

200  
136  
100-76  
OFR 55-3

UNITED STATES DEPARTMENT OF THE INTERIOR

U.S. GEOLOGICAL SURVEY

(Report No. 100-76-1)

GEOLOGY OF THE EDISON AREA, SUSSEX COUNTY, NEW JERSEY

By

Donald Roy Baker



REPRODUCED FROM BEST AVAILABLE COPY

This report is preliminary and has  
not been edited or reviewed for  
conformity with Geological Survey  
standards or nomenclature.

OPEN FILE

## CONTENTS

	Page
ABSTRACT . . . . .	xiii
INTRODUCTION . . . . .	1

## PART I GEOLOGIC SETTING

1. REGIONAL GEOLOGIC SETTING . . . . .	5
- INTRODUCTION . . . . .	5
THE NEW JERSEY HIGHLANDS . . . . .	5
General . . . . .	5
Historical . . . . .	6
Comparison to Adirondacks . . . . .	8
BASIC STRUCTURAL FRAMEWORK OF THE FRANKLIN FURNACE AREA . . . . .	10
- Introduction . . . . .	10
- Structural blocks . . . . .	10
2. GENERAL GEOLOGY OF THE EDISON BLOCK . . . . .	13
- INTRODUCTION . . . . .	13
LITHOLOGIC UNITS . . . . .	13
General . . . . .	13
Age relationships . . . . .	15
STRUCTURE . . . . .	16
REGIONAL METAMORPHISM AND METASOMATISM . . . . .	17
MAGNETITE DEPOSITS . . . . .	18

## PART II GEOLOGIC DESCRIPTION

3. LITHOLOGIC UNITS OF THE EDISON TYPE . . . . .	20
- INTRODUCTION . . . . .	20
EDISON UNIT . . . . .	20
SAND HILLS UNIT . . . . .	22
NO AFEE UNIT . . . . .	24
SHERMAN UNIT . . . . .	25
COMPARISON . . . . .	27
4. PETROLOGY OF THE EDISON AREA . . . . .	28
INTRODUCTION . . . . .	28

	Page
WALL ROCK UNITS . . . . .	28
Quartz-oligoclase gneiss . . . . .	28
Pyroxene syenite gneiss . . . . .	30
Pyroxene granite . . . . .	34
Hypersthene granite . . . . .	38
Hornblende granite . . . . .	39
Biotite alaskite . . . . .	40
Contaminated hornblende granite . . . . .	41
Garnet-biotite-quartz-feldspar gneiss and related facies . . . . .	42
EDISON UNIT . . . . .	43
Mixed gneiss subunit . . . . .	43
Introduction . . . . .	43
Mineralogy . . . . .	44
Magnetite-quartz-K-feldspar gneiss . . . . .	45
Sillimanite . . . . .	48
Lithologic variations . . . . .	52
Pegmatites . . . . .	58
Fabric . . . . .	60
Sulfide zone . . . . .	62
Quartz-K-feldspar gneiss . . . . .	65
Introduction . . . . .	65
Mineralogy and composition . . . . .	65
Fabric . . . . .	66
Classification . . . . .	69
Relationship to other rocks . . . . .	70
Biotite-quartz-feldspar gneiss . . . . .	72
Introduction . . . . .	72
Mineralogy . . . . .	72
Fabric . . . . .	73
Composition . . . . .	74
Lithologic variations . . . . .	77
Relationship to other rocks . . . . .	77
Epidote-scapolite-quartz-gneiss and related facies . . . . .	77
Introduction . . . . .	77
Mineralogy . . . . .	78
Fabric . . . . .	81
Lithologic variations . . . . .	82
5. STRUCTURE OF THE EDISON AREA . . . . .	85
INTRODUCTION . . . . .	85
POLIATION . . . . .	85
LINEATION . . . . .	87
FOLDS . . . . .	88
FAULTS AND JOINTS . . . . .	90

	Page
6. DETAILED MINERALOGY OF THE EDISON UNIT IN THE EDISON AREA . . .	92
K-FELDSPAR . . . . .	92
Introduction . . . . .	92
Composition . . . . .	92
Twining . . . . .	92
Terthitic intergrowth . . . . .	94
X-ray data . . . . .	95
Summary and petrologic significance . . . . .	103
ZIRCON . . . . .	106
GARNET . . . . .	107
MAGNETITE-HEMATITE-ILMENITE-RUTILE PARAGENESIS . . . . .	110
Introduction . . . . .	110
Magnetite-ilmenite and magnetite-hematite systems . . . . .	111
Introduction . . . . .	111
Magnetite-ilmenite . . . . .	113
Magnetite-hematite (martite) . . . . .	114
Hematite-ilmenite-rutile system . . . . .	117
Introduction . . . . .	117
Hematite-ilmenite with minor rutile . . . . .	118
Hematite-rutile with minor ilmenite . . . . .	123
Intergrowths of magnetite with non-magnetic iron and titanium oxides . . . . .	126
Alteration of ilmenite . . . . .	130
Iron and titanium oxides of the other rocks of the Edison unit . . . . .	132
7. GEOCHEMISTRY OF THE MIXED GNEISS SUBUNIT . . . . .	136
PARTIAL CHEMICAL ANALYSIS OF THE MAGNETITE-QUARTZ-K-FELDSPAR GNEISS AND MAGNETITE RICH LAYER . . . . .	136
GEOCHEMISTRY OF MANGANESE, TITANIUM, PHOSPHORUS AND SULFUR IN THE MIXED GNEISS SUBUNIT . . . . .	139
Manganese . . . . .	139
Titanium . . . . .	139
Phosphorus . . . . .	140
Sulfur . . . . .	142
GEOCHEMISTRY OF IRON WITH SPECIAL REFERENCE TO THE DISTRIBUTION OF MAGNETITE AND HEMATITE . . . . .	143
Introduction . . . . .	143
Distribution of iron . . . . .	144
Distribution of magnetite and hematite . . . . .	144
Introduction . . . . .	144
Petrographic data . . . . .	144
Drill core data . . . . .	145
Summary . . . . .	150

	Page
8. ECONOMIC GEOLOGY OF THE EDISON AREA . . . . .	151
INTRODUCTION . . . . .	151
DISTRIBUTION . . . . .	151
SOURCES OF DATA . . . . .	152
PETROLOGY AND MINERALOGY . . . . .	153
CONTACT RELATIONSHIPS . . . . .	155
STRUCTURE . . . . .	156
RESERVES . . . . .	157
9. EXPERIMENTAL AND THERMODYNAMIC DATA FOR THE MAGNETITE-HEMATITE-ILMENITE-RUTILE-WATER SYSTEM . . . . .	160
INTRODUCTION . . . . .	160
THE MAGNETITE-HEMATITE REACTION . . . . .	163
Introduction . . . . .	163
Experimental data . . . . .	163
Thermodynamic data . . . . .	166
Calculation of the equilibrium constant . . . . .	169
Determination of $\Delta F$ at high pressures for the magnetite-hematite reaction . . . . .	174
Calculation of $p(O_2)$ . . . . .	181
THE OXIDATION OF ILMENITE . . . . .	184
THE WATER REACTION . . . . .	188
Introduction . . . . .	188
Experimental data for the water reaction . . . . .	189
Water reaction at high pressures and temperatures . . . . .	192
Calculation of $p(O_2)$ for the water reaction . . . . .	194
Influence of other volatiles on the water reaction . . . . .	196
COMPARISON OF THE WATER REACTION WITH THE MAGNETITE-HEMATITE REACTION . . . . .	197
PART III INTERPRETATION	
10. SIGNIFICANCE OF THE IRON AND TITANIUM OXIDE PARAGENESIS IN THE EDISON UNIT . . . . .	202
MAGNETITE-PRIMARY HEMATITE . . . . .	202
MAGNETITE-MARTITE . . . . .	204
OXIDATION OF ILMENITE . . . . .	206
SIGNIFICANCE OF INTERGROWTHS OF MAGNETITE WITH NON-MAGNETIC IRON AND TITANIUM OXIDES . . . . .	207
11. ORIGIN OF THE EDISON UNIT . . . . .	211
INTRODUCTION . . . . .	211

	Page
' ORIGIN OF THE MIXED GNEISS SUBUNIT . . . . .	212
✓ Sedimentary affinities . . . . .	212
✓ Metamorphism . . . . .	214
✓ Metasomatism . . . . .	215
/ ORIGIN OF THE LIME RICH SUBUNIT . . . . .	216
✓ Sedimentary affinity . . . . .	219
✓ Metamorphism . . . . .	219
✓ Metasomatism . . . . .	220
' ORIGIN OF THE BIOTITE-QUARTZ-FELDSPAR GNEISS . . . . .	221
' ORIGIN OF THE QUARTZ-K-FELDSPAR GNEISS . . . . .	225
 12. ORIGIN OF THE MAGNETITE DEPOSITS IN THE EDISON AREA	
INTRODUCTION . . . . .	230
SOURCE OF IRON FOR MAGNETITE DEPOSITS . . . . .	234
MODE OF TRANSPORTATION OF THE IRON . . . . .	239
MODE AND TIME OF EMPLACEMENT OF THE MAGNETITE . . . . .	241
SUMMARY . . . . .	244
 REFERENCES CITED . . . . .	269

## TABLES

Table	Page
1. Chemical composition of (graphitic)-biotite-oligoclase gneiss from the New Jersey Highlands, tabulated with the average composition of a similar gneiss from the Northwest Adirondacks and with the average composition of some graywacke sandstones . . . . .	9
2. Partial Chemical Analysis and Mineral Recalculation of Ilmonomagnetite from the Pyroxene Syenite Gneiss . . . . .	34
3. Chemical analysis and recalculation of ferrohedenbergite from pyroxene granite (Specimen No. Ed-1924). . . . .	37
4A. Partial chemical analyses of magnetic and non-magnetic fractions of iron and titanium oxides from eight samples of magnetite-quartz-K-feldspar gneiss from the Edison area and Sherman unit . . . . .	46
4B. Petrographic data of the eight samples from Table 4A . . . . .	47
5. Mineral analyses of thirty-six samples of magnetite-quartz-K-feldspar gneiss from the Edison area and Sherman unit . . . .	50
6. Mineral analyses of miscellaneous samples from the mixed gneiss subunit . . . . .	54
7. Lithologic profile, Old Ogden Mine, Edison, New Jersey . . . .	56
8. Mineral analyses of sixteen samples of quartz-K-feldspar gneiss from the Edison area . . . . .	67
9. Mineral analyses of twenty-two samples of biotite-quartz-feldspar gneiss from the Edison unit . . . . .	75
10. Partial chemical analyses of quartz-feldspar concentrates from the mixed gneiss subunit . . . . .	93
11. Partial X-ray powder diffraction data on K-feldspar . . . . .	98
12. Chemical composition of garnet . . . . .	108
13. MnO analyses of garnets . . . . .	109
14. Petrographic criteria for identification of iron and titanium oxide minerals . . . . .	119

## TABLES

Table	Page
/ 15. Partial chemical analyses of magnetic and non-magnetic fractions of iron and titanium oxides and petrographic data for two miscellaneous gneisses . . . . .	134
/ 16. Volumetric modes, weight modes and partial chemical analyses of magnetite-quartz-K-feldspar gneiss and a magnetite rich layer tabulated with the chemical composition of a sillimanite-quartz-microcline granitic gneiss from the Adirondacks . . . . .	137
/ 17. Estimate of Magnetite Ore Reserves in the Edison area, New Jersey . . . . .	159
/ 18. Experimental, thermodynamic and equilibrium data for the magnetite-hematite reaction for 1 atmosphere total pressure.	165
/ 19. Activity of $\text{Fe}_3\text{O}_4$ in Magnetite . . . . .	171
/ 20. Virial coefficients for equation of state for $\text{O}_2$ . . . . .	177
/ 21. Thermodynamic and equilibrium data for the magnetite-hematite reaction for selected high temperatures and pressures . . .	179
/ 22. Thermodynamic data for iron and titanium oxide reactions at 25°C and one atmosphere pressure . . . . .	185
/ 23. Experimental, thermodynamic and equilibrium data for the $\text{H}_2\text{O}$ reaction for selected temperatures and pressures . . . .	190
/ 24. Equilibrium $p(\text{H}_2)$ for a pure $\text{H}_2\text{O}$ system and a $\text{H}_2\text{O}$ -magnetite-hematite system for selected temperatures and pressures . . .	199
25. Average mineral composition of the quartz-K-feldspar gneiss of the Edison area and garnet alaskite of the Adirondacks . . .	227

## FIGURES

Figure	Page
✓ 1. Index map showing the location of the Franklin Furnace area, Sussex and Morris counties, N. J. . . . .	2
✓ 2. Highly generalized map showing the basic structural framework of the Franklin Furnace area and the location of the Edison area . . . . .	11
✓ 3. Variation in mineralogical composition of magnetite-quartz-K- feldspar gneiss . . . . .	49
✓ 4. Relation of sillimanite to K-feldspar in the mixed gneiss subunit . . . . .	51
✓ 5. Variation in mineralogical composition of quartz-K-feldspar gneiss . . . . .	63
✓ 6. Variation in mineralogical composition of biotite-quartz- feldspar gneiss . . . . .	76
✓ 7. Triangular diagram of the iron and titanium oxide system showing possible minerals . . . . .	112
✓ 8. Tentative subsolidus temperature-composition phase diagram for a portion of the hematite-ilmenite-rutile system based on data from Table 4 . . . . .	127
✓ 9a. Total iron as moles of magnetite versus phosphorus as moles of apatite from eighty-seven assayed samples of the mixed gneiss subunit . . . . .	141
✓ 9b. Histogram showing ratio of magnetite to apatite in the assayed samples . . . . .	141
✓ 10. Total iron as moles of magnetite versus the ratio of magnetite to hematite for assayed samples of the mixed gneiss subunit	143
✓ 11. Total iron as moles of magnetite versus the ratio of magnetite to hematite for assayed samples of the mixed gneiss sub- unit . . . . .	149
✓ 12. Isobars showing variation of free energy increase with temper- ature for the magnetite-hematite reaction . . . . .	170
✓ 13. Isobars showing variation of the equilibrium constants with temperature for the magnetite-hematite and water reactions	173

## FIGURES

Figure	Page
14. Isotherms showing variation of free energy increase with pressure for the magnetite-hematite reaction . . . . .	180
15. Isotherms showing variation of free energy increase with pressure for the water reaction . . . . . . . . .	182
16. Univariant isobars showing variation of the equilibrium $p(O_2)$ with temperature for the magnetite-hematite and water reactions . . . . . . . . .	183
17. Isobars showing variation of free energy with temperature for the water reaction . . . . . . . . .	191
18. Isobars showing variation of the equilibrium $p(H_2)$ with temperature for the water reaction and for a water-magnetite-hematite system . . . . . . . . .	200

## PLATES

Plate	Page
1. Geologic map of the area of the Edison Magnetite Deposits, Sussex County, New Jersey . . . . .	Map pocket
Explanation to Plate 1 . . . . .	245
2. Amphibolite layer intruded by pegmatite . . . . .	248
3. Photomicrograph sample 140, magnetite-quartz-K-feldspar gneiss from the Edison area . . . . .	249
4. Photomicrograph sample 143, magnetite-K-feldspar-quartz gneiss from the Edison area . . . . .	250
5a. Photomicrograph sample 145, magnetite-quartz-K-feldspar gneiss from the Edison area . . . . .	251
5b. Photomicrograph sample 145 . . . . .	252
6a. Photomicrograph sample B-151f, magnetite-biotite-millimanite- quartz gneiss from the Edison area . . . . .	253
6b. Photomicrograph sample B-151f . . . . .	254
7. Photomicrograph sample Ed-177, quartz-K-feldspar gneiss from the Edison area . . . . .	255
8. Photomicrograph sample Ed-241a, biotite-quartz-feldspar gneiss from the Edison area . . . . .	256
9. Pegmatite lode in the mixed gneiss subunit . . . . .	257
10. Interlayers of biotite alaskite, biotite-quartz-feldspar gneiss and quartz-K-feldspar gneiss in the Edison area . .	258
11. Handspecimen (Ed-2544) which illustrates interlayering of biotite alaskite, biotite-quartz-feldspar gneiss and quartz-K-feldspar gneiss . . . . .	259
12. Photomicrograph sample 144, ilmenomagnetite with martite .	260
13. Photomicrograph sample 149, ilmenohematite and magneto- ilmenohematite . . . . .	261
14. Photomicrograph sample 149, ilmenohematite . . . . .	262

## PLATES

Plate	Page
15. Photomicrograph sample 149, magneto-hemoilmenite . . . . .	263
16. Photomicrograph sample 145, ilmeno-rutilehomatite . . . . .	264
17. Photomicrograph sample 153, hemorutile . . . . . . . . .	265
18. Photomicrograph sample 153, magneto-rutilehematite . . . . .	266
19. Photomicrograph sample 154, magneto-rutile . . . . . . . . .	267
20. Handspecimen showing contact relations between magnetite-quartz-K-feldspar gneiss and magnetite-quartz gneiss . .	268

## ABBREVIATIONS OF MINERAL NAMES

acc.	accessory	mt. or M	magnetite
al.	allanite	ilm. or I	ilmenite
alt. pl.	altered plagioclase	hem. or H	hematite
ap.	apatite	rut. or R	rutile
bi.	biotite	IM	ilmenomagnetite
ch.	chlorite	HI	hemoilmenite
co.	corundum	IH	ilmenohematite
ep.	epidote	R-IH	rutilo-ilmenohematite
feld.	feldspar	I-RH	ilmeno-rutilohematite
fl.	fluorite	RH	rutilohematite
gar.	garnet	HR	hemorutile
hb.	hornblende	PY.	pyrite
K-fd.	K-feldspar	S.	ephalerite
mcc.	micro complex		
mic.	microcline		
nz.	nzemite		
musco.	muscovite		
oc.	oligoclase		
pl.	plagioclase		
qts.	quartz		
ser.	sericitic		
ser.-ep.	sericitic plus epidote		
sill.	sillimanite		
sph.	sphene		
sp.	spinel		
sr.	sircon		

## ABSTRACT

The Edison area is in the New Jersey Highlands three miles south of Franklin, New Jersey and is a part of a structural block, which trends northeast and is bounded by high-angle faults on the northwest and southeast. An older complex of sedimentary rocks (Grenville type), modified by regional metamorphism and metasomatism and intruded by younger igneous rocks, underlies the region. Lithologic units define a major anticline which plunges 30° northeast and is overturned to the northwest. Foliation and lineation are structures within lithologic units. In the Edison area magnetite ore zones are tubular-shaped bodies which pinch-out in the foliation plane in a direction parallel to the lineation.

The Edison gneiss, a major lithologic unit in the Edison area, is divided into four subunits. The mixed gneiss subunit is a complex of interlayered gneisses, pegmatite and magnetite zones. Quartz, K-feldspar and magnetite are major minerals; minor minerals include biotite, sillimanite, garnet, ilmenohematite, apatite, monazite, zircon, hemoilmenite, ilmenite, rutile, martite and sulfides. Magnetite-quartz-K-feldspar gneiss is predominant but layers with metasedimentary affinity are abundant. The biotite-quartz-feldspar gneiss subunit is composed of oligoclase, K-feldspar, biotite and garnet with hornblende, ilmenomagnetite, ilmenite, and apatite. Epidote-scapolite-quartz gneiss (lime-rich subunit) with layers varying from metaquartzite to quartz-feldspar gneiss is composed of quartz, oligoclase, microcline,

epidote, scapolite, actinolite, salite, phlogopite; and sphene, calcite, magnetite, martite, ilmenohematite, and garnet. The quartz-K-feldspar gneiss is a uniform subunit composed of perthitic K-feldspar, garnet, ilmenomagnetite, biotite and zircon. Wall rocks to these subunits are of igneous origin and include pyroxene syenite gneiss, hornblende granite and pyroxene granite.

X-ray observations prove that K-feldspar from magnetite-rich layers is monoclinic, but K-feldspar from magnetite-quartz-K-feldspar gneiss is microcline with 0.9 triclinicity. K-feldspar from biotite-quartz-feldspar gneiss and quartz-K-feldspar gneiss is a mixture of triclinic and monoclinic polymorphs.

The primary iron-titanium oxide paragenesis in the Edison unit includes ilmenomagnetite, ilmenite, hematite, hawilmenite, ilmenohematite, rutile-ilmenohematite, rutilehematite, hemorutile and rutile. Magnetite is altered to martite. The other intergrowths are exsolution products. A tentative subsolidus temperature-composition diagram for the hematite-ilmenite-rutile system is presented.

The chemical composition of magnetite-quartz-K-feldspar gneiss is similar to sillimanite-quartz-microcline granite gneiss of the Adirondacks which is a metasomatized metasediment. In the mixed gneiss sub-unit, Ba and Mn are enriched in magnetite layers;  $TiO_2$  varies from 0.2 to 2.0 wt. % and occurs in a constant proportion to iron; sulfur (0.01 to 0.5 wt. %) is from sulfides which crystallized later than magnetite; phosphorus (0.1 - 0.8 wt. %) and iron (up to 60 wt. %) are in a constant ratio which is believed to be a reflection of the composition of

a parent ore fluid. Primary hematite is enriched over magnetite in rocks of metasedimentary type and the magnetite/hematite ratio (oxidation degree) decreases linearly with increase in total iron.

New thermodynamic calculations enabled the construction of univariant isobars for the magnetite-hematite reaction ( $2\text{Fe}_3\text{O}_4 + \frac{1}{2}\text{O}_2 = 3\text{Fe}_2\text{O}_3$ ) and water reaction ( $2\text{H}_2 + \text{O}_2 = 2\text{H}_2\text{O}$ ) for temperatures from  $25^\circ - 1300^\circ\text{C}$  and pressures from 1 - 7000 atm. Assuming magnetite and hematite formed at equilibrium at a given temperature and pressure, the equilibrium  $p(\text{O}_2)$  and  $p(\text{H}_2)$  for the petrologic system are obtained directly from the univariant curves. The univariant curves indicate that in cooling from a magnetite-hematite equilibrium there is a continual production of "excess"  $\text{O}_2$  (due to  $\text{H}_2\text{O}$  dissociation) so that magnetite is continually oxidized to hematite; hence, magnetite is considered a retrograde mineral.

It is concluded that the mixed gneiss subunit represents argillaceous and arenaceous sedimentary rocks which have been recrystallized to gneisses of amphibolite grade by regional metamorphism and reconstituted by Fe-and-K-metasomatism. Similarly, the lime-rich subunit originated by the regional metamorphism and K-metasomatism of calcareous sedimentary rocks. The biotite-quartz-feldspar gneiss is a facsimile of gneisses in the Adirondacks which are regional metamorphosed (amphibolite grade) and K-metasomatized graywacke. The quartz-K-feldspar gneiss crystallized directly from the K-rich fluids which chemically reconstituted the other gneisses.

The magnetite deposits in the mixed gneiss subunit formed during regional metamorphism and metasomatism. The initial source of the iron was from residual fluids developed from the progressive crystallization of granitic magma. Some of the ferric iron may be of sedimentary (exogene) origin. The iron-rich fluids permeated and metasomatically replaced the co-existing rock material.

## INTRODUCTION

The Franklin Furnace area occupies about 70 square miles in Sussex and Morris counties, New Jersey, and includes parts of the Franklin Furnace, Hamburg, Newfoundland, Wawayanda, Dover, and Stanhope 7 1/2 minute quadrangles. The area is about 14 miles long extending from Woodport, New Jersey on the southeast to Vernon, New Jersey on the northeast, and is from 3 to 6 miles in average width. New York City is about 40 miles to the southeast (see Figure 1.)

The Franklin Furnace area is within the New Jersey Highlands which is within the Reading Prong of the New England physiographic province. The area is characterized by northeast trending ridges that are separated by broad and narrow valleys. Altitudes range from 500 to 1400 feet. The topography is moderately rugged and was developed by stream erosion which was controlled by the structure and lithology of the bedrock. Pleistocene glaciation has modified the pre-existing fluvial erosion pattern to different degrees. The area is well north of the terminal moraine of the Wisconsin stage of glaciation so that bedrock exposures are very numerous although some small areas are covered with glacial drift. The uplands of the area are wooded with second-growth forest and have abundant bedrock exposures. The lowlands of the area which are cleared and farmed have relatively few bedrock exposures.

The Edison area is located near the center of the Franklin Furnace area at Edison, New Jersey which is 2 miles southeast of the village of Ogdensburg. The Edison area is about 2 miles long and a mile wide. Within this area are the Edison magnetite deposits. These magnetite deposits and

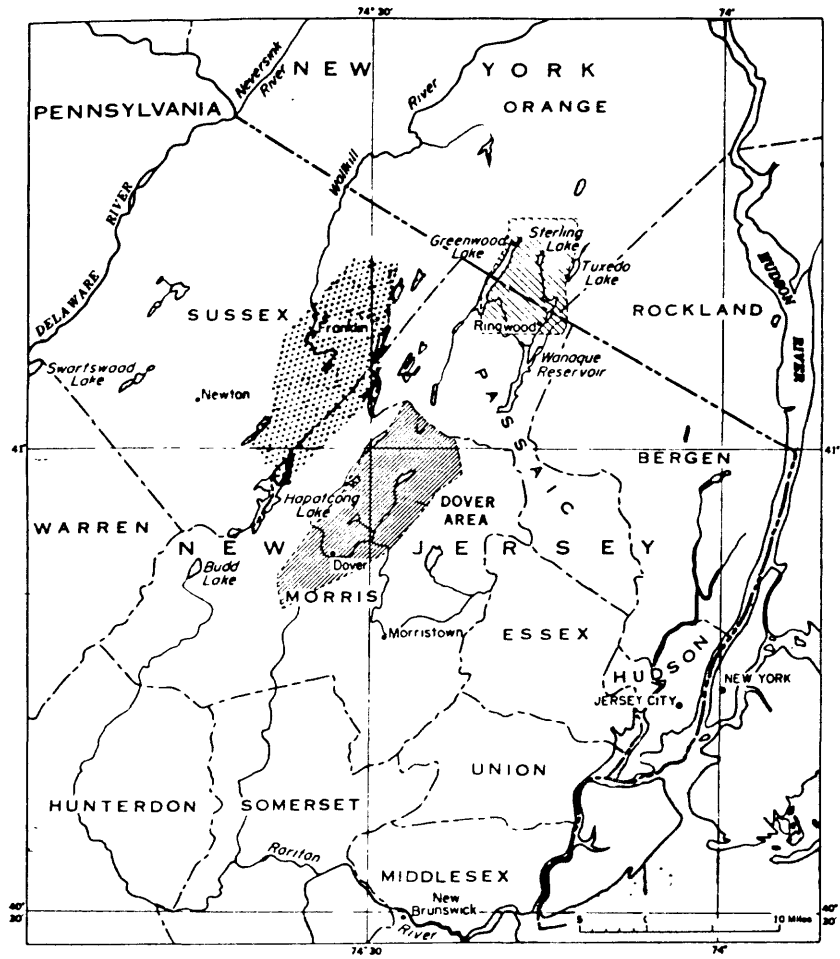


**Figure 1.** Index map showing the location of the Franklin Furnace area, Sussex and Morris counties, N. J. Dover district (Sims, 1953) and Sterling Lake-Ringwood district (Hotz, 1952) are also shown.  
(Figure modified after Sims, 1953.)

associated rocks are the principal subject of this report.

During the summers of 1952 and 1953 the writer assisted A. F. Buddington in the areal geologic mapping of the pre-Cambrian rocks of much of the Franklin Furnace area for the U. S. Geological Survey. During these summers about six weeks were spent in the detailed geologic mapping and study of the Edison area. The base map for the Edison area was prepared from a plane table survey made by A. F. Buddington during the summer of 1951. During the years 1952-54 laboratory studies on rock samples collected from the Edison area were carried on in the geology department of Princeton University. The laboratory work included the study of 150 thin and 50 polished sections. In addition a number of chemical analyses of rocks and minerals from the Edison area and Franklin Furnace area were obtained. The writer did a small amount of X-ray work during the year 1953-54.

The purpose of this research was to describe the nature of the magnetite deposits and closely allied rocks in the Edison area. In the first part of this report a summary of the regional geology is presented. The bulk of the descriptive data are presented in the second part of the report. In the last part of the report the descriptive data are synthesized in an attempt to explain the genesis of the magnetite deposits and rocks of the Edison area.

The cooperation of the Edison Company for making available the magnetic anomaly map of the Edison area and other useful data is gratefully acknowledged. In addition the generosity of the Pittsburgh Coke and Iron Company for making available the drill core from seven holes which they drilled in 1943 is gratefully acknowledged.

The writer is gratefully indebted to Mr. Cleaves L. Rogers of the U. S. Geological Survey for helpful geologic data which he collected during an earlier phase of the study of the Edison area.

The writer is greatly indebted to A. F. Buddington of Princeton University for guidance and counsel during the course of the investigation. The support of the U. S. Geological Survey for the field and part of the laboratory studies is gratefully acknowledged. The partial chemical analyses of the iron and titanium oxides were made by J. Fahey and A. Vlisidis of the U. S. Geological Survey. The additional chemical analyses were furnished by Princeton University.

PART I

GEOLoGIC SETTING

## CHAPTER 1

### REGIONAL GEOLOGIC SETTING

#### INTRODUCTION

In order to describe and interpret the detailed studies of the Edison area it is necessary to obtain a reasonably complete picture of the regional geologic setting. It is the purpose of this part to establish this prerequisite descriptive background, so that the detailed studies may be evaluated with an understanding of the regional geologic picture and not in the light of a few detailed observations which may prove very deceptive when viewed alone.

#### THE NEW JERSEY HIGHLANDS

##### General

The New Jersey Highlands is a physiographic province in the northern part of the state which is characterized by greater elevation and relief than the coastal plain and Triassic lowlands to the south. The Highlands are underlain by pre-Cambrian and Paleozoic rocks and form a portion of the Reading Prong. The Reading Prong extends for a total of 350 miles from the southwest near Reading, Pennsylvania to the northeast as far as Vermont. It has a maximum width in the New Jersey Highlands where it averages about 15 miles. The northwest boundary of the New Jersey Highlands, and hence the Reading Prong, is adjacent to the northeast continuation of the Great Valley physiographic province. In New Jersey the Great Valley is as narrow as 8 to 10 miles and is underlain by Cambro-Ordovician

deformed sedimentary rocks. The New Jersey Highlands, and hence the Reading Frong, terminate on the southeast along a high angle fault against the Triassic rocks of the Newark series. To the southwest the Reading Frong continually narrows until near Reading, Pennsylvania it disappears between fault contacts against Triassic rocks and fault and unconformable contacts against Paleozoic rocks. In its northern extension the Reading Frong forms a thin slice of pre-Cambrian rocks which are often in thrust contact with Paleozoic rocks on the east and west. These faults are probably of Taconic age; however, the exact relationships of the pre-Cambrian to the Paleozoic in the region north of New Jersey is often unknown.

#### Historical

Despite their accessibility the pre-Cambrian rocks of the New Jersey Highlands have been the subject of few comprehensive studies. The most important early geologic studies that were made in the region are those of Rogers (1836, 1840), Kitchell (1856), Cook (1863), Putnam (1886), Mason (1889), Walff (1894), Bayley (1908, 1910, 1914), Spencer (1908), and Smith (1933). Earlier geologists were concerned chiefly with the exploration and production of ore deposits. The report of Bayley (1910) is the most complete source of data on the iron mines and mining in the region, but it gives only a brief summary of the geology. The first comprehensive geologic work was done by Spencer (1908) who divided the pre-Cambrian rocks into the following categories, (1) Pochuck gneiss, a general field term applied to dark mafic gneisses (see Hotz, 1953 for a complete discussion of the term), (2) Franklin marble, (3) Lossee gneiss, granitic gneisses distinguished by light color and the predominance of

Na-Feldspar, and (4) the Byram gneisses, granitic rocks with predominant K-feldspar. Spencer postulated that the Losoe and Byram gneisses were of igneous origin but regarded the Pochuck as of unknown origin. This classification of the pre-Cambrian rocks of the New Jersey Highlands, has been used by many workers; however, detailed geologic mapping and petrographic study indicate that Spencer's classification is very inadequate. Hence, no attempt is made in this report to utilize this classification.

Fchner (1914) in a classic paper presented a wealth of ideas concerning the origin of the gneisses of the New Jersey Highlands. From his detailed studies of a small area he proposed that the gneisses originated through, "a process involving the injection of a thinly fluid granitic magma between the layers of an original rock of laminated structure." In addition he pointed out that structures within the gneiss indicate "that the process of injection was carried out in a most quiet and gradual manner, and possessed many of the characteristics of a substitution of the original material by the magmatic solution rather than the features of a violent intrusion."

The most recent and comprehensive geologic studies in the New Jersey Highlands have been done by various geologists associated with the U. S. Geological Survey (Sims and Leonard 1952, Notz, 1953, Sims 1950, and 1953). All these geologists have recognized two broad categories of pre-Cambrian rocks, (1) those of metasedimentary origin, and (2) those of igneous origin. In addition rocks of complex origin, i. e. migmatites, metasomites, etc., have been recognized. The consensus among later geologists is that the greatest part of the rocks of igneous origin were intruded into the older metasedimentary rocks, "during the waning stages

of the tectonic activity that deformed the earlier rocks," (Hotz, 1953). In all cases only one major period of pre-Cambrian tectonic activity with its consequent igneous activity is recognized.

Comparison to the Adirondacks

Engel and Engel (1953) have called attention to the close similarity between the Grenville series, as found in the Grenville subprovince of Canada and the Adirondacks, and many of the pre-Cambrian gneisses of New Jersey. The Franklin marble is analogous to the Grenville marbles of the Adirondacks, and in addition many of the paragneisses of the two regions are very similar. Especially striking are the similarities between biotite-quartz-plagioclase gneisses from the two regions. The average chemical composition of such paragneiss from the northwest Adirondacks (Engel and Engel, 1953) is listed in Table 1 together with a single chemical analysis for the same type of paragneiss from the New Jersey Highlands. The similarity in chemical composition is very close. It appears conclusive that many of the gneisses of the New Jersey Highlands are of Grenville type in the sense that they are lithologically similar to but possibly of different age from the characteristic gneisses of the Grenville subprovince proper.

Thus, the most important general comparison is that both the Adirondacks and the New Jersey Highlands are characterized by an older complex of sedimentary rocks (Grenville series in the Adirondacks) which have been greatly modified by regional metamorphism and metasomatism and which are intruded by younger igneous rocks. However, the two regions differ in some respects. No major anorthosite bodies have been located in the New Jersey Highlands although some small masses have been mapped

Table 1. Chemical composition of (graphitic)-biotite-quartz-oligoclase gneiss from the New Jersey Highlands, tabulated with the average composition of a similar gneiss from the Northwest Adirondacks and with the average composition of some graywacke sandstones.

	El-1663	QbA	A	B
SiO <sub>2</sub>	67.69	70.90	69.69	64.2
TiO <sub>2</sub>	0.48	0.32	0.40	0.5
Al <sub>2</sub> O <sub>3</sub>	15.99	12.17	13.53	14.1
Fe <sub>2</sub> O <sub>3</sub>	0.64	1.31	0.74	1.0
FeO	2.42	4.12	3.10	4.2
MnO	0.05	0.04	0.01	0.1
NiO	1.16	2.32	2.00	2.9
CaO	2.88	1.55	1.95	3.5
MgO	4.64	3.74	4.21	3.4
K <sub>2</sub> O	2.86	2.87	1.71	2.0
RbO	0.16			
BaO +	0.35	0.21	2.03	2.1
HgO -	0.14	0.05	0.26	0.1
P <sub>2</sub> O <sub>5</sub>	0.16		0.10	0.1
CO <sub>2</sub>	0.04		0.23	1.6
S	0.04			
Total	99.70	99.60	100.01	99.8

El-1663 - (Graphitic)-biotite-quartz-oligoclase gneiss, from extreme northwest corner of Newfoundland Quadrangle, New Jersey (analyst:

QbA - Analysis of composite sample of 24 least altered layers of quartz-biotite-oligoclase gneiss (after Engel and Engel, 1953, p. 1085).

A - Average of 3 analyses, Franciscan graywacke (after Tulaferro, 1973, p. 136).

B - Average of 11 graywackes (after Pettijohn, 1949, p. 250).

in Pennsylvania (Biscom and Stose, 1938 and Smith, 1923). This is in marked contrast to the situation in the Adirondacks. Also rocks of cataclastic origin are lacking in the New Jersey Highlands, whereas they are very conspicuous in the northwest Adirondacks (Buddington, 1939). To date only a single major period of igneous activity is recognized in the New Jersey Highlands, but in the Adirondacks at least three distinct periods of igneous activity are established (Buddington, 1939, 1952). Finally, the grade of metamorphism in the New Jersey Highlands as well as it is known is the amphibolite facies, whereas in the Adirondacks the grade varies from the amphibolite to the granulite facies (Buddington 1952, p. 79-83).

#### BASIC STRUCTURAL FRAMEWORK OF THE FRANKLIN FURNACE AREA

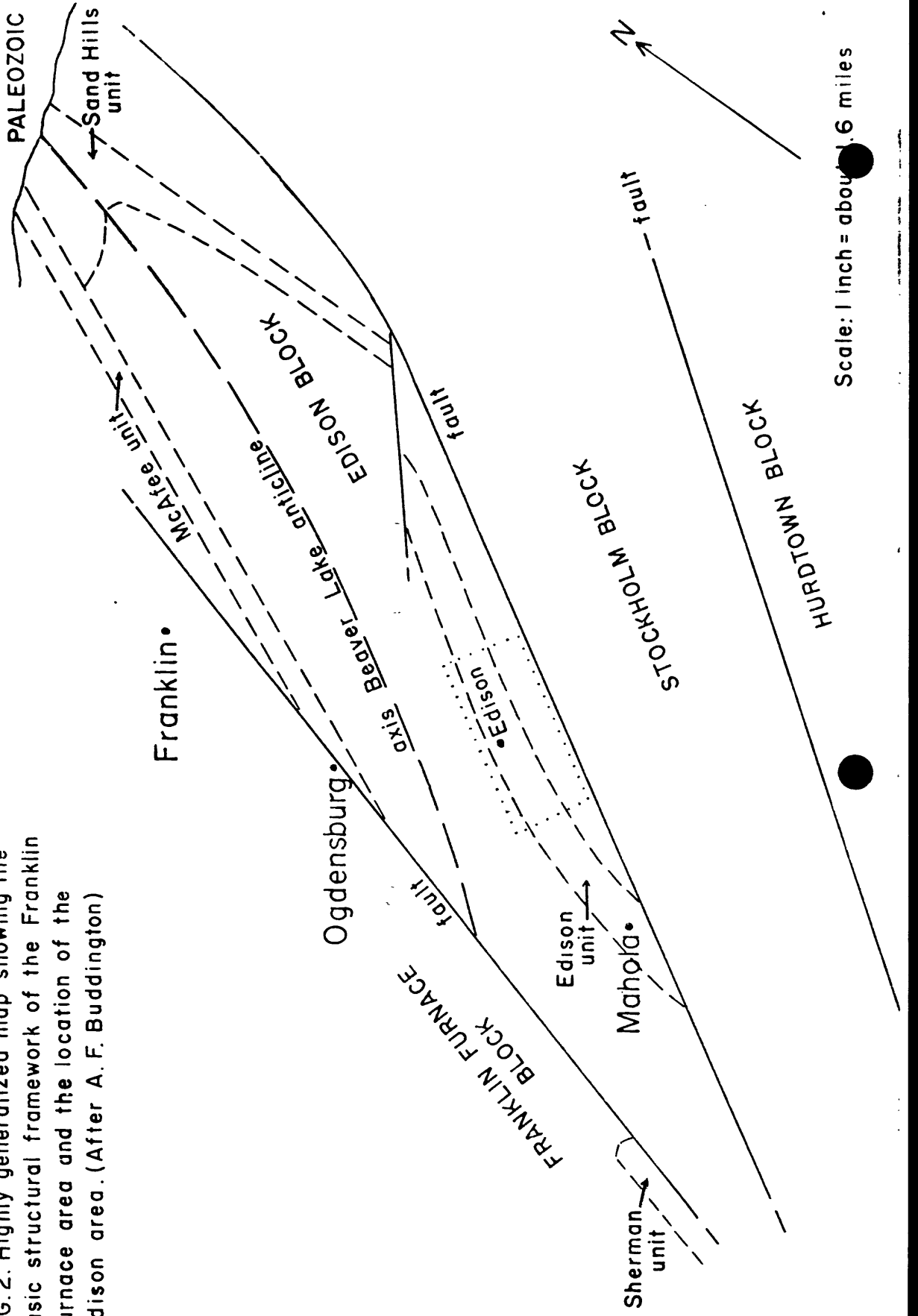
##### Introduction

The Franklin Furnace area includes all of the Franklin Furnace quadrangle and much of the adjacent quadrangles (Figure 2). The following section attempts to describe the principal structural aspects of this area.

##### Structural blocks

The area is divided into separate fault blocks by high angle, north-east trending faults. The pre-Cambrian rocks have been faulted against younger Paleozoic rocks and other pre-Cambrian rocks. It is very likely that some of the faults are of pre-Cambrian age, and there is evidence which suggests that pre-Cambrian faults were rejuvenated during a later period. However, as the youngest displaced rocks are of Devonian age (Skunneumunk conglomerate, Spencer et al., 1908) some of the faulting must

FIG. 2. Highly generalized map showing the basic structural framework of the Franklin Furnace area and the location of the Edison area. (After A. F. Buddington)



be post Devonian. These faults are similar to the Triassic-Jurassic faults of the Newark basin; so it is very likely that some of the faulting in the New Jersey Highlands could be of similar age.

Within the Franklin Furnace area four structural blocks separated by such faults are well defined (Figure 2). The Franklin Furnace block farthest to the northeast is a graben and is underlain mostly by Paleozoic rocks which are described by Mummel (1908). The Edison block is immediately to the southeast and is underlain entirely by pre-Cambrian rocks. Within this block is the Edison area. The fault which separates the Edison block from the Stockholm block became apparent only after detailed mapping within the pre-Cambrian terrain, although the fault has displaced the Paleozoic rocks at the locality of Vernon. The Hurdtown block lies on the extreme southeast of the area and is faulted against the Stockholm block.

Actual exposures of the fault planes are very rare. However, the straight trends of the fault lines indicate high angle fault planes. The faults have been traced for distances of 10-12 miles and may extend much farther. No independent evidence was found which would indicate whether the faults were normal or reverse types and it is possible that some of them could be strike-slip faults. It is very difficult to assess actual displacements; however, vertical offset must certainly be on the order of 1000 feet or more (Spencer, 1908, p. 19), and it is possible that horizontal offset on some of the pre-Cambrian faults could be on the order of miles. There is usually a narrow zone of fracturing on each side of the fault. Generally the fractures are filled with epidote and other minerals.

## CHAPTER 2

### GENERAL GEOLOGY OF THE EDISON BLOCK

#### INTRODUCTION

The Edison block is a structural unit which is separated on the northwest and southeast from the adjacent structural blocks by two major faults which trend northeast (Figure 2). To the northeast the Edison block is covered unconformably by Paleozoic rocks. The southwest limit of this block has not been established. The block is known to have a minimum length of 14 miles and a width of up to 2.5 miles and is a long narrow horst of pre-Cambrian rocks.

#### LITHOLOGIC UNITS

##### General

Within all major structural blocks and in particular the Edison block distinct lithologic units are recognizable. The units possess a distinct form and physical continuity and hence are structural units.

Most of the lithologic units are composed of a mixture of older Grenville type material and younger introduced materials. Mixing of older and younger rock forming materials may have been a mechanical, e.g. (injection) or a chemical e.g. (metasomatic) process or a combination of both. The most important and difficult problems in the study of these rocks are to distinguish between older Grenville type material and younger introduced material and to decipher the nature of the physical and chemical processes which gave rise to the final rock product. Only by the

accumulation of detailed field, petrographic and chemical data can the problem be solved.

Within the Edison block there are several lithologic units composed mostly of Grenville type gneisses. The Edison type gneisses are the most important of this group and are separated into four distinct lithologic units which are discussed in more detail subsequently. The Edison type gneisses are largely of metasedimentary and metasomatic origin and include such rocks as magnetite-quartz-K-feldspar gneiss, magnetite ore, garnet-sillimanite-biotite-quartz gneiss, biotite-quartz-feldspar gneiss, quartz-K-feldspar gneiss, epidote-scapolite-quartz gneiss, and various hornblende and pyroxene gneisses.

The largest proportion of the Edison block is composed of rocks which because of their bulk composition and general uniformity are believed to be of ultimate igneous origin. The principal igneous rocks in the Edison block are hornblende-micropertite granite and alaskite, which are either mixed with Grenville type gneisses or occur as uniform structural units. Of particular interest is a pyroxene syenite gneiss which is composed of microcline and oligoclase with some micropertite and ferro-augite. Green pyroxene granite and alaskite are igneous rocks of major importance in other structural blocks but are of limited occurrence in the Edison block.

A quartz-oligoclase gneiss, which carries minor garnet, biotite, chlorite, microcline and ores, is a major lithologic unit in the Edison block. It is interlayered with much amphibolite and in places both quartz veins and metaquartzite layers are included. It is difficult to

ally this unit with either the older Grenville type gneisses or the younger introduced rocks.

Age relationships

Within the Edison structural block rocks of at least two distinct age categories are recognized. The older group of rocks includes the types which are similar to the Grenville series, such as the Franklin marble, paragneisses and complex gneisses of mixed origin. The bulk of the igneous rocks such as pyroxene and hornblende granites and alaskites are younger than the Grenville types. A difference in age is evident in two very positive ways, (1) the granites are always unmetamorphosed or distinctly less metamorphosed than the Grenville types, and (2) in many places there is positive evidence that the granites have intruded and cross-cut the Grenville rocks. On the other hand the pyroxene syenite gneiss, which is well metamorphosed, is an example of an igneous rock which is older than the younger granites.

The younger granites are generally emplaced conformable to the structures of the older Grenville rocks in such forms as sheets and phacoliths. However, in some places the younger granites cross-cut structures in the Grenville rocks. Thus, there is good evidence that the Grenville rocks had been deformed prior to the intrusion of the younger granites. However, inasmuch as the younger granites are themselves slightly deformed, it is probable that they were emplaced before the complete cessation of the tectonic forces responsible for the deformation of the older Grenville rocks. Therefore, it is postulated that the granites were emplaced during the waning stages of the regional metamorphism and are thus paratectonic or late paratectonic. This inter-

pretation is in agreement with Hots (1953) and Sims (1950, 1953).

#### STRUCTURE

The pre-Cambrian lithologic units within the Edison block define a single major anticline as the most important internal structure. The crest of the anticline (hereafter the Beaver Lake anticline) which is underlain by the quartz-oligoclase gneiss has been traced along the entire known length of the Edison block (14 miles). The crest of the fold lies about in the middle of the block, trends northeast and has not been cut by either border fault. Instead both the northwest and southeast limbs of the fold have been truncated at a very small angle by the border faults. In general the trend of the faults parallels the trend of the limbs of the fold; therefore, the latter may have controlled the development of the faults. The anticline is isoclinal and overturned slightly to the northwest. The regional dip of the limbs and axial plane of the fold averages between  $70^{\circ}$ - $80^{\circ}$  southeast and varies from  $60^{\circ}$  southeast to  $80^{\circ}$  northwest. Linear structures on the limbs of the fold and particularly along the crest of the fold indicate a plunge which varies from  $15^{\circ}$  to  $40^{\circ}$  and averages  $25^{\circ}$  northeast. No southeast plunging linear elements were found..

Foliation and lineation are the most important structures within each lithologic unit. Both axial plane cleavage and compositional layering are well developed. Such foliation is parallel to the strike of the lithologic units along the limbs of the fold; indeed, these rock units are simply large scale compositional layers. Most of the lithologic units are greatly thickened along the crest of the fold and in

some cases a unit is more than five times as thick at the crest as on the limbs. At the crest of the anticline the compositional layers remain parallel to the boundaries of the lithologic units, whereas cleavage often trends across the compositional layers, so that it remains parallel to the axial plane of the fold. Generally lineation is predominant along the crest of the fold and foliation dominates in the limbs. In some places lineation and foliation cannot be distinguished, because the linear elements tend to group in the plane of foliation. It appears that lineation grades into foliation and that along the crest of the fold they are genetically equivalent.

Throughout the Edison block and Franklin Furnace area a well developed set of cross joints which are subperpendicular to the lineation is present.

#### REGIONAL METAMORPHISM AND METASOMATISM

The Grenville type rocks of the New Jersey Highlands have been modified by both regional metamorphism and metasomatism. It is a difficult petrologic task to separate the effects of these two processes. In most cases metasomatism has been superimposed upon the effects of the regional metamorphism.

Potash metasomatism (granitization) has been the most prevalent kind of metasomatic action. This type is most likely related to the younger granites, although it is possible that the actual source of metasomatic fluids could be from other Grenville type rocks, i. e. differential fusion, etc. Iron metasomatism has also been important, and is responsible for the genesis of many of the magnetite deposits in the Highlands region (Sims, 1953).

Deformation has accompanied the regional metamorphism. This has produced the foliation, lineation and folds described previously.

The grade of regional metamorphism is best determined by a critical study of particular metamorphic rocks such as amphibolite and pyroxene syenite gneiss. The amphibolites carry no epidote and are thus certainly above the grade of the epidote-amphibolite facies. Only a few of the amphibolites carry pyroxene. This suggests that the presence of pyroxene in amphibolite is dependent upon the bulk composition of the rock and not upon the pressure and temperature of formation. Hence, the amphibolites do not belong to the granulite facies. The pyroxene syenite gneiss carries microcline and oligoclase as well as relic micropertite. The metamorphism has caused the primary micropertite to recrystallize into two distinct alkali feldspars, rather than a single solid solution alkali feldspar, which indicates that the recrystallization probably took place at a temperature less than 650°C (Bowen and Tuttle, 1950). In addition no mineral such as garnet which is characteristic of the granulite facies as for example in metamorphosed syenites of the Adirondacks (Euddington, 1952), has developed in this syenite gneiss. It is concluded that the regional metamorphism of the Edison block has been of the amphibolite grade.

#### MAGNETITE DEPOSITS

The magnetite deposits of the New Jersey Highlands are regarded by most geologists as metasomatic replacements of pre-existing rocks, (Hotz, 1953; Sims, 1950, 1953; Sims and Leonard, 1952). The ultimate origin of the iron is postulated to be from the extreme fractionation of granite or

alaskite magma. The nature of the metasomatic fluids is postulated as pneumatolitic or hydrothermal. It is postulated that position of ore bodies is controlled by the presence of favorable sites for replacements. Such sites may be related to mechanical effects, e.g. microbrecciation, (Sims, 1950, 1953), or chemical effects, e.g. replacement of marble, (Sims and Leonard, 1952). In either case it is generally proposed that the structure of the magnetite deposits is inherited from the replaced country rock.

The magnetite deposits are classified according to the nature of the rock in which they occur. In general the deposits in the New Jersey Highlands occur in the same kinds of rocks as the magnetite deposits in the Adirondacks. The most important of these are, (1) pyroxene and hornblende skarns (Sims and Leonard, 1952); (2) amphibolite (Hotz, 1953); (3) microcline granite gneiss (Leonard, 1951); (4) quartz-oligoclase gneiss or oligoclase granite (Sims, 1950, 1953), and (5) pegmatites.

Most of the magnetite deposits mentioned above are represented in the Franklin Furnace area. Much of this report is devoted to the study of the Edison magnetite deposits which are very similar to the deposits in the microcline granite gneiss at the Benson mines in the Adirondacks (Leonard, 1951).

PART II  
GEOLOGIC DESCRIPTION

## CHAPTER 3

### LITHOLOGIC UNITS OF THE EDISON TYPE

#### INTRODUCTION

The gneisses of the Edison type constitute a major lithologic unit which may be traced from the southeast limb of the Beaver Lake anticline around the anticlinal axis to the northwest limb of the fold (Figure 2). For purposes of concise discussion the Edison type gneisses are divided into four distinct lithologic units, (1) the Edison unit, which is located on the southeast flank of the anticline; (2) the Sand Hills unit, which is the thickened part of the Edison unit and is located at the nose of the anticline; (3) the McAfee unit, which is located on the northwest limb of the anticline, and (4) the Sherman unit which is located in the extreme southwest on the northwest flank of the fold. These four units are all a part of the same general lithologic unit, i. e., the Edison type gneisses, and all occupy the same stratigraphic position relative to other distinctive lithologic units.

#### EDISON UNIT

The Edison unit is a complex of gneisses of mixed origin. The unit has the form of a tabular sheet and occupies a structural position on the southeast limb of the Beaver Lake anticline. The outcrop length of the sheet parallel to the strike of the fold axis is over 6 miles. The average thickness of the sheet is about 0.4 miles. The sheet is terminated about 1 mile southwest of Mahola against the fault which separates the

Edison block from the Stockholm block. The sheet terminates in the north-east, at a point near Highway 23, along an oblique fault which has displaced the Edison unit as much as 1.5 miles to the northeast. The footwall to the Edison unit is a pyroxene syenite gneiss. The contact between the two is very abrupt. Frequently, amphibolite is located in this contact zone but the exact relationships within the zone are difficult to interpret. The hanging wall rocks on the southeast of the Edison unit are largely of igneous affinities. These include hornblende granite and alaskite, pyroxene granite and alaskite and some hypersthene granites as well as much pegmatite interlayered with the granites.

Four main lithologic subunits are present within the Edison unit. The mixed gneiss subunit is a complex group of gneisses and magnetite concentrations and is the most prevalent and economically the only important rock type within the Edison unit. It consists of magnetite-quartz-K-feldspar gneiss which is characterized by the virtual absence of plagioclase. In addition there are numerous gneisses of distinct metasedimentary affinities within the complex such as biotite, garnet and sillimanite rich quartz gneisses. The entire mixed gneiss subunit is full of seams, lenses and pods of pegmatite. A second important lithologic subunit within the Edison unit is a garnet or (garnetiferous)-biotite-quartz-feldspar gneiss. In it the feldspars are oligoclase and microcline or slightly perthitic microcline. In places the biotite gneiss subunit is intimately interlayered with a third subunit which is a quartz-K-feldspar gneiss. It is a uniform, fine grained rock, which always carries accessory garnet and magnetite. The fourth distinct lithologic subunit within the Edison unit is composed of a group of gneisses

which differ from the other rocks in their high content of lime and silica. These gneisses, which are called the lime rich subunit, consist of epidote-scapolite-quartz gneiss and related hornblende and pyroxene-quartz-feldspar gneiss, biotite-hornblende-quartz-feldspar gneisses, epidote quartzites and other types consisting of the same minerals but in different proportions. The gneisses of the lime rich subunit have a much higher plagioclase content than do any of the other gneisses of the Edison unit. These four lithologic subunits of the Edison unit are the subject of more detailed study in subsequent sections.

#### SAND HILLS UNIT

The Sand Hills unit of the Edison type gneisses is located on the nose of the Beaver Lake anticline. It forms a relatively small unit of about one square mile in area and represents the thickened axial portion of the Edison unit. On the south, southeast, and east, the Sand Hills unit is in contact with hornblende granite and alaskite and to the west is in contact with the McAfes unit.

In general the Sand Hills unit has a well developed foliation which follows the regional pattern (northeast strike and steep southeast dips). However, near the axis of the major anticline the foliation disappears in favor of lineation which plunges to the northeast at an average angle of 20 to 30 degrees.

The predominant rock type in the Sand Hills unit is a pink, fine-medium grained, fairly even grained and xenoblastic quartz-microcline gneiss which is frequently rich in sillimanite and garnet. The rock

does not possess a strong gneissic structure but instead is moderately gneissic and has some compositional layering. Accessory minerals include magnetite, hematite, biotite, plagioclase, sericite, muscovite and apatite. The microcline is slightly perthitic. In terms of texture, structure and mineral composition this gneiss is very similar to the quartz-K-feldspar gneiss of the Edison unit.

Biotite-quartz-feldspar gneiss is frequently interlayered with the quartz-microcline gneiss of the Sand Hills unit. The former gneiss is generally medium grained and xenoblastic. Its structure varies from schistose to gneissic depending upon the percentage of biotite in the rock. Varietal minerals in this gneiss include sillimanite and garnet. Hornblende, sericite, sphene, zircon, apatite, magnetite and ilmenite are accessory minerals. The biotite-quartz-feldspar gneiss is definitely more heterogeneous than the associated quartz-microcline gneiss. This is due to alternate layers of biotite-rich and biotite-poor gneiss. As in the quartz-microcline gneiss the K-feldspar is a slightly perthitic microcline.

It is not uncommon to find layers and sheets of hornblende granite and alaskite interlayered with the gneisses of the Sand Hills unit. This is not surprising in view of the fact that the unit is more or less surrounded by such igneous granites. Pegmatite layers and veins, amphibolite, and migmatitic amphibolite are a common rock type interlayered with the other gneisses of the Sand Hills unit. Amphibolite is particularly abundant near the footwall contact of the unit.

The K-feldspar of the granites and alaskites adjacent to the Sand Hills unit is microperthite. The fact that the K-feldspar of the gneisses

in the unit are only slightly perthitic indicates that the granites and alaskites crystallized at a somewhat higher temperature than the gneisses (Bowen and Tuttle, 1950). If the granites are of the same age or younger than the gneisses, then it appears evident that a rather abrupt thermal gradient existed between these two rock types at the time the igneous rocks were emplaced.

#### McAfee Unit

The McAfee unit is the rock mass of tabular shape which is the stratigraphic equivalent to the Edison and Sand Hills units on the north-west limb of the Beaver Lake anticline. This tabular body extends from the village of McAfee on the northeast to a point just north of Ogdensburg (six miles to the southwest) where it is faulted against lower Paleozoic sedimentary rocks. The width of the unit varies from 500 to 1000 feet. The footwall zone of the McAfee unit to the northwest is a sheet of hornblende granite which extends parallel to the McAfee unit for most of its length. The hanging wall to the McAfee unit is largely hornblende syenite gneiss; however, to the northeast the unit makes contact along its hanging wall with hornblende granite and the Sand Hills unit. The McAfee unit is structurally the extension of the Sand Hills unit along the north-west flank of the Beaver Lake fold and is therefore stratigraphically identical to the Sand Hills unit; however, there are marked differences in lithology between the two units.

The predominant rocks of the McAfee unit are an interlayered complex of metaquartzites and quartz-feldspar gneisses. The interlayering of these two types is locally on a scale of inches. The quartzite layers

which weather out in high relief impart a "ribbed" structure to the weathered outcrop. The same minerals are common to both kinds of layers; however, the proportions of these minerals in the rock types differ markedly. Epidote, plagioclase and microcline are generally present in every rock sample. Varistal and accessory minerals include hornblende, pyroxene, sphene, allanite, calcite, scapolite, garnet and ores. Thus, typical lithologic types include, (1) epidote metaquartzite, (2) epidote-plagioclase-microcline metaquartzite, (3) epidote-plagioclase-microcline-quartz gneiss, (4) epidote-pyroxene-quartz-feldspar gneiss, etc. The interlayering of these various rock types yields a rock of banded character. The metaquartzites have a distinct gneissic structure which is caused by the quartz which is deformed and sheared out into lenses and lenticles which parallel the foliation. On the other hand gneisses with a large proportion of feldspar are less gneissic and much less deformed than the metaquartzite. Most of the gneisses are medium grained, fairly even grained and xenoblastic. It is apparent from the discussion above that the gneisses of the McAfee unit show strong calcareous and arenaceous affinities. Beside the group of gneisses discussed above there are frequent layers and sheets of biotite-quartz-feldspar gneiss, granite and many layers, bands and nests of pegmatite, included in the McAfee unit.

#### SHERMAN UNIT

The Sherman unit is located on the northwest limb of the Beaver Lake anticline at the extreme southwest end of the Franklin Furnace quadrangle. The unit appears to be a tabular shaped mass which extends parallel to the

regional foliation for a distance of at least 2 miles. The average thickness of the unit is 1000-1500 feet. Stratigraphically the Sherman unit appears to occupy a structural position similar to the Edison unit; however, its relationship to the surrounding rocks is somewhat obscured by faulting. Detailed studies of the Sherman unit have been confined to the general area of the Sherman magnetite mines which are located 1.5 miles southwest of Nahola.

The principal gneiss of the Sherman unit is magnetite-quartz-K-feldspar gneiss which is almost identical to the principal variety in the mixed gneiss subunit of the Edison unit. By increase in the proportion of magnetite the gneiss of the Sherman unit passes into magnetite ore. Variental minerals in the gneiss include sillimanite, chlorite, biotite, rutile and hematite. Accessory minerals may include plagioclase, sericite, epidote, apatite, zircon, garnet and ilmenite. The gneiss is usually medium grained, but fine and coarse grain facies are abundant. In addition it is fairly even grained and xenoblastic. The gneiss may be banded due to the alternation of layers of slightly different composition or texture. Some samples are strongly gneissic due to the preferred orientation of lenticular shaped grains or aggregates of quartz and magnetite. The preferred orientation of sillimanite-needles also contributes to the gneissic structure. The magnetite-quartz-K-feldspar gneiss is mixed with layers, seams, and nests of pegmatite but is otherwise fairly uniform.

Rocks interlayered with the magnetite-quartz-K-feldspar gneiss include chlorite-quartz-feldspar gneiss (Table 15), fluorite slaskite and hornblende granite. The former is fine grained, even grained,

xenoblastic and interlayered with much granite and pegmatite.

The Sherman magnetite area appears to be complexly folded into a group of minor folds. In addition there are frequent crushed and brecciated zones which are mineralized with epidote and are probably related to the period of major faulting.

#### COMPARISON

The regional mapping indicates that the four units of Edison type gneisses all represent the same stratigraphic zone. Structurally the Edison unit, McAfee unit, and Sherman unit are all similar in that they form a part of the limbs of the major anticline. The Sand Hills unit is distinct in occupying the axial position on the anticline and consequently is greatly thickened. The units all show distinct similarities in lithology. Perhaps most significant is the similar calcareous and arenaceous character of the metaquartzites and feldspathic metaquartzites of the McAfee and Edison units. Also, the magnetite-quartz-K-feldspar gneiss and magnetite ore of the Sherman unit are very similar to gneisses and ores of the Edison unit. In addition the quartz-K-feldspar gneiss of the Edison unit is nearly identical to the principal gneiss of the Sand Hills unit. Biotite-quartz-feldspar gneiss, sheets and interlayered seams and nests of pegmatite are common to the four units.

CHAPTER 4  
PETROLOGY OF THE EDISON AREA

INTRODUCTION

The Edison area is a 1.6 mile region centered about the magnetite ore deposits at Edison, New Jersey. Plate 1 is a geologic map of this area to the scale of 1/3600, (1 inch equals 300 feet).

The Edison unit which is traceable through the Edison area has been divided into 4 subunits. Economically the only important subunit is the mixed gneiss which includes magnetite concentrations. In addition (garnetiferous)-biotite-quartz-feldspar gneiss, quartz-K-feldspar gneiss, and the lime rich gneisses are important subunits closely associated with and related to the mixed gneiss subunit and magnetite deposits. Associated with the Edison unit in this area are a variety of rock types which are lithologically and structurally distinct from the Edison unit and form the wall rocks to the unit. These include such rocks as quartz-oligoclase gneiss, pyroxene syenite gneiss, biotite alaskite, hornblende granite, hypersthene granite, and pyroxene granite.

WALL ROCK UNITS

Quartz-oligoclase gneiss

The quartz-oligoclase gneiss is exposed in the northwest part of the area and is but a small portion of the much larger lithologic unit which forms the exposed core of the Beaver Lake anticline. The gneiss is generally leucocratic and very white but frequently is spotted with pale

green blotches of chlorite. The bulk composition of this rock corresponds to an oligoclase alaskite. Oligoclase and quartz are the two important minerals and biotite and chlorite are the only important varietal minerals. The chlorite may be secondary after hornblende. Accessory minerals include epidote, (in part secondary), microcline, garnet (locally), and opaque oxides. The rock is striking for its distinct paucity of K-feldspar.

The gneiss is generally medium and even grained, but fine and coarse grained types are abundant. It has distinct foliation manifested by interlayers of variable composition and texture and by a strong gneissic structure. The latter is caused by the preferred orientation of lenticular shaped grains and aggregates of quartz.

Biotite- and chlorite-rich facies of the quartz-oligoclase gneiss are locally interlayered with the normal leucocratic type. In addition amphibolite and quartz-oligoclase gneiss may be interlayered on a scale of feet to fractions of an inch. In places it appears as if the amphibolite has been injected and impregnated by the quartz-oligoclase gneiss.

Two varieties of pegmatite have been observed in the quartz-oligoclase gneiss. The most abundant is a white, strongly gneissic pegmatite which is conformably interlayered with the gneiss. Mineralogically these white pegmatites appear very similar to the leucocratic facies of the quartz-oligoclase gneiss. It is proposed that these pegmatites are simply very coarse grained variants of the normal white gneiss. The less abundant type is a pink, massive, magnetite-hornblende pegmatite which cross cuts the foliation of the quartz-oligoclase gneiss and interlayered amphibolite. The evidence suggests that this variety of pegmatite was emplaced after the crystallization and deformation of the

quartz-oligoclase gneiss.

Thin layers or veins, pods and lenses of white, massive, milky quartz are often conformably interlayered with the quartz-oligoclase gneiss. Quite distinct from this vein quartz are rare interlayers of metaquartzite. These are texturally and structurally distinct from the massive vein quartz. The metaquartzite layers are less than a foot thick and are strongly deformed into tight minor folds and crenulations. The limbs of these minor folds are often broken up and pulled apart and surrounded by quartz-oligoclase gneiss in a boudinage fashion.

The origin of the quartz-oligoclase gneiss is problematical. Dic-tite-rich facies, amphibolites and metaquartzites all indicate meta-sedimentary affinities. However, the bulk composition of the gneiss (oligoclase alkali-feldspar) does not correspond with the composition of any common sedimentary rock. If the gneiss is of ultimate magmatic origin the problem of generating such a soda-rich magma is difficult to solve, (Buddington, p. 32-40, 1948; Sims, p. 261, 1953). Of course it is possible that the gneiss is of metasonatic origin. Further detailed studies are necessary before a definite conclusion can be proposed.

Pyroxene syenite gneiss

The pyroxene syenite gneiss is a sheet-shaped body which averages about 700-800 feet thick in the Edison area. It is one of the most distinctive regional lithologic units and may be traced from the south-east limb of the Beaver Lake anticline around the nose of the fold to the northeast and for a considerable distance on the northwest limb of the fold. On the nose of the anticline the gneiss is nearly 10 times its normal thickness. The pyroxene syenite gneiss forms the immediate

footwall to the Edison unit. The gneiss is interpreted as a meta-morphosed igneous pyroxene syenite.

The pyroxene syenite gneiss is an extremely uniform rock. The gneissic structure is due to the lenticular form of mineral grains and aggregates. There is little compositional layering, and except for rare amphibolite inclusions the gneiss is extremely homogeneous. Generally, the gneiss is medium grained and even grained; however, finer grained facies and pegmatitic seams are present.

Oligoclase and microcline are the two most important minerals in the pyroxene syenite gneiss. The oligoclase is generally twinned and occasionally the twin lawes are bent which indicates some post crystallization deformation. However, no cataclastic textures or structures have been observed within the sheet. The K-feldspar varies from a slightly perthitic microcline (about 10% intergrown Na-feldspar) to microperthite (up to 40% intergrown Na-feldspar). Even in a single thin section both extremes may be present, but in other samples only oligoclase and slightly perthitic microcline are present. Occasionally a sample which has only microperthite with a rare grain of oligoclase and slightly perthitic microcline has been observed. These petrographic observations indicate that the primary feldspar was a solid solution of Na and K-feldspar. Subsequent slow cooling of this solid solution caused exsolution with the development of the microperthite. Metamorphism of the original pyroxene syenite caused the recrystallization of much of the microperthite into discrete grains of oligoclase and slightly perthitic microcline. The frequent relics of microperthite and of perthitic microcline testify that the recrystallization process was

not complete. The feldspar assemblage indicates that the probable temperature of recrystallization was below 660°C (Bowen and Tuttle, 1950).

Ferroaugite is the most important ferromagnesium mineral in the pyroxene syenite gneiss. It is free of any exsolved minerals. Frequently, it is partially altered to hornblende, reddish brown biotite or chlorite. Green hornblende in discrete grains is a minor accessory mineral in the pyroxene syenite gneiss of the Edison area, but to the northeast, hornblende becomes increasingly abundant until near the axial portion of the gneiss, pyroxene is absent and hornblende is the only important ferromagnesian mineral. Whether the hornblende is regarded as being of igneous or metamorphic origin, it is postulated that it occurs in place of ferroaugite in zones which were relatively enriched in H<sub>2</sub>O, such as the axial zones of the pyroxene syenite gneiss may have been.

Accessory minerals in the pyroxene syenite gneiss include ilmenomagnosite, ilmenite, sphene, quartz, euhedral zircon and apatite. Ilmenite occurs as euhedral grains along the boundaries of magnetite. It seems likely that this "border phase" represents ilmenite which was completely exsolved from an original titaniferous magnetite during the cooling process and particularly during the metamorphic recrystallization of the pyroxene syenite. Rarely a veinlet or spike of hematite (martite) replaces magnetite. Sphene, which generally occurs as a corona around the iron and titanium oxides, probably developed in this titanium rich milieu during the metamorphic recrystallization. Quartz is always present in the gneiss and occasionally may form as much as 10 to 15 per cent of the rock.

The metaigneous pyroxene syenite gneiss affords an opportunity to compare the regional metamorphism of the Edison area to the regional metamorphism in the northwest Adirondacks. Buddington (1952) has pointed out that in metaigneous pyroxene syenite and quartz syenites of the Adirondacks, garnet (pyrope-almandite) may develop as a product of regional metamorphism providing the grade of metamorphism is high enough. On the basis of metamorphic garnet developed in gabbros, syenites and quartz syenites, etc., Buddington (1952, p. 79-80) has recognized three zones of different metamorphic grade. Garnet has developed in the pyroxene syenites and quartz syenites only in the zone of most intense metamorphism which is designated as the granulite facies. In the zone of intermediate metamorphic grade regional metamorphic garnet has developed only in gabbroic rocks. In the third metamorphic zone, which is designated as the amphibolite facies, regional metamorphic garnets are not developed in any of these igneous rock types. No garnet was found in the pyroxene syenite gneiss of the Edison area. Therefore, it seems clear that the gneisses of this area do not belong to the granulite facies as described by Buddington in the Adirondacks but instead belong to a lower metamorphic facies. Buddington (1953) has pointed out that the  $TiO_2$  content of ilmenomagnetite from Adirondack igneous and metamorphic rocks varies as a function of temperature of crystallization. His data indicated that the  $TiO_2$  content of ilmenomagnetites from gneisses reconstituted in the granulite and upper temperature range of the amphibolite facies is 3.1 to 4.1 per cent; however, the  $TiO_2$  content is only 1 to 2 per cent for the ilmenomagnetite from gneisses formed in the "lower" temperature range of the amphibolite facies. In Table 2

below a partial analysis of the ilmenomagnetite from the pyroxene syenite gneiss of the Edison area is presented. The  $TiO_2$  content is less than 1 per cent, which is very low and corresponds with the "lower" temperature range of the amphibolite facies in the Adirondacks. If the pyroxene syenite gneiss of the Edison area was reconstituted in the "lower" amphibolite facies, the presence of unaltered ferrcaugite can best be explained by assuming that the gneiss was extremely dry so that sufficient  $P_2O_5$  was not present to enable hornblende to form during the recrystallization. On the basis of the above discussion it is postulated that the pyroxene syenite gneiss of the Edison area was regionally metamorphosed in the amphibolite facies or more precisely the "lower" amphibolite facies of the Adirondacks.

Table 2. Partial Chemical Analysis and Mineral Recalculation  
of Ilmenomagnetite from the Pyroxene Syenite Gneiss

Partial Chemical Analysis Mineral Recalculation to 100 Weight Per Cent

	<u>Weight Per Cent</u>		<u>Weight Per Cent</u>
$Fe_2O_3$	63.03	Magnetite	97.09
FeO	30.18	Hematite	none
$TiO_2$	0.92	Ilmenite	1.86
Total	<u>94.13</u>	Excess FeO	<u>1.05</u>
		Total	100.00

Analyist: J. Fahey, 1953

#### Pyroxene granite

Pyroxene granite is in the hanging-wall zone of the Edison unit. The portion exposed in the Edison area is only a small part of a much larger

mass of similar granite which outcrops to the southeast. It is postulated that the pyroxene granite is of igneous origin.

On fresh surface the pyroxene granite is a definite green to whitish-green color. This is due to the pale greenish color of the feldspar. The pyroxene granites and associated alkali-silicates are generally medium and even grained, but pegmatite seams and veins are present. The rock is always hypidiomorphic and gneissoid to almost massive. Lenticular shaped quartz grains contribute most to the gneissoid structure. Generally the gneissoid structure is very obvious, but in occasional outcrops the rock is so slightly deformed that it appears almost massive. In the Wilson area the pyroxene granite is uniform except for occasional layers of biotite gneiss and amphibolite.

Quartz, microantiperthite and microperthite are the most abundant minerals in the pyroxene granites and alkali-silicates. Generally these perthites have a typical exsolution morphology with oriented films, lenses, rods, etc., of guest feldspar enclosed in the host. However, in some of the granites the perthitic intergrowths are of patch or checkerboard types and are very irregular. This suggests that some recrystallization of an original uniform perthite has taken place. Contrary to the pyroxene-syenite gneiss discrete grains of plagioclase and microcline are rare; generally the two are intergrown in perthitic fashion in the pyroxene granites. Visual estimates of the bulk composition of the microperthites and microantiperthite indicate that the host feldspar usually comprises as much as 60 per cent of the intergrowth.

The single pyroxene in these granites is quite free of any exsolved material, is generally medium to dark green and occasionally is altered slightly to hornblende and chlorite (?). A single chemical analysis of

the pyroxene (Table 3) proves it to be a ferrohedenbergite (Poldervaart and Hess, 1951).

Ilmenomagnetite is the most important accessory mineral. Locally it may form as much as 5 per cent of the rock. The  $TiO_2$  content of one ilmenomagnetite sample from the pyroxene granite is 7.97 weight per cent. This is considerably more than in the hornblende microperthite granites of the Adirondacks which carry 5 to 6.7 per cent  $TiO_2$  (Fuddington et al., 1953). The high  $TiO_2$  content of the pyroxene granites indicates a higher temperature of crystallization than that of the hornblende microperthite granites. Other accessory minerals include sphene, zircon, apatite and rare hornblende and biotite.

The homogeneity and bulk compositions of the pyroxene granite, the very high  $TiO_2$  content of its ilmenomagnetite, and the nature of its alkali feldspar (perthite) are features which indicate that the pyroxene granite crystallized at high temperatures and is of magmatic origin. The paragenesis of microantiperthite and microperthite, which are frequently present together in a single thin section, suggests that equilibrium was established between the two alkali feldspar solid solutions at some temperature just below the crest of the alkali feldspar solvus curve. If the pyroxene granite is magmatic, this paragenesis indicates that the liquidus field was depressed so as to intersect the alkali feldspar solvus curve near its crest. According to the experimental data of Bowen and Tuttle (1950) this would be near the temperature of  $660^{\circ}C$  for a pure alkali feldspar system. This is postulated as the minimum temperature of crystallization of the pyroxene granite and associated alaskite.

Table 3. Chemical analysis and recalculation<sup>a</sup> of ferrohedenbergite from pyroxene granite (Specimen No. Ed-1924).

Atomic Ratios				Na	Al	Ti	2Al	Al	Al	Z	W	Y	Cations to Six O
													Fe <sup>3+</sup>
				Na	Al	Ti	2Al	Al	Al	Z	W	Y	Fe <sup>3+</sup>
SiO <sub>2</sub>	43.18	Si	802										
Al <sub>2</sub> O <sub>3</sub>	1.76												
Fe <sub>2</sub> O <sub>3</sub>	4.07	Al	35	--	--	--	--	--	--	--	--	--	
FOO	23.71												
MgO	1.93	Fe <sup>3+</sup>	51	23									
CaO	16.59	Fe	330										
MnO	0.61	Mn	13.5										
K <sub>2</sub> O	0.17	Mg	47										
H <sub>2</sub> O <sup>+</sup>	0.90	Ca	296										
H <sub>2</sub> O <sup>-</sup>	0.35	Na	19.5	19.5									
TiO <sub>2</sub>	0.23	K	3.5	3.5									
MnO	0.97	Ti	3.5										
		O	2433.0										
	93.39												

Analyst: John Maxwell, 1954

Ca<sub>33.8</sub>Al<sub>6.2</sub>Fe<sub>55.0</sub>

<sup>a</sup>See Hess, R. H., Chemical composition and optical properties of common clinopyroxenes, Part I, Amer. Min. 34, 621-66, 1949, for method of recalculation.

<sup>b</sup>Deviation from the perfect pyroxene cation to anion ratio is probably due to minor alteration of the sample to hornblende.

### Hypersthene granite

The hypersthene granite outcrops as a thin sheet about 300 feet thick and forms the footwall rock to the pyroxene granite in the Edison area. The sheet is well exposed for about one-half mile along its strike. The hypersthene granite belongs to the charnockite suite of rocks. It is tentatively assumed to be of igneous origin and specifically a modified facies of the closely associated pyroxene granite.

On a fresh surface the hypersthene granite is a greenish buff color but is either drab or a rusty buff on the weathered outcrop. The granite is medium or slightly finer grained and is usually even grained. However, fine grained to pegmatitic zones are abundant. The hypersthene granite is not a layered rock but various features impart a distinct foliation to it. These features include, (1) a somewhat irregular distribution of accessory biotite into particular zones, the preferred orientation of the biotite flakes and the rusty weathering of biotitic zones indicate this feature; (2) slight textural variations such as the alteration of fine and medium grained zones across the foliation plane; (3) the tendency for quartz grains to have a lenticular shape and to occur as thin lenticular bands parallel to foliation. The hypersthene granite is not as uniform as the closely associated pyroxene granite. Besides the irregular distribution of biotite, there are included layers of biotite-quartz-feldspar gneiss, quartz-K-feldspar gneiss and sheets of hornblende granite within the hypersthene granite.

As in the pyroxene granite the most abundant minerals in the hypersthene granite are quartz, microantiperthite and microperthite. Some samples carry plagioclase and perthitic microcline. The feldspar

assemblage is so similar to that of the pyroxene granite that a genetic relationship between the two is assumed. Hypersthene and biotite are the important varietal minerals. The hypersthene is pleochroic in pale greens (Z=pale green, X and Y=flesh pink) and is partially altered to mica. Biotite is reddish brown or green (X=pale yellow to yellowish brown, Y=dark reddish brown, Z=very dark brown or reddish brown, sometimes opaque) and is present in nearly all samples of the hypersthene granite. Opaque oxides, zircon (anhedral), apatite, sphene and hornblende are accessory minerals.

It has frequently been pointed out that the charnockites occur in zones of plutonic metamorphism and are usually associated with rocks of the granulite facies (Barth, 1952; Turner and Verhoogen, 1951; Tyrrell, 1948). One contention is that the charnockitic granites originate from the metamorphism of normal granites under conditions allied to the granulite facies. To the contrary, Huntington (1939, 1943, 1952) has established the igneous origin of the charnockitic syenites and quartz syenites of the Adirondacks. The hypersthene granite and the pyroxene granite of the Edison area have no features which suggest that they have been metamorphosed. Their structure, texture and mineralogic character indicate that they have been but slightly deformed and recrystallized. Therefore, it is postulated that the hypersthene granite is a hybrid igneous rock and represents a border facies of the pyroxene granite which has been contaminated by the incorporation of older metasedimentary gneisses.

#### Hornblende granite

The hornblende granite in the Edison area is a sheet shaped mass

in its southwest portion but passes into a phacolithic body to the north-east in the zone near the Edison Pond syncline (Plate 1). The hornblende granite is in the immediate footwall zone of the hypersthene granite. The contact between these two granites is parallel to the foliation.

The hornblende granite is a pink to pinkish buff color. It is medium or coarsely medium grained and fairly even grained. It is distinctly coarser grained than the hypersthene or pyroxene granites. The hornblende granite is gneissoid, and foliation is quite distinct due to slight textural variations across the foliation plane and due to frequent interlayers of amphibolite and pegmatite. The latter is much more abundant in the hornblende granite than in the hypersthene and pyroxene granites.

Quartz, and microperthite are the essential minerals of the hornblende granite. In some samples perthitic microcline and oligoclase form the bulk of the feldspar which suggests that locally the mineral assemblage came to equilibrium at a lower temperature than did the bulk of the hornblende granite. This could be related to local recrystallization of the original microperthite. Green hornblende is the principal accessory mineral, but in addition biotite, magnetite, zircon and apatite are present.

It is postulated that the hornblende granite is of igneous origin.

#### Biotite alaskite

Biotite alaskite in the Edison area forms a small lenticular sheet which is only 3500 feet long and about 150 feet thick. The mass forms the immediate footwall to the hornblende granite and is probably related to it.

The alaskite is pink, coarse grained and massive. Frequently, it is so coarse grained as to be classed as pegmatite. The alaskite is free of amphibolite layers except in the contact zone with the hornblende granite where a continuous 10 to 15 foot layer of amphibolite is present. In its footwall zone the alaskite is interlayered with biotite-quartz-feldspar gneiss and quartz-K-feldspar gneiss of the Edison unit (Plates 10 and 11).

Quartz, oligoclase and perthitic microcline are the essential minerals of the biotite alaskite. In contrast to the associated hornblende granite no microperthite is present, indicating that the alaskite came to equilibrium at a lower temperature than the granite. Biotite and hornblende are the most important accessory minerals, but magnetite, zircon and apatite are also present.

It is postulated that the biotite alaskite is of igneous origin and is related to the hornblende granite. The variations in the nature of the K-feldspar from microperthite in the hornblende granite to perthitic microcline in the biotite alaskite definitely indicates a higher temperature of crystallization for the former. It is possible that the hornblende granite and biotite alaskite are related to the large mass of pyroxene granite to the southeast.

#### Contaminated hornblende granite

The contaminated hornblende granite is located in the east-northeast corner of the Edison area and probably is the northeast continuation of the hornblende granite sheet. Its contacts are conformable with the surrounding gneisses and granites.

The contaminated hornblende granite is medium grained, even grained

xenoblastic and gneissoid. It is extremely heterogeneous due to numerous interlayers of gneiss which show definite metasedimentary affinities such as, (1) pyroxene skarn, (2) biotite, hypersthene and pyroxene amphibolites, (3) hornblende-pyroxene-plagioclase gneiss, (4) pyroxene-hornblende-feldspar gneiss, (5) sphene-pyroxene-feldspar gneiss, (6) quartz-pyroxene-plagioclase gneiss, etc. In addition there are sheets and layers of alkali feldspar and pegmatite within the granite.

The essential minerals in the contaminated granite are quartz and microperthite. Many samples show evidence of a lower temperature of equilibrium in that they carry plagioclase and perthitic microcline rather than microperthite. Accessory minerals in the contaminated hornblende granite include hornblende, magnetite, apatite and sphene.

It is postulated that the contaminated hornblende granite is a facies of the hornblende granite which has been modified by the incorporation of older metasedimentary gneisses.

#### Garnet-biotite-quartz-feldspar gneiss and related facies

The garnet-biotite-quartz-feldspar gneiss is located in the east-northeast corner of the Edison area (Plate 1) between the phacolithic mass of hornblende granite and the contaminated hornblende granite. Its contacts are conformable to the surrounding rocks.

The gneiss is medium and even grained, although some coarse grained facies are present. The rock is xenoblastic with a marked gneissic structure.

The predominant rock type is composed of quartz, oligoclase and perthitic microcline. Varistal minerals include garnet and biotite;

whereas hornblende, ores and occasionally hypersthene are accessory minerals. The rock is quite heterogeneous due to many interlayers of such rocks as biotite amphibolite, biotite-hypersthene amphibolite or biotitic rich facies of the normal gneiss. In addition hornblende granite, alkali-feldspar and pegmatite are interlayered.

To the northeast the gneiss lenses out in favor of the contaminated hornblende granite (Plate 1).

It is postulated that the garnet-biotite-quartz-feldspar gneiss and related facies were originally Grenville type metasediments which have been intruded and modified by younger granitic rocks.

#### EDISON UNIT

##### Mixed gneiss subunit

Introduction. The mixed gneiss subunit with the associated magnetite concentrations is the most important subunit in the Edison area. It is a sheet shaped body about 700 feet thick in the southwest part of the area. To the northeast it is split into two thinner sheet shaped masses. The epidote-scapolite-quartz gneiss and related facies (lime-rich subunit) separate these two portions of the mixed gneiss northeast of the Victor Mine. The pyroxene syncline gneiss forms the footwall and the biotite-quartz-feldspar gneiss and quartz-K-feldspar gneiss form the hanging wall to the mixed gneiss subunit. The contacts with the wall rocks appear to be conformable.

The mixed gneiss subunit is a heterogeneous complex of interlayered rock types. The predominant variety of rock is a magnetite-quartz-K-

feldspar gneiss. This type is generally the immediate wall rock to magnetite rich layers and by an increase in per cent of magnetite this type appears to pass gradually into heavy ore. Subordinate types consist of variations of the magnetite-quartz-K-feldspar gneiss and of inter-layers which show metasedimentary affinities in that they carry large quantities of garnet, biotite, sillimanite and quartz. In brief, the mixed gneiss subunit is characterized by very abrupt and radical chemical (compositional) discontinuities from layer to layer across the foliation plane. This feature is certainly the most significant descriptive fact and recognition of it is the first prerequisite to a reasonable petrologic interpretation of the mixed gneiss subunit.

Mineralogy. In general the various rock types which are interlayered to make up the mixed gneiss subunit may be considered as related rocks which have crystallized under more or less the same physical conditions (pressure and temperature); so that the same mineral phases were stable throughout. However, because of large differences in chemical composition from layer to layer the proportions of the different mineral phases varies widely from rock to rock within the mixed gneiss subunit.

Quartz, K-feldspar (microcline and monoclinic E-feldspar) and magnetite are essential minerals in nearly all the rock types found within the mixed gneiss subunit. Plagioclase is virtually absent from the subunit except in rare layers. Important varietal minerals include biotite, sillimanite, garnet and ilmenohematite. Accessory minerals include apatite, monazite, zircon, spinel, corundum, epidote, fluorite, hematite-ilmenite, ilmenite, rutile, pyrite, molybdenite, bornite, and chalcopyrite. Secondary minerals are chlorite, sericite, epidote and hematite(martite).

In a subsequent chapter the mineralogy of the mixed gneiss subunit is treated in detail.

Magnetite-quartz-K-feldspar gneiss. The principal type of rock interlayer in the mixed gneiss subunit is composed of variable proportions of quartz, K-feldspar, and magnetite with only minor amounts of the other minerals as accessory constituents. At one extreme of composition this principal type is a magnetite-quartz gneiss (metaquartzite?); at another extreme it is a K-feldspar-quartz-magnetite gneiss, i. e., magnetite ore. However, field and laboratory observations indicate that the most abundant variety is composed of subequal proportions of quartz and K-feldspar with subordinate magnetite and is a medium grained magnetite-quartz-K-feldspar gneiss.

Modal analyses of 8 specimens (5 from the Edison area and 3 from the Sherman unit) of magnetite-quartz-K-feldspar gneiss are presented in Table 4B. These specimens were collected from uniform layers less than 1 foot thick. Three thin sections per specimen, two of which were stained to enable the easy and accurate determination of K-feldspar (for staining methods see Keith, 1939 and Chayes, 1952), were analyzed on an integrating stage. The variation obtained between reanalyses of the same thin sections was considerably less than the variation from section to section for the same specimen. Thus the largest source of uncertainty lies in the inhomogeneity of the narrow rock layer itself. This uncertainty can only be alleviated by an increase in the number of thin sections per specimen. In addition the modal analysis of a single thin section from each of 36 randomly chosen samples (from the Edison area and Sherman unit) of magnetite-quartz-K-feldspar gneiss are presented in Table 5.

-15-

**Table 4. A. Partial chemical analyses of magnetic and non-magnetic fractions of iron and titanium oxides from eight samples of magnetite-quartz-K-feldspar gneiss from the Edison Area and Sherman unit.**

	146	145	149	143	144	154	153	151
<b>Magnetic fraction</b>								
Fe <sub>2</sub> O <sub>3</sub>	64.93	70.23	63.49	70.37	68.17	63.94	66.77	65.82
FeO	26.02	21.77	25.27	22.15	25.62	26.45	24.52	27.66
TiO <sub>2</sub>	0.14	1.01	0.33	1.11	0.54	1.39	1.10	0.54
Total	91.09	93.01	94.64	93.63	94.33	91.78	92.39	91.02
<b>Non-magnetic fraction</b>								
Fe <sub>2</sub> O <sub>3</sub>	74.36	56.61	46.59	n. d.	21.69	29.10	59.18	39.79
FeO	2.29	2.33	16.32	n. d.	16.06	12.79	9.82	13.62
TiO <sub>2</sub>	10.45	16.16	22.67	n. d.	40.03	20.63	16.55	24.43
Total	87.10	75.60	36.58		77.78	72.52	65.55	31.84
Wt. per cent Fe and Ti oxides in rock								
Mt.	3.31	3.05	12.6	18.87	39.01	11.2	13.7	24.00
Hem.	1.71	1.29	4.3	6.46	6.07	1.03	2.93	1.55
Ilm.	0.10	0.11	1.8	0.58	0.69	0.36	0.37	0.33
Rut.	0.15	0.05	0.4	tr.	0.15	0.06	0.16	0.02
Composition magnetic fraction to 100 mole per cent								
Mt.	83.3	65.2	77.7	65.0	30.8	34.1	75.8	90.3
Hem.	11.3	32.1	20.0	32.0	17.3	11.8	21.0	8.1
Ilm.	0.4	2.7	2.3	3.0	1.4	4.1	3.2	1.6
Composition non-magnetic fraction to 100 mole per cent								
Hem.	73.2	63.3	44.8	n. d.	21.4	0.8	40.6	9.9
Ilm.	5.3	7.2	34.0	n. d.	35.0	tr.	0	0
Rut.	16.5	29.5	16.2	n. d.	43.6	67.8	35.8	58.8
Mt.	0	0	5.0	n. d.	0	31.4	23.6	31.3

Analysts: J. Malvey and A. Ulrich, 1962-62.

Table 4. B. Petrographic data of the eight samples from Table 4, A.

	146	145	149	143	144	154	153	151	Mean
Mineral analysis, volume per cent									
qtz.	49.3	45.1	24.0	60.7	33.8	27.7	33.7	38.3	39.1
K-fd.	40.0	45.0	62.3	17.1	25.6	62.5	51.9	44.2	43.5
pl.	0	0	0	1.5	0	0.2	x	0	0.2
bi.	0.2	2.0	0.5	x	1.1		x	0.5	
mcc.	1.0		x			0.9	0.5		0.3
ser.		2.3	1.7	2.2	x	0.7	2.6	0.4	1.2
ch.						x		0.4	0.1
scr. & ep.	5.3				8.5				1.7
sill.	1.0	2.6	x		x	x	1.2		0.6
grn.			x						x
ep.	0.7								0.1
ap.	x	x	0.5	0.7	3.1	0.3		0.8	0.7
zr.	x	x	x	x	x	0.1	x	x	x
sp.	x								x
acc.	x	x	0.1	0.6	0.9	0.3	x	x	0.3
ores	2.5	3.0	10.9	17.2	27.0	7.3	10.1	15.9	11.7
IM	1.9	2.5	8.5	17.2	27.0	6.3	8.3	15.2	
HI			0.4						
IH				x	x				
R-IH			2.0						
I-RH	0.6	0.5					x	1.2	x
RH								0.6	0.7
HR									
R			x	x	x	1.0			0.1
I						x			

146 - 300 feet northwest of Copper Mine, Edison Area; ilmeno-rutilehematite = I<sub>5</sub>R<sub>16</sub>H<sub>79</sub>.

145 - northeast end of Condon Cut, Edison Area; ilmeno-rutilehematite = I<sub>7</sub>R<sub>30</sub>H<sub>63</sub>.

149 - Big Cut, Edison Area; hemoilmenite = R<sub>0-5</sub>O<sub>10</sub>(H<sub>25</sub>I<sub>75</sub>), i.e., magnetite tablets intergrown with hemoilmenite; rutile-ilmenohematite = R<sub>0-13</sub>O<sub>10</sub>(I<sub>37</sub>H<sub>63</sub>), i.e., magnetite tablets intergrown with rutile-ilmenohematite.

143 - Big Cut, Edison Area.

144 - northeast end of Condon Cut, Edison Area.

154 - Sherman unit, Sherman Area; rutilehematite = (R<sub>30</sub>H<sub>70</sub>); rutile = H<sub>32</sub>R<sub>68</sub>, i.e., magnetite tablets intergrown with rutile.

153 - Sherman unit, Sherman Area; rutilehematite = M<sub>0-20</sub>(R<sub>22</sub>H<sub>72</sub>), i.e., magnetite tablets intergrown with rutilehematite; hemorutile = (H<sub>10</sub>R<sub>90</sub>).

151 - Sherman unit, Sherman Area; hemorutile and rutile = H<sub>31</sub>H<sub>10</sub>R<sub>59</sub>, i.e., magnetite tablets intergrown with hemorutile and rutile.

In Figure 3 the proportions of quartz, K-feldspar and opaque oxides (largely magnetite) recalculated to 100 per cent for these 44 specimens are plotted in a triangular diagram. The tables and figure show that there is considerable variation in the mineral composition of these samples (note the variance values in Table 5). The composition varies from a magnetite-quartz gneiss (metaquartzite?) to a magnetite-K-feldspar gneiss (garnite?). However, it is also apparent from the figure and tables that most of the samples are in the compositional range of a magnetite-quartz-K-feldspar gneiss or a magnetite-K-feldspar-quartz gneiss in that the per cent of magnetite is generally subordinate to the quartz and K-feldspar and about half the samples have more K-feldspar than quartz and the other half more quartz than K-feldspar. Thus the petrographic data emphatically substantiate the field observations that the interlayers which are composed largely of quartz, K-feldspar and magnetite and which are the principal rock type within the mixed gneisses exhibit are best classified as magnetite-quartz-K-feldspar gneisses which are somewhat variable with feldspar, quartz, and magnetite rich extremes.

Sillimanite. In the mixed gneiss subunit sillimanite is ubiquitous but occurs in highly variable proportions. The volume percentages of sillimanite and K-feldspar in the samples of magnetite-quartz-K-feldspar gneiss from Tables 4 and 5 are plotted in Figure 4. The figure shows that samples with greater than 50 per cent K-feldspar rarely carry accessory sillimanite, and samples with 30 to 50 per cent K-feldspar usually carry up to 5 per cent accessory sillimanite. In addition samples with less than 30 per cent K-feldspar may carry up to 20 per cent sillimanite. The four samples clustered near the origin of the

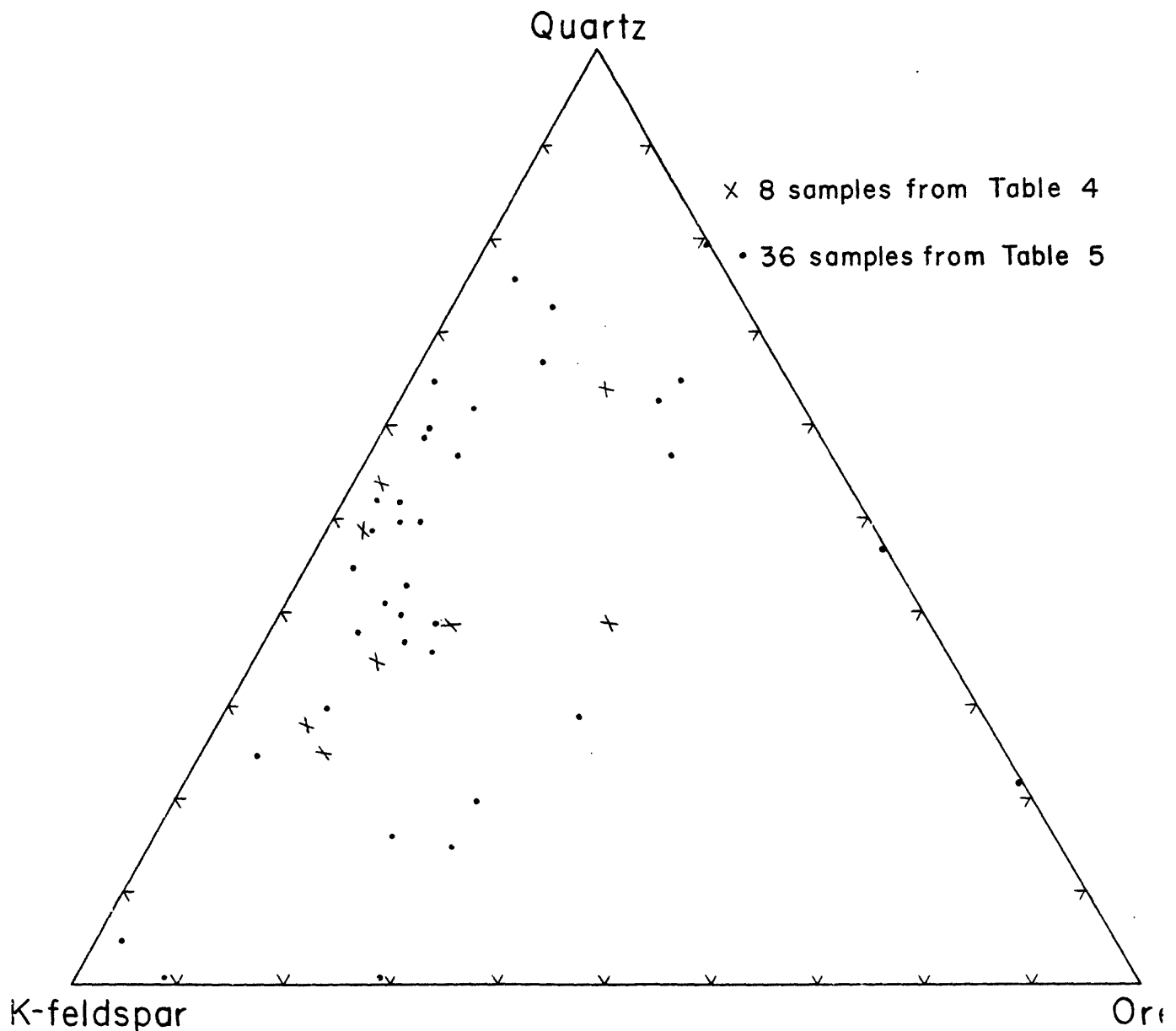


Figure 3. Variation in mineralogical composition of magnetite-quartz-K-feldspar gneiss



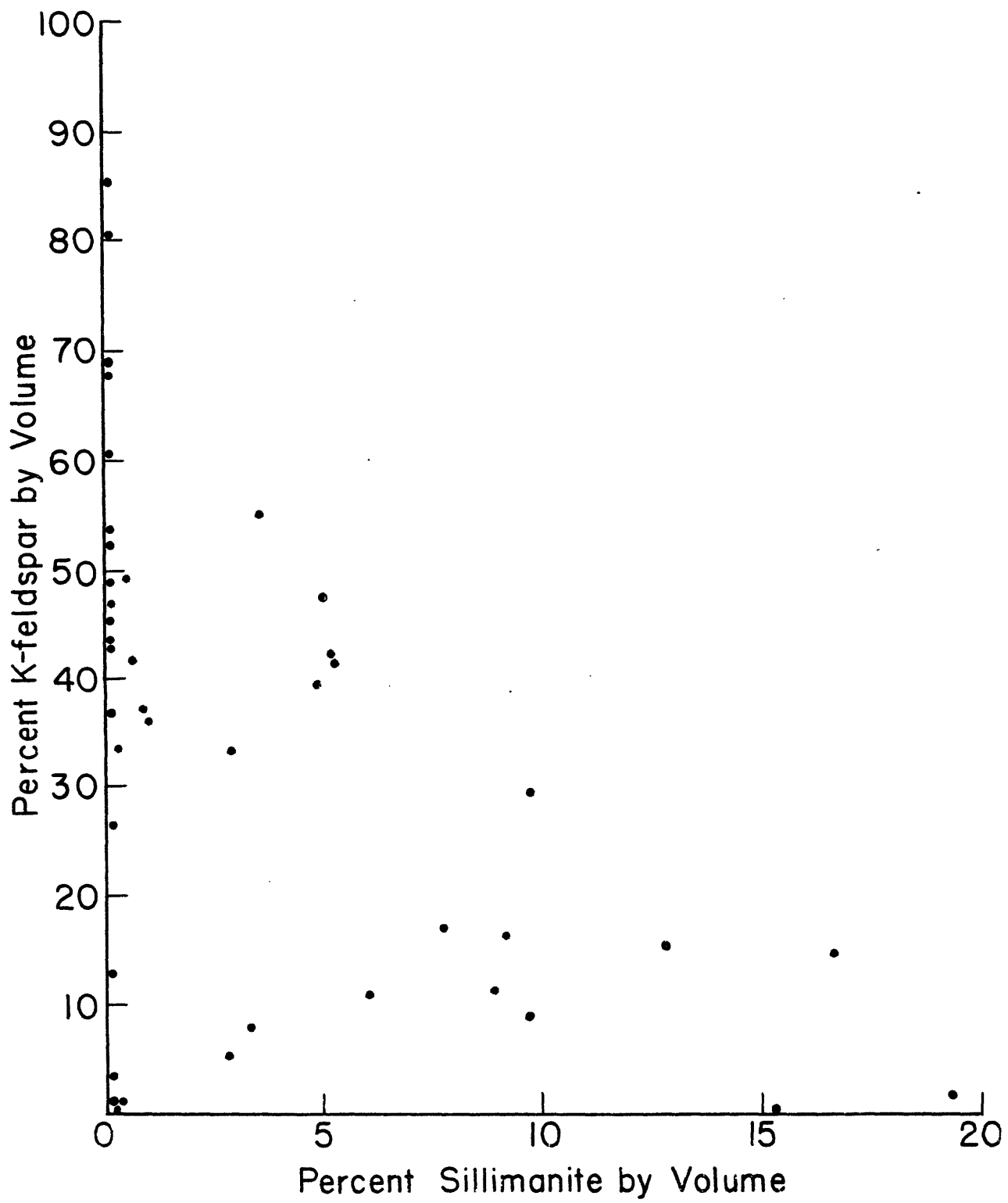
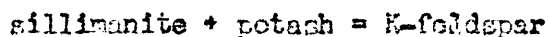


Figure 4. Relation of sillimanite to K-feldspar in the mixed gneiss subunit

figure are magnetite-quartz gneiss (metaquartzite?) and are apparently as free of sillimanite as of K-feldspar. Within the limits of accuracy of the sampling procedure and modal analyses, the figure indicates that there is an inverse relationship between the amount of K-feldspar and sillimanite. The data suggest that either there is a reaction relation between the two minerals such that sillimanite by addition of  $K^{+1}$  was transformed to K-feldspar or that the two minerals crystallized at equilibrium and that the mineral proportions varied as a function of the bulk chemical composition of the milieu. The former case may be chemically expressed as:



and the latter case as:



As there is no independent evidence to suggest that one mineral replaces the other, it is concluded that sillimanite and K-feldspar crystallized together, substantially at equilibrium, and that the proportions of each mineral varied with the bulk composition of the immediate environment.

Lithologic variations. Other rock types within the mixed gneiss subunit are intimately interlayered with the more abundant magnetite-quartz-K-feldspar gneisses. One or all of the minerals quartz, K-feldspar or magnetite form an essential constituent of these other rock varieties, but in addition such minerals as biotite, sillimanite and garnet are very important constituents. Some of these layers are nothing more than biotitic, sillimanitic or garnetiferous varieties of the predominant magnetite-quartz-K-feldspar gneiss. However, many of these layers have mineral compositions which are markedly different from the predominant

magnetite-quartz-K-feldspar gneiss. Some of these distinct types include, (1) garnet-biotite-sillimanite-quartz gneiss (metaquartzite?), (2) sillimanite-biotite-quartz gneiss and rarely, (3) biotite-quartz-feldspar gneiss, as well as numerous other varieties which differ from each other only in the proportion of the various mineral phases. (See modal analyses in Table 6) It is not difficult to find layers which represent all gradations between the predominant magnetite-quartz-K-feldspar gneiss and these other types. The irregular distribution of such minerals as biotite, sillimanite and garnet (these vary from 0 to 20 per cent from layer to layer) as well as the three principals, quartz, K-feldspar and magnetite, impart great heterogeneity to the mixed gneiss subunit. This irregular distribution has led to the interlayering of different related rock varieties which carry the same minerals but in widely different proportions. In order to more clearly describe the nature of these variations two detailed profiles are described.

Summarized below is a 160 foot lithologic profile made across the stripped northeast portion of the Roberts Mine (Plate 1). Five distinct zones are separated. Zone 1 on the northwest is about 80 feet thick and consists of magnetite-quartz-K-feldspar gneiss (B-151a, Table 5) in which there are interlayers, lenses and thin seams rich in biotite, garnet and sillimanite. In addition there are pegmatite seams and layers as well as occasional "vugs" containing coarse grained plates of biotite. Extreme varieties include a 1 to 3 foot layer of garnetiferous-biotite-sillimanite-quartz gneiss (metaquartzite?), (B-151f, Table 6). Zone 2 is a continuous (traced about 50 feet) 3 feet thick pegmatite. On the whole it is very coarse grained with feldspar crystals sometimes as large as 4 by 8 inches

Table 6. Mineral analyses of miscellaneous samples from the mixed gneiss subunit.

Sample No.	qtz.	K-fd.	pl.	alt. pl.	ores	M	H	H	R-H	bi.	ser.	ch.	sill.	gar.	ep.	ap.	m.z.	zr.	spl.	acc.
B-140a	30.8	5.8		32.7	9.7	x		x		17.0	x		2.8		x	1.0	x	x	0.2	
B-142a	30.5	18.0	33.5		8.5					8.5			0.6		x	x	0.4			
B-142c	43.3	9.5	13.8		8.5					13.1			9.8		x		1.5			
B-142d	49.7	15.7	5.1		10.2					3.5			12.8	3.0	x		x			
B-142e	47.1	8.1			39.0					x			3.3	1.0	x	x	x	1.5		
B-142f	27.3	36.8	19.2		5.3					9.3	x		1.0		x	x		1.1		
B-143a	46.0	11.1			8.3	25.1	x	x	x	3.0	x		6.0		x	x	0.5			
B-151f	59.8				9.8	6.0	4.2	1.8		8.7	x		15.3	x	x	x	x	0.4		
B-170c	39.7	7.2	33.8							8.0	10.5	x		x	0.8	x	x	0.1		
B-170e	51.9	1.1	3.5		14.6					7.6			19.4					1.9		

in cross-section. Its contacts with the adjacent gneiss appear conformable. The pegmatite is uniform and massive except for an occasional thin layer or seam enriched in magnetite and biotite. Sillimanite and garnet are absent from the pegmatite. Zone 3 is about 30 feet thick and is a fairly uniform magnetite-quartz-K-feldspar gneiss (B-151g, Table 5). Biotite is a minor accessory in this zone and garnet and sillimanite are virtually absent. Except for a single 1 foot layer of magnetite-quartz gneiss (ret quartzite?) (B-151h, Table 5) and the usual pegmatite seams and layers the composition of zone 3 is very uniform and would correspond to the average magnetite-quartz-K-feldspar gneiss. Zone 4 which contains a considerable amount of magnetite is about 40 feet thick and is the immediate hanging wall to zone 3. This zone is an interlayered complex of typical magnetite-quartz-K-feldspar gneiss alternating with bands (up to 3 to 4 inches thick) of magnetite, (B-151k1 and k2, Table 5). In places garnet is enriched and locally massive quartz is abundant. Sillimanite is absent in zone 4 and biotite is a minor accessory. Particularly characteristic of zone 4 are accessory sulfide minerals which include much pyrite and some molybdenite (see paragraph on sulfide zones). Zone 5 overhangs the magnetite rich zone 4 and is very similar to zone 1 in that it is magnetite-quartz-K-feldspar gneiss with variations rich in biotite, garnet and sillimanite.

The above description illustrates the nature of the large scale lithologic variations in the mixed gneiss subunit. The small scale variations, such as indicated in zone 1 above, may be better illustrated by describing a lithologic profile exposed at the Old Ogden Mine (Plate 1). This description, which is summarized in Table 7, illustrates the rapid

Table 7. Lithologic profile, Old Order Mine, Edison, New Jersey.

Thickness (Spec. No.)	Mineral Composition	Rock Name	Fabric	Remarks
2 inches		biotite-magne- tite-quartz- feldspar gneiss	coarse grained	
6 inches (B-142a)	qtz. 30.5 mic. 18.0 ol. 33.5 bi. 8.5 sill. 0.6 ores 8.5 acc. 0.4	biotite-magne- tite-quartz- feldspar gneiss	fine-medium, uneven grained	slightly peg- matitic
3/4 inch		biotite-magne- tite rock		
13 inches		sillimanite- biotite-magne- tite-quartz- feldspar gneiss	fine-medium grained	includes a 1½ inch layer of pegmatite
2 inches		biotite-magne- tite pegmatite	massive	
10 inches (B-142c)	qtz. 43.8 mic. 9.5 ol. 13.8 bi. 13.1 sill. 9.8 ores 8.5 acc. 1.5	magnetite- sillimanite- biotite-feld- spar-quartz gneiss	fine to medium grained; bio- tite, sill- imanite, and quartz and magnetite lenses in preferred orientation	
10 inches (B-142d)	qtz. 49.7 mic. 15.7 pl. 5.1 bi. 3.5 sill. 12.8 gar. 3.0 ores 10.2	garnet-biotite- magnetite-sill- imanite-feld- spar-quartz gneiss	fine grained, nearly schistose	sillimanite needles lined
4-5 inches (B-142e)	qtz. 47.1 mic. 8.1 bi. x sill. 3.3 gar. 1.0 ores 39.0 acc. 1.5	sillimanitic- microcline- magnetite- quartz gneiss	medium grained	
8 inches		sillimanitic- biotite-magne- tite-quartz- feldspar gneiss	fine grained	

Table 7. (Continued)

Thickness (Spec. No.)	Mineral Composition	Rock Name	Fabric	Remarks
8 inches		biotite-magne- tite pegmatite	massive	rare biotite rich layers; accessory gar- net
8 feet (S-142f)	qtz. 27.3 mic. 36.8 pl. 19.2 bi. 9.3 sill. 1.0 ores 5.3 acc. 1.1	magnetite-q quartz-k- feldspar gneiss	fine-medium grained	garnet absent

and extreme variations in composition and texture between various rock interlayers in the mixed gneiss subunit. However, as was illustrated in the profile at the Roberts Mine the entire subunit is not as variable as this detailed profile would suggest; to the contrary, there are frequent thick zones which are uniform magnetite-quartz-K-feldspar gneiss e. g., zone 3 at the Roberts Mine.

Pegmatites. Pegmatites composed of quartz and K-feldspar with a minor amount of magnetite, biotite and occasionally sillimanite are mixed with all the various rock types which make up the mixed gneiss sub-unit. Mineralogically the pegmatites are very similar to some varieties of the magnetite-quartz-K-feldspar gneiss; however, in general they carry far less magnetite and more K-feldspar than the typical gneiss. The pegmatites are massive and vary in grain size from coarse grained to extremely coarse grained (K-feldspar crystals up to 3 inches long).

Pegmatite bodies vary from narrow seams and lenses less than one inch wide to layers as thick as 3 feet. All the pegmatites which were well enough exposed to enable the tracing of their boundaries proved to be ductless. In other words they either lance out into the surrounding gneiss or fade away into the gneiss. The contacts between the pegmatites and the adjacent gneiss are always abrupt but are never sharp or dike like. Instead, the contacts are gradational over a distance of an inch or two. At the actual pegmatite-gneiss boundary the grains of each type are intergrown across the boundary so that the contact is slightly irregular and is of the same nature as the irregular grain boundary contacts between adjacent layers within the gneiss.

Although the pegmatites usually are conformably interlayered with

the gneiss, they occasionally cross-cut adjacent gneiss (Plate 9). It is clear from the plate that the pegmatite lode cross-cuts the gneissic structure of the adjacent magnetite-quartz-K-feldspar gneiss as well as a layer of biotite-sillimanite-magnetite-quartz-K-feldspar gneiss. This pegmatite is massive and very coarse grained in its central part. It grades into the adjacent gneiss by a progressive decrease in grain size towards the borders until at the contact the granularity of the massive pegmatite lode is identical to the granularity of the medium grained gneissic wall rock. Note also that this pegmatite "sends off" conformable stringers which also grade into the enclosing gneiss. Elsewhere thin ductless pegmatite veins and layers cross-cut the foliation of the gneiss at very small angles and in some places actually distort the adjacent layers of gneiss.

Thus the pegmatites appear to be structurally distinct from the enclosing gneiss and were probably emplaced subsequent to the development of the foliation of the bulk of the gneiss. In addition it is critical to note that the pegmatites carry only accessory magnetite. They never appear to be "mineralized" with magnetite, as immediately adjacent quartz-K-feldspar gneiss may be. Indeed, the pegmatites actually cross-cut gneiss which carries a fair proportion of magnetite (Plate 9). These observations indicate that the pegmatites were emplaced not only after the development of the predominant rock types but also after the emplacement, fixation etc., of the magnetite. It is suggested that the pegmatites represent late stage products of crystallization. The implication is that a certain amount of material in equilibrium with the magnetite-quartz-K-feldspar gneiss remained in the dispersed state, i. e., not

fixed or crystallized, until the temperature dropped or some other physical changes took place (such as the development of low pressure sites along shear zones) which caused the crystallization of this dispersed material into discrete pegmatite bodies.

Fabric. Textural variations in the mixed gneiss subunit are as frequent as compositional variations and the causes for both of these variations are probably related. The predominant magnetite-quartz-K-feldspar gneiss as well as the other subordinate compositional types including the magnetite concentrations are medium grained or fine-medium grained and fairly even grained. However, some fine grained layers are present and coarse grained to pegmatitic layers are quite abundant (see discussion of pegmatites). Quartz, K-feldspar and all opaque oxides are xenoblastic and either fairly equidimensional or of distinct lenticular morphology (Plates 3, 4 and 5). Sillimanite is usually in the form of elongated needles with well developed pinacoidal faces but generally without terminations (Plates 5 and 6). Biotite occurs as thin plates. Garnet occurs either as disseminated xenoblastic grains or in porphyroblasts in an otherwise medium grained gneiss. These porphyroblasts are best developed and most apparent in biotite-rich and sillimanite-rich varieties of the magnetite-quartz-K-feldspar gneiss.

The nature of the structure of the rocks in the mixed gneiss subunit also appears to vary somewhat with rock composition. The predominant magnetite-quartz-K-feldspar gneiss has a distinct gneissic structure due to the preferred orientation of the lenticular shaped grains of quartz and magnetite. It is extremely interesting that the variety magnetite-quartz gneiss (metaquartzite?) appears considerably more

deformed than any feldspathic varieties of the gneiss. Both the quartz and the magnetite in this variety are drawn out into long thin lenticles which testify to rather intense deformation. There appears to be a definite inverse correlation between the amount of K-feldspar in the rock and the intensity of its deformation fabric; such that samples low in K-feldspar appear to have a stronger gneissic structure than do samples rich in K-feldspar (compare Plates 4 and 6 with Plates 3 and 5).

In the magnetite-quartz-K-feldspar gneiss magnetite is generally disseminated in lenticular grains. As the per cent of magnetite progressively increases in the gneiss the magnetite begins to occur as lenticular aggregates and thin discontinuous layers all of which contribute to the planar fabric. Finally, the magnetite is so enriched as to occur in definite thick layers (1/4 inch to 3 inches wide) which alternate with typical magnetite-quartz-K-feldspar gneiss. In these magnetite-rich layers the same gneissic structure appears evident as in the magnetite poor wall rock gneiss. However, in these layers the gneissic structure is due to lenticular aggregates and streaks of quartz and K-feldspar as opposed to streaks and lenticles of magnetite in the silicate-rich gneisses. Thus the fabric in the magnetite-rich (ore) layers appears to be essentially the same as the fabric in the typical magnetite-quartz-K-feldspar gneiss.

The rock varieties which are enriched in biotite and sillimanite show a very strong structure due to the preferred orientation of these inequidimensional minerals (Plate 6). Biotite plates and sillimanite needles are always oriented in the foliation plane. The sillimanite may or may not have a preferred linear fabric. This structure may be called schistose with as much accuracy as gneissic. Actually, such rocks consist

of schistose biotite and sillimanite-rich layers alternating with gneissic quartzose-feldspathic layers. Thus it is clear that the precise nature of the fabric is a function of composition as well as of deformation.

Sulfide zone. There is a distinct zone which is characterized by above normal content of sulfide minerals which may be clearly distinguished from the normal mixed gneisses at the Old Cyden and Roberts Mine (Plate 1). In these two places the zone is about 40 feet thick and is located in the southeast workings of each of the mines. The zone has been traced as far southwest as to the shaft just southeast of the Davenport Mine. In the field the higher content of sulfide minerals relative to adjacent gneisses is made particularly evident by the more intense weathering of the gneisses in the sulfide zone. In addition assay data (see Chapter 8) from diamond drill holes 1 and 2 (Plate 1) which include total sulfur determinations, substantiate the existence of a distinct sulfide zone. In each hole the sulfur content in the sulfide-rich zone averages 1.5-3.5 per cent, but the sulfur content of the sulfide-poor gneiss is always less than 0.5 per cent and generally less than 0.1 per cent. The drill core data also show that the sulfide zone is a zone of enrichment in magnetite. However, it should be emphasized that other magnetite rich zones which also have been assayed are not enriched in sulfur. The sulfide zone is conformable to the foliation of the gneisses, and it is interesting to note that the zone is always in the same "stratigraphic" position relative to adjacent gneisses. Thus, there appears to be no doubt that this zone is more or less traceable for at least 2500 feet from the shaft southeast of the Davenport Mine to the northeast end of

the Roberts Mine. It is interesting that far to the northeast sulfide minerals are rather abundant at the Copper Mine shaft (Plate 1). Although it could not be substantiated by field observations, it is possible that the sulfide zone is continuous or perhaps discontinuous all the way to the Copper Mine.

The sulfide minerals in the Old Ogden and Roberts Mine portions of the zone are pyrite, chalcopyrite and some molybdenite. The zone is rather rich in magnetite and on the whole appears to carry more garnet than many of the adjacent rocks. In addition pegmatite constitutes a large portion of the sulfide zone at the Old Ogden Mine, but at the Roberts Mine the zone appears to be more quartzose than adjacent gneisses.

The chalcopyrite and pyrite in the sulfide zone in the Old Ogden and Roberts Mines are frequently intergrown. Often the pyrite rims the chalcopyrite. The relationships between the magnetite and the sulfides is quite clear. Frequently pyrite rims the magnetite and occasionally a veinlet of pyrite cuts across magnetite grains. The textural evidence suggests strongly that the sulfides are later than the iron oxides.

The sulfide bearing rocks at the Copper Mine are rich in biotite, garnet and sillimanite and are particularly heterogeneous. As usual the predominant type is a magnetite-quartz-K-feldspar gneiss; however, there are numerous biotitic, garnetiferous and sillimanitic varieties. The gneisses all carry a considerable amount of magnetite (10-50 per cent). Sulfide minerals are disseminated throughout the gneiss and probably form about 1-2 per cent of the rock. Accessory minerals include apatite, zircon, fluorite and some plagioclase. The heterogeneous character of these rocks is strongly emphasized by seams, thin layers and bands of

pegmatite which alternate with the layers of gneiss, and in which the K-feldspar occurs as coarse grained porphyroblasts.

The principal ores at the Copper Mine are magnetite (sometimes martitic) and bornite. Accessory ores include ilmenohematite, hematite, ilmenite, chalcopyrite, covellite and some pyrite and molybdenite. The magnetite carries no ilmenite blades; however, in one reaction zone with bornite the magnetite carries a few blebs of ilmenite which indicates that some ilmenite was in solid solution in the magnetite (reaction with bornite released this ilmenite). There are three types of bornite. The first consists of independent grains of brownish bornite which carry chalcopyrite exsolution films whose orientation is strictly controlled by crystallographic planes. The second is pinkish bornite which may occur as independent grains but more frequently occurs as cuboidal intergrowths with magnetite. This type carries exsolution chalcopyrite in the form of blebs or droplets and as strings which wind in a tortuous pattern within the bornite. Both types of chalcopyrite are confined to the central part of the host crystal. This type frequently grades into type three. The third type is bladed bornite, i. e., blades of bornite (with exsolved chalcopyrite blebs) alternating with blades which consist of a mixture of limonite, rutile (?) and ilmenite. This type is found adjacent to magnetite and definitely replaces some magnetite. The copper sulfides have been partly oxidized to covellite along fractures and at grain boundaries.

It seems evident that the copper sulfides are younger than the magnetite. Bornite of the first type probably crystallized directly from "copper solutions"; whereas the second and third types of bornite

were probably formed by replacement of magnetite by "copper solutions." In this case the bladed bornite would represent the early stages of this replacement process.

#### Quartz-K-feldspar gneiss

Introduction. The quartz-K-feldspar gneiss is a very uniform subunit which is conformable to and forms part of the hanging wall to the mixed gneiss subunit. In the southwest part of the Edison area the quartz-K-feldspar gneiss interfingers and lenses out into the biotite-quartz-feldspar gneiss subunit. To the northeast the gneiss has thinned or pinched to a thickness of about 150 feet and is conformable between the northeast extensions of the mixed gneiss subunit and contaminated hornblende granite. In its central portion the quartz-K-feldspar gneiss is about 900 feet thick. Thus, the shape of this subunit in horizontal cross section (Plate 1) is that of a large lens with a length of 2000 feet and a maximum thickness of 900 feet.

Mineralogy and composition. The mineralogy of the quartz-K-feldspar gneiss is very simple. Quartz and perthitic K-feldspar (see Chapter 6) are the two major minerals. Garnet and ilmenomagnetite are the two principal accessory minerals. As in the case of the magnetite-quartz-K-feldspar gneiss, plagioclase is always absent in the quartz-K-feldspar gneiss except in some samples taken from zones which are closely associated with the biotite-quartz-feldspar gneiss. Other accessory minerals include biotite, zircon, allanite and apatite. Secondary minerals are sericite, chlorite and rarely hematite (martite). Chlorite may occur exclusive of biotite but frequently it is interlayered with biotite as an alteration product. Sericite could be an alteration product of

plagioclase. Hematitic alteration of ilmenomagnetite (martite) is usually not present; however, occasional samples contain traces of martite (never more than 1-2 per cent of the ilmenomagnetite).

The quartz-K-feldspar gneiss is a very uniform rock. The modal analyses of 16 samples of this gneiss are presented in Table 8 along with the arithmetic means and variances. In Figure 5 the modal percentage of quartz-K-feldspar and magnetite, recalculated to 100 per cent are plotted in a triangular diagram. The diagram and variances conclusively substantiate the field impression that the gneiss has a very uniform composition. It is particularly interesting and significant to note that the variability of the quartz-K-feldspar gneiss is much less than that of the magnetite-quartz-K-feldspar gneiss (compare Figure 3 with 5 and Table 5 with 8).

Fabric. The texture of the quartz-K-feldspar gneiss is as uniform as its composition. The unweathered gneiss is either a pinkish buff or grayish white color; it weathers to a rusty orange color. The rock is fine grained and equigranular (Plate 7), although fine-medium grained zones are present and garnet grains are often clumped together in porphyroblastic like aggregates. The minerals are all equidimensional. Magnetite occurs as disseminated grains but may be enriched slightly in thin seams. Some magnetite grains are subhedral; zircon is usually euhedral (with some slight resorption ?); otherwise, the minerals are all xenoblastic. The minerals are not intergrown much along grain boundaries. Instead the contacts between grains are slightly irregular but smooth, i. e., the grains are not intergrown along a tortuous (suture) boundary (Plate 7). In summary the texture is fine grained, equigranular, equidimensional and xenoblastic.

Table 8. Mineral analyses of sixteen samples of quartz-K-feldspar gneiss from the Edison Area.

Sample No.	qts.	K-fd.	pl.	ores	M	T	bi.	musc.	ser.	ch.	gar.	sp.	sp.	acc.
E-40	41.9	51.4		4.5	x	2.2				x		x		
E-61	40.0	57.3		2.7	x	x				x	x	x		
E-65	35.9	57.7		1.0	x				5.4	x		x		
E-50	45.9	45.1		1.8	x			3.7	0.3	3.1		0.1		
E-75b	41.1	53.4		3.3	x					1.8	x	0.4		
Ed-21a	48.2	47.4		3.8	x					0.6	x	x		
Ed-168	39.8	53.8		3.2	x	x			1.2	2.0	x	x		
Ed-170	41.7	47.0		3.0	x	3.9	0.3			4.1	x	x	x	
Ed-177	35.8	59.7		3.0	x	0.3			1.0	x	x	0.2		
Ed-205c	42.8	51.1		3.7	x	0.4			x	2.0	x	x		
Ed-217	39.9	53.9		3.9	x		x		2.3		x	x		
Ed-265a	13.9	60.1		1.3	x	6.0				18.7		x		
Ed-931b	53.8	36.7		4.4						5.1	x	x		
Ed-932	53.9	41.2		1.6					1.6	0.8	x	x		
Ed-2544a <sup>a</sup>	42.4	41.2	9.1	2.8		0.1				4.4	x	x		
E-145c	37.2	56.5		5.5	x	0.3				0.4	x	x	0.1	
Mean	40.2	50.8	0.6	3.1	x	x	0.8	x	0.2	0.7	2.8	x	x	0.1
Variance	81.2	50.4		1.5										
<u>qts.</u>														
<u>K-fd.</u>														
<u>qts.</u>														
<u>K-fd. + ore</u>														

<sup>a</sup>From contact zone with biotite-quartz-feldspar gneiss.

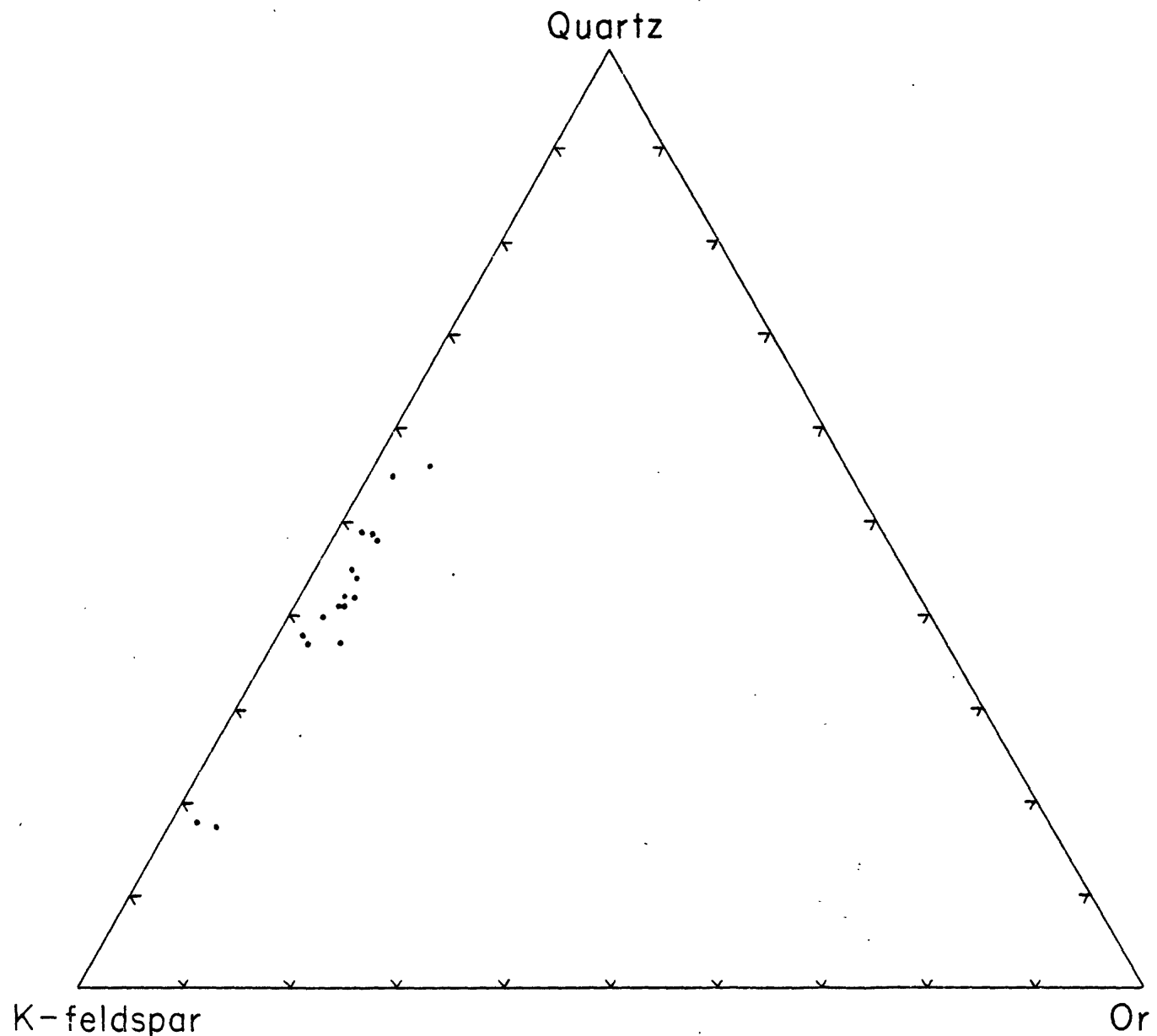


FIG. 5. Variation in mineralogical composition of quartz-K-feldspar gneiss

The structure of the quartz-K-feldspar gneiss is granulose (Tyrrell, p. 274, 1948) with some bands and streaks of prophyroblastic aggregates of garnet which impart a rough foliation to the rock. The streaks and lenses of garnet are from 1/2 to 3/4 inches thick and usually 1-3 inches long. The distribution of these garnet aggregates is somewhat irregular and in zones free of much garnet the rock is usually very massive. As indicated previously all the minerals of the quartz-K-feldspar gneiss are equidimensional; they are seldom of lenticular shapes or in other forms which would suggest that the rock has been deformed (Plate 7). Even the grains of garnet which occur in lenticular aggregates appear undeformed. Thus, the structure of the gneiss is extremely faint and is due to the presence of lenses and streaks of distinct mineral composition, i. e., garnet aggregates. It is interesting to note that this structure is conformable with that developed in adjacent gneisses, but it should be emphasized that the fabric of the quartz-K-feldspar gneiss is much less developed than that of any of the adjacent gneisses.

Classification. The average mineralogic composition of the quartz-K-feldspar gneiss is given in Table 8. The striking features of the composition are the high quartz content and absence of plagioclase feldspar. The composition, as well as texture, correspond closely to garnet alaskite of the Adirondacks (Buddington, 1951) or a granite-aplite (Johanssen, p. 302, 1932). However, because of the nature of the geologic occurrence and the slight foliation, it seems more sensible to give a general name to the rock instead of a specific name such as aplite. Therefore the rock is descriptively classed as a quartz-K-feldspar gneiss. (See Chapter 11 for a further discussion.)

Relationship to other rocks. The contact of the quartz-K-feldspar gneiss is conformable to the foliation of the mixed gneiss subunit. This contact is very well exposed on the northeast end of the Old Ogden Mine. Here the contact of the quartz-K-feldspar gneiss is with the magnetite-quartz-K-feldspar gneisses of the sulfide zone. The contact is conformable and very sharp with no observable gradational zone. There appears to be no interlayering of the two rock types. The fabric changes at the contact are quite apparent. The mineralogical changes have been studied in detail. Samples of each type were taken at distances of 1 to 2 feet from each other across the contact. On the whole the mineralogy is similar in that quartz and K-feldspar are common essential minerals. Biotite, apatite, zircon and magnetite are common accessory minerals. Garnet is limited to the quartz-K-feldspar gneiss. The two rocks differ most in the nature of the oxide and sulfide minerals. Pyrite and chalcopyrite are accessory minerals in the sulfide zone but are absent in the immediately adjacent quartz-K-feldspar gneiss. Magnetite is more abundant in the magnetite-quartz-K-feldspar gneiss and is partially altered (about 15 per cent) to hematite (martite). The magnetite in the quartz-K-feldspar gneiss is entirely free of any martite. Although these features are not of great magnitude it is interesting that such variations occur over such small distances.

In its southwest extension the quartz-K-feldspar gneiss lenses cut completely in favor of the biotite-quartz-feldspar gneiss. To the northeast the opposite is the case in that the biotite-quartz-feldspar gneiss lenses out into the quartz-K-feldspar gneiss. In the zone immediately southeast of Edison the two gneisses as well as some biotite alkaliite are strongly interlayered. The representation on the Edison area map,

Plate 1, is highly diagrammatic in that the entire zone southeast of Edison is a complex interlayered mixture of the quartz-K-feldspar gneiss and the biotite-quartz-feldspar gneiss as well as biotite alaskite. The zones as mapped seem to consist predominantly of the indicated variety but the other kind of gneiss as well as biotite alaskite layers are ubiquitous. The scale of the interlayering of these three types may be small enough to be seen in a single thin section. In the field layers as thin as 1/2 inch lenses out into one another (Plates 10 and 11). The contacts between all three rock types are extremely abrupt. The contacts are not vein or dike like but instead are simply the irregular interlocking grain boundaries between the minerals of the particular rock layers (Plate 11). The width of the contact zone is no greater than the width of the coarsest grain along the boundary. No gradational contacts were observed.

Only minor variations from the normal of the two gneisses and the biotite alaskite are noticed in this complex interlayered zone. The textures of the three rock types remain the same as in non-interlayered zones. The coarse grained character of the biotite alaskite is in sharp contrast to the medium grained biotite-quartz-feldspar gneiss and the fine grained quartz-K-feldspar gneiss. In such complex zones the quartz-K-feldspar gneiss sometimes carries a few per cent of accessory plagioclase. This appears to be its only mineralogical change from the normal. In the contact zone between biotite-quartz-feldspar gneiss and biotite alaskite altered hypersthene (?) is present. In addition the biotite quartz-feldspar gneiss has a small but significant increase in K-feldspar content in the interlayered zone (see next section).

Otherwise there appears to be no significant mineralogical deviations from the normal varieties found in non-interlayered zones.

Biotite-quartz-feldspar gneiss

Introduction. The biotite-quartz-feldspar gneiss forms the hanging wall to the mixed gneiss subunit in the southwest part of the Edicon area. The gneiss lenses cut into the quartz-K-feldspar gneiss to the northeast and has been traced to the southwest outside the Edicon area to the line where the Edicon unit is faulted. Thus the biotite-quartz-feldspar gneiss subunit is a sheet shaped mass which is conformable to all the surrounding rocks.

Mineralogy. The essential minerals of this gneiss are quartz, plagioclase (oligoclase) and slightly perthitic K-feldspar. Biotite is always the most important varietal mineral and garnet is either a varietal or major accessory mineral. Subordinate accessory minerals include hornblende, ilmenomagnetite, ilmenite (locally hexa-ilmenite) rutile, apatite, zircon, hypersthene and allanite. Secondary minerals are epidote, chlorite, sericite, rutile and hematite.

The plagioclase is in the oligoclase range of composition ( $An\ 20 \frac{1}{3}$ ). It is partially altered to sericite and sometimes epidote. Both triclinic (microcline) and monoclinic K-feldspar are present in the biotite-quartz-feldspar gneiss (see the discussion in Chapter 6). In contrast to the plagioclase the K-feldspar is free from alteration. Quartz is highly strained but never crushed or granulated. Biotite is a reddish brown to a very dark brown variety:

X=medium straw yellow

Y=dark reddish brown

Z=very dark brown, near opaque

The biotite is partially altered to epidote and chlorite. Hornblende is a dark green variety and is unaltered. Hypersthene is a flesh color and generally intensely altered to a micaceous mineral and an opaque oxide (hematite?). Hypersthene has been found only in the gneiss which is closely associated with alaskite, and is interpreted as having formed as a consequence of this relationship. It is interesting to note that no martite is present in the ilmenomagnetite; however, the ilmenite blades within the magnetite and the free ilmenite grains are frequently altered to a mottled aggregate of rutile and hematite.

Fabric. The biotite-quartz-feldspar gneiss is a grayish white to reddish buff color on fresh surface. The gneiss is medium or coarse-medium grained but fine-medium and coarse grained varieties are present. The gneiss is even grained but is considerably less so than the quartz-K-feldspar gneiss (Plate 8). In places porphyroblasts of K-feldspar (Plate 11) and porphyroblastic aggregates of garnet are present. The minerals with the exception of zircon and apatite are xenoblastic. In some samples the quartz and feldspar may have a slightly lenticular shape, but usually they are equidimensional grains which are of amoeboid character in that they have very irregular shapes and grain boundaries (Plate 8). Biotite occurs as thin plates which are oriented in the fabric plane.

The biotite-quartz-feldspar gneiss has a distinct planar structure. This is due to the preferred orientation of biotite plates and to slight textural and compositional variations within the gneiss. In addition conformable interlayers of distinct rock types, such as the quartz-K-feldspar gneiss, emphasize the structure. Locally the biotite content becomes so rich that the rock has the fabric of a biotite schist. The

planar structure is also intensified by the occasional lenticular shape of the quartz and feldspar.

The structure of the biotite-quartz-feldspar gneiss is not as gneissic (in the sense that the bulk of the minerals are "sheared" out into thin lenses and lenticles) as is the structure of the rocks of the mixed gneiss subunit. Instead its structure is intermediate between the nearly massive quartz-K-feldspar gneiss and the very gneissic mixed gneiss subunit.

Composition. In Table 9 the modal analyses of twenty-two samples of biotite-quartz-feldspar gneisses (one thin section per sample) are presented. The amounts of quartz, plagioclase and K-feldspar for each of these samples has been recalculated to 100 per cent and plotted in a triangular diagram (Figure 6). The diagram indicates that the modal composition of the gneiss is somewhat variable but that there appears to be a definite concentration of samples whose quartz content is from 20 to 35 per cent. Within this range the K-feldspar content varies from 0 to 62 per cent as the plagioclase content varies from 79 to 25 per cent. On the basis of the feldspar proportions two distinct zones are recognizable within the biotite-quartz-feldspar gneiss subunit. Zone B includes those gneisses in the area southeast of Edison which are intimately mixed with the quartz-K-feldspar gneiss and biotite alkali-syenite (Plate 1). Zone A includes those gneisses well southwest of this mixed zone. From the diagram and the means in Table 9 it is apparent that the gneisses in zone A have an average content of plagioclase somewhat higher than that of the gneisses of zone B. Thus it is clear that K-feldspar is increasing in proportion to the northeast toward the quartz-K-feldspar gneiss. Despite this remarkable variation it should be

Table 9. Mineral analyses of 22 samples of biotite-quartz-feldspar gneiss from the Edison unit.

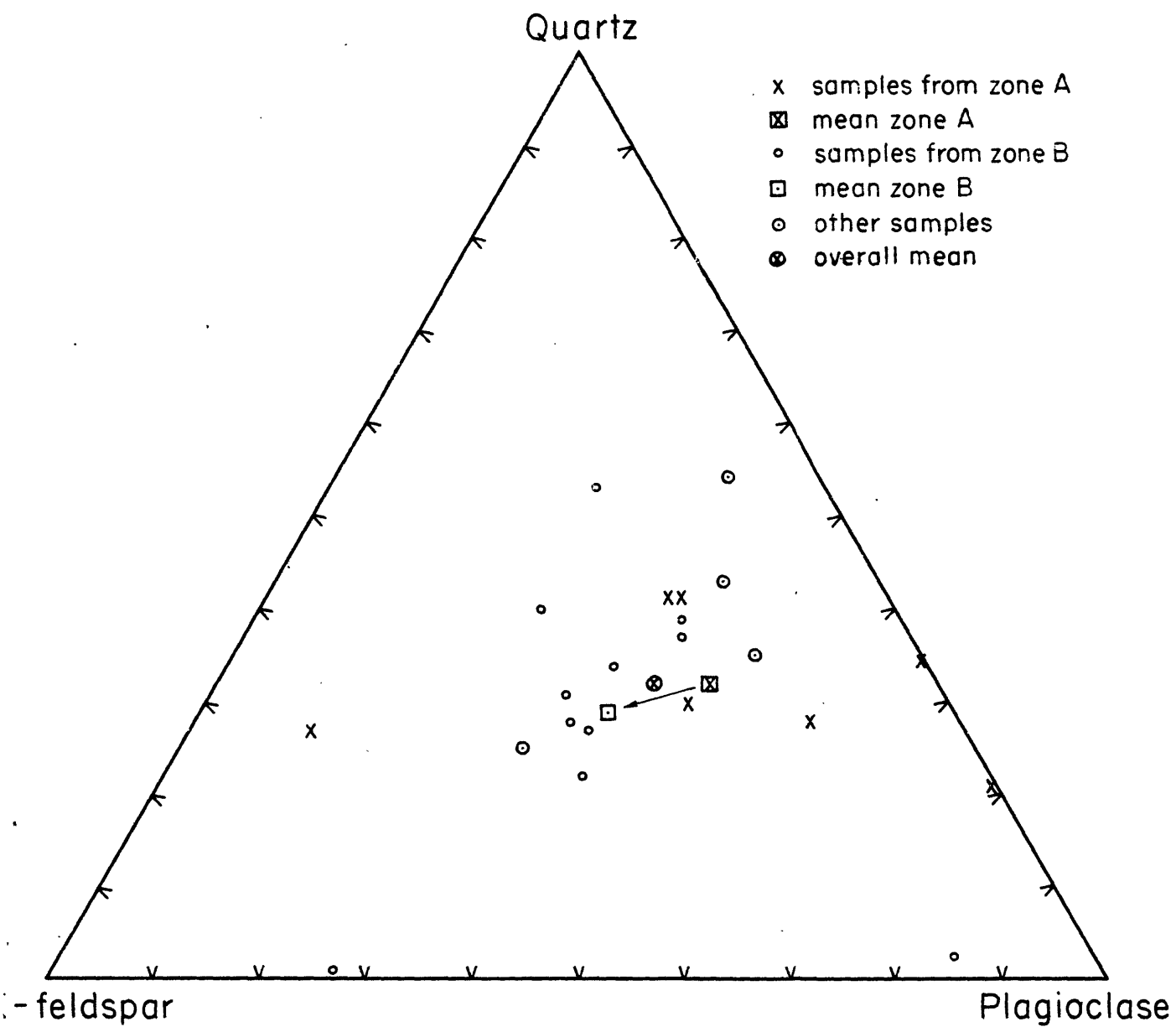


Fig. 6. Variation in mineralogical composition of biotite - quartz - feldspar gneiss

emphasized that there is not a continual variation from biotite-quartz-plagioclase gneiss to quartz-K-feldspar gneiss. The two types were always distinct in the field and as can be seen from Figures 5 and 6 there is a distinct compositional discontinuity between them. In addition there is a marked textural and fabric discontinuity. In other words there is no evidence to suggest that the quartz-K-feldspar gneiss was formed by continual enrichment of K-feldspar in a biotite-quartz-plagioclase gneiss.

Lithologic variations. In some places the biotite-quartz-feldspar gneiss appears uniform and the only apparent variations are due to the slightly irregular distribution of the biotite and garnet. Generally the gneiss is interlayered with other rock types. This interlayering may be on a scale of 1/2 to 1 inch, or it may be on a scale of 1 to 10 feet. In its northeast extent the gneiss is considerably interlayered with biotite slates and quartz-K-feldspar gneiss (Pls. 10 and 11). As can be observed in the plates the rocks are interlayered on a scale of inches. Additional rock layers mixed with the gneiss include pegmatite, some biotite schist, garnet rich layers (syenitic), biotite amphibolite and pyroxene-plagioclase-hornblende skarn.

Relationship to other rocks. The biotite-quartz-feldspar gneiss is conformable to all adjacent rock types. Its contact relations to the quartz-K-feldspar gneiss and biotite slate are discussed in the section on the former gneiss.

#### Epidote-scapolite-quartz gneiss and related facies

Introduction. The epidote-scapolite-quartz gneiss subunit (here-

after the lime rich subunit) occurs in the northeast part of the Edison area and extends to the northeast to the line of termination of the Edison unit at the oblique fault near Highway 23 (Figure 2). The subunit lenses out very rapidly into the mixed gneiss subunit; one zone of the lime rich subunit was mapped within the southwest portion of the mixed gneiss subunit, otherwise no interlayering of the two types is apparent (Plate 1). The McAfee unit on the northwest limb of the Beaver Lake anticline (Figure 2) is probably the stratigraphic equivalent to the lime rich subunit. No lime rich equivalent was located in the Sand Hills unit. The lime rich subunit is always conformable to adjacent rocks.

The lime rich subunit is composed of a variety of interlayered rock types which vary from metaquartzites to quartz-feldspar gneisses. Intermediate types include feldspathic metaquartzites and feldspar-quartz gneisses. All these varieties are characterized by the same suite of varietal and accessory minerals which on the whole are lime rich. Usually the feldspar rich layers weather out more readily than the quartz rich layers so that the layering is emphasized by a ribbed-like structure which gives the gneiss a "migmatitic" aspect.

Mineralogy. The minerals in the lime rich subunit are quite distinct from those in other subunits. The outstanding mineralogic feature is the high content of quartz and of lime rich minerals. The major minerals throughout the subunit are quartz, plagioclase and microcline. Varietal minerals are epidote, scapolite, hornblende, pyroxene, biotite and sphene. Accessory minerals include calcite, magnetite, hematite, garnet, clinzoisite, allanite, muscovite, apatite, and zircon. Secondary minerals are sericite, epidote (clinzoisite), hematite (martite) and two varieties

of chlorite.

Quartz is always highly strained. Microcline is always very clear, unaltered and has good cross-hatched twinning. It is usually completely non-perthitic, but locally slightly perthitic microcline is present. Plagioclase varies in composition from An 20 - An 30 ± 5. It is always partially altered and sometimes completely altered to sericite and epidote (clinozoisite).

Pyroxene is a pale green monoclinic variety. Two of its optical properties are listed below:

$$\begin{aligned}Ng &= 1.692 \pm 0.001 \\2V &= + 58^\circ \text{ to } + 61^\circ\end{aligned}$$

The pyroxene is clear and unaltered. Its properties prove that it is not an augite (Hess, 1949) but instead corresponds to a non-aluminous pyroxene of the diopside-hedenbergite series. The 2V and Ng values correspond very closely to the optical property curves for Adirondack sharn pyroxenes (Hess, 1949). Using these curves the pyroxene is identified as enstatite with about 14 atomic per cent Fe. The curves indicate the total  $\text{Al}_2\text{O}_3$  may be about 3 weight per cent.

Hornblende is an abundant varietal and accessory mineral, and throughout the entire lime rich subunit a single variety is present. Characteristically its color formula is:

X = light yellowish brown with a pale greenish hue,  
Y = medium green with a yellowish hue,  
Z = medium green with a faint bluish hue.

Its 2V varies from -78° to -85°. The absorption colors and 2V measurements correspond to hornblendes of the tremolite-actinolite group and to the actinolite variety specifically (Winchell 1951; Sundius, 1946). Usually the hornblende is clear and unaltered; occasionally, it is

intergrown with biotite in a fashion which suggests the biotite replaced the hornblende, and often it is altered to chlorite (see secondary minerals).

Biotite in the lime rich subunit differs considerably from the biotite elsewhere in the Edison unit. Its color formula is always:

X = colorless to very pale yellow-brown,  
Y = pale yellow-brown,  
Z = medium yellow-brown.

These colors correspond to those of magnesium rich biotite, i. e., phlogopite. Usually the biotite is unaltered; however, it may be altered to epidote and chlorite along layers parallel to the OOl plane (see section on secondary minerals).

Scapolite occurs as discrete grains. Its birefringence is rather high (0.02 to 0.03) which indicates that its composition is K-silicate<sub>40-60</sub> (Winchell, 1951). The scapolite does not appear to have developed as an alteration of plagioclase. The two minerals frequently occur side by side in a single thin section and both appear to be of primary origin, i. e., formed during metamorphic recrystallization. Scapolite is sometimes altered to sericite.

Sphene occurs as disseminated grains and as coronas around iron oxides.

Epidote appears to be both primary and secondary. Secondary epidote is an alteration product of biotite and plagioclase. Primary epidote may occur as discrete grains or in discrete aggregates of many small grains. It is a pale to medium green variety which appears somewhat zoned. Frequently at least two kinds of primary epidote are present in a single rock. One type has high relief and birefringence and is a medium green color and strongly pleochroic. The other type is colorless

has anomalous blue interference color and is of low relief. The colorless variety corresponds to clinozoisite while the green variety corresponds to an epidote somewhat richer in iron. The iron rich type shows strong zoning. It may be that there is a continual compositional variation between these two types.

The principal iron oxides in the lime rich subunit are varieties of hematite. These are ilmenohematite ( $I_{35}H_{65}$ ) and rutile-ilmenohematite ( $R_5-I_{10}-H_{70}-S_5$ ); hemoilmenite was not observed. Magnetite [which is partially altered (< 10%) to hematite (magrite)] is subordinate to hematite.

Calcite occurs as discrete grains and definitely appears to be primary.

Sericite is the most abundant secondary mineral. It occurs as an alteration product of plagioclase and sometimes scapolite. It is frequently accompanied by clinzoisite.

Petrographically two varieties of chlorite are recognized. The most abundant type has a very pale green color, weak pleochroism, anomalous yellow-brown interference color and is length fast. This variety corresponds to clinoclore (?) (Winchell, 1951). The second variety has a low birefringence, anomalous blue interference color and is colorless to very pale green and length slow. This variety corresponds to penninite (?) (Winchell, 1951). Generally the two are interlayered parallel to OOL in a sort of layered chlorite complex. Hornblende is frequently altered to such a complex in which clinoclore (?) is more abundant. Biotite is also altered to this chlorite complex; however, penninite (?) is probably more abundant in this alteration.

Fabric. The bulk of the rocks in the lime rich subunit are medium

grained or fine-medium grained; however, some coarser grained varieties and pegmatitic facies are present. Usually the rocks are even grained. Quartz and feldspar and most of the other minerals are xenoblastic. However, some of the varietal and accessory minerals such as hornblende, pyroxene, epidote, scapolite, biotite and iron oxides may have subhedral outlines. Biotite occurs as plates slightly elongated parallel to the trace of the OOl plane. Hornblende, despite its general anhedral character, is usually elongated parallel to crystallographic c. Feldspar is always equidimensional, but quartz is sometimes of lenticular shape.

The rocks of the lime rich subunit have a distinct gneissic structure. The intensity of this structure varies from specimen to specimen. There seems to be a general correlation between intensity of the gneissic structure and the percentage of feldspar in the rock; such that rocks low in feldspar and high in quartz have a better developed structure. In general the structure is due to the preferred orientation of biotite plates, elongated hornblende grains and lenticular shaped grains of quartz. In samples rich in feldspar or with equidimensional quartz the structure is due to the oriented mafic minerals. The gneissic structure is emphasized by distinct compositional layering. This is caused either by a disproportionate distribution of such minerals as biotite, hornblende, pyroxene, iron oxides, etc., or is less subtle and is caused by the alteration of layers of quite different compositions, such as metaqueartzite and quartz-feldspar gneiss.

Lithologic variations. As indicated previously the rocks of the lime rich subunit vary from metaqueartzites to quartz-feldspar gneisses and all carry the same general suite of lime rich varietal and accessory

minerals. This suite of minerals is common to all the rock types within the subunit but the mineral proportions vary considerably from rock to rock. The rock varieties occur as distinct layers which vary from fractions of an inch to 1 to 2 feet thick. Typical rock varieties include such gneisses as, (1) scapolite-epidote-pyroxene metaquartzite; (2) epidote-pyroxene-quartz-feldspar gneiss; (3) epidote-biotite-hornblende-feldspar-quartz gneiss; (4) epidote-sphene-pyroxene-quartz-microcline gneiss; (5) epidote-garnet pyroxene-scapolite-quartz-microcline gneiss; (6) pyroxene-hornblende-quartz-feldspar gneiss; (7) scapolite-biotite-hornblende-quartz-feldspar gneiss (scapolite and plagioclase both present); (8) scapolite-epidote-pyroxene-quartz-feldspar gneiss; (9) feldspar-epidote-calcite metaparbitite, etc. It is particularly interesting to note that pyroxene and hornblende occur side by side in the same rock with no apparent reaction or replacement relationship. Also, scapolite and plagioclase may occur side by side. In very lime rich rock, i. e., high in epidote as (4) above, plagioclase may be absent. These general relationships suggest that bulk chemical composition was the main controlling factor in determining the final mineral assemblage. It seems certain that more or less identical pressures and temperatures prevailed throughout the entire lime rich subunit during the period of crystallization. Hence, all the minerals found in the subunit would have been stable throughout the entire subunit if the bulk chemistry of the immediate milieu was proper for their development (see Yoder, 1952). For example, in rocks which carry abundant Ca rich minerals, microcline and quartz, as (4) above, it seems logical to conclude that plagioclase is absent from such rocks because the Na content was too low to enable its formation.

and not because the pressure and temperature were beyond the stability limits of plagioclase. In addition where scapolite is absent or closely associated with plagioclase, as in (7) and (8) above, it seems likely that there was only limited amounts of  $\text{Cl}^{-1}$  and  $\text{CO}_3^{-2}$ , etc., in the rock forming milieu. Very likely the absence of hornblende in favor of pyroxene, as in (2) above, and their association together, as in (6) above, indicate that a limited amount of  $\text{H}_2\text{O}$  was present in the rock forming system (Yoder, 1952).

## CHAPTER 5

### STRUCTURE OF THE EDISON AREA

#### INTRODUCTION

The structural features of the Edison area are related to the regional structural pattern. The Edison area is on the southeast limb of the Beaver Lake anticline which is the major structure within the Edison block (Figure 2). On the whole the structural pattern of the Edison area is simple and consists of tabular shaped lithologic units which are oriented parallel to the axial plane of the major fold (north-east strike and steep southeast dip) and extend across the entire area (Plate 1). The quartz-oligoclase gneiss, the pyroxene granitic gneiss and the Edison unit all outcrop as relatively narrow units which trend north-east across the area. However, in detail the structure of the area is quite complex. The principal structural features include foliation, lineation, folds, faults and joints.

#### FOLIATION

Foliation is the most prevalent and obvious internal structure within the lithologic units. The term foliation is applied to any planar structure within the rock. Foliation is manifest either by the preferred orientation of inequidimensional minerals or mineral aggregates such as kyanite, amphibole, sillimanite, lensoid quartz and feldspar aggregates, etc., or by distinct rock layers with compositions different from adjacent layers. The former kind of foliation is called cleavage and the latter

compositional layering.

The lithologic units represent the largest scale case of such compositional layering. The best examples of compositional layering are amphibolite layers interlayered with quartz-feldspar gneiss or with granite (Plate 2). Such layering is on a scale of fractions of an inch to tens of feet. In the Edison area the mixed gneiss subunit, the biotite-quartz-feldspar gneiss and the quartz-oligoclase gneiss all show marked compositional layering. On the other hand the pyroxene syenite gneiss, quartz-K-feldspar gneiss and various granites in the area are rather uniform and have little compositional layering.

Cleavage is due to the preferred orientation of minerals and mineral aggregates and is present to some degree in almost every rock type. It is particularly well developed in the quartz-oligoclase gneiss, the pyroxene syenite gneiss and rocks of the mixed gneiss subunit.

On the whole the foliation strikes uniformly northeast and dips vertically or steeply to the southeast. Hence, compositional layering and cleavage are generally parallel. However, in places the lithologic units are contorted into minor folds. In such cases the compositional layers remain parallel to the larger lithologic units, whereas cleavage either remains parallel to the axial plane of the fold or disappears in favor of lineation. Hence, although the compositional layering is directly related to the larger lithologic units, cleavage is related to the folding, i. e., the Beaver Lake anticline, and is properly called an axial plane cleavage.

### LINEATION

Lineation is the second most prevalent internal structure in the lithologic units. The term lineation is applied to any linear structure within a rock. Lineation caused by the preferred orientation of elongated minerals or mineral aggregates such as amphibole, sillimanite, quartz rods etc., is called mineral lineation. Lineation caused by the directional alignment of elongated rock masses with compositions different from adjacent rocks is called compositional lineation.

Compositional lineation is caused either by the fold axes of contorted compositional layers or by oriented masses of rock which are either rod or lath shaped (Plate 2). Such masses are on the order of inches to tens of feet long. Such small scale linear elements are similar to large scale features involving whole lithologic units. Compositional lineation is abundant along both the axes and limbs of folds. There is good evidence to indicate that many of the magnetite rich layers in the mixed gneiss subunit are such lath shaped linear elements.

Mineral lineation manifested by the preferred orientation of elongated minerals or mineral aggregates is particularly obvious in the mixed gneiss subunit. Sillimanite needles are oriented in the foliation plane and generally in a preferred linear pattern. In addition elongated aggregates rich in magnetite, biotite or other minerals are oriented in the foliation plane and also in a preferred linear pattern.

Where both compositional and mineral lineation are present they are parallel. In the Ediron area the strike and plunge of the lineation are always to the northeast, i. e., parallel to and in the plane of the foliation. The plunge of the lineation varies from 10° northeast to

nearly vertical and averages about  $50^{\circ}$  northeast. Compositional lineation is related to compositional layering and hence to the major lithologic units. Mineral lineation is related to cleavage and appears equivalent to it at the crest of folds. When viewed in terms of its relationship to the major Beaver Lake anticline and the minor folds the lineation in the Edison area corresponds to the b axis of the regional movement picture of deformation (Turner, p. 532, 1951).

#### FOLDS

There are numerous small folds and crenulations in the Edison area. This folding involves compositional layers which vary in thickness from fractions of an inch to tens of feet. All such structures are interpreted as minor folds related to the major Beaver Lake anticline. In essence most of them are considered as drag folds on the limbs of the major fold. Although the dip of the axial plane of most folds in the Edison area is parallel to that of the Beaver Lake anticline (steep southeast), the plunge of the minor fold axes in the area averages  $45^{\circ}$ - $55^{\circ}$  northeast and is therefore somewhat greater than that of the Beaver Lake anticline.

At the Old Ogden Mine minor folding is obvious on the central ridge of the open pit and involves compositional layers 2 inches to 2 feet thick (Plate 1). A syncline with a breadth of about 4 feet is evident along the crest of the ridge. The axial plane of the syncline dips steeply ( $75^{\circ}$ - $85^{\circ}$ ) to the southeast and the axis plunges  $55^{\circ}$ - $60^{\circ}$  northeast. There is a certain amount of minor crenulation associated with the structure. Obviously this syncline is best interpreted as a minor drag fold on the limbs of the major Beaver Lake anticline.

In the Roberts Mine there is an excellent example of a minor drag fold exposed in the stripped southwest part of the open pit (Plate 1). At that locality a 10 to 15 feet thick magnetite-quartz gneiss layer is tightly folded into a minor syncline and anticline. The axial planes of these folds dip steeply to the southeast and the axes plunge at about  $50^{\circ}$ - $60^{\circ}$  northeast. Hence the architecture of the minor folds is geometrically similar to the Beaver Lake anticline. Within the folded magnetite-quartz gneiss layer and adjacent gneisses there are many tightly crumpled and crenulated layers. In the magnetite-quartz gneiss layer thin layers of quartz alternate with thin layers of magnetite in such crumpled structures. Both the magnetite and quartz in this layer are sheared out into lenticular grains and aggregates but neither appear crushed nor brecciated. The evidence indicates that the folding took place while the rock was at a relatively high temperature and hence was able to recrystallize during deformation.

The syncline in the southeast part of the Edicon area (Plate 1) is the largest fold within the area. The axial plane of the syncline is about vertical and its axis plunges  $30^{\circ}$ - $40^{\circ}$  northeast. The breadth of the syncline is about 1200-1500 feet and the fold is relatively open. The structure is best defined by the garnet-tiotite-quartz-feldspar gneiss and by minor mafic rich layers which are present in the contaminated hornblende granite. The northeast extension of the hornblende granite plunges beneath the trough of the syncline as a phacolithic body. That there is no continuation of this fold to the northwest is an enigma. It is postulated that the original relationships have been obscured either by the subsequent emplacement of the quartz-K-feldspar gneiss

or by pre-Cambrian faulting along a plane near the northwest contact of the garnet-biotite-quartz-feldspar gneiss.

#### FAULTS AND JOINTS

The northeast trending high angle faults are the major fractures in the region and were discussed in detail in Chapter 1. It is interesting that within the major fault blocks very little minor faulting of any type is present. It appears as if all crustal adjustment has taken place along the few major faults which divide the area into structural blocks.

}

Joints are the most prevalent kind of fracture in the Edison area. A set of joints which strikes northwest and dips steeply to the southwest is ubiquitous. This set which is about perpendicular to the lineation and foliation of the lithologic units is a good example of transverse or a c joints. The spacing of these joints varies from fractions of an inch to 1 to 3 feet and depends upon the kind of rock fractured. In relatively massive rocks such as the hornblende granite the joints are widely spaced and in heterogeneous rocks such as the mixed gneiss subunit they are closely spaced.

In addition to the transverse joints there is a less well developed set of longitudinal joints present in the mixed gneiss subunit. This set trends northeast parallel to the strike of the foliation and dips 15° to 20° northwest. These joints are spaced inches apart and unlike the transverse joints are not smooth extensive planes but are rough discontinuous planes. In places where both transverse and longitudinal joints are well developed, layers in the mixed gneiss subunit break out as small

parallelepiped polyhedra bounded by two joint planes and the foliation plane.

In some places a joint set which trends northwest and dips gently northeast (parallel to the plunge of the lineation) is present.

The minor faulting in the Edison area is parallel to the transverse joints and probably is genetically related to them. Such minor faults are interpreted as transverse joints along which there has been minor displacement. The only fault of any significance in the Edison area is located 600 feet southwest of the Big Cut. There the horizontal offset of a magnetite rich layer is 150 feet.

## CHAPTER 6

### DETAILED MINERALOGY OF THE EDISON UNIT IN THE EDISON AREA

#### K-FELDSPAR

##### Introduction

The most important mineral in terms of its volume per cent in the Edison area is K-feldspar. Even within this small area the K-feldspar shows considerable variation in terms of composition, twinning, porphyritic intergrowth and X-ray powder patterns. In particular, differences are noted between the K-feldspar from the biotite-quartz-feldspar gneiss, quartz-K-feldspar gneiss and from magnetite-quartz-K-feldspar gneiss and magnetite rich layers within the mixed gneiss subunit.

##### Composition

Two quartz-feldspar concentrates taken from rocks within the mixed gneiss subunit were analyzed for CaO, Na<sub>2</sub>O, K<sub>2</sub>O and BaO. Sample 1/4 is from a magnetite rich layer and sample 145 is from the adjacent (wall rock) magnetite-quartz-K-feldspar gneiss (see Table 4B for mineralogic data on these rocks). The analytical data are presented in Table 10 along with recalculations to the usual feldspar molecules. The very low albite content of both these concentrates substantiates petrographic and X-ray observations that little or no albite was present in either rock sample. The very high celsian content of the feldspar from the magnetite rich layer (144) is in marked contrast to the low celsian content of the feldspar from the magnetite-quartz-K-feldspar wall rock gneiss (145). No other K-feldspars were analyzed.

Table 10. Partial chemical analyses of quartz-feldspar concentrates from the mixed gneiss subunit.

144				145			
Wt. % oxides	Feldspar molecules	Wt. % oxides	Feldspar molecules	Wt. % oxides	Feldspar molecules	Wt. % oxides	Feldspar molecules
CaO	0.09	An	1.0	CaO	0.04	An	0.5
Na <sub>2</sub> O	0.45	Ab	9.0	Na <sub>2</sub> O	0.46	Ab	10.6
K <sub>2</sub> O	6.09	Or	80.7	K <sub>2</sub> O	5.82	Or	83.6
BaO	2.28	Cel	9.3	BaO	0.06	Cel	0.3
	8.91		100.0		6.33		100.0

144 - Concentrate from a magnetite rich layer, Condon Cut, Edi. sp., N. J.

145 - Concentrate from magnetite-quartz-K-feldspar gneiss (wall rock to 144), Condon Cut, Edison, N. J.

Analyst: Doris Thaelitz, 1954.

### Twinning

The K-feldspar associated with magnetite rich layers is always untwinned. This is in contrast to the K-feldspar in the wall rock magnetite-quartz-K-feldspar gneiss which always has distinct cross-hatched (grid) twinning. The bulk of the K-feldspar in both the biotite-quartz-feldspar gneiss and the quartz-K-feldspar gneiss also has distinct cross-hatched microcline twinning. However, K-feldspar porphyroblasts (Plate 11) within the biotite-quartz-feldspar gneiss are always untwinned. Where microcline grid twinning is present it may be very obvious with wide and clear cross-hatched lamellae, or it may be extremely faint, so that without a very detailed examination it could be mistaken for undulate extinction. The degree of twinning often varies progressively in a single grain from a well twinned portion of the grain into an apparently untwinned portion.

### Berthitic intergrowth

The K-feldspars from the magnetite rich layers and from the magnetite-quartz-K-feldspar gneiss from the mixed gneiss subunit carry only rare films and lenses of albite and are thus decidedly non-berthitic. The partial analyses in Table 10 of the quartz-feldspar concentrates from such rocks prove that the albite content is very low. Thus, the analytical data are consistent with the petrographic observation that there are but few films and lenses of exolved albite in the K-feldspar and that there is no free albite in these rocks. In addition the analyses show that there could be only a few mole per cent of albite remaining in solid solution within the K-feldspar.

Visual estimates of the amount of perthitic intergrowth in the K-feldspars from the biotite-quartz-feldspar gneiss and the quartz-K-feldspar gneiss indicate that there are more films, lenses, blebs and veins of exsolved albite in the K-feldspar of the latter rock than in the K-feldspar of the former rock. Estimates of guest albite intergrown with the K-feldspar of the quartz-K-feldspar gneiss range from 10-40 per cent and appear to average near 20 per cent. Similar estimates of the guest albite in the K-feldspar porphyroblasts and matrix feldspar from the biotite-quartz-feldspar gneiss are lower and appear to average about 10 per cent. These petrographic observations are substantiated by X-ray powder data. Specifically, two K-feldspar samples from the quartz-K-feldspar gneiss gave X-ray diagrams with distinct albite peaks for 040 (the hkl plane with greatest intensity, Goodyear and Duffin, 1954). In contrast two K-feldspar porphyroblasts from the biotite-quartz-feldspar gneiss gave X-ray diagrams with a clearly discernible but very weak 040 albite peak. Absolutely no 040 albite peaks were visible in the X-ray diagrams of the K-feldspar from the magnetite rich layer and the adjacent magnetite-quartz-K-feldspar gneiss (Samples 144 and 145). Thus the X-ray data substantiate the petrographic and chemical data that the K-feldspars from the mixed gneiss subunit are very low in albite and that the K-feldspar porphyroblasts from the biotite-quartz-feldspar gneiss contain considerably less intergrown albite than the K-feldspar from the quartz-K-feldspar gneiss.

#### X-ray data

Goldsmith and Ives (1954) have presented the 2θ and d values for the principal reflections in powder diagrams for microcline and sanidine.

They point out that the reflections from the  $1\bar{3}0$ ,  $1\bar{3}0$ ,  $1\bar{3}1$ , and  $1\bar{3}1$  planes were very useful for distinguishing between monoclinic and triclinic K-feldspar. In the case of monoclinic K-feldspar of course the  $1\bar{3}0$  and  $1\bar{3}1$  lines are absent. In addition Goldsmith and Laves proposed that the degree of triclinic character (triclinicity) of K-feldspar is a function of the degree of ordering of Al and Si. K-feldspar with completely disordered Al and Si would be monoclinic (sanidine) and K-feldspar with complete Al and Si ordering would be microcline with a maximum degree of triclinicity. They established that the spacing between the  $1\bar{3}1$  and  $1\bar{3}1$  lines was a measure of the ordering of Al and Si in K-feldspar; therefore, they used these two reflections in order to calculate triclinicity according to the following empirical formula:

$$(\text{triclinicity}) = 12.5 \frac{d(1\bar{3}1) - d(1\bar{3}1)}{d(1\bar{3}1)}$$

In the case of sanidine where the  $1\bar{3}1$  and  $1\bar{3}1$  lines merged into a single  $1\bar{3}1$  line, the triclinicity would be zero. The constant, 12.5, was chosen so that the most ordered microcline (maximum microcline) which they have X-rayed would have a triclinicity value of unity. In the present study K-feldspars from samples 144 and 145 from the mixed gneiss subunit (see above), and two samples of K-feldspar from the quartz-K-feldspar gneiss (1903 and 2544-a) and two K-feldspar porphyroblasts (2544-c 1 and 2544-c 2) from the biotite-quartz-feldspar gneiss were studied by means of X-ray powder diagrams.

The untwinned, high celsian K-feldspar from the magnetite rich layer (144) gave a distinct monoclinic X-ray pattern. In addition both the untwinned K-feldspar porphyroblasts (samples 2544-c, 1 and 2) from the biotite-quartz-feldspar gneiss gave distinct monoclinic X-ray patterns.

In Table II the observed  $2\theta$  values for selected reflections from these three samples are listed along with the  $2\theta$  values given by Goldsmith and Laves (1954) for sanidine. The distinct  $130$  and  $1\bar{3}1$  reflections and the complete absence of  $\bar{1}\bar{3}0$  and  $1\bar{3}1$  reflections definitely prove the monoclinic character of these three samples. The selected reflections for the high celsian sample (144) appear to agree better with the data for sanidine than do the reflections from the other monoclinic samples. However, none of the  $2\theta$  values from the three samples differs by more than 0.15 degrees from the corresponding  $2\theta$  value of sanidine.

The sample of K-feldspar from the quartz-ite-quartz-K-feldspar gneiss (145) gave a triclinic X-ray powder pattern. The sample gave distinct reflections for both the  $131$  and  $1\bar{3}1$  planes as well as for the  $130$  and  $\bar{1}\bar{3}0$  planes (see Table II). All the  $2\theta$  values for the selected reflections agree within 0.1 degrees with the data of Goldsmith and Laves for microcline. The triclinicity as calculated from the formula of Goldsmith and Laves is 0.9. This corresponds to a relatively high degree of ordering of Al and Si.

The X-ray data from the K-feldspar samples from the quartz-K-feldspar gneiss (1903 and 2544-a) are very difficult to interpret. Both these samples contain many grains which show distinct microcline grid twinning, so it was expected that the X-ray powder diagrams would be more or less identical to that of sample 145. This identity was evident for all the selected reflections except the  $130$ ,  $1\bar{3}0$ ,  $131$  and  $1\bar{3}1$ , (see Table II). Instead of giving distinct doublets for these two pairs of reflections, both samples gave a single broad asymmetric peak on the spectrogram in the ranges where doublets were expected. However, superimposed upon these

Table 11. Partial X-ray powder diffraction data on K-feldspar.

Monoclinic K-feldspar									
hkl	Calculated FeK	$d^a$	$\frac{2\theta}{CuK}$	1	2 $\theta$ , observed, CuK				
					144	2544c (1)	2544c (2)	1903	2544a
201	26.4	4.2390	20.94						
111	28.4	3.9460	22.51	22.5	22.5	22.5	22.4	22.5	
200	29.0	3.8661	22.93						
130	29.6	3.7394	23.46	23.55	23.6	23.6	23.53	23.6	
131	31.0	3.6222	24.56					24.3	
202	34.3	3.2327	27.14		27.03	27.02	27.09	27.05	
040	34.6	3.2551	27.38	27.55	27.55	27.55	27.52	27.53	
002	35.0	3.2190	27.63						
131	37.7	2.9960	29.80	29.82	29.88	29.87	29.85	29.89	
222	38.5	2.9360	30.42						
041	38.9	2.9370	30.73	30.78	30.85	30.85	30.85		
Triclinic K-feldspar									
hkl	Calculated FeK	$d^b$	$\frac{2\theta}{CuK}$	1	2 $\theta$ , observed, CuK				
					145			1903	2544a
201	26.5	4.2233	21.02						
111	28.1	3.9373	22.23	22.3					
200	29.1	3.8531	23.08				23.1		
130	29.3	3.8273	23.22	23.25			23.1-23.2	?	
130	30.3	3.7038	24.01	24.02			24.0	23.9	
131	30.7	3.6567	24.32						
202	34.2	3.2920	27.06	27.04			27.09	27.05	

Table 11, (continued)

hkl	FeK Calculated	Triclinic K-feldspar					
		d <sup>b</sup>	CuK <sub>1</sub>	2θ <sup>b</sup>			2θ, observed, CuK <sub>1</sub>
				145	1908	2544a	
220	34.6	3.2551	27.38				
002	34.7	3.2460	27.45				
040	34.8	3.2370	27.53 27.52		27.52	27.53	
131	37.3	3.0270	29.43 29.47		29.6	-?	
222	38.2	2.9562	30.18				
131	38.3	2.9508	30.26 30.19		30.15	30.15	
022	38.9	2.9070	30.73				
041	38.9	2.9070	30.73 30.83		30.83	-	

<sup>a</sup>Data for sanidine from Goldsmith and Iaves, 1954.

<sup>b</sup>Data for microcline from Goldsmith and Iaves, 1954.

144, from magnetite rich layer, mixed gneiss subunit.

145, from magnetite-quartz-K-feldspar gneiss, mixed gneiss subunit (wall rock to 144).

2544c, (1) and (2), porphyroblasts from biotite-quartz-feldspar gneiss.

1908 and 2544a, from quartz-K-feldspar gneiss.

broad peaks are identifiable subsidiary peaks.

In sample 1903 a very strong and distinct subsidiary reflection is present at  $2\theta = 23.58$ , which corresponds to the  $1\bar{3}0$  reflection of monoclinic K-feldspar. A second less distinct but very obvious subsidiary reflection in 1903 is present at  $2\theta = 24.00$ , which corresponds to the  $\bar{1}\bar{3}0$  reflection of microcline. In addition a rather faint subsidiary reflection may be present at  $2\theta = 25.1 - 25.2$  which would correspond to the  $1\bar{3}0$  reflection of microcline. Furthermore, sample 1903 has a distinct subsidiary reflection superimposed on the broad reflection at  $2\theta = 30.15$ , which would correspond with the  $\bar{1}\bar{3}1$  reflection of microcline. In addition there are very faint but distinct subsidiary reflections at  $2\theta = 29.85$  and  $2\theta = 29.6$  which would correspond to the  $1\bar{3}1$  reflection of monoclinic K-feldspar and microcline respectively.

Sample 2544-a has a very strong subsidiary peak at  $2\theta = 23.6$  which corresponds exactly to the  $1\bar{3}0$  reflection of monoclinic K-feldspar. In addition there is a distinct but weak subsidiary reflection at  $2\theta = 23.9$  which corresponds to the  $\bar{1}\bar{3}0$  reflection of microcline. Also in sample 2544-a there is a very strong subsidiary reflection at  $2\theta = 29.39$  which corresponds closely with the  $1\bar{3}1$  reflection of monoclinic K-feldspar. There is a suggestion of a subsidiary reflection of  $2\theta = 30.15$  which corresponds very closely to the  $\bar{1}\bar{3}1$  reflection of microcline. No subsidiary reflections corresponding to the  $1\bar{3}0$  and  $1\bar{3}1$  planes of microcline are clearly apparent in sample 2544-a.

Inasmuch as albite is intergrown in perthitic fashion with K-feldspars 1903 and 2544-a, it is necessary to consider the effect this will have on the X-ray diagrams. Goodyear and Duffin (1954) have presented the X-ray

powder data for a series of low and high temperature plagioclase feldspars. The 040 reflection for low albite (the reflection of greatest intensity) was compared with the corresponding reflection for K-feldspar in both samples. In each sample the 040 reflection for K-feldspar was from 4 to 5 times more intense than was the 040 reflection from the intergrown albite. The data of Goodyear and Duffin (1954) for low temperature albite-oligoclase indicate a 111 reflection with a  $2\theta$  value between 23.6 and 23.68. This albite-oligoclase reflection would not interfere with the 130 or  $\bar{1}30$  reflections of microcline, but it could amplify the 130 reflection of monoclinic K-feldspar. However, in the light of the large intensity factor (4-5) in favor of K-feldspar, it seems highly improbable that this 111 reflection could cause or even influence the very definite and rather strong subsidiary reflection at  $2\theta = 23.55$  and 23.6 which has been noted to correspond to the 130 reflection of monoclinic K-feldspar in samples 1903 and 2544-a. The  $\bar{1}31$  reflection of albite-oligoclase is in the  $2\theta$  range of 30.0 - 30.25. This reflection undoubtedly has influenced the strong subsidiary reflection in sample 1903 at a  $2\theta$  value of 30.15 ( $\bar{1}31$  microcline). Again the intensity factor in favor of K-feldspar makes it unlikely that the influence of this  $\bar{1}31$  albite-oligoclase reflection could be great enough to independently cause the subsidiary peak at  $2\theta = 30.15$ . In addition no albite-oligoclase reflections are indicated which could cause the very faint but distinct subsidiary reflections at  $2\theta = 29.85$  and 29.6 (131 of monoclinic and triclinic K-feldspar respectively). Therefore, it is concluded that the influence of the intergrown low temperature albite-oligoclase on the K-feldspar X-ray powder diagram for the two samples (1903 and

2544-a) from the quartz-K-feldspar gneiss is not adequate or of the character to markedly alter the diagram. It seems even more unlikely that the albite-oligoclase could influence the K-feldspar diagram in such a way as to produce the two broad reflections with the particular subsidiary reflections. Especially difficult to explain on the basis of albite-oligoclase effects is the very distinct and strong subsidiary reflection at  $2\theta = 23.58$  and  $23.6$  (in 1903 and 2544-a respectively) which correspond to the  $130$  reflection of monoclinic K-feldspar.

There are two interpretations of the X-ray powder diagrams of samples 1903 and 2544-a from the quartz-K-feldspar gneiss. First, it is quite possible that these K-feldspars correspond to microcline of such low triclinicity that the doublets  $131-1\bar{3}1$  and  $130-1\bar{3}0$  are near or at the point of merging, so that instead of getting two distinct reflections in these ranges, as was the case for the microcline, one obtains the two broad reflections with the subsidiary reflections superimposed. However, if much faith is placed upon these subsidiary reflections a wholly different interpretation is apparent. In brief these K-feldspar samples may consist of a mixture of triclinic microcline and monoclinic K-feldspar. As indicated previously the subsidiary reflections correspond in part to microcline reflections and in part to monoclinic K-feldspar reflections. Such a mixture might originate by the incomplete inversion of an original monoclinic K-feldspar to microcline (Laves, 1950, 1952). However, the possibilities for developing such a mixture are unlimited. Goldsmith and Laves (1950) have examined single crystals of K-feldspar in which there are areas of monoclinic and triclinic symmetry. In addition Harker (1954) has reported granite gneiss in which orthoclase and microcline occur

together, not infrequently in the same crystal. Furthermore, Mackenzie (1954) reports the occurrence of orthoclase and microcline in the same rock as well as in the same crystal. These observations lend some substantiation to the hypothesis of mixed K-feldspar polymorphs. More significant is the fact that the samples 1908 and 2544-a from quartz-K-feldspar gneiss are very closely associated with the biotite-quartz-feldspar gneiss which carries the monoclinic K-feldspar porphyroblasts. Sample 2544-a actually comes from the identical handspecimen, (shown in Plate II) as monoclinic K-feldspar porphyroblasts 2544-c, 1 and 2. Thus it would not be surprising to find monoclinic K-feldspar mixed with well twinned (triclinic) microcline in the quartz-K-feldspar gneiss. Very likely the same situation would exist in the matrix K-feldspar in the biotite-quartz-feldspar gneiss.

#### Summary and petrologic significance

It has been shown that the untwinned K-feldspar which is associated with magnetite rich layers is monoclinic and carries up to 10 per cent celsian in solid solution. In addition the K-feldspar porphyroblasts from the biotite-quartz-feldspar gneiss are monoclinic. The K-feldspar from the magnetite-quartz-K-feldspar gneiss of the mixed gneiss subunit is microcline with a triclinicity of about 0.9 and has less than 0.5 per cent celsian in solid solution. X-ray data indicate that the K-feldspar from the quartz-K-feldspar gneiss is not a true triclinic microcline, but it is either microcline with very low triclinicity or more likely it is a mixture of both triclinic K-feldspar (microcline) and uninverted monoclinic K-feldspar. In either case the bulk triclinicity value of the K-feldspar from the quartz-K-feldspar gneiss is considerably less

than that of the microcline from the mixed gneiss subunit. Chemical, petrographic and X-ray data all indicate that the amount of exsolved albite intergrown in perthitic fashion is 11 per cent or less in the K-feldspar from the mixed gneiss subunit, 10 to 15 per cent in the K-feldspar from the biotite-quartz-feldspar gneiss and as much as 20 per cent in the K-feldspar of the quartz-K-feldspar gneiss.

The monoclinic symmetry of the celsian rich K-feldspar from magnetite rich layers is difficult to explain. Inasmuch as there are so many unsolved problems concerning the stability relationships of the alkali feldspars (Laves, 1952, 1954), it is inappropriate to propose a special set of physical conditions (pressure, temperature, thermal history, etc.) to account for the monoclinic symmetry of the high celsian K-feldspar. Laves (1950) has proposed that microcline grid twinning is a transformation type twin which develops during the inversion of monoclinic K-feldspar to triclinic K-feldspar. In the light of this hypothesis it seems likely that the celsian rich K-feldspar formed under the same general physical conditions (composition excepted) as the wall rock microcline, but because of its high celsian content it did not invert from the monoclinic to triclinic form as did the low celsian wall rock microcline.

The variable content of exsolved albite in the various K-feldspars as indicated above is petrologically very significant. It is evident from the alkali feldspar solvus curve (Bowen and Tuttle, 1950) that all these K-feldspars, which are only slightly perthitic and are not true microperthites, probably came to a final equilibrium at temperatures less than 660°C. The difference in albite content of the K-feldspars indicates

that the quartz-K-feldspar gneiss came to a final equilibrium at a significantly higher temperature than did the K-feldspar porphyroblasts or matrix microcline in the biotite-quartz-feldspar gneiss. As the magnetite-quartz-K-feldspar gneiss is unsaturated in albite it is difficult to compare the low albite content of its K-feldspar with that of the other two rock types. It is difficult to explain why there should be significant temperature difference between the biotite-quartz-feldspar gneiss and the intimately associated quartz-K-feldspar gneiss. It is suggested that the quartz-K-feldspar gneiss may have crystallized from a fluid (magma) which intruded and permeated older rocks and by  $Z$ -metasomatism has caused the development of the less perthitic K-feldspar in the biotite-quartz-feldspar gneiss.

The low triclinicity of the K-feldspar from the biotite-quartz-feldspar gneiss and quartz-K-feldspar gneiss as compared to the highly triclinic microcline from the mixed gneiss subunit suggests that the latter gneisses originated under somewhat different physical conditions than the other two subunits. Tentatively it is suggested that the microcline in the mixed gneiss subunit crystallized at a lower temperature and possibly was cooled at a slower rate enabling greater ordering of  $\text{Al}^{3+}$  and  $\text{Si}^{4+}$  than in the K-feldspars in the other two gneisses. This hypothesis is in keeping with the idea that the quartz-K-feldspar gneiss was possibly an igneous rock which crystallized at a higher temperature (as indicated by the greater perthitic intergrowth) and probably cooled at a more rapid rate than the mixed gneiss subunit. Hence, the K-feldspar of the former gneiss did not completely invert to microcline but instead retained much of its original monoclinic character, i. e., greater disorder of  $\text{Al}^{3+}$  and  $\text{Si}^{4+}$ .

ZIRCON

The zircons in the mixed gneiss subunit are quite distinct. They are very small spherical shaped, disseminated grains and are colorless in thin section. Rarely are the zircons elongated and in this case they usually have rounded terminations. Zircons were separated from a layer of garnet-biotite-sillimanite-quartz gneiss (B-151f, Table 6) from the mixed gneiss subunit. There were at least two varieties of zircon in the concentrate. The most abundant type is a pinkish brown color and had the following color formula:

c = brownish yellow,  
Lc = lighter brownish yellow.

The second variety of zircon in the concentrate is less abundant and is of distinctly lighter color. It is pale lemon yellow with no brownish tints. It appears almost colorless which is in marked contrast to the pinkish brown of the principal variety. Both of these varieties of zircon are distinctly rounded. Some grains are perfect spheres but others are slightly elongated with rounded terminations. The presence of two kinds of rounded zircons in a gneiss which has such strong metasedimentary affinities is indeed suggestive of a clastic origin for the zircons.

Zircon in the quartz-K-feldspar gneiss is of a single distinct type. It is a dark reddish brown color and fairly pleochroic. It usually occurs as disseminated, stubby, euhedral crystals. The crystal faces are sometimes slightly rounded (resorbed?). This zircon is quite distinct in color and morphology from the zircons described above and corresponds to what might be considered a primary igneous zircon.

From the above description it might be concluded that the zircons

from the mixed gneiss subunit are of sedimentary origin and indicate the sedimentary affinities of much of the mixed gneiss subunit. In contrast it is suggested that the zircons of the quartz-K-feldspar gneiss are of primary origin and indicate that the gneiss is a magmatic rock.

#### GARNET

Within the Edison unit in the Edison area garnet is present in all the principal rock types. However, its distribution is quite irregular within these rock types. Garnet occurs as disseminated grains and as porphyroblastic aggregates of grains usually oriented in the fabric plane of the rock. Generally, the garnet is intergrown with iron oxides and quartz in a poikilitic fashion. All the garnets are a pink to red color.

In Table 12 is listed a complete chemical analysis of a garnet (E-153a) which was separated from a magnetite rich layer from the Roberts Mine. The garnet is a spessartite-almandite with less than 15 mole per cent of the other garnet molecules. For comparison an analysis of a garnet from a partially granitized paragneiss from the Adirondacks (Engel and Engel, 1953) is included in Table 12. A weight per cent modal analysis of the rock from which the garnet was separated also is given in Table 12 (E-153a). The rock corresponds to an ore and might be called a garnet-K-feldspar-quartz-magnetite gneiss.

A sample of garnet was also separated from a layer of garnet-biotite-sillimanite-quartz gneiss (E-151f, Table 6) from the mixed gneiss subunit and analyzed only for MnO. The analysis is listed in Table 13. The composition of the rock corresponds to a rock of metasedimentary character

Table 12. Chemical composition of garnet.

	B-153a	*	Mode, B-153a, Wt. %
SiO <sub>2</sub>	36.38	39.03	39 ± 2.0
Al <sub>2</sub> O <sub>3</sub>	20.82	22.05	13 ± 1.0
TiO <sub>2</sub>	0.05	0.07	33 ± 2.0
Fe <sub>2</sub> O <sub>3</sub>	1.50	0.59	biotite
FeO	21.92	22.43	garnet
MnO	14.51	1.57	accessories <sup>a</sup>
MgO	1.11	6.49	100
CaO	3.58	1.80	
H <sub>2</sub> O +	0.04	0.13	
H <sub>2</sub> O -	0.03	0.06	
P <sub>2</sub> O <sub>5</sub>	n.d.	0.05	
	99.97	100.27	

Mode

Pyrope	4.5
Almandite	50.7
Spessartite	34.2
Andradite	4.6
Grossularite	6.0
	100.0

B-153a, Garnet from magnetite rich gneiss (ore), Roberts Mine,  
Edison, New Jersey; d = 4.157, Doris Thaelitz, analyst, 1954.

\* Garnet from partly granitized paragneiss, Adirondacks, Engel and  
Engel, 1953.

<sup>a</sup> Apatite, fluorite, zircon and monazite.

although the proportion of ore is fairly high. The MnO content of the garnet is  $12.7 \pm 1.3$  weight per cent, which corresponds to about 30 mole per cent spessartite.

A sample of garnet was also separated from the quartz-K-feldspar gneiss and analyzed for MnO. The analysis (1908) is listed in Table 13. This garnet carries only  $4.9 \pm 0.5$  weight per cent MnO which corresponds to 11 mole per cent spessartite.

Table 13. MnO analyses of garnets.

	B-151f*	1908*
MnO (wt. %)	$12.7 \pm 1.3$	$4.9 \pm 0.5$

B-151f, from a garnet-biotite-sillimanite-quartz gneiss within the mixed gneiss subunit.  
1908, from quartz-K-feldspar gneiss.

\* Analyzed by the Minnesota Rock Analysis Laboratory, 1954.

Miyashiro (1953) has pointed out that at high metamorphic grade, amphibolite facies or higher, the composition field of pyrospilites is enlarged such that Fe and Mg rich garnets can form as readily as Mn rich garnets. In essence at such metamorphic temperatures garnet does not distinguish between the 3 ions and as a result the composition of the garnet is a consequence of the composition of the petrologic system. Thus the differences in MnO content as described above indicate differences in the MnO content of the rock forming system. Therefore, it seems safe to conclude that Mn is enriched in the mixed gneiss subunit (ore zone) relative to the iron poor wall rocks such as the quartz-K-feldspar gneiss.

### MAGNETITE-HEMATITE-ILMENITE-RUTILE PARAGENESIS

#### Introduction

The following section is devoted to the detailed description of the magnetite-hematite-ilmenite-rutile paragenesis (iron and titanium oxides) of the magnetite-quartz-K-feldspar gneiss and the related rocks of the Edison unit. The observations have been made mostly on the samples taken from the Edison area although the data apply to the Edison unit as a whole. The magnetite-quartz-K-feldspar gneiss of the Sherman unit has been included in this discussion.

The examination of the iron and titanium oxides has been of a petrographic and chemical nature. Numerous polished surfaces of the magnetite-quartz-K-feldspar gneiss and its variations as well as a limited number of polished surfaces of the biotite-quartz-feldspar gneiss, quartz-K-feldspar gneiss and lime rich subunit were examined. These petrographic data are summarized in Tables 4B, 5, 6, 8, and 9. The chemical data include the partial chemical analyses of the magnetic and non-magnetic iron and titanium oxide fractions of five samples of magnetite-quartz-K-feldspar gneiss from the Edison area and three samples from the Sherman unit. The magnetic fraction includes magnetite and any intergrown minerals such as ilmenite and hematite. The non-magnetic fraction includes hematite, ilmenite, and rutile which generally occur in various intergrown assemblages. The partial chemical analysis of each of these fractions involved the determination of FeO,  $Fe_2O_3$  and  $TiO_2$ . These partial chemical analyses of the two fractions from the eight samples are listed in Table 4A along with the modal analyses of the rocks from which the samples were taken (Table 4B). The modal analyses were made

from three thin sections (two of which were stained for K-feldspar; Keith, 1939; Chayes, 1952) and two polished surfaces of each sample. The partial analysis of each fraction has been recalculated to 100 per cent for iron and titanium oxide minerals as found in the polished surface examination of the particular sample. These recalculations are also listed in Table 4A. Knowing the weight proportion of the magnetic and non-magnetic fractions in each sample it has been possible to calculate the actual weight per cent of the iron and titanium oxide minerals in each rock, these data are also listed in Table 4A.

The iron and titanium oxide system is best represented by the  $\text{FeO} - \text{Fe}_2\text{O}_3 - \text{TiO}_2$  triangular diagram (Figure 7). All the oxide assemblages discussed in this section with the exception of that from the quartz-K-feldspar gneiss have a bulk composition well to the  $\text{Fe}_2\text{O}_3$  side of the magnetite-ilmenite join. The first part of this description deals with the iron and titanium oxides in the magnetite-quartz-K-feldspar gneiss and its lithologic variations; in the last part a brief description of the iron and titanium oxides in the other subunits of the Edison unit is presented. The entire discussion is centered about various portions of the iron and titanium oxide system. First, the magnetite-ilmenite-hematite portion of the system which includes the magnetic fraction is discussed. Second, the ilmenite-hematite-rutile portion of the system which includes the non-magnetic fraction is discussed. Finally, some special iron and titanium oxide intergrowths are described.

#### Hematite-ilmenite and magnetite-hematite systems

Introduction. It is well known that magnetite may carry a considerable amount of titanium in its structure at elevated temperatures

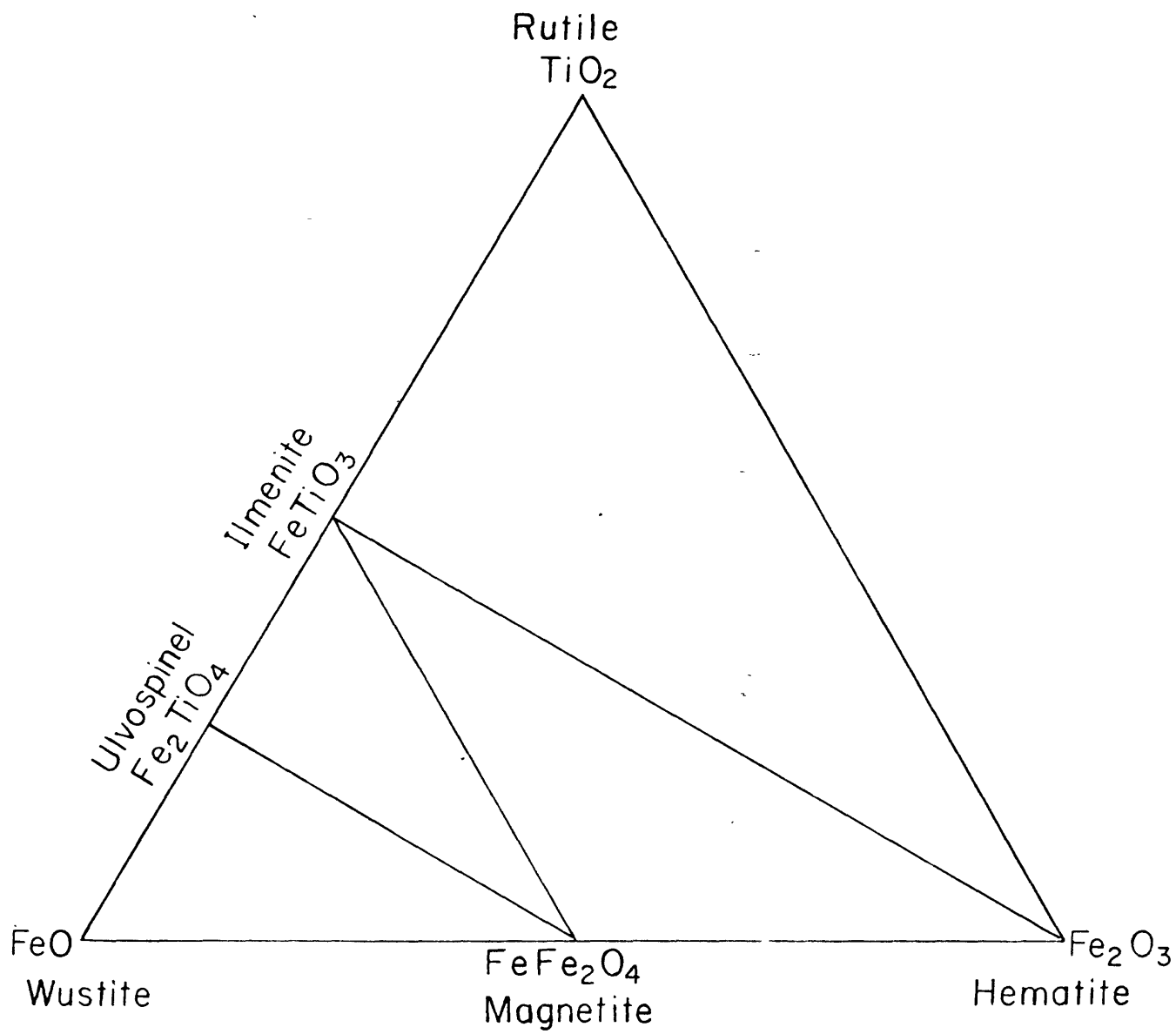


FIG. 7. Triangular diagram of the iron and titanium oxide system showing possible minerals

(Randohr, 1926, 1939, p. 660, 1950; Edwards, 1938, 1952; Chevallier, 1950; Foslie, 1928; Jouravsky, 1936; Pouillard, 1949, 1950 and Buddington et al., 1953). Many analyses of such titaniferous magnetites recalculate to compositions very near the magnetite-ilmenite join. Generally the excess titanium has exsolved as ilmenite from the magnetite structure. Frequently, however, analyzed magnetites carry FeO in excess of that required for the formation of the ilmenite molecule and therefore are recalculated into ilvospinel ( $\text{Fe}_2\text{TiO}_4$ ), ilmenite and magnetite or just ilvospinel and magnetite. These samples frequently carry exsolved ilvospinel as lenses parallel to the cube plane (Hogenboom, 1946; Randohr, 1953; Girault, 1953). The experimental data of Darken and Gurry (1946) shows that pure magnetite never carries excess whitite (FeO) in its structure at any temperature. However, there are a few natural magnetites which carry FeO in excess of that which can combine with  $\text{TiO}_2$  to form ilvospinel or with another sesquioxide to form some other spinel molecule, (Buddington, personal communication). There appears to be no obvious answer to this discrepancy between the synthetic and natural magnetites. Many samples of analyzed magnetite carry excess  $\text{Fe}_2\text{O}_3$ . These are generally intergrown to some extent with hematite. All the analyzed magnetites from the magnetite-quartz-feldspar gneiss are intergrown with hematite so that the partial analyses always recalculate with excess  $\text{Fe}_2\text{O}_3$ .

Magnetite-ilmenite. All the samples of magnetite which have been examined in polished surface are intergrown with ilmenite to some extent and may therefore be called ilmenomagnetite. As can be seen from the analyses of the magnetic fraction (Table 4A) the mole per cent of inter-

grown ilmenite varies from 0.4 to 4.1. In polished surface cross section the intergrown ilmenite has the form of long thin "blades" which are oriented parallel to the octahedral plane of the host magnetite (Plate 12). These "blades" terminate by lensing or pinching out. The "blades" are from 0.02 to 0.10 mm thick and may be 20 to 50 times as long. In three dimensions the intergrown ilmenite must be in the form of planar disks or thin tablets which are oriented in the octahedral plane. Sometimes ilmenite is intergrown as irregular shaped grains which are concentrated near the borders of the host magnetite.

Although no experimental data are available on the magnetite-ilmenite system, in view of the present knowledge of titaniferous magnetites (Randehr, 1950; Buddington et al., 1953; loc. cit.) it seems certain that the intergrown ilmenite is of exsolution origin. The actual content of solid solution  $TiO_2$  is extremely low, and varies from 0.14 to 1.29 weight per cent of the magnetic fraction. Using the  $TiO_2$  content it is noted that the temperature of formation of the magnetite-quartz-K-feldspar gneiss corresponds to that of the lower range of the amphibolite facies of the Adirondacks (Buddington, et al., 1953).

Magnetite-hematite (magnetite). All the magnetite within the magnetite-quartz-K-feldspar gneiss is intergrown to some extent with hematite. As can be seen in Table 4A the mole per cent of intergrown hematite varies from 8.1 to 32.1 of the host magnetite. In polished surface cross section the intergrown hematite has the form of thin films or triangular spikes which are consistently oriented in the octahedral plane of the host magnetite (Plate 12). Thus the actual shape of the intergrown bodies of hematite is that of thin planar disks (films) and thin wedges (spikes)

both oriented in the octahedral plane. These bodies may be so small that even the finest grinding would not enable their clean separation from the host magnetite. They are much smaller than the ilmenite bodies. When the hematite content is high, the films and spikes form an interlocking octahedral network. In very hematitic magnetite the films and spikes coalesce to yield blebs and grains of hematite of less regular form than the films and spikes. Thus magnetite with sparse hematite in a very regular octahedral pattern passes into magnetite with a very large proportion of hematite as films, spikes, irregular blebs, grains and patches. Occasionally actual veinlets of hematite cut across the host magnetite.

In a single grain of magnetite the distribution of hematite varies considerably. Often the hematite is concentrated along the border of the host grain. In this case the films and spikes of hematite project in from the borders of the magnetite and shortly die out into the grain. Even more striking is the distribution of hematite along the borders of cracks and veinlets within the host magnetite. The cracks and veinlets are rarely filled with hematite but films and spikes of hematite project outward from the border of the fractures and die out rapidly away from them. It appears evident that the distribution of hematite is controlled by such cracks and veinlets as well as by the magnetite grain boundaries.

The amount of intergrown hematite varies radically from grain to grain within a single polished surface. Thus, one magnetite grain may carry as much as 70-80 volume per cent of hematite and an adjacent grain as little as 10-15 per cent.

In the magnetite the intergrown hematite always shows a consistent

textural relationship to the intergrown ilmenite tablets. Films and spikes of hematite are oriented parallel to and athwart individual octahedral tablets of ilmenite. Those at an angle sharply terminate against the ilmenite "blades" but never cross cut them (Plate 12). Such sharply terminated films and spikes of hematite are never found to have a continuous half on the opposite side of the ilmenite "blade", as though the ilmenite replaced a section through the middle of a film or spike of hematite. These textural relationships suggest that the ilmenite disks formed before the intergrown films and spikes of hematite and that the latter grew in the host magnetite up to the ilmenite-magnetite interface at which point their growth abruptly terminated.

Darken and Gurry (1946) as well as Greig, et. al. (1935) and Schnabl (1941) have shown that magnetite takes excess  $\text{Fe}^{3+}$  into solid solution only above  $1000^{\circ}\text{C}$ . This fact indicates that the magnetite-hematite intergrowths are not of exsolution origin. To the contrary the experimental data coupled with the distinct textural relationships described above prove that the intergrown hematite is an alteration product of the host magnetite and thus may be correctly called martite. The delicate nature of the intergrowth and the octahedral control show that the alteration was of replacement nature. The alteration is considered to be of a retrograde nature in that it is postulated that the martite developed during the cooling stages of the rock in response to changing physical conditions. This hypothesis is developed in more detail in a subsequent section which deals with the physical chemistry of the iron and titanium oxide system.

### Hematite-ilmenite-rutile system

Introduction. In nearly all the samples of magnetite-quartz-K-feldspar gneiss which were examined minerals of the non-magnetic iron and titanium oxide fraction were observed. These include the minerals hematite, ilmenite, rutile and various distinctive intergrowths of them. Of the eight samples of magnetite-quartz-K-feldspar gneiss which were used for analysis (Table 4A) all but sample 143 carried sufficient non-magnetic oxides to enable a simple separation and partial chemical analysis. The non-magnetic oxide fraction of these eight samples includes all the various intergrowths which have been found throughout the mixed gneiss subunit. Thus the eight samples are very representative and provide a good analytical framework on which to base interpretation for the mixed gneiss subunit.

As can be seen from Table 4B, the three non-magnetic oxides, hematite, ilmenite, and rutile, occur in at least eight different varieties. The varieties are various kinds of intergrowths of the three minerals. In addition some of the samples, such as 149, 154, 153 and 151, have small amounts of magnetite (martitic) intergrown with the non-magnetic oxides. Where this has been observed the composition of the non-magnetic fraction has been recalculated to include some magnetite (Table 4A). The bulk compositions of the various intergrowths have been estimated from the chemical analyses and from petrographic measurements. These estimates are indicated in Table 4B by numerical subscripts. The compositions of the various intergrowths are plotted in a hematite-ilmenite-rutile diagram (Figure 8). The diagram shows that the intergrowths belong to two groups. One group has compositions near to the

hematite-ilmenite join and the other group has compositions near to the hematite-rutile join. These two groups are discussed separately below.

The non-magnetic oxides, hematite, ilmenite and rutile, and their various intergrowths with the exception of martite and a peculiar alteration of ilmenite (composed of rutile and hematite) are all considered to be of primary origin. There are no textural relationships which suggest that these oxides are of secondary origin. These oxides appear equivalent texturally to the associated magnetite and are believed to have formed contemporaneously with it. In addition primary hematite is quite distinct from obvious secondary hematite (martite). The most important distinction is that martite is always devoid of any intergrown ilmenite or rutile while adjacent grains of primary hematite are well intergrown with these other oxides. In addition there are clear color differences between primary and secondary hematite as described in Table 14.

It is very difficult to recognize all the mineral phases in the various intergrowths of non-magnetic oxides. This is particularly true in the extremely fine intergrowths. Where possible petrographic observations were substantiated by chemical data. Listed in Table 14 are the petrographic criteria which were found most definitive for identification purposes.

Hematite-ilmenite with minor rutile. There are two principal intergrowths which have compositions nearly on the hematite-ilmenite join. Ilmenohematite is the intergrowth richer in hematite and hemoilmenite is the intergrowth richer in ilmenite. Frequently both these are intergrown with minor amounts of rutile. In such cases the prefix rutile has been

Table 14. Petrographic criteria for identification of iron and titanium oxide minerals.

	Magnetite	Rommatite	Ilmenite	Rutile
Isotropic	Strongly anisotropic	Strongly anisotropic	Strongly anisotropic brownish-yellow internal reflections in grains but rarely in thin disks and lenses	
Color	Ilmenite-bright white Hematite-brownish White	Magnetite-very white Ilmenite-very bright white	Magnetite-brownish gray Hematite-violet tinged brown	Hematite-nearly equi- valent Hematite-brownish, darker
Morphology	Rutile-nearly equivalent	Rutile-bright white Magnetite-brownish Violet-white, duller	Rutile-distinctly darker	Ilmenite-distinctly brighter, very dif- ficult to see dif- ference in fine intergrowths
HCl	Positive	Negative	Negative	Negative
	Occurs as tablets parallel to 0001 in ilmenite-hematite intergrowths and rutile	Lenses and disks parallel to 0001 in ilmenite-hematite intergrowths. Disks and wedges in magnetite (rarely)	Lenses and disks parallel to 0001 in ilmenite-hematite intergrowths. Tab-lets parallel to 111 in magnetite.	Disk's parallel to rhombohedral plane in ilmenite-hematite intergrowths. Rhombo- hedral disks and thin lenses parallel to 0001 in rutile-hematite

added as a modifier to the principal name.

Ilmenohematite consists of host hematite with intergrown ilmenite (Plates 13 and 14). The ilmenite is intergrown in two distinct forms. The largest portion of the intergrown ilmenite (probably 70-80 per cent of it) is in the form of thick lenses. The remainder of the intergrown ilmenite is in the form of very thin disks which appear as thin lenticular films in polished surface cross section. Both the lenses and films are oriented in the basal plane of the host hematite. The cross section of individual thick lenses may be as much as 1/10 to 1/5 the width of the entire grain of ilmenohematite. There are rarely more than 6-10 such lenses in any single grain. The cross section of individual films is about 1/100 the width of the host grain. There is definitely a size discontinuity between the thick lenses and thin disks of intergrown ilmenite (Plate 14). There is no indication that a continuous size gradation exists between the thick lenses and thin disks. It is interesting that the hematite host immediately next to the thick lenses of ilmenite is quite devoid of any thin disks of ilmenite (Plate 14). In addition within the thick lenses of ilmenite, thin disks of hematite are usually present. These disks of hematite are similar in form, size, and orientation to the ilmenite disks within the hematite host.

Hemoilmenite consists of host ilmenite with intergrown hematite (Plate 15). This intergrowth is entirely similar to the ilmenohematite. In hemoilmenite hematite occurs as thick lenses and thin disks in host ilmenite. Within the thick lenses of hematite are thin disks of ilmenite. In addition the host ilmenite is more or less devoid of disks of hematite adjacent to the thick lenses of hematite. All the lenses and films are

oriented in the basal plane. Obviously this intergrowth is quite homologous to the ilmenohematite intergrowth.

Intergrown rutile in the hemoilmenite is seldom present. When present it occurs as irregular lenses and as included small grains. Rutile intergrown with ilmenohematite may be in such lens and grain form but usually it is in the form of long thin flat disks which are oriented in the rhombohedral (?) plane of the host hematite. Thus, the rutile disks are perpendicular and at oblique angles to the lenses and films of ilmenite which are oriented in the basal plane of the host hematite. No clear evidence was observed which suggests that the rutile disks formed other than simultaneously with the whole intergrowth.

The preferred orientation of lenses and films parallel to the basal plane and of rutile disks parallel to the rhombohedral (?) plane impart a great uniformity to the intergrowths of hemoilmenite, ilmenohematite and rutile-ilmenohematite. This is the single most striking feature of those intergrowths.

In most samples of the magnetite-quartz-K-feldspar gneiss ilmenohematite or rutile-ilmenohematite is present. Frequently hemoilmenite is also present, but it is less abundant than ilmenohematite. Randohr (1926, 1950) proposed a hypothetical temperature-composition phase diagram for the ilmenite-hematite system in which there is complete solid solution at elevated temperatures. Certainly the relationships described above can be simply interpreted as due to the exsolution of various solid solutions between ilmenite and hematite. Thus, hemoilmenite represents the solid solution member richer in ilmenite and the ilmenohematite represents the solid solution member richer in hematite. As some samples,

such as 149 (Table 4) carry both these solid solution members, it may be concluded that the magnetite-quartz-K-feldspar gneiss came to equilibrium at a temperature below the crest of the solvus curve so that two solid solution members were in equilibrium. With cooling these two solid solutions would exsolve to yield the independent intergrowth of hemo-ilmenite and ilmenohematite. Frequently samples carry only ilmenohematite or rutile-ilmenohematite without the corresponding solid solution member, i. e., hematite. Generally the composition of such intergrowths is more hematitic than if hemoilmenite were present. This suggests that the rock formed at the same temperature, but that the bulk composition of the oxide fraction was to the hematite side of the solvus curve so that only a single solid solution member formed, which exsolved upon cooling when the solvus curve was intersected.

Unfortunately there are no experimental data on the ilmenite-hematite system which would allow a rigorous interpretation of the solid solution relationships. However, from the relationships found in the magnetite-quartz-K-feldspar gneiss it is possible to speculate as to the specific nature of the solvus curve for the system. Many of the compositions of the hemoilmenite and ilmenohematite intergrowths are within 10-15 per cent of being 50:50 mixtures of the two mineral phases. This means that the two solid solution members have formed at a temperature only slightly below the temperature of the crest of the solvus curve. If the non-magnetic oxides are of primary origin this means that the crest of the solvus curve must be near to the temperature at which the mixed gneiss subunit came to equilibrium, which is assumed to be of the order of  $500^{\circ} \text{ C} \pm 50^{\circ}$ .

The textural relationships in the solid solution intergrowths allow some speculation on the shape of the solvus curve. It is postulated that the ilmenite-hematite solvus curve has a very flat broad crown. Thus, if a solid solution pair form at a temperature just below the crest of the solvus and if the solvus curve has a broad crown, then the bulk of the exsolution would take place during a very small temperature drop in the upper temperature interval. It is during this interval that the thick lenses of ilmenite and hematite would form. Thus, their large proportion and size can be attributed to the fact that the largest proportion of ilmenite and hematite was exsolved during this small temperature interval and to the fact that the ion diffusion rate was greater in this upper temperature interval which enabled a rapid migration of ions into fewer but larger exsolution bodies. In such an interpretation the very thin disks of ilmenite and hematite are the excess material which was exsolved from the host crystal and thick lenses during the final stages of cooling along the steep slopes of the solvus curve. This stage corresponds to a very large temperature interval with very minor changes in the compositions of the solid solutions. Utilizing such an interpretation makes it unnecessary to assume polymorphic changes to account for the odd exsolution textures (Lindahl, 1926; pp. 701-704, 1950). A proposed solvus curve for the ilmenite-hematite system is presented in a portion of Figure 8.

Hematite-rutile with minor ilmenite. Intergrowths of hematite, rutile and ilmenite which have bulk composition nearly on the hematite-rutile join are very common in the magnetite-quartz-K-feldspar gneiss. As indicated in Table 4 and Figure 8, the intergrowths include hemorutile,

rutilohematite, and ilmeno-rutilohematite in addition to pure rutile. After Remdohr (1939) it is postulated that a solid solution series exists between hematite and rutile and that these intergrowths result from the exsolution of various solid solutions in this series, although in some cases alteration effects are superimposed upon the primary solid solution intergrowths.

Ilmeno-rutilohematite occurs in samples 145 and 146 of the magnetite-quartz-K-feldspar gneiss (Table 4 and Plate 16). The compositions of these intergrowths as estimated from the partial chemical analysis are given in Table 4. In this variety hematite forms the host mineral and rutile is intergrown as thin lenses which are oriented parallel to the basal plane of the hematite. In addition rutile occurs as thin flat disks oriented in the rhombchedral (?) plane of the hematite. Ilmenite occurs as thin lenses parallel to the basal plane and appears to be altered in various degrees to a mixture of rutile and hematite (see subsequent section).

Rutilohematite is morphologically very similar to ilmeno-rutilohematite. Rutile is again intergrown as lenses parallel to the basal plane and as disks parallel to the rhombchedral (?) plane. Sometimes rutile occurs as irregular grains and masses near the border of the host hematite grain. No ilmenite is present. Occasionally a dark gray (non-opaque) mineral is intergrown with the hematite. Rutilohematite is present in samples 154, 153, and 151 (Table 4), which are all from the Sherman unit.

Hemorutile is a third variety of intergrowth which consists of host rutile with intergrown hematite (Plate 17). The hematite occurs as small

lenses and forms no more than 10 per cent of the intergrowth. Usually a dark gray non-opaque mineral (corundum?) in long lenticular blades is intergrown with the rutile. Hemorutile is present in samples 153 and 151 (Table 4), both of which are from the Sherman unit.

It is postulated that there is limited solid solution between hematite and rutile at the temperature of formation of the magnetite-quartz-K-feldspar gneiss. Hemorutile and rutilohematite are thus exsolution intergrowths of two primary solid solution mixtures. Samples 151 and 153 carry both these intergrowths and therefore give the approximate limits of solid solution for the temperature of formation of this gneiss (Figure 8). Sample 146 differs from the other samples only in its slight content of ilmenite. Sample 145 is anomalous and may be an original ilmenohematite in which the ilmenite has been partially altered to rutile and hematite so that the bulk composition of the intergrowth does not represent the original solid solution. It is apparent from Figure 8 that although there is almost complete solid solution between hematite and ilmenite at the temperature of formation of the magnetite-quartz-K-feldspar gneiss there is only limited solid solution between hematite and rutile; compare the compositions of the non-magnetic oxide intergrowths of 149 to 151, 154, 153, and 146. Thus it seems likely that the crest of the postulated solvus curve between hematite and rutile will be at a somewhat higher temperature than the solvus of the hematite-ilmenite system. On the basis of the partial chemical analyses and petrographic data described above a hypothetical subsolidus temperature-composition phase diagram for the ilmenite-hematite-rutile system is presented in Figure 8. The compositions of the supposed primary solid

solutions for seven of the samples listed in Table 4 are plotted in the diagram for the postulated temperature of crystallization of the magnetite-quartz-K-feldspar gneiss. In addition the compositions of the non-magnetic oxides from samples 148 and 152 (Table 15) are indicated in the diagram.

#### Intergrowths of magnetite with non-magnetic iron and titanium oxides

Frequently magnetite is intergrown with the non-magnetic iron and titanium oxides in the magnetite-quartz-K-feldspar gneiss. The bulk compositions of such intergrowths have been estimated from the partial chemical analyses and petrographic observations and are indicated in Table 4 by the usual subscripts. Magnetite is intergrown with hematite and ilmenohematite (Plates 13 and 15) but is particularly abundant in the hematite-rutile intergrowths (Plates 18 and 19).

In such intergrowths magnetite occurs as thick (up to 1/10 the width of the grain) tablets (blades or laths in polished surface cross section) which are oriented parallel to the basal plane of the host and usually extend completely across the host grain. Thus the magnetite tablets are more continuous than the lenses of ilmenite, hematite, etc. If the magnetite tablets terminate within the host grain they lens out abruptly. The intergrown magnetite is always slightly martitic (5-10 per cent). The martite occurs as film and spikes parallel to the octahedral plane of the magnetite. Magnetite tablets in hematilmenite (Plate 15) and ilmenohematite (Plate 13) never make contact with the hematite member of the intergrowth. Instead there is always a thin layer or selvage of ilmenite separating the magnetite tablet from the rest of the intergrowth. However, this is not the case in intergrowths of magnetite

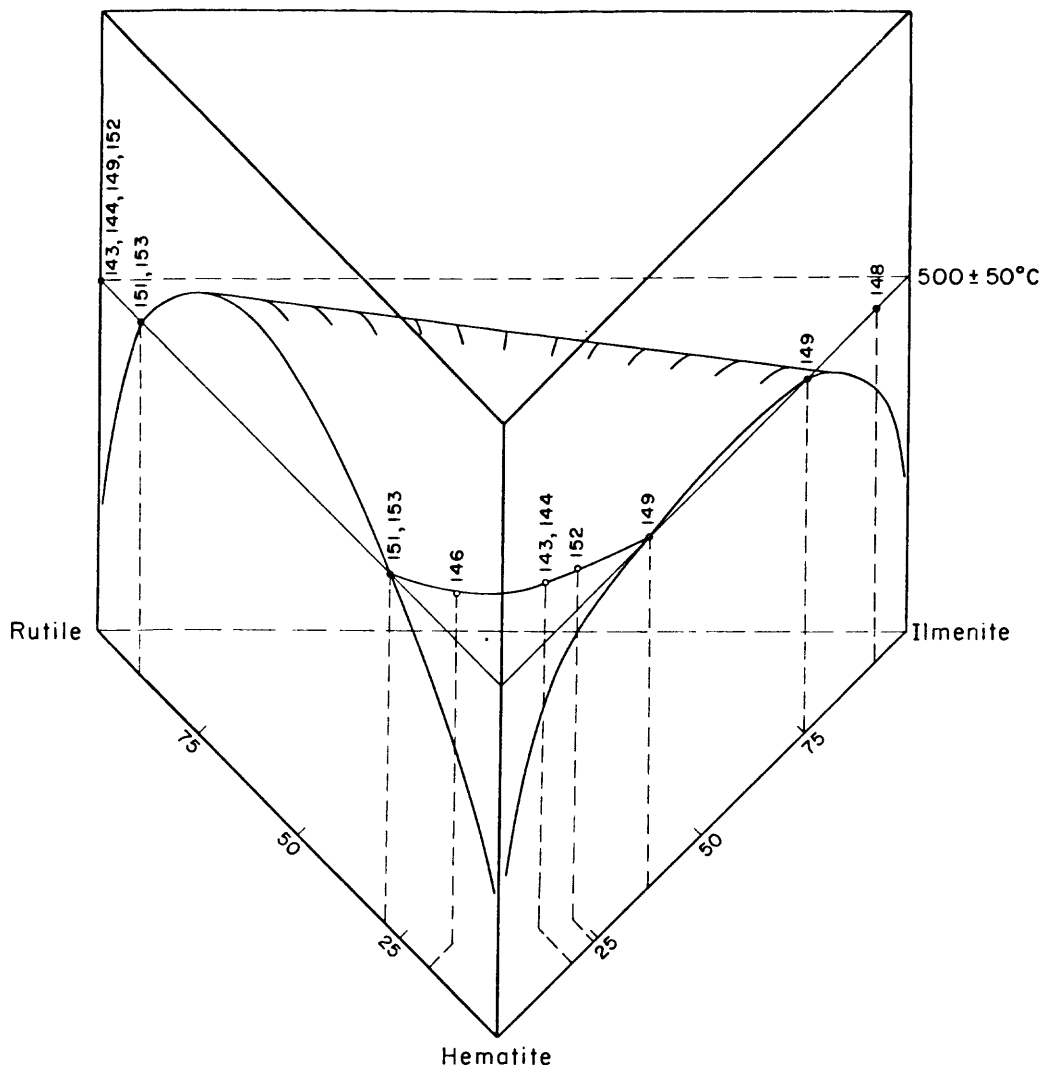


Fig. 8 Tentative subsolidus temperature - composition phase diagram for a portion of the hematite-ilmenite-rutile system based on data from Table 4

with rutillohematite (Plate 18), hemorutile or rutile (Plate 19) (samples 154, 153 and 151, Table 4). In these types the magnetite tablets make contact directly with hematite and rutile. The intergrowths of magnetite and rutile are particularly striking and occur in the magnetite-quartz-K-feldspar gneiss of the Sherran unit.

Characteristically the per cent of intergrown magnetite varies over wide limits from sample to sample and from grain to grain within the same sample. Thus in the Edison area, the amount of magnetite intergrown with the ilmenite-hematite series varies from 0 to 10 per cent. Even in a single sample, such as 149, the magnetite content varies from 0 to 10 per cent from grain to grain of ilmenohematite and hemobilmenite. The per cent of magnetite intergrown with the hematite-rutile series and particularly rutile is much greater than that intergrown with the ilmenite-hematite series. However, the per cent of intergrowth is just as variable and varies from 0-50 per cent from sample to sample as well as from grain to grain within a single sample.

There are several possible interpretations for these intergrowths of magnetite with non-magnetic iron and titanium oxides. It seems unlikely that these intergrowths could result from the simple exsolution of a solid solution between magnetite-hematite-ilmenite and rutile. Experimental data are available (Barker and Gurry, 1946) which show that there is no solid solution of magnetite in hematite. In addition rarely has ilmenite with exsolution intergrowths of magnetite been reported (Ferdot and Gaffrey, 1952). It is also difficult to explain on the basis of a solid solution theory why the amount of magnetite varies so radically from grain to grain within a single sample.

Another possible interpretation is that primary magnetite was replaced by hematite, ilmenite and rutile. However, it seems unlikely that such regular intergrowths could develop by this process.

A third interpretation is really a modification of a solid solution theory and might be termed incongruent exsolution because of its similarity to incongruent melting. Incongruent exsolution takes place when one or both of the solid solution end members exsolve as different compounds either by mutual reaction between the two end members or by the actual break up of a single end member into two compounds. In this case it is conceivable that a solid solution between hematite and ilmenite upon cooling could exsolve as a mixture of hematite, ilmenite, rutile and magnetite simply by the reaction of hematite and ilmenite as indicated below to yield magnetite and rutile.



If the process went to completion the original solid solution of hematite and ilmenite could be changed to a nearly pure mixture of magnetite and rutile (depending upon the original composition of the solid solution). If such a process took place the amount of magnetite and rutile in such intergrowth should be about identical. This is not always the case in the samples studied. However, it is possible that during such an incongruent exsolution process there would be considerable redistribution of material so that the primary composition of the grains would be changed. For such a process to take place it seems necessary to postulate special physical conditions under which magnetite and rutile are more stable than hematite and ilmenite. In this connection it is interesting that Landohr (1939) recorded that solid solutions of hematite-ilmenite were replaced

by a mixture of magnetite and rutile.

The most probable explanation for the intergrowths of non-magnetic iron and titanium oxides and magnetite is that of simultaneous crystallization of magnetite with the respective solid solution of the non-magnetic iron and titanium oxides. During cooling the solid solution of hematite-ilmenite or hematite-rutile would exsolve. It is postulated that the ilmenite rim or selvage around the magnetite tablets developed during the exsolution process and represents a physical arrangement of minimum energy.

It is postulated that the martite which is present within the magnetite tablets developed at the same time and under the same conditions as did the martite in the free magnetite grains.

Ramdohr (1929) recorded the presence of intergrowths of magnetite with ilmenohematite and hemobilmenite. He did not record the presence or absence of an ilmenite selvage around the magnetite tablets. As described above, the magnetite tablets which he observed were oriented parallel to the basal plane of the host ilmenite-hematite intergrowth. Ramdohr postulated that such intergrowths were caused by the reduction of hematite lenses to magnetite. He proposed a change to zero reducing conditions to produce such a reaction, but he did not attempt to quantitatively evaluate how such a change in the physical conditions could take place or what the important physical factors were. His theory is certainly worthy of more specific evaluation and will be discussed in a section on the physical chemistry of the iron and titanium oxides.

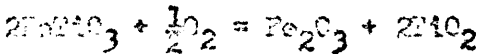
#### Alteration of ilmenite

Both the tablets of ilmenite in magnetite and the ilmenite intergrow-

with hematite are in some places partially or completely altered to a very fine grained aggregate of several minerals. Usually the alteration occurs in small patches (Plate 15) with no obvious structural control, but occasionally an entire ilmenite body is altered.

The alteration consists of a sort of "mottled aggregate" which is composed of 2 to 3 discrete minerals. The over all color of the aggregate in polished surface is whitish gray. The aggregate appears distinctly brighter than the host ilmenite and has a strong internal reflection with a yellow to brownish-red color under crossed nicols. Under extreme high power and with the use of immersion oil lenses it was possible to recognize both rutile and hematite in all the aggregates. In addition relic grains of ilmenite were sometimes present.

Thus, the alteration of ilmenite appears to be a simple oxidation of ilmenite to rutile and hematite. Such an alteration could take place according to the following chemical reaction:



Visual estimates of the "mottled aggregates" indicate that rutile is considerably more abundant than hematite. This of course should be the case if the alteration process took place as indicated above, as 2 moles of rutile are produced per 1 mole of hematite. Thus the petrographic estimates substantiate the proposed theory of alteration.

In the magnetite-quartz-K-feldspar gneiss martite is ubiquitous. However, in many samples ilmenite is unaltered. Although the martitization of magnetite and the alteration of ilmenite to rutile and hematite are both secondary oxidation processes, it seems likely that they take place under slightly different conditions. It appears as though martite

develops more readily than the "mottled aggregate". It may be that the reactions require slightly different  $p(O_2)$ . (See section on physical chemistry of iron and titanium oxides.)

Randohr (1939) has recorded the alteration of ilmenite to rutile plus hematite and to anatase plus hematite. He believes such alteration to be of hydrothermal origin. His observations and interpretations agree in principle with those presented here.

#### Iron and titanium oxides of the other rocks of the Edisen Unit

Sufficient detailed studies of the iron and titanium oxides of the lime rich subunit, the biotite-quartz-feldspar gneiss and the quartz-K-feldspar gneiss have been done to enable some general comparisons with the magnetite-quartz-K-feldspar gneiss.

The iron and titanium oxide mineral assemblage in the lime rich subunit is very similar to the assemblage in the magnetite-quartz-K-feldspar gneiss. The magnetite carries about the same amount of intergrown ilmenite and is always slightly martitic. Primary ilmenohematite or rutilohematite is always present. These intergrowths are morphologically quite similar to those described from the magnetite-quartz-K-feldspar gneiss and are also interpreted as exsolved solid solutions. Ilmenite may be partly altered to rutile and hematite. The proportion of primary hematite relative to magnetite is somewhat greater in the lime rich gneisses than in the magnetite-quartz-K-feldspar gneiss. In addition no hemoilmenite was observed, which indicated that the bulk composition of the non-magnetic fraction was near the hematite end of the hematite-ilmenite join. These facts indicate a high oxidation degree for the lime rich subunit.

The biotite-quartz-feldspar gneiss carries accessory ilmenomagnetite and ilmenite and rarely hemoilmenite ( $H_5I_{95}$ ). Primary hematite as well as martite are absent. Ilmenite is partially altered to rutile and hematite. This assemblage is distinct from that in the magnetite-quartz-K-feldspar gneiss where the iron and titanium oxides consist of a variety of intergrowths.

The quartz-K-feldspar gneiss carries ilmenomagnetite as a major accessory and only minor ilmenite. No primary hematite or rutile are present and only rarely is a very minor amount (less than 1 to 2 per cent of the host magnetite) of martite present. Ilmenite is usually partially altered to rutile and hematite. In Table 15 is listed the partial analysis of the magnetic and non-magnetic fractions from a sample (L3) of the quartz-K-feldspar gneiss. The non-magnetic analysis as expected corresponds to ilmenite with about 7.5 mole per cent of hematite in solid solution. The composition of this phase is plotted in Figure 8. The magnetite analysis recalculates as magnetite with 8.2 mole per cent ilmenite (2.80 wt. per cent  $TiO_2$ ) and about 14.0 mole per cent excess  $FeO$ . Intergrown parallel to the cube plane in the magnetite are very minute disks or lenses of a dark gray non-opaque mineral. This is probably exsolved Fe rich spinel, such as hercynite, and would account for the excess  $FeO$  in the analysis. The high  $TiO_2$  content (2.80 wt. per cent) of the magnetite is in contrast to the low  $TiO_2$  (0.14-1.39 wt. per cent) content of magnetite from the magnetite-quartz-K-feldspar gneiss. According to the data of Puddington (1953) this difference suggests that the quartz-K-feldspar gneiss crystallized at a slightly higher temperature than the magnetite-quartz-K-feldspar gneiss, and in addition the quartz-K-feldspar

Table 15. Partial chemical analyses of magnetic and non-magnetic fractions of iron and titanium oxides and petrographic data for two miscellaneous gneisses.

	148	152
Magnetic fraction		
Fe <sub>2</sub> O <sub>3</sub>	53.72	59.00
FeO	31.06	25.43
TiO <sub>2</sub>	<u>2.80</u>	<u>1.52</u>
Total	87.58	85.95
Non-magnetic fraction		
Fe <sub>2</sub> O <sub>3</sub>	6.44	n. d.
FeO	41.45	n. d.
TiO <sub>2</sub>	<u>40.44</u>	n. d.
Total	38.33	
Weight per cent Fe and Ti oxides in rock		
Mt.	16.0	1.20
Hem.	0.03	0.80
Ilm.	1.38	0.04
Rut.	0	tr.
FeO (excess)	0.92	
Composition magnetic fraction to 100 mole per cent		
Mt.	77.3	86.3
Hem.	0	8.7
Ilm.	3.2	5.0
FeO (excess)	14.0	
Composition non-magnetic fraction to 100 mole per cent		
Hem.	7.5	n. d.
Ilm.	92.5	n. d.
Rut.	0	n. d.
Mineral analysis		
Qtz.	0	43.0
K-fd.	65.8	36.0
Pl.	0.9	11.7
Bi.	8.3	
Ch.		7.6
Var.	6.6	
Ep.		x
Ap.	0.7	
Zr.	x	x
Zoc.	x	0.5
Ores	14.7	1.2
IM	13.1	0.9
R-IM		0.1
R		0.3
I	1.6	

- 148 - Garnet-biotite-K-feldspar gneiss, on Edison railroad, 0.65 miles north of Mahola road, Franklin Furnace Quadrangle, New Jersey.  
 149 - Chlorite-quartz-feldspar gneiss, Sherman Arch, Franklin Furnace Quadrangle, New Jersey; ratio ilmenohematite = (R<sub>5</sub>I<sub>22</sub>H<sub>73</sub>) ± 5.

gneiss formed at about the same temperature as microcline rich "granitized" rocks of the Adirondacks which are believed to have formed at temperatures lower than magmatic.

## CHAPTER 7

### GEOCHEMISTRY OF THE MIXED GNEISS SUBUNIT

#### PARTIAL CHEMICAL ANALYSIS OF THE MAGNETITE-QUARTZ-K-FELDSPAR GNEISS AND MAGNETITE RICH LAYER

Sufficient data are available to recalculate the approximate chemical composition of a sample of magnetite-quartz-K-feldspar gneiss (145) and a sample from a magnetite rich layer (144) both from the Condon Cut in the Edison area. During the separation of the quartz-feldspar concentrate from both these samples (see K-feldspar section) a partial mode (weight per cent) was determined, (a representative portion from a 2 kilogram sample ground to -30 mesh was used for each nodal analysis). Using this weight mode, the partial analysis of the quartz-feldspar concentrate (Table 10) and the partial analyses of the iron and titanium oxide fractions (Table 4A), it was possible to recalculate a partial chemical analysis for the two samples. In Table 16 the weight mode, the partial chemical analysis and the volumetric mode (taken from Table 4B) for the two samples are presented.

A comparison of the volumetric and weight modes of sample 145 indicates considerable differences. In particular the proportion of the quartz and feldspar is radically different and the quartz/feldspar ratios differ by nearly a factor of one-half. The discrepancy is probably due to insufficient or poor sampling for the petrographic thin section analysis. Thus the weight mode is considered more reliable. The volumetric and weight modes for sample 144 compare very well when allowance is made for density differences of the minerals; note the quartz/feldspar

Table 16. Volumetric modes, weight modes and partial chemical analyses of magnetite-quartz-K-feldspar gneiss and a magnetite rich layer tabulated with the chemical composition of a sillimanite-quartz-microcline granitic gneiss from the Adirondacks.

	Volumetric Mode		Weight Mode		Chemical Composition		
	145	144	145	144	145	144	B-13
qtz.	45.1	33.8	qtz.	54.3	21.6	SiO <sub>2</sub>	76.4
K-fd.	45.0	25.6	feld.	34.1	18.8	Al <sub>2</sub> O <sub>3</sub>	6.3
pl.	0	0	mt.	3.0	47.9	Fe <sub>2</sub> O <sub>3</sub>	3.41
bi.	2.0	1.1	hem.	1.3		FeO	1.00
ser.	2.3	x	ilm.	0.1		MgO	n. d.
ser. & ep.	0	5.5	rut.	0.1		CaO	0.04
sill.	2.6	x	rest	7.1	11.7	Na <sub>2</sub> O	0.41
ep.	x	2.1				P <sub>2</sub> O <sub>5</sub>	5.15
sr.	x	x				FeO	0.05
ep.	x					Fe <sub>2</sub> O +	n. d.
I-M	2.5	27.0				Fe <sub>2</sub> O -	n. d.
I-M		x				TiO <sub>2</sub>	0.10
I-W	0.5					P <sub>2</sub> O <sub>5</sub>	n. d.
R.		x				MnO	n. d.
						rest	7.13 <sup>a</sup>
feld.	1.0	1.3		1.6	1.1	Total	100.00
							100.00
							99.76

145 - Magnetite-quartz-K-feldspar gneiss, Conlin Cut, Wilson Area, Franklin Furnace Quadrangle, New Jersey.

144 - Magnetite rich layer, adjacent to 145.

B-13 - Sillimanite-quartz-microcline granitic gneiss, Skate Creek, Cowegatchie Quadrangle, New York. Analyst, Lee C. Peck. (Quoted from A. F. Buddington, 1951)

<sup>a</sup>Consists mostly of SiO<sub>2</sub>, Al<sub>2</sub>O<sub>3</sub> and K<sub>2</sub>O from biotite and sillimanite and minor Fe<sub>2</sub>O<sub>3</sub>, FeO, MgO, CaO and P<sub>2</sub>O<sub>5</sub>.

<sup>b</sup>Consists mostly of SiO<sub>2</sub>, Al<sub>2</sub>O<sub>3</sub>, CaO and P<sub>2</sub>O<sub>5</sub> from biotite, apatite, sericite and epidote.

ratios are very similar.

The striking chemical features of sample 145 are the very high  $\text{SiO}_2$  content, the high ratio of  $\text{Fe}_2\text{O}_3$  to  $\text{FeO}$ , and the very high ratio of  $\text{K}_2\text{O}$  to  $\text{Na}_2\text{O}$ . The average  $\text{SiO}_2$  content of granites as listed by Daly (1933) is 70.18%. None of the granites listed by Daly exceed 71.06%  $\text{SiO}_2$ . The  $\text{K}_2\text{O}$  to  $\text{Na}_2\text{O}$  and  $\text{Fe}_2\text{O}_3$  to  $\text{FeO}$  ratios in granites from Daly's list do not approach the high values present in sample 145. According to the compilations of Nockolds (1954) biotite alkali granite with an average of 75.01%  $\text{SiO}_2$  has the maximum average  $\text{SiO}_2$  content of all granites. None of the average compositions of calc-alkali or alkali granites, as listed by Nockolds, has as high a  $\text{SiO}_2$  content or  $\text{K}_2\text{O}$  to  $\text{Na}_2\text{O}$  and  $\text{Fe}_2\text{O}_3$  to  $\text{FeO}$  ratios as does sample 145. Clearly the magnetite-quartz-K-feldspar gneiss (sample 145) does not belong to the normal granite clan. Although the  $\text{SiO}_2$  content of sample 145 well exceeds that of similar gneisses of the Adirondacks, the over-all composition of the sample corresponds closely to a sillimanite-quartz-mica-schist granite gneiss of the Adirondacks (Engel and Engel, 1953, sec E-13 in Table 16) which is interpreted as a metasomatized metasediment.

Naturally the striking feature of the partial chemical analysis of the magnetite rich layer, sample 144, is the high content of  $\text{Fe}_2\text{O}_3$  and  $\text{FeO}$ . The ratios of these are of course very near to the ratio in magnetite. It is interesting to note that the quartz to feldspar ratio is not too different in the two samples. It can be concluded that the quartz and feldspar decrease together as magnetite increases. The ratio of  $\text{K}_2\text{O}$  to  $\text{Na}_2\text{O}$  is also about the same as in sample 145. However,  $\text{BaO}$  which is carried by K-feldspar, is enriched in sample 144. This increase

in BaO in magnetite rich rocks corresponds very well with the observation at the Benson Mines made by Leonard (1951), where it was noted that the BaO content in K-feldspar separated from magnetite rich rocks was somewhat greater than in K-feldspar from wall rock gneiss very similar to those of the mixed gneiss subunit.

GEOCHEMISTRY OF MANGANESE, TITANIUM, PHOSPHORUS AND SULFUR IN THE  
MIXED GNEISS SUBUNIT

Manganese

As reviewed in the section on garnet it is clear that the manganese content of the mixed gneiss subunit is higher than the manganese content of the quartz-K-feldspar gneiss. It seems reasonable to conclude that this high manganese content is related to the high iron content. In other words the manganese followed the iron during the genesis of the magnetite-quartz-K-feldspar gneiss and magnetite rich layers. In its high manganese content the mixed gneiss subunit is homologous to similar gneisses at the Benson Mines in the Adirondacks (Leonard, 1951).

Titanium

The  $TiO_2$  content of the magnetite-quartz-K-feldspar gneiss and associated magnetite rich layers is very low. As can be judged from Table 4A the  $TiO_2$  never exceeds 1.40 weight per cent and is usually less than 0.5 weight per cent. For the samples in Table 4 the mole ratio of magnetite to ilmenite + rutile varies from 42.7 to 3.1. Magnetite is relatively enriched over  $TiO_2$  in the samples from the Sherman unit (154, 153, and 151). The data suggest that the  $TiO_2$  content increases in

about the same proportion with the iron content as though the titanium and iron "ran together." Additional data are needed to substantiate this conclusion.

### Phosphorus

Considerable data are available on the phosphorus content of the magnetite rich layers and magnetite-quartz-K-feldspar gneiss of the Edison area. The data stem entirely from drill core assays which were made by the Pittsburgh Coke and Iron Company in 1943 (Chapter 8). All the core was assayed in short lengths (5 feet or less) for iron, and some of the core was assayed for phosphorus. The phosphorus content of individual assayed samples varies from 1.45 to 0.032 weight per cent. The average phosphorus content is between 0.1 and 0.8 weight per cent. Phosphorus is carried by apatite; thus, for several of the assayed drill cores the phosphorus content for the individual assayed samples has been recalculated in terms of moles of apatite per  $10^3$  liters of sample. For the same samples the total iron content has been recalculated as moles of magnetite per liter of sample. In Figure 9a these two values for each assayed sample have been plotted. Although there is a wide distribution of points the graph indicates unequivocally that apatite increases with magnetite. The distribution of points determines a zone which has a 45° slope and originates near the origin. In Figure 9b the ratios of moles of magnetite to moles apatite in each assayed sample is plotted in a histogram. The plot shows a very strong concentration of samples in the 10-50 portion of the diagram. The mean value of the ratio is near 35 and suggests that the magnetite to apatite ratio for the entire bulk of the mixed gneiss subunit may be near this value.

The most general interpretation of these data is simply that iron and phosphorus "ran together" in a more or less constant ratio. There are several geochemical principles which might be invoked to explain this relationship. However, the most simple explanation is that the iron and phosphorus were both carried by an ore fluid in which the iron and phosphorus content was fixed so that when the fluid precipitated, the ratio of iron and phosphorus was maintained. In other words the relationship between magnetite and apatite is simply a reflection of a parent ore fluid.

#### Sulfur

The distribution of sulfur has been discussed previously with reference to the sulfide rich zone. Several of the drill cores were assayed for sulfur as well as iron and phosphorus. Each assayed sample was a 5 foot or smaller length of core. The sulfur content of these samples, which is never more than 0.5 per cent and generally less than 0.1 per cent (except in the sulfide zone), was compared to their iron and phosphorus content. There appears to be no systematic relationship between the sulfur content of the assayed samples and their iron and phosphorus contents. Thus, while it is quite evident that the iron and phosphorus contents are in some way dependent upon one another (see phosphorus section) it is equally clear that the sulfur content is independent of iron and phosphorus contents.

Thus it may be concluded that sulfur has acted independently of iron and phosphorus during the genesis of the mixed gneiss subunit. As was suggested previously it is believed that the relationship between iron and phosphorus is a reflection of the composition of a primary ore fluid.

Although the source of the sulfur was probably the parent ore fluid, the ratio of sulfur to iron and phosphorus in the ore fluid was not maintained in the crystallized product simply because sulfur acted independently of the other constituents. Textural evidence cited in a previous section (Chapter 3) indicated that the sulfide minerals crystallized later than iron and titanium oxides. Thus it is postulated that the irregular distribution of sulfur relative to iron and phosphorus is a result of crystallization of sulfide minerals at a late stage. This late "finition" enabled the sulfur to "move around" so that any primary relationship which existed between sulfur and iron and phosphorus would be obliterated.

THE CHEMISTRY OF IRON WITH SPECIAL REFERENCE TO THE DISTRIBUTION OF  
MAGNETITE AND HEMATITE

Introduction

The associated magnetite rich layers are the most important aspect of the mixed gneiss subunit. The iron is chiefly in magnetite although a considerable amount of it is in hematite and some in ilmenite. As described in a previous section the entire mixed gneiss subunit is enriched in iron relative to adjacent wall rocks. The contacts with the wall rocks are abrupt chemical discontinuities. Particular zones within the mixed gneiss subunit are extremely rich in iron and form high grade magnetite veins. It is the purpose of this section to evaluate quantitatively the distribution of iron throughout the mixed gneiss subunit particularly with reference to the two principal iron oxides, magnetite and hematite.

### Distribution of iron

The total iron content of assayed samples from the drill core varies from 6.70 to 61.20 weight per cent. The average assayed sample carries 20-30 weight per cent Fe. The overall average total iron content of the mixed gneiss subunit is considerably less and is near 10 weight per cent.

The distribution of iron in the mixed gneiss subunit is highly irregular. A detailed study of the assayed drill core data indicates that particular zones (veins?) of the gneiss from 5 to 15 feet thick are greatly enriched in iron and may carry up to 5 times more iron than adjacent zones. Any theory pertaining to the origin of the mixed gneiss subunit must account for this irregular distribution of iron.

### Distribution of magnetite and hematite

Introduction. In this section the distribution of magnetite and hematite in the rock layers of the mixed gneiss subunit is described. The data concerning the distribution of those two iron oxides stems from two sources, (1) petrographic data, largely of a semi-quantitative nature, and (2) drill core assay data. The discussion pertains only to primary hematite and not to martite.

Petrographic data. The general petrographic examination of polished surfaces suggests that hematite is more abundant in rocks which are not particularly rich in magnetite. Thus samples of magnetite-quartz-K-feldspar gneiss in which magnetite is less than 10 volume per cent appear to carry a larger proportion of hematite than do adjacent rock layers which are enriched in magnetite. Accurate and abundant modal analyses are needed to establish these relationships quantitatively. Such data are lacking; however, an examination of the modal analyses of the samples in

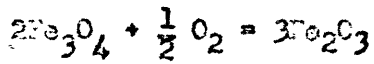
Table 4E indicate in a general way that these qualitative observations are true. Clearly samples 146, 145, 149, 154, and 153 which are poor in magnetite all carry more hematite than do samples 143, 144, 151 which are rich in magnetite.

There are some petrographic data which indicate that rocks from the mixed gneiss subunit, which have strong metasedimentary affinities (high sillimanite, garnet, biotite and quartz contents) are enriched in hematite relative to magnetite. Sample B-151f (Table 6) which is a garnetiferous-biotite-sillimanite-quartz gneiss, is particularly interesting in this respect. The modal analysis of this rock is known both from thin section analysis and from a separation of the magnetic and non-magnetic oxides from a representative sample of the rock. It carries 6 Volume per cent iron and titanium oxides of which 4.2 per cent is magnetite and 1.8 per cent hematite (both with a subordinate amount of intergrown minerals). The ratio of magnetite to hematite is 2.4 to 1, which as will be pointed out later is low relative to many of the other samples, i. e., the sample is enriched in hematite relative to magnetite.

Drill core data. It is not necessary to rely entirely on the semi-quantitative petrographic data to establish the fact that hematite decreases in samples which are enriched in magnetite. Several of the drill cores were assayed both for magnetic iron and soluble iron. In the former case the magnetic fraction was separated from the core sample and analyzed for iron. Thus magnetic iron is from magnetite but does include intergrown ilmenite and martite. The soluble iron is not only from magnetite but also from primary oxides such as ilmenite and hematite and is thus the total iron from oxides in the sample. It is believed that very little

of the soluble iron would come from dissolved iron silicates inasmuch as such minerals are subordinate to the iron and titanium oxides and are less readily decomposed. Hematite is always more abundant than ilmenite in all samples examined petrographically. Thus, the algebraic difference between soluble iron (total iron) and magnetic iron will be approximately equal to the iron from the hematite in the sample. Thus, for all the core samples which have been assayed for both soluble and magnetic iron it has been possible to recalculate the assays into moles of magnetite (magnetic iron) and moles hematite (soluble iron minus magnetic iron) per unit volume of the sample. In this way it has been possible to study on a large scale and quantitatively the distribution and relationships between magnetite and hematite.

As is discussed in a subsequent section on the physical chemistry of the iron oxides (Chapter 9) there is an oxidation-reduction relationship between magnetite and hematite which may be expressed as follows:



In a system involving the iron oxides, magnetite and hematite, it is possible that the degree of oxidation could be great enough that hematite was the predominant phase; or if the degree of oxidation was low, magnetite could be the predominant phase. All variations from pure magnetite to pure hematite are possible in such a system depending upon the physical conditions and the way in which the mineral assemblage formed. Thus a simple way of expressing the oxidation grade of such an iron oxide system would be in terms of the ratio of magnetite to hematite. In rocks of low oxidation grade the ratio would be very high i. e., magnetite much greater than hematite. In cases of high oxidation grade the ratio would

approach zero, i. e., magnetite much less than hematite. In Figure 10 the total iron (soluble iron) as moles of magnetite per liter of rock is plotted versus the magnetite to hematite ratio for each drill core sample which was assayed for magnetic and soluble iron. The points determine a linear zone which passes through the origin and has a steep positive slope. The diagram clearly shows that the oxidation degree decreases with increase in the proportion of iron. It might be argued that there is a common term (magnetite) in both the coordinates and that the distribution of points is a natural consequence. This would be true in a case where magnetite was plotted versus a ratio involving magnetite and a phase such as quartz or feldspar which did not have a chemical reaction with the magnetite. As there is an oxidation-reduction reaction between magnetite and hematite, it is quite conceivable that with increase of total iron the oxidation degree could easily increase providing the proper physical conditions ( $pO_2$ ) prevailed. Thus when considered in this way the diagram is a valid presentation of the relationship.

In eight samples from forty feet of continuous drill core the total iron oxide is always less than 10 mole per cent of the assayed samples. Hence, these eight samples as far as iron oxide content is concerned correspond very well with the typical magnetite-quartz-K-feldspar granite. In Figure 11 the total iron (soluble iron) as moles of magnetite per liter of sample is plotted versus the magnetite to hematite ratio for each of these eight samples. The distribution of points is about a straight line which has a positive slope and whose extension passes near to the origin. It is clear from the graph that the decrease in oxidation grade with increase in iron content is even more strikingly apparent in

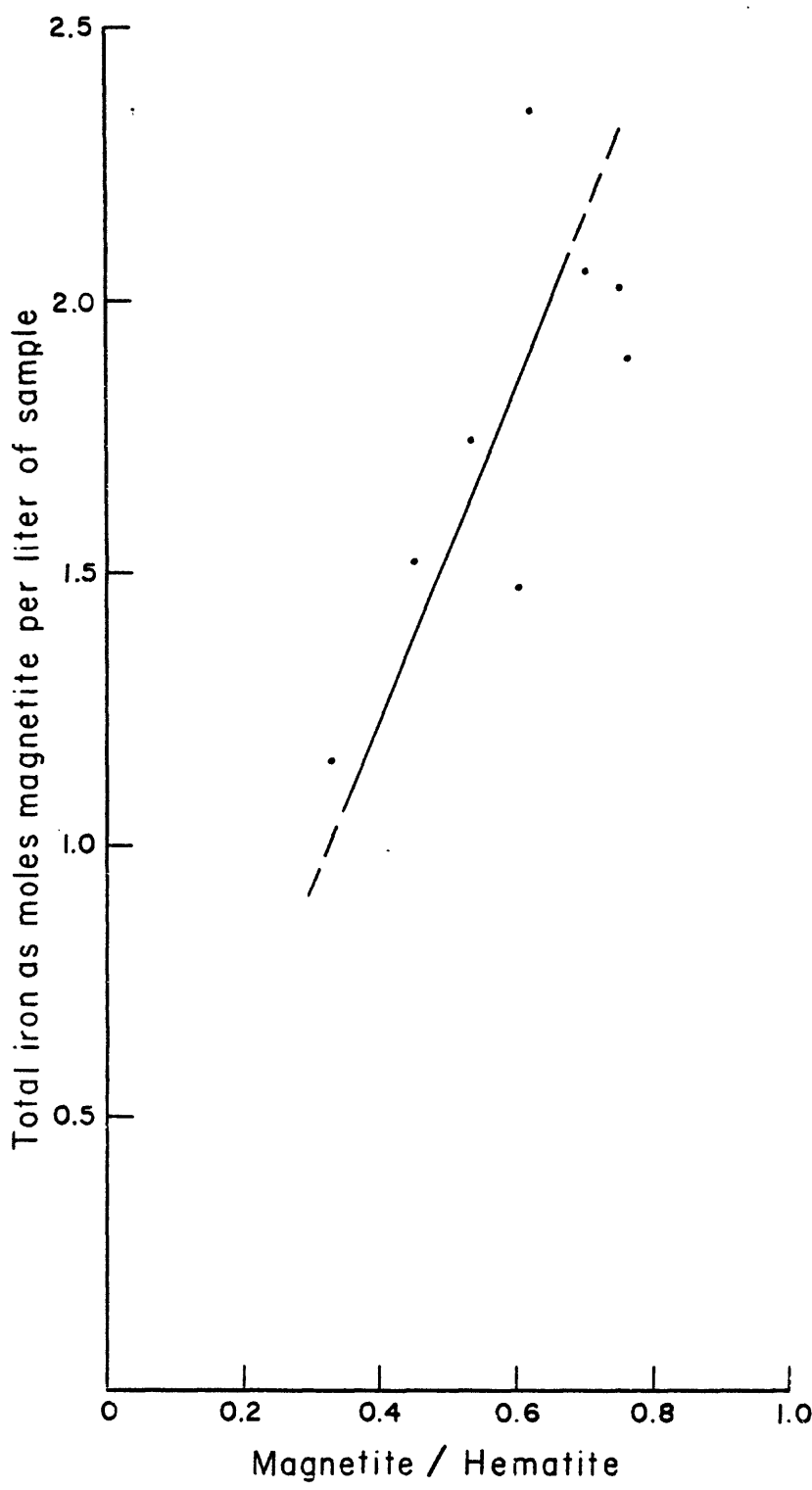


FIG. II. Total iron as moles of magnetite versus the ratio of magnetite to hematite for assayed samples of the mixed gneiss subunit

the magnetite-quartz-K-feldspar gneiss than it is in the bulk of the rocks in the mixed gneiss subunit, i. e., compare Figures 10 and 11.

Summary. The principal conclusion which can be drawn from these petrographic and drill core data is that the degree of oxidation decreases in a regular fashion (linearly) with increase in magnetite or total iron content. The theoretical reasons for this relationship are discussed in a subsequent section dealing with the physical chemical relations between the iron and titanium oxides.

## CHAPTER 6

### ECONOMIC GEOLOGY OF THE EDISON AREA

#### INTRODUCTION

The heterogeneous nature of the mixed gneiss subunit is expressed in the frequent concentration of the magnetite into distinct layers as well as the variation in proportions of other minerals. Such enriched zones may consist of a single magnetite rich layer or of several magnetite rich layers separated by lean gneiss. The magnetite rich zones are locally thick enough and of large enough extent to constitute iron ore of workable grade. Assay data from the drill cores indicate that the magnetite rich layers carry up to 55-60 weight per cent magnetic Fe. These extremely rich layers generally grade off into leaner wall rock which may carry as little as 2 weight per cent magnetic Fe. However, there are cases where magnetite rich layers make an abrupt contact with the wall rock gneiss.

In the subsequent sections the iron ores are discussed from an economic standpoint. In Chapter 12 of this report the origin of the ores is discussed.

#### DISTRIBUTION

In the Edison area the magnetite ore deposits are confined to a narrow belt within the mixed gneiss subunit. This belt extends parallel to the trend of the subunit for 7500 feet and averages 150 to 200 feet in width.

Several distinct magnetite rich zones are present within this belt, and are shown on Plate 1, either as inferred or indicated. Indicated ore zones are well established by drill core data and previous workings, whereas inferred ore zones are established by dip needle and surface observations. The most important ore zones include, (1) the ore zone in the southeast workings of the Old Ogden and Roberts Mines (this corresponds to the sulfide zone); (2) the ore zone which passes thru the northwest workings of the Old Ogden and Roberts Mine and extends from the Victor Mine as far southwest as the Davenport Mine; (3) the ore zone which is located to the northwest of the Davenport Mine and is apparently displaced along a minor fault just southwest of the Big Cut, and (4) the ore zone passing through the Vulcan Mine. In addition numerous smaller magnetite rich layers are present; however, it is doubtful if these are large enough to constitute an ore zone. It is possible that other ore zones may be present in the northwest portion of the mixed gneiss subunit particularly at the Iron Hill Mine and possibly in the zone passing thru the Copper Shaft. However, additional data are needed to identify other ore zones.

#### SOURCES OF DATA

Seven diamond drill holes, which total 3967 feet, were made by the Pittsburgh Coke and Iron Company in 1943. The core was assayed for magnetic iron and some zones were assayed for soluble iron, phosphorus and sulfur as well. In 1920 Bethlehem Steel Company diamond drilled five holes which total 3015 feet. In addition they made 10 channel samples between the Roberts Mine and the Victor Mine along the magnetite rich

zone which passes through the Condon Cut. The Bethlehem Steel Company assayed the drill core and channel samples only for magnetic iron.

The old surface workings in the Edison area not only provide information as to the locale of the magnetite rich zones but also provide the best exposures of the zones. The surface workings which are located on the base map (Plate 1) are open pits and from the southwest to the northeast are called the Big Cut, Davenport Mine, Old Ogden Mine, Roberts Mine, Condon Cut, Victor Mine and Iron Hill Cut. The underground workings were on the same magnetite rich zones and from the southwest to northeast include the Vulcan Mine, Davenport Mine, Old Ogden Mine, Roberts Mine, Victor Mine and the Copper Mine. Thus, most of the magnetite rich zones were worked both on the surface and underground. All the underground workings are now flooded and inaccessible; however, Bayley's report (1916) provides some data pertaining to them.

A modified version of a dip needle survey made by the Edison Company is plotted on the base map (Plate 1). Forty and sixty degree contours are used. The sixty degree contour corresponds to an absolute reading of  $70.30^\circ$  with a standard Gurley, Lake Superior dip needle calibrated to read  $-21^\circ$  over hornblende granite.

#### EATROLOGY AND MINERALOGY

At least two varieties of magnetite concentration can be recognised in the mixed gneiss subunit. The first of these is related to the typical magnetite-quartz-K-feldspar gneiss and is the most important type. In this type magnetite may be enriched in definite bands (up to 3-5 inches thick) which may have fairly sharp contacts to the wall rock gneiss; or

more often magnetite lean wall rock gneiss grades abruptly into a magnetite rich layer by a progressive increase in magnetite. In this latter case magnetite increases from disseminated grains in the lean wall rock, to thin discontinuous bands in rich wall rock and finally into heavy solid bands of magnetite 3-5 inches thick. In general the same mineral phases are found in these magnetite rich layers as in the lean wall rock; however, the proportions of the minerals vary greatly (Tables 4 and 5, Figure 3). Ilmenohematite is generally absent from magnetite rich layers, but it is often a major accessory in the immediate wall rock (see Chapter 7). K-feldspar is often absent in the magnetite rich layers but when present is always an untwinned variety (see Chapter 6 on K-feldspar). Quartz is always a major mineral in such layers. Apatite is generally enriched in magnetite rich layers and fluorite has been observed. Minerals of retasedimentary affinities such as biotite, garnet and sillimanite are subordinate in the magnetite rich layers, but sulfides (pyrite, molybdenite, chalcopyrite and bornite) are locally enriched (see section on sulfide zone).

The second variety of magnetite rich layer is composed of magnetite and quartz and is probably related to the magnetite-quartz gneiss (meta-quartzite?). This type occurs as distinct layers enclosed within the predominant magnetite-quartz-K-feldspar gneiss. Layers of this variety are generally 6 inches to 1-10 feet thick and may pinch out along strike in 20-50 feet. Internally such layers are uniform in that magnetite and quartz are evenly distributed. Magnetite and quartz are the principal minerals of this type of ore layer; K-feldspar is absent except adjacent to the contacts of magnetite-quartz-K-feldspar gneiss. In addition

ilmenohematite and hemoilmenite are absent, whereas biotite, muscovite and apatite are the chief accessory minerals. As quartz and magnetite form over 95 per cent of the rock, this type of ore layer is mineralogically very simple.

In general the texture of the two types of magnetite concentrations are similar in that they are medium, even grained and xenoblastic. However, the structures of the two types are in marked contrast. The magnetite concentrations which are related to the magnetite-quartz-K-feldspar gneiss have a gneissic structure very similar to that of the adjacent gneisses. In contrast the magnetite-quartz variety has a very strong gneissic structure due to the greater lenticularity (deformed character) of the minerals. These differences were discussed in more detail in the section devoted to the petrology of the mixed gneiss subunit.

#### CONTACT RELATIONSHIPS

The contact relationships between the magnetite-quartz gneiss and the magnetite-quartz-K-feldspar gneiss is well illustrated by Plate 20. As can be seen in the plate the contact with the magnetite-quartz-K-feldspar gneiss is very sharp but slightly irregular. It is not the planar contact of fissure nature but it is the natural grain boundary contact between the adjacent layers of gneiss. At the contact there is an abrupt change in texture as well as composition. Magnetite is enriched in the magnetite-quartz-K-feldspar gneiss along the contact; however, texturally this enriched zone of magnetite is quite distinct and separate from the magnetite in the magnetite-quartz gneiss layer. Within the magnetite-quartz gneiss are lenses of magnetite-quartz-K-feldspar gneiss

which have well developed K-feldspar porphyroblasts. These lenses appear more intimately mixed with the magnetite-quartz gneiss than do the distinct layers of the magnetite-quartz-K-feldspar gneiss. In addition there are K-feldspar porphyroblasts completely isolated from any lenses or layers of magnetite-quartz-K-feldspar gneiss. These relationships suggest that at least some of the K-feldspar and perhaps the magnetite-quartz-K-feldspar gneiss were formed after the formation of the magnetite-quartz gneiss.

#### STRUCTURE

The ore zones are conformable to the foliation of the gneisses. In no cases do magnetite rich layers cross-cut the foliation of adjacent gneisses. Structurally the magnetite rich layers are equivalent to the adjacent rock layers. The drill core data show that magnetite zones vary from 10 to about 30 feet in thickness. The thicker zones are always a composite of several magnetite rich layers which alternate with layers which are less rich in magnetite. The thinner ore zones are generally a single uniform magnetite rich layer.

The drill core data, dip needle observations, and field observations definitely prove that the ore zones pinch and swell parallel to the strike of the foliation. Thus the ore zones shown on Plate 1 are discontinuous along the strike; where such discontinuities are expected the ore zone is inferred. Actually, the data indicate that the ore zones pinch out in the foliation plane but in a direction parallel to the linear structure in the gneisses. Thus the ore zones are tabular shaped bodies with the two major dimensions oriented in the foliation plane and with one of

these dimensions oriented parallel to the lineation. The lineation plunges 55-60° northeast in the Old Ogden Mine and about 50° northeast in the Iron Hill Cut. Drill core data prove that some of the ore zones extend to a depth at least 700 feet from the surface; however, it is uncertain how far down the linear structure the ore zones may be projected.

Like the adjacent gneisses the magnetite rich layers are sometimes deformed into minor folds. Such a fold was described from the Roberts Mine in Chapter 5. As such folds are tight, magnetite layers are essentially doubled in thickness along the crest of the fold and form a linear shaped ore body which plunges along the fold axis. Such ore bodies have a distinct cap and bottom rock. Although linear shaped magnetite ore bodies along the axes of folds form important ore deposits elsewhere in the New Jersey Highlands (Sims, 1953), it is certain that they are subordinate in the Edison area. The major ore zones are tabular shaped bodies as previously described, and such linear shaped bodies that may exist are only the result of minor folding of the larger planar ore bodies.

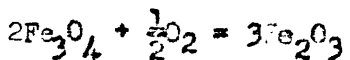
Jointing and faulting of the magnetite zone is identical to that described in the chapter on structure.

## CHAPTER 9

### EXPERIMENTAL AND THERMODYNAMIC DATA FOR THE MAGNETITE-HEMATITE-ILMENITE-RUTILE-WATER SYSTEM (OXIDATION - REDUCTION EQUILIBRIA IN METAMORPHIC AND METASOMATIC ROCKS)

#### INTRODUCTION

In order to obtain any reasonable petrologic interpretation of rocks which bear iron and titanium oxide minerals (magnetite, hematite, ilmenite and rutile), it is necessary that the stability relationships of these various minerals be well understood. Experimental data are lacking for the iron and titanium oxide system except at very high temperatures. Fortunately reliable thermodynamic data are available for magnetite, hematite and  $O_2$  over a range from low to high temperature. In addition some thermodynamic data are available for ilmenite and rutile. Therefore, it has been possible to calculate more important energetic data for the magnetite-hematite-ilmenite-rutile system. Specifically, the free energy increase ( $\Delta F$ ) and the equilibrium constant for the reaction



(hereafter the magnetite-hematite reaction) have been determined for a range of temperatures from 200°C to 1400°C and a range of pressures from 1 to 7000 atmospheres. In addition the free energy increase for the reactions,  $2\text{FeTiO}_3 + \frac{1}{2}\text{O}_2 = \text{Fe}_2\text{O}_3 + 2\text{TiO}_2$  (hereafter the ilmenite-hematite reaction) and  $3\text{FeTiO}_3 + \frac{1}{2}\text{O}_2 = \text{Fe}_3\text{O}_4 + 3\text{TiO}_2$  (hereafter the ilmenite-magnetite reaction) have been compared in a semi-quantitative way to that for the magnetite-hematite reaction and it is concluded that the three reactions are energetically very similar.

Recently excellent data pertaining to the dissociation of water ( $2H_2O = 2H_2 + O_2$ ) at high temperatures have become available (Dwyer and Oldenborg, 1944). In a petrologic system which contains magnetite and water the oxidation of magnetite to hematite is a potential chemical reaction. In order to evaluate the effect of water on the magnetite-hematite equilibrium the free energy increase and the equilibrium constant for the formation of water have been evaluated for a range of temperatures from 400° to 1000°C and over a range of pressures from 1 to 2000 atmospheres. The data for the dissociation of water as given by Dwyer and Oldenborg (1944) for 1 atmosphere pressure over this range of temperature were used. His equilibrium constants were extended to higher pressures by standard thermodynamic calculations.

With the approximate evaluation of the equilibrium constants for the reactions  $2Fe_3O_4 + \frac{1}{2}O_2 = 3Fe_2O_3$  and  $2H_2 + O_2 = 2H_2O$  it is then possible to evaluate in a quantitative fashion the significance of a given oxidation grade (iron oxide paragenesis) in a metamorphic or metasomatic rock. Thus, these data are utilized in an effort to interpret the iron and titanium oxide paragenesis in the rocks and magnetite deposits of the Edison unit in the Edison area.

The chemical reaction between magnetite, hematite and oxygen as well as the reaction between ilmenite, hematite, rutile and oxygen have been considered as reactions between solid phases and a gas phase. Therefore, the data presented are only applicable to metamorphic and metasomatic rocks in which the mineral paragenesis developed in a physical environment which consisted largely of solid phases and a minor amount of disperse phase (Barth, p. 315, 1952). The disperse phase

includes all material in the gas or fluid phase as well as material so highly activated that it has not become permanently fixed in any solid phase. Nevertheless, these studies apply to igneous rocks once a solid phase such as magnetite has formed. Indeed, the application of these studies to the cooling stages of a crystallized igneous rock may reveal important information pertaining to the physical conditions which existed during the deuteric stage.

Probably the most serious limitation of this treatment is that the iron and titanium oxide - water system is considered as isolated from the remainder of the petrologic system. Other solid phases will of course have a definite solubility in the disperse phase and in particular other solids which contain iron may influence the stability field of the iron oxides. Obviously, these difficulties are impossible to evaluate in a quantitative way; therefore, more ideal conditions have been assumed in this discussion.

It might be argued that the treatment presented here is invalid because the chemical reactions as written probably do not represent the real reaction which took place. For example, the oxidation of magnetite to hematite may have involved several intermediate chemical exchanges which cannot be predicted. If such is the case it can be stated with certainty that the reaction rates will be considerably modified. However, the thermodynamic treatment employed is perfectly general and the energetic changes which take place are not dependent upon the path of the reaction but only upon the initial and final states of the system. Therefore, the treatment employed is applicable despite the fact that the exact nature of the chemical reactions cannot be evaluated.

## THE MAGNETITE-HEMATITE ( $2\text{Fe}_3\text{O}_4 + \frac{1}{2}\text{O}_2 = 3\text{Fe}_2\text{O}_3$ ) REACTION

### Introduction

The significance of the magnetite-hematite chemical reaction can best be emphasized by pointing out that it is a potential chemical reaction in every rock which bears the mineral magnetite. The reaction is sensitive to the partial pressure of  $\text{O}_2$  [ $p(\text{O}_2)$ ]. Thus, if it is possible to determine the equilibrium partial pressure of  $\text{O}_2$ , i. e., the dissociation  $p(\text{O}_2)$  for hematite, for the reaction over a range of temperature and pressure it would be possible to obtain some quantitative idea of the  $p(\text{O}_2)$  present in a rock forming system. If the gas  $\text{O}_2$  is in equilibrium with other components, such as  $\text{H}_2\text{O}$ ,  $\text{CO}_2$ ,  $\text{H}_2$ , etc., with certain assumptions and other equilibrium data it might be possible to calculate the partial pressures of some of these other volatile components of the rock forming system (Kennedy, 1943).

It is the purpose of this section to utilize all the available data in order to calculate the equilibrium constant and  $p(\text{O}_2)$  for the magnetite-hematite reaction for a series of temperatures and pressures. The data are of two types, (1) experimental and (2) thermodynamic.

### Experimental data

Various workers have studied the magnetite-hematite-oxygen system at high temperatures and at a total pressure of one atmosphere. The studies of Greig et al., 1935), Schumhl (1941) and Darken and Curry (1946) stand out as the best modern treatments of the system.

Greig and his co-workers determined the equilibrium temperature for the magnetite-hematite reaction for partial pressures of  $\text{O}_2$  equal to

760 mm Hg and 159 mm Hg. In addition they determined the degree of solid solution of hematite in magnetite at temperatures between 1100° and 1450°C. These equilibrium temperatures at the indicated  $p(O_2)$  are listed in Table 18. They found that at 1450°C magnetite will take up to 25 weight per cent of hematite in solid solution. However, as the temperature drops the degree of solid solution drops very rapidly, so that at 1100°C there is less than 10 weight per cent hematite in the magnetite. The implication of their work is that at intermediate and low petrologic temperatures the percentage of hematite in solid solution with magnetite is negligible.

The experimental data of Schmahl (1941) are also listed in Table 18. He determined the equilibrium  $p(O_2)$  at a series of temperatures for the magnetite-hematite reaction. His data agree very well with Greig's. He worked at temperatures as low as 1310°C and also found that there is very limited solid solution of hematite in magnetite at such a temperature. In addition he found that there is essentially no magnetite in solid solution in hematite at temperatures less than 1200°C.

The work of Darken and Gerry (1945, 1946, 1953, pp. 347-359) is by far the best available treatment of the magnetite-hematite-oxygen system. Their experiments have enabled the construction of a temperature-composition diagram for the Fe-O<sub>2</sub> system (loc. cit. p. 351, 1953). The equilibrium values of the  $p(O_2)$  for the magnetite-hematite reaction as found by them are listed in Table 18. It is apparent that these  $p(O_2)$  agree very well with those determined by Greig (1935) and by Schmahl (1941). The temperature-composition diagram of Darken and Gerry (1953) reveals some very important facts. First, the diagram indicates that hematite takes no

Table 18. Coefficients,  $\Delta H$  and  $\Delta S$  for the magnetite-hematite reaction  
 $(2\text{Fe}_3\text{O}_4 + \text{O}_2 = 3\text{Fe}_2\text{O}_3)$  for 1 atm. of  $\text{O}_2$  total pressure.

T°C	$\Delta H$ cal./mole	$\Delta S$ cal./mole	$\Delta F$ kcal./mole	$K_1^*$	$\log K_1$	$p(\text{O}_2) \text{ atm.}$	$\log p(\text{O}_2) \text{ atm.}$
(a) 1457 1730	-55,474	-30.63	-2.47	2.075	0.32	339	4.46x10 <sup>-1</sup>
(b) 1450 1723	-56,240	-30.94	-1.12	1.384	0.14	760	1.0
(a) 1392 1665	-56,240	-30.94	-4.74	4.19	0.62	760	1.0
(c) 1390 1663	-55,474	-30.63	-3.23	2.70	0.43	66	8.63x10 <sup>-2</sup>
(b) 1390 1663	-55,474	-30.63	-3.23	2.70	0.43	159	2.09x10 <sup>-1</sup>
(c) 1370 1643	-56,438	-31.27	-6.29	7.19	0.36	159	1.97x10 <sup>-1</sup>
(c) 1350 1623	-56,438	-31.27	-5.25	5.25	0.72	53	0.76x10 <sup>-1</sup>
(c) 1330 1603	-56,438	-31.27	-6.98	9.17	0.96	20.1	2.65x10 <sup>-2</sup>
(c) 1313 1586	-56,576	-31.27	-5.56	5.85	0.77	37.7	4.96x10 <sup>-2</sup>
(e) 1313 1586	-57,052	-31.72	-12.55	9.03x10 <sup>-3</sup>	1.96	12.1	1.59x10 <sup>-2</sup>
(c) 1310 1583	-57,052	-31.72	-19.0	2.92x10 <sup>-3</sup>	3.47	29.6	3.90x10 <sup>-2</sup>
1130 1403	-57,052	-31.72	-32.2	5.93x10 <sup>-3</sup>	6.77	23.5	3.10x10 <sup>-2</sup>
927 1200	-57,387	-31.95	-32.97	-33.5	1.06x10 <sup>-4</sup>	14.03	1.33x10 <sup>-4</sup>
527 800	-58,556	-30.43	-46.5	1.23x10 <sup>-4</sup>	34.09	6.76x10 <sup>-6</sup>	1.22x10 <sup>-7</sup>
327 600	-56,730	-30.50	-46.5	1.23x10 <sup>-4</sup>	34.09	8.91x10 <sup>-6</sup>	2.84x10 <sup>-18</sup>
25 298	-55,500	-30.50	-46.5	1.23x10 <sup>-4</sup>	34.09	6.60x10 <sup>-6</sup>	-17.5%
							-28.05

$$* K_1 = \frac{(\text{act Fe}_2\text{O}_3)^3}{(\text{act Fe}_3\text{O}_4)^2 p(\text{O}_2)^{\frac{1}{2}}} ; \quad \ln K_1 = -\frac{\Delta F}{RT} ;$$

act  $\text{Fe}_2\text{O}_3$  = unity at all temperatures  
 act  $\text{Fe}_3\text{O}_4$  = unity at temperatures less than 1100°C and as in Table at temperatures greater than 1100°C.

- (a) Experimental data, Darken and Curry, 1946
- (b) Experimental data, Grotz, et al., 1935
- (c) Experimental data, Schrehl, 1941

magnetite into solid solution at any temperature. Second, magnetite takes only limited amounts of hematite into solid solution even at very high temperatures, and essentially none at temperatures less than 1000°C. In addition, although it is of no particular significance to the magnetite-hematite system, it is important to note that magnetite takes no wüstite ( $\text{FeO}$ ) into solid solution at any temperature or composition. Finally, Darken and Gurry have evaluated the equilibrium  $p(\text{O}_2)$  for the dissociation of magnetite into wüstite plus  $\text{O}_2$  and for the dissociation of wüstite into native iron and  $\text{O}_2$  for temperatures above 1100°C.

In summary the experimental data indicates the following major facts concerning the magnetite-hematite-oxygen system. First, there is essentially no solid solution between magnetite and hematite at temperatures less than 1000°C. Second, the dissociation  $p(\text{O}_2)$  for hematite, i. e., the equilibrium  $p(\text{O}_2)$  for the magnetite-hematite reaction, decreases very rapidly from a value of 1 atmosphere at 1457°C to a value near 23.5 mm Hg at about 1310°C. It is therefore clear that at temperatures less than 1000°C the equilibrium  $p(\text{O}_2)$  will decrease to very small values so that hematite will readily form from magnetite if the  $p(\text{O}_2)$  approaches any appreciable level. It is the purpose of the remainder of this section to evaluate the equilibrium  $p(\text{O}_2)$  for the magnetite-hematite reaction at temperatures less than 1000°C and at pressures from 1 to 7000 atmospheres.

#### Thermodynamic data

One form of the Gibbs-Helmholtz equation which applies to any chemical reaction which takes place in a closed system, at equilibrium with the external pressure and isothermally is  $\Delta F = \Delta H - T\Delta S$ , where  $\Delta F$ ,  $\Delta H$  and

$\Delta S$  represent the increase in free energy, heat content and entropy respectively for the given isothermal process (Glasstone, 1947 p.206). Thus, if the heat content and the entropy for the reactants and products of the magnetite-hematite reaction are known for a range of temperatures at standard pressure, it would be possible to calculate the free energy increase ( $\Delta F$ ) for the chemical reaction over the temperature interval. Fortunately, the heat content and entropy increments for  $\text{FeO}$ ,  $\text{Fe}_3\text{O}_4$  and  $\text{Fe}_2\text{O}_3$  for temperatures between  $298.1^\circ\text{K}$  and  $1800^\circ\text{K}$ , at one atmosphere total pressure, have recently become available (Coughlin, King and Bornickson, 1951). In addition essentially the same thermodynamic data for  $\text{O}_2$  are available (Rosini, 1952).

Utilizing these heat content and entropy data it has been possible to calculate the free energy increase for the magnetite-hematite reaction for a series of temperatures at standard pressure. The sample calculation below for a temperature of  $1200^\circ\text{K}$  will illustrate the method.



$F_1$        $F_2$        $F_3$       (free energy)

$H_1$        $H_2$        $H_3$       (heat content)

$S_1$        $S_2$        $S_3$       (entropy)

$T = 1200^\circ\text{C}$ ,  $P = 1$  atm.

Heat content and entropy values at  $298.16^\circ\text{K}$  ( $25^\circ\text{C}$ ) are:

	$\text{Fe}_3\text{O}_4$	$\text{Fe}_2\text{O}_3$	$\text{O}_2$
$H_{25}$ (cal/mole)	-267,000	-196,500	0.000
$S_{25}$ (cal/deg.mole)	35.0	21.5	49.003

and heat content and entropy increments for 1200°K are:

	<u>Fe<sub>3</sub>O<sub>4</sub></u>	<u>Fe<sub>2</sub>O<sub>3</sub></u>	<u>O<sub>2</sub></u>
H <sub>T</sub> - H <sub>25</sub> (cal/mole)	44,950	30,870	9183.6
S <sub>T</sub> - S <sub>25</sub> (cal/deg.mole)	66.9	45.80	10.73

The heat content (entropy) increment is the difference between the heat content (entropy) at the temperature T (1200°K in this example) and the heat content (entropy) at 25°C, i. e., H<sub>T</sub> - H<sub>25</sub> (S<sub>T</sub> - S<sub>25</sub>). Hence, by adding the heat content (entropy) increment to the heat content (entropy) at 25°C (H<sub>25</sub>), it is possible to obtain the heat content (entropy) per mole for the temperature T (H<sub>T</sub>) for magnetite, oxygen and hematite. By multiplying these molar values by the appropriate coefficients the heat content (entropy) values for the reactants and products of the magnetite-hematite reaction may be obtained:

$$H_3 = 3H_T = 3(20,870 + 196,500) = -496,890 \text{ cal/mole}$$

$$H_2 = \frac{1}{2}H_T = \frac{1}{2}(9183.6 + 0.000) = +4591.8 \text{ cal/mole}$$

$$H_1 = 2H_T = 2(44,950 - 267,000) = -44,100 \text{ cal/mole}$$

$$\Delta H = H_3 - (H_2 + H_1)$$

$$\Delta H = -57,387 \text{ cal/mole}$$

$$S_3 = 3S_T = 3(45.80 + 21.5) = 201.9 \text{ cal/deg.mole}$$

$$S_2 = \frac{1}{2}S_T = \frac{1}{2}(10.73 + 49.00) = 29.865 \text{ cal/deg.mole}$$

$$S_1 = 2S_T = 2(66.99 + 35.0) = 203.98 \text{ cal/deg.mole}$$

$$\Delta S = S_3 - (S_2 + S_1)$$

$$\Delta S = -31.95 \text{ cal/deg.mole}$$

hence:  $\Delta F = \Delta H - T\Delta S$

$$\Delta F = -57,382 - 1200(-31.95)$$

$$\Delta F = -19,032 \text{ cal/mole}$$

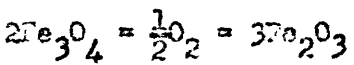
$$= 19.0 \text{ Kcal/mole}$$

In the same manner by utilizing analogous heat and entropy data (for the appropriate temperature) the free energy increase for the magnetite-hematite reaction was calculated for a temperature interval from 25°C to about 1400°C, at one atmosphere total pressure. These values are plotted versus temperature in Figure 12 and along with the appropriate  $\Delta H$ ,  $\Delta S$  and  $\Delta F$  values are tabulated in Table 18.

Other workers (Richardson and Jeffes, 1948) also calculated the free energy increase for the magnetite-hematite reaction over the same temperature interval at one atmosphere total pressure. They used the same method as outlined above but utilized older heat content and entropy data. Their values of  $\Delta F$  versus temperature also are plotted in Figure 12. It is obvious that the agreement between their curve and the one calculated with the more recent data is very good, especially in the temperature range of 500° to 1000°C.

#### Calculation of the equilibrium constant

The equilibrium constant for the magnetite-hematite reaction



is  $K_1 = \frac{(\text{act Fe}_2\text{O}_3)^3}{(\text{act Fe}_3\text{O}_4)^2 (\text{act O}_2)^{\frac{1}{2}}}$

By the mass action law the activity of a pure solid is equal to unity. Durkin and Curry (1946) evaluated the activity of  $\text{Fe}_3\text{O}_4$  in magnetite at one atmosphere total pressure and at temperatures above 1100°C. Their values for various temperatures are listed in Table 19.

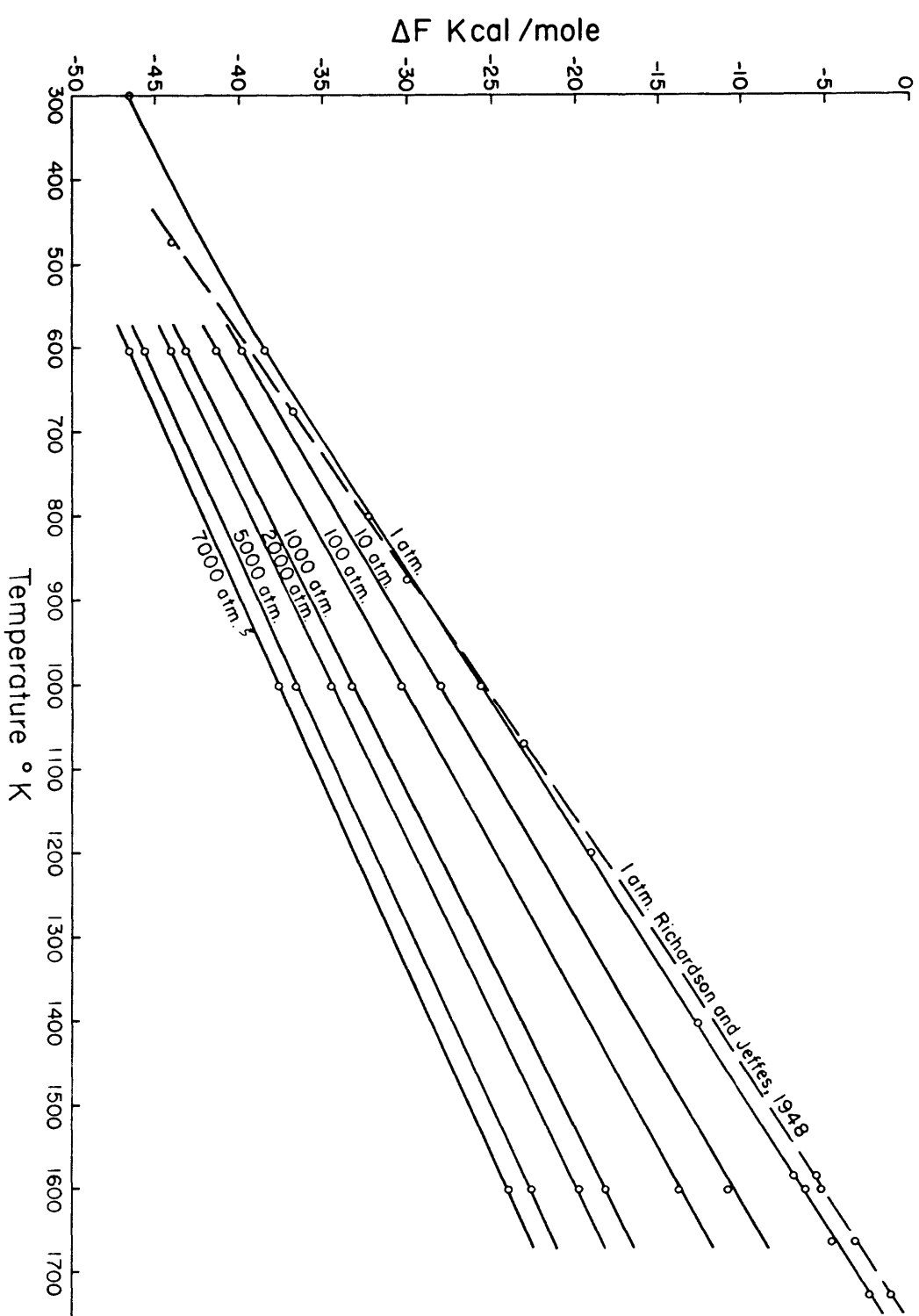


Fig. 12 Isobars showing variation of free energy increase ( $\Delta F$ ) with temperature for the magnetite - hematite reaction

Table 19. Activity of  $\text{Fe}_3\text{O}_4$  in Magnetite

T°C	act $\text{Fe}_3\text{O}_4$
1457	0.85
1392	0.90
1330	0.925
1313	0.93
1130	0.98

Inasmuch as below  $1100^{\circ}\text{C}$  at 1 atmosphere total pressure, solid solution of hematite in magnetite is negligible (Darken and Gurry, 1953), the activity of  $\text{Fe}_3\text{O}_4$  in magnetite will be unity below this temperature. As hematite takes no magnetite into solid solution, its activity is unity at all temperatures and at one atmosphere total pressure. If it is assumed that the solid solution relationships between magnetite and hematite are not influenced by pressure, which seems likely in view of the fact that their coefficients of thermal expansion and compressibility are nearly identical (Birch, 1942), then it may be concluded that the activities of both hematite and magnetite are unity for all temperatures below  $1000^{\circ}\text{C}$  and at all geologic pressures for a system consisting only of magnetite, hematite and oxygen. Thus the equilibrium constant for the reaction may be simply expressed as

$$K_1 = \frac{1}{(act O_2)^2}$$

Inasmuch as the concentration of oxygen will be very small it is permissible to substitute the partial pressure  $O_2$  for its activity. At low concentrations they will be identical. Thus the final equilibrium

constant is simply expressed as  $K_1 = \frac{1}{\frac{1}{p(O_2)^2}}$

The activities of both  $Fe_3O_4$  and  $Fe_2O_3$  will deviate markedly from unity in a normal petrologic system in which various solid solutions with other compounds are formed. The significance of such deviations will be evaluated subsequently.

Using the relationships  $\Delta F_T = -RT\ln K$  which is derived from the reaction isotherm (Glasscock, p. 283, 1947), it is possible to calculate the equilibrium constant for the magnetite-hematite reaction at any temperature if the free energy increase is known. Thus, using the  $\Delta F$  values obtained from the thermodynamic data, the equilibrium constants ( $K_1$ ) were calculated and are listed in Table 18. In Figure 13  $\log K_1$  is plotted versus  $\frac{1}{T}$  for one atmosphere pressure.

If the equilibrium  $p(O_2)$  for the magnetite-hematite reaction is known from experimental data and the activities of  $Fe_2O_3$  and  $Fe_3O_4$  are known for the appropriate temperatures,  $K_1$  can be directly evaluated. It is then possible to calculate free energy increase ( $\Delta F$ ) by using the expression  $\Delta F = -RT\ln K_1$ . This has been done for the high temperature experimental data of Darken and Curry (1946). The three calculated values of  $\Delta F$  are listed in Table 18 and are plotted in Figure 12, where they fall on the curve of Richardson and Jeffes (1948). This agreement is expected inasmuch as Richardson and Jeffes used similar experimental data in order to plot the upper portion of their curve. The upper portion of the  $\Delta F$  curve of Richardson and Jeffes, which coincides with the experimental data of Darken and Curry, is a well defined straight line and has essentially the same slope as the curve established

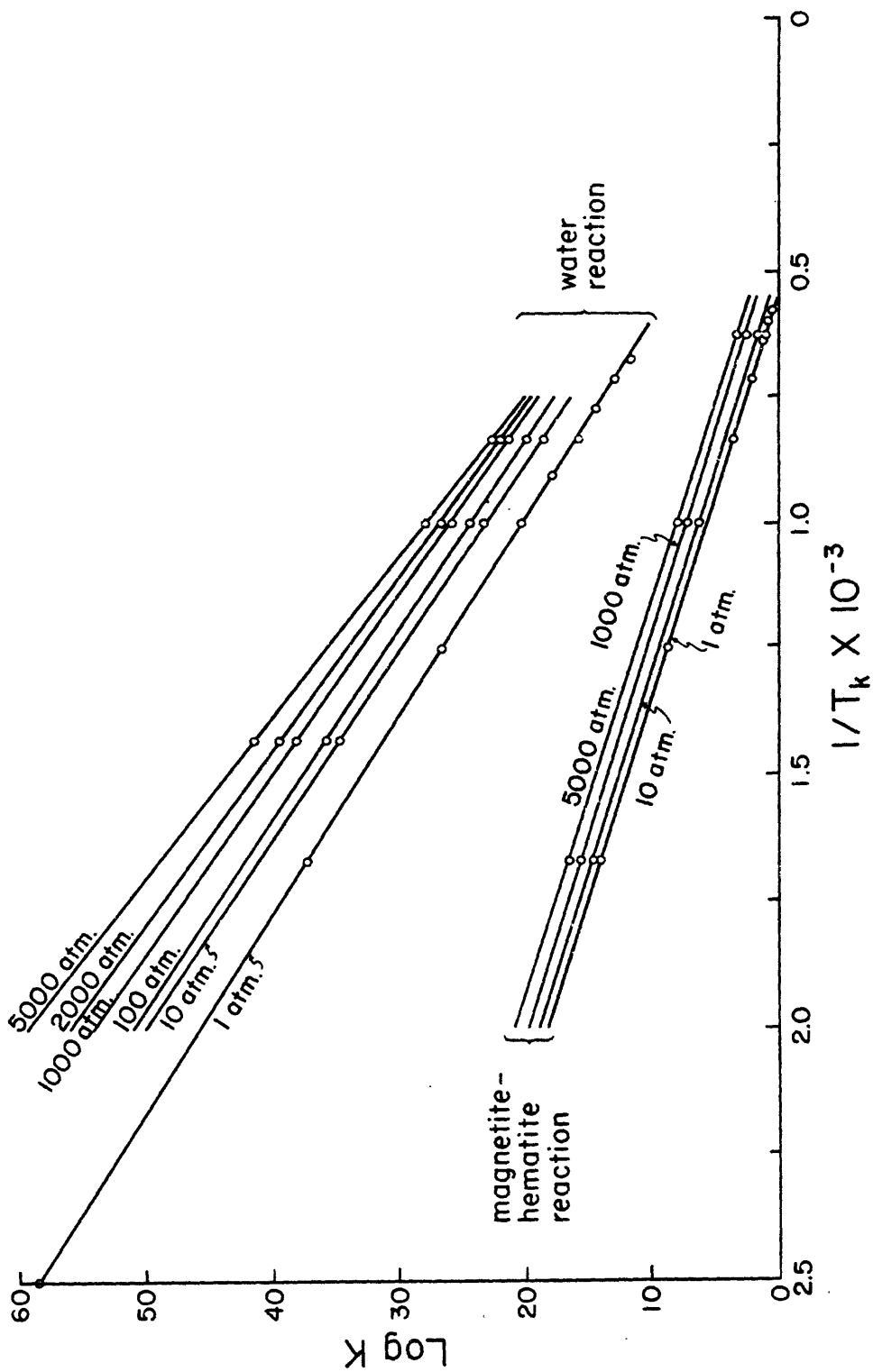


Fig. 13. Isobars showing variation of the equilibrium constants with temperature for the magnetite-hematite and water reactions

thermodynamically in this paper but is displaced +1.4 Kcal/mole from the latter. Darken and Curry claim an accuracy of about 1 per cent in their  $p(O_2)$  determinations, which is not sufficient to explain the difference between the two curves. Coughlin, et al. (1951) claim an accuracy of only 1 to 2 per cent for the bulk of their thermodynamic data. An error of this magnitude could explain the discrepancy between the two curves. Very likely the error in the thermodynamic quantities is even less at lower temperatures, so that the error in the  $\Delta F$  values calculated thermodynamically for the low temperature range is probably less than  $\pm 1$  Kcal. This small error will have very little effect on the calculated values of the equilibrium constant  $K_1$ .

#### Approximation of $\Delta F$ at high pressures for the reaction (1) at 25°C.

All the thermodynamic data utilized in evaluating the free energy change and equilibrium constant for the reaction (1) at 25°C. which have been for a total pressure equal to one atmosphere. The application of the  $\Delta F$  data to pressures higher than one atmosphere adjustment can be made for high pressure. Inasmuch as the reaction involves a gas phase ( $O_2$ ) it is certain that pressure will have a large influence on the position of equilibrium. Therefore, it is necessary to evaluate the free energy change ( $\Delta F$ ) for reactions of high pressures. The basic thermodynamic relationship which relates  $\Delta F$  to pressure is  $\left[\frac{d(\Delta F)}{dP}\right]_T = -V$ , where  $d(\Delta F)$  is the increment change in the free energy increase per liter at constant temperature T;  $dP$  is constant T; and  $-V$  is the molar volume change for the reaction at the temperature T (Glasstone, 1946, p. 231, 232), which for the reaction



$v_1 \quad v_2 \quad v_3$  (specific volumes of reactants and products),

$$\text{is } \Delta V = v_3 - (v_1 + v_2)$$

In order to evaluate the change in the free energy increase it is necessary to integrate the above expression,

$$d(\Delta F) = \Delta V dP$$

$$\Delta(\Delta F) = \int_1^P \Delta V dP, T = \text{constant}$$

The limits of the integration are from 1 atmosphere total pressure to the desired pressure  $P$ . Therefore,  $\left[ \Delta(\Delta F) \right]_T = \left[ \Delta F_P - \Delta F_1 \right]_T$  where

$\Delta F_P$  is the free energy increase at the high pressure,  $P$ ; and  $\Delta F_1$  is the free energy increase at a pressure of one atmosphere. Thus, the expression for the free energy increase at any pressure  $P$  and temperature  $T$  is

$$(\Delta F_P)_T = \left[ \Delta F_1 + \int_1^P -\Delta V dP \right]_T$$

As the values of  $\Delta F_1$  have already been determined for a series of temperatures (Table 13, Figure 12), it is only necessary to evaluate the integral term for the same set of temperatures in order to evaluate  $\Delta F_P$ .

The molar volume change,  $\Delta V$ , is itself a function of the total pressure and temperature. Therefore, in order to evaluate the integral it was necessary to determine  $\Delta V$  for a series of pressures (at three specified temperatures) and then to plot three  $\Delta V$  versus  $P$  isotherms. The area beneath an isotherm between one atmospheric and any other pressure  $P$  is the value of the integral,  $\int_1^P \Delta V dP$ , for the particular pressure

interval at the particular temperature. The addition of this area to the free energy increase for the reaction at one atmosphere pressure,  $\Delta F_1$ , (for the specified temperature) will give the free energy increase for the reaction at the higher pressure,  $\Delta F_p$ , for the specified temperature.

In order to evaluate  $\Delta V$  it is necessary to know the molar volumes of magnetite, hematite and oxygen at any specified temperature and pressure. This necessitates a knowledge of the compressibility and thermal expansion coefficients for the two solids and also an equation of state for oxygen which would be suitable for high temperatures and pressures. It is obvious that the magnitude of the change in the molar volumes of the two solid phases will be very much less than the change in the molar volume of  $O_2$  for a unit change in pressure or temperature. Thus in the expression  $\Delta V = V_3 - (V_1 + V_2)$ , the value of  $(V_3 - V_1)$  may be considered constant throughout the temperature and pressure range of interest. In other words the compressibility and thermal expansion of the gas  $O_2$  are so much greater than the similar constants for magnetite and hematite (Birch, 1942) that any change in the molar volume of the solids due to increase in temperature and pressure will be insignificant relative to the change in the molar volume of  $O_2$ . Therefore, the problem of evaluating  $\Delta V$  is reduced to the problem of evaluating the molar volume of  $O_2$  at high temperatures and pressures.

Fortunately the following modern empirical equation of state for  $O_2$  at high pressures and temperatures is available (Taylor, 1952).

$$\frac{PV}{nRT} = 1 + \frac{b}{V} + .625 \frac{b^2}{V^2} + .2869 \frac{b^3}{V^3} + .1928 \frac{b^4}{V^4}$$

This equation also is applicable to a number of gases including H<sub>2</sub> and H<sub>2</sub>O. The values of the second virial coefficient (b) and the third, fourth and fifth virial coefficients (b<sub>o</sub>) are given in Table 20 below, (Taylor, 1952).

Table 20

	b cm <sup>3</sup> /mole	b <sub>o</sub> cm <sup>3</sup> /mole
O <sub>2</sub>	30.5	57.75
H <sub>2</sub>	14.0	26.12
H <sub>2</sub> O	7.9	22.9

Therefore, it was possible to determine the molar volume of O<sub>2</sub> at any high temperature and pressure by performing a graphical solution to the above equation.

Using 5.2 g/cm<sup>3</sup> as the best density value for pure magnetite and hematite the volume of magnetite is 44.5 x 10<sup>-3</sup> liter/mole and the volume of hematite 30.7 x 10<sup>-3</sup> liter/mole. Thus the difference (V<sub>3</sub> - V<sub>1</sub>) is equal to 3.1 x 10<sup>-3</sup> liters. With the graphically obtained value of the molar volume of the O<sub>2</sub> and the above value of (V<sub>3</sub> - V<sub>1</sub>) (assumed as constant at high temperature and pressure) the value of  $\Delta V$  was obtained for a series of pressures from 1 to 7000 atmospheres for the three temperatures 600°, 1000° and 1600°K. These values of  $\Delta V$  were plotted versus pressure for these three isotherms. The area under each of these three isothermal curves/measured for the pressure intervals of 1-10, 1-100,

1-1000, 1-2000, 1-5000 and 1-7000 atmospheres. These areas which were in units of liter-atmospheres/mole were converted to units of kilocalories/mole and were then added to the value of  $\Delta F_1$  (free energy increase at 1 atmosphere pressure) for the proper temperature. Inasmuch as  $\Delta V$  is a negative value the change in free energy increase with increase in pressure is negative, so that at higher pressures the  $\Delta F$  assumes a higher negative value which simply indicates that the equilibrium for the magnetite-hematite reaction is shifted to the right.

The  $\Delta F$  data for total pressures of 10, 100, 1000, 2000, 5000, and 7000 atmospheres, at temperatures of 600°, 1000°, and 1600°K are listed in Table 21.  $\Delta F$  versus P is plotted for those three isotherms in Figure 11. It is apparent from the figure that pressure has a very significant effect upon the value of  $\Delta F$ , but that the influence of pressure is greatest in the interval from 1-1000 atmospheres, after which the effect of pressure becomes steadily less significant.  $\Delta F$  versus T is plotted for the isobars, 10, 100, 1000, 2000, 5000, and 7000 atmospheres in Figure 12.

Using the relationship  $\Delta F_T = -RT\ln K$  as before, the equilibrium constants for the magnetite-hematite reaction were evaluated for the higher pressures. These values of  $K_1$  are listed in Table 21 at the appropriate temperatures and pressures. The  $\log K_1$  versus  $\frac{1}{T_K}$  are plotted in Figure 13 for the various isobars.

Thus by using Figures 12 and 13 it is possible to determine readily the free energy increase ( $\Delta F$ ) and equilibrium constant ( $K_1$ ) respectively, for the magnetite-hematite reaction at any significant temperature and pressure.

Table 21. Thermodynamic and equilibrium data for the magnetite-hematite reaction ( $2\text{Fe}_3\text{O}_4 + \frac{1}{2}\text{O}_2 = 3\text{Fe}_2\text{O}_3$ ) for selected high temperatures and pressures.

Total Gas Pressure	$T^{\circ}\text{C}$	$T^{\circ}\text{K}$	$\Delta F$ Kcal/mole	$K_1^a$	$\log K_1^a$	$p(\text{O}_2)^b$ atm.	$\log p(\text{O}_2)$
10 atm.	327	600	-39.9	$3.67 \times 10^{14}$	14.52	$7.43 \times 10^{-30}$	-29.13
10 atm.	727	1000	-23.0	$1.35 \times 10^6$	6.11	$5.48 \times 10^{-13}$	-12.26
10 atm.	1327	1600	-10.1	$2.17 \times 10$	1.38	$2.90 \times 10^{-3}$	-2.54
100 atm.	327	600	-41.3	$1.22 \times 10^{15}$	15.00	$6.71 \times 10^{-31}$	-30.17
100 atm.	727	1000	-30.3	$4.26 \times 10^6$	6.61	$5.52 \times 10^{-14}$	-13.26
100 atm.	1327	1600	-13.9	$7.90 \times 10$	1.90	$2.19 \times 10^{-4}$	-3.66
1000 atm.	327	600	-43.2	$6.18 \times 10^{15}$	15.70	$2.62 \times 10^{-32}$	-31.58
1000 atm.	727	1000	-33.3	$1.92 \times 10^7$	7.25	$2.71 \times 10^{-15}$	-14.57
1000 atm.	1327	1600	-18.2	$3.07 \times 10^2$	2.48	$1.45 \times 10^{-5}$	-4.34
2000 atm.	327	600	-44.0	$1.22 \times 10^{16}$	16.05	$6.71 \times 10^{-33}$	-32.17
2000 atm.	727	1000	-34.5	$3.67 \times 10^7$	7.55	$7.43 \times 10^{-16}$	-15.13
2000 atm.	1327	1600	-19.9	$5.21 \times 10^2$	2.71	$5.03 \times 10^{-6}$	-5.30
5000 atm.	327	600	-45.6	$4.95 \times 10^{16}$	16.63	$4.07 \times 10^{-34}$	-33.39
5000 atm.	727	1000	-35.6	$1.00 \times 10^8$	8.00	$1.00 \times 10^{-16}$	-16.00
5000 atm.	1327	1600	-22.7	$1.23 \times 10^3$	3.10	$8.33 \times 10^{-7}$	-6.08
7000 atm.	327	600	-46.5	$1.00 \times 10^{17}$	17.00	$1.00 \times 10^{-34}$	-34.00
7000 atm.	727	1000	-37.6	$1.73 \times 10^3$	9.21	$3.34 \times 10^{-17}$	-16.48
7000 atm.	1327	1600	-24.0	$1.92 \times 10^3$	3.28	$3.70 \times 10^{-7}$	-6.43

$$^a \ln K_1 = - \frac{\Delta F}{RT}$$

$$^b p(\text{O}_2)^{\frac{1}{2}} = \frac{(\text{act Fe}_2\text{O}_3)^3}{(\text{act Fe}_3\text{O}_4)^2 K_1},$$

act  $\text{Fe}_2\text{O}_3$  = unity at all temperatures and pressures.

act  $\text{Fe}_3\text{O}_4$  = 0.925 at 1327°C (Table 19) and unity at 327 and 727°C for all pressures.

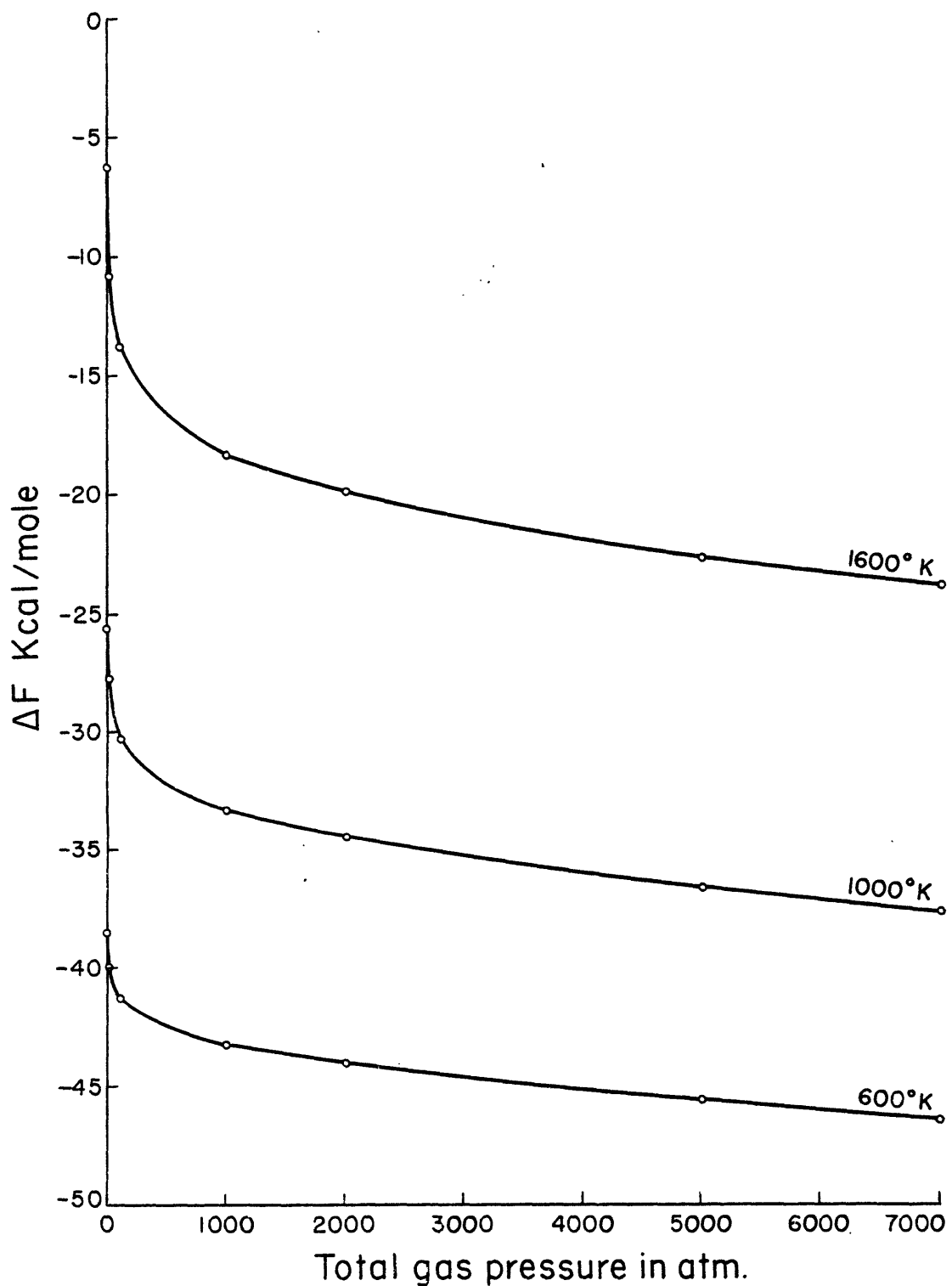


Fig. 14. Isotherms showing variation of free energy increase ( $\Delta F$ ) with pressure for the magnetite-hematite reaction

### Calculation of $p(O_2)$

By using an activity coefficient of unity for hematite at all temperatures and an activity coefficient as calculated by Darken and Gurry for magnetite (Table 19), at temperatures greater than 1100°C, and an activity coefficient of unity for magnetite for temperatures less than 1100°C, and knowing the equilibrium constant for the magnetite-hematite reaction it is possible to calculate  $p(O_2)$  for equilibrium at any temperature and pressure for the magnetite-hematite reaction. This has been done for a series of temperatures at one atmosphere pressure, see Table 18. In addition, utilizing the high temperature and pressure equilibrium constants as calculated in the previous section, the  $p(O_2)$  for equilibrium in the magnetite-hematite reaction has been calculated for three temperatures (600°, 1000°, and 1600°K) at total pressures of 10, 100, 1000, 2000, 5000, 7000 atmospheres. These values are listed in Table 21. In Figure 16 the  $\log p(O_2)$  versus  $\frac{1}{T}$  is plotted for the above isobars. It

is clear from the figure that there is a linear dependence of  $\log p(O_2)$  on  $\frac{1}{T}$ , so that the  $\log p(O_2)$  increases with a decrease in  $\frac{1}{T}$  i. e.,  $p(O_2)$  increases with T. This of course is merely a confirmation of the empirically established fact that the dissociation pressure of hematite increases with temperature. The figure also shows that the equilibrium  $p(O_2)$  decreases very rapidly with increase in pressure at constant temperature, up to about 1000 atmospheres, after which the change in  $p(O_2)$  with pressure is relatively small. This is of course a reflection of the similar relation of  $\Delta F$  to P (Figure 14).

The unique aspect of Figure 16, is that it enables one to obtain

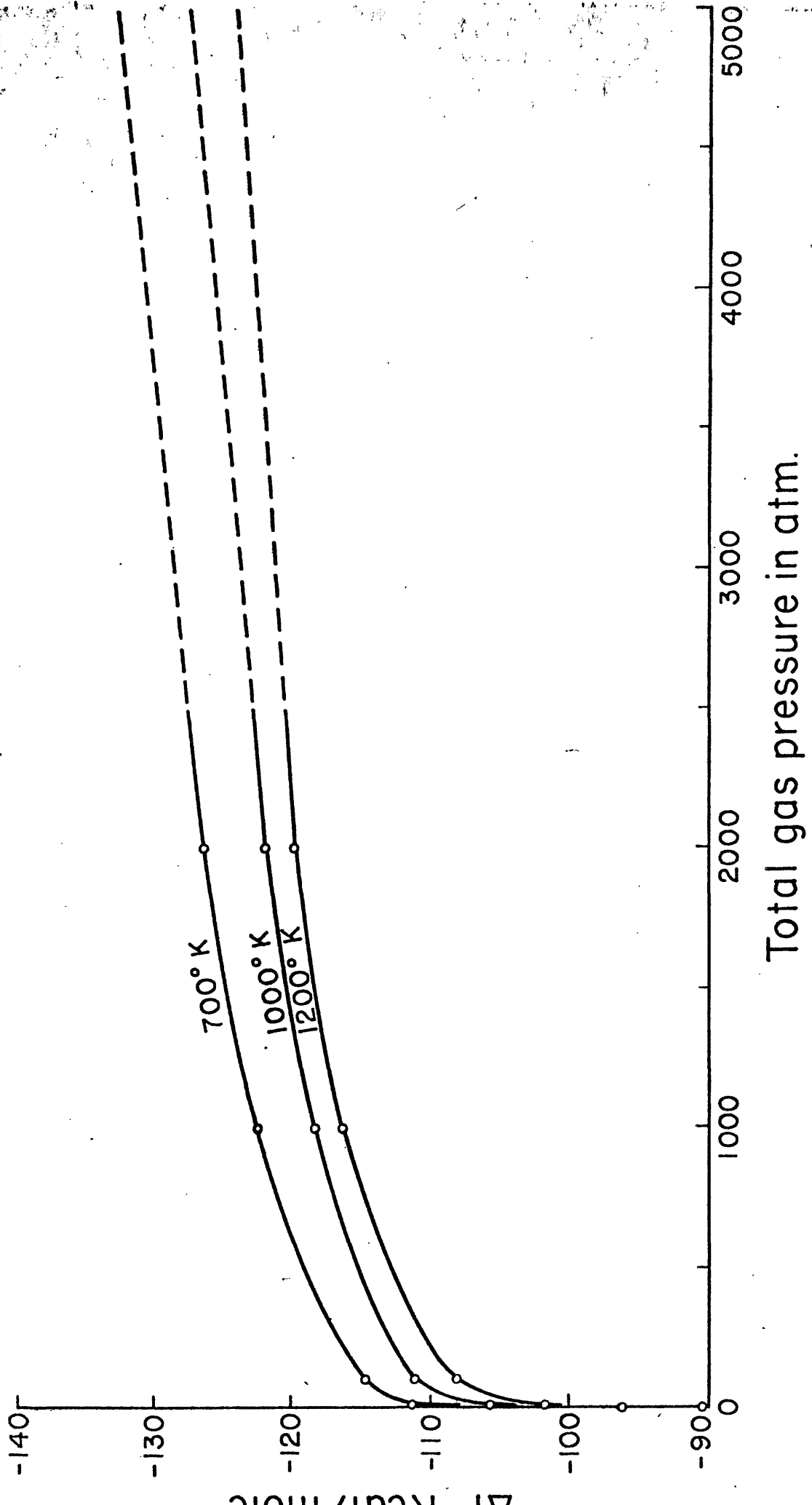


Fig. 15. Isotherms showing variation of free energy increase ( $\Delta F$ ) with pressure for the water reaction

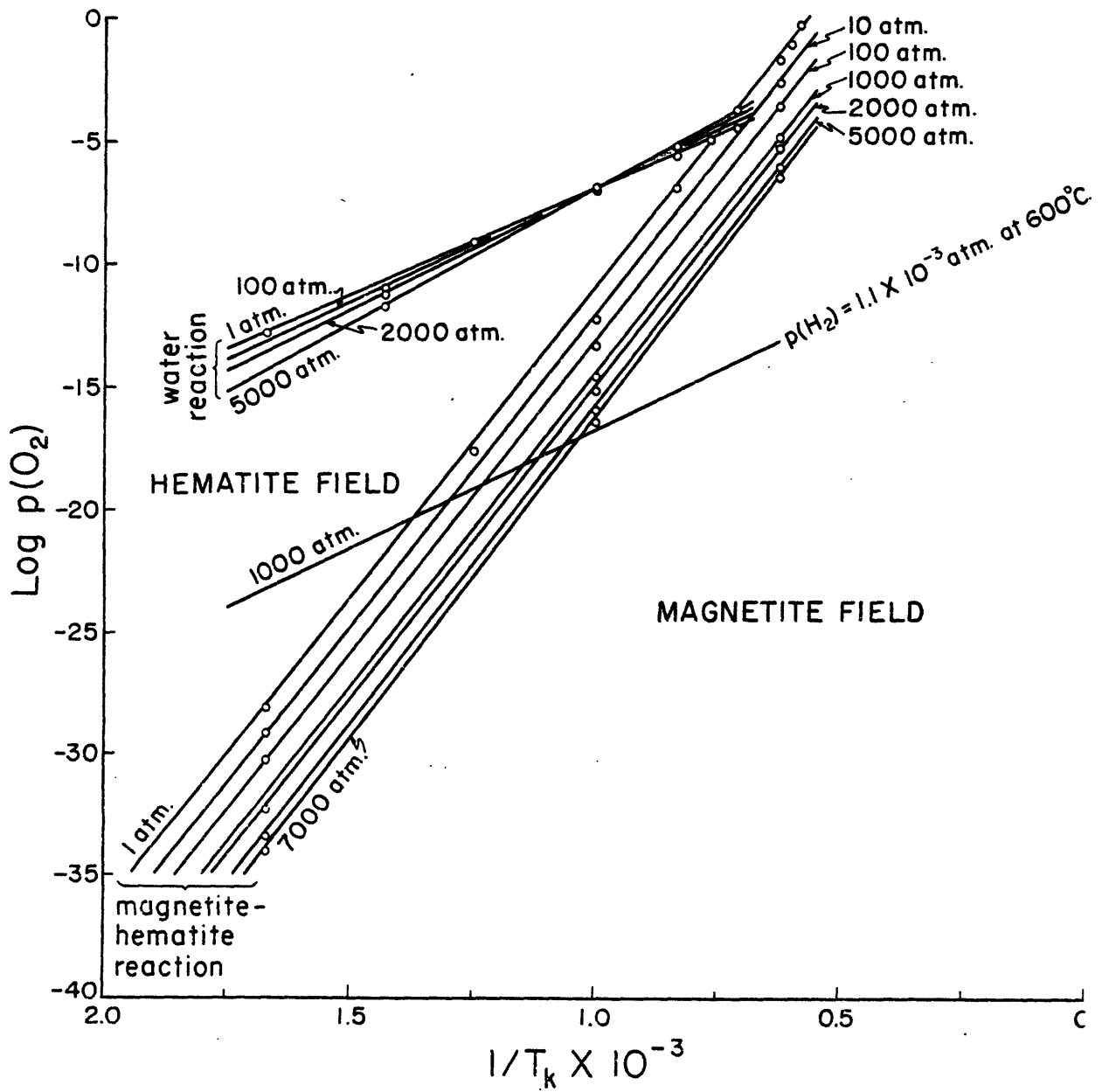
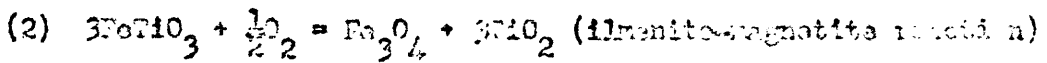
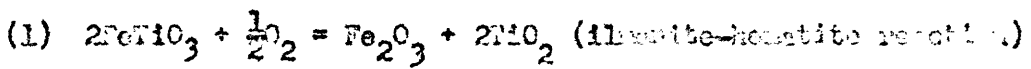


FIG. 16. Univariant isobars showing variation of the equilibrium  $p(O_2)$  with temperature for the magnetite-hematite and water reactions

a value for the  $p(O_2)$  at any reasonable geologic pressure and for temperatures which have not been amenable to experimental investigation [largely because of the low equilibrium  $p(O_2)$  at such temperatures]. Thus the figure is suitable for application to petrologic systems, whereas the available experimental data have been limited to low pressure and high temperature (slag) conditions.

#### THE COMBINATION OF ILMENITE

In nature the iron oxides do not occur exclusive of other elements. Titanium is usually an important constituent and is distributed in such minerals as ilmenite, rutile, ulvöspinel and in solid solution with iron oxides. Of particular interest in many metasomatic and metaclastic rocks are ilmenite and rutile which frequently occur with magnetite and hematite. If these minerals crystallized at equilibrium, then it is clear that there must be some one or group of chemical reactions which describes the equilibrium. The equilibrium between ilmenite and the iron oxides may be expressed by two simple chemical reactions.



There are some thermodynamic data (heat content and entropy) available for ilmenite and rutile at room temperature and one atmosphere pressure. With these data and the analogous data for hematite, magnetite and oxygen it is possible to calculate the free energy increase for the two reactions as written above. The results of these calculations are listed with the same data for the magnetite-hematite reaction in Table 22.

Table 22. Thermodynamic data for iron and titanium oxide reactions at 25°C and one atmosphere pressure

	magnetite-hematite	ilmenite-hematite	ilmenite-magnetite
$\Delta F$ Kcal/mole	-46.50	-46.90	-46.4
$\Delta H$ Kcal/mole	-55.5	-55.5	-55.5
$\Delta S$ cal/deg.mole	-30.5	-29.58	-29.36
$\left[ \frac{d(\Delta F)}{dT} \right]_P = -\Delta S$	+30.5	+29.58	+29.36

It is obvious from the table that the thermodynamic data for all the reactions at a temperature of 25°C and 1 atmosphere pressure are essentially identical. Perhaps more important, the entropy changes are the same, thus indicating that the  $\Delta F$  values for the three reactions will still be the same even at higher temperatures. The conclusion emerges from the fundamental equation which relates free energy to temperature, i. e.,  $\left[ \frac{d(\Delta F)}{dT} \right]_P = -\Delta S$  (Glasstone, 1946, p.231). Thus the slope of the  $\Delta F$  versus T curve for each of the three reactions will be about the same.

It was stated previously that the sensitivity of the magnetite-hematite reaction to pressure is due to the influence of pressure on the gas phase and not on the solid phases. Thus it seems reasonable to assume that the influence of increased pressure on the free energy increase for the two ilmenite reactions will not be greatly different from the influence of pressure on the magnetite-hematite reaction. In thermodynamic terms it seems likely that  $\left[ \frac{d(\Delta F)}{dP} \right]_T = -V$  is the same for all of the three

reactions. Thus, in a rather qualitative way it can be stated that the free energy increase for these three reactions will be about identical for all significant temperatures and pressures. Likewise the values of equilibrium constants ( $\Delta F = -RT\ln K$ ) for the three reactions should be about the same at any particular pressure and temperature.

The equilibrium constants for these three reactions may be expressed as below:

$$K_1 = \frac{(\text{act } \text{Fe}_2\text{O}_3)^3}{(\text{act } \text{Fe}_3\text{O}_4)^2 P(\text{O}_2)^{\frac{1}{2}}}$$

$$K_2 = \frac{(\text{act } \text{Fe}_2\text{O}_3) (\text{act } \text{TiO}_2)^2}{(\text{act } \text{FeTiO}_3)^2 P(\text{O}_2)^{\frac{1}{2}}}$$

$$K_3 = \frac{(\text{act } \text{Fe}_3\text{O}_4) (\text{act } \text{TiO}_2)^3}{(\text{act } \text{FeTiO}_3)^3 P(\text{O}_2)^{\frac{1}{2}}}$$

As discussed previously the activities of magnetite and hematite in a system involving no other components will be equal to unity at most petrologic temperatures and pressures. In an oxide system of iron and titanium there can be considerable solid solution between magnetite and ilmenite, ilmenite and hematite, and limited solid solution between rutile and ilmenite or hematite (Chapter 6). Thus, in such a system the activities of the solid phases will deviate from unity according to the degree of solid solution. Inasmuch as the degree of solid solution is chiefly a function of temperature, the activities will vary with temperature.

From a consideration of the degree of solid solution, by definition never greater than 50 per cent, it seems likely that the activity of any solid phase will never be less than .5 or .6. Thus a brief calculation shows that the value of the equilibrium  $p(O_2)$  as calculated from the equilibrium constant and the minimum possible activities of the solid phases will differ at very most by a factor of 10 from the  $p(O_2)$  as calculated from the equilibrium constant and unit activities for the solid phases. A factor of 10 is not too significant when the value of  $p(O_2)$  may be of the order of  $10^{-10}$  to  $10^{-20}$  atmospheres.

Actually the concept of activity makes it conceivable that the  $p(O_2)$  for the three reactions can be equal when the equilibrium constants for the three reactions are not quite equal. The deviations of the activities of the solid phases from unity in effect compensate for any small difference in the equilibrium constants, so that it is entirely feasible that the  $p(O_2)$  for the three reactions can be identical for any particular pressure and temperature despite small differences between the values of equilibrium constants. That the  $p(O_2)$  be identical for the reactions is a necessity if magnetite, hematite, ilmenite and rutile are all to occur together at chemical equilibrium.

Therefore, it may be concluded that thermodynamically it is possible and even expected to find that all these solid phases crystallized side by side. The energetic treatment substantiates the idea that ilmenomagnetite, hemoilmenite, ilmenohematite, and rutile all could crystallize as a single paragenesis under a single set of physical conditions. It is energetically unnecessary to postulate a variable set of physical conditions to account for this paragenesis. Had this thermodynamic data

indicated widely different stability relations i. e.,  $p(O_2)$ , for the solid phases in these chemical reactions, then perhaps it would be necessary to postulate several changing sets of physical conditions to account for such a mineral assemblage.

### THE WATER REACTION ( $2H_2 + O_2 = 2H_2O$ )

#### Introduction

Kennedy (1948) has called attention to the importance of the volatile constituents and the iron oxides of igneous rocks. He has presented data with which it is possible to calculate the partial pressure of  $O_2$  in a rock melt with a particular ferric-ferrous iron ratio for a particular temperature. He points out that the  $O_2$  pressure also must be in equilibrium with the volatiles in the melt and presents data which enable him to calculate the partial pressure of  $H_2$  which would be in equilibrium with  $H_2O$ ,  $O_2$  and a particular ferrous-  
iron ratio at a given temperature and gas pressure. As  $H_2O$  is certainly the most important volatile constituent in the principal petrologic systems the significance of his computations are apparent.

The same general treatment as employed by Kennedy may be used in the case of metamorphic and metasomatic rocks. From the data for the magnetite-hematite reaction it is possible to obtain the equilibrium  $p(O_2)$  from Figure 16 for any important temperature and pressure. If there is excess  $H_2O$  in the petrologic system (which certainly must be the case in almost any crystallizing metamorphic or metasomatic rock), it is necessary that for chemical equilibrium to be maintained, the requisite  $p(O_2)$  for the magnetite-hematite reaction must be identical

with the  $p(O_2)$  in equilibrium with  $H_2O$  for the given temperature and pressure. Thus if the equilibrium constant for the formation of  $H_2O$ , ( $2H_2 + O_2 = 2H_2O$ , hereafter the water reaction),

$$K_w = \frac{p(H_2O)^2}{p(H_2)^2 p(O_2)}$$

were known for significant temperatures and pressures it would be possible to calculate the partial pressure of  $H_2$  [ $p(H_2)$ ] in equilibrium in a system of  $H_2O$ , magnetite and hematite. In addition if the equilibrium constant for the water reaction were known it would be possible to evaluate in a quantitative way the oxidizing or reducing effect that  $H_2O$  would have on a magnetite-hematite system upon coming to equilibrium with such a system. Thus it is critical to evaluate the equilibrium constant for the water reaction for a series of significant temperatures and pressures.

#### Experimental data for the water reaction

Dwyer and Oldenberg (1944) have experimentally determined the equilibrium constants for the water reaction for a series of temperatures from 400° to 1500°K at a total pressure of 1 atmosphere. These data are presented in Table 23. The  $\log K_w$  versus  $\frac{1}{T_K}$  for 1 atmosphere pressure is plotted in Figure 13. Utilizing the relationship  $\Delta F_w = -RT \ln K_w$  the value of the free energy increase for the reaction has been determined and is listed in Table 23 and plotted versus  $T_K$  in Figure 17. Note how well the values of  $\log K_w$  and  $\Delta F_w$  fall in straight lines. Utilizing Dwyer and Oldenberg's data and some additional thermodynamic data it is possible to evaluate the free energy increase and the equil-

Table 23. Experimental, thermodynamic and equilibrium data for the  $H_2O$  reaction ( $2H_2 + O_2 = 2H_2O$ ) for selected temperatures and pressures.

Total Gas Pressure	T°C	T°K	$\Delta F$ Kcal/mole	$\log K_w^a$	$K_w$	$p(O_2)$ atm.	$\log p(O_2)$
b	1 atm.	127	400	-107.0	58.53	$3.39 \times 10^{53}$	$1.95 \times 10^{-20}$
	1 atm.	327	600	-106.5	37.30	$2.00 \times 10^{37}$	$2.32 \times 10^{-13}$
	1 atm.	527	800	-101.5	26.60	$3.93 \times 10^{26}$	$8.57 \times 10^{-10}$
	1 atm.	727	1000	-96.1	20.14	$1.38 \times 10^{20}$	$1.22 \times 10^{-7}$
	1 atm.	827	1100	-93.2	17.79	$6.17 \times 10^{17}$	$7.40 \times 10^{-7}$
	1 atm.	927	1200	-90.5	15.32	$6.61 \times 10^{15}$	$3.36 \times 10^{-6}$
	1 atm.	1027	1300	-87.8	14.15	$1.41 \times 10^{14}$	$1.21 \times 10^{-5}$
	1 atm.	1127	1400	-84.9	12.71	$5.13 \times 10^{12}$	$3.66 \times 10^{-5}$
	1 atm.	1227	1500	-82.0	11.46	$2.83 \times 10^{11}$	$9.60 \times 10^{-5}$
	10 atm.	427	700	-111.3	34.8	$6.3 \times 10^{34}$	$7.4 \times 10^{-12}$
	10 atm.	727	1000	-105.9	23.1	$1.3 \times 10^{23}$	$5.8 \times 10^{-8}$
	10 atm.	927	1200	-101.9	18.5	$3.2 \times 10^{18}$	$2.0 \times 10^{-6}$
	100 atm.	427	700	-114.8	35.3	$6.3 \times 10^{35}$	$1.6 \times 10^{-11}$
	100 atm.	727	1000	-111.1	24.2	$1.6 \times 10^{24}$	$1.1 \times 10^{-7}$
	100 atm.	927	1200	-103.1	19.9	$7.9 \times 10^{19}$	$3.2 \times 10^{-6}$
	1000 atm.	427	700	-122.6	38.2	$1.6 \times 10^{38}$	$1.1 \times 10^{-11}$
	1000 atm.	727	1000	-113.4	25.9	$7.9 \times 10^{25}$	$1.5 \times 10^{-7}$
	1000 atm.	927	1200	-116.3	21.2	$1.6 \times 10^{21}$	$5.4 \times 10^{-6}$
	2000 atm.	427	700	-126.5	39.5	$3.2 \times 10^{39}$	$6.3 \times 10^{-12}$
	2000 atm.	727	1000	-122.0	26.6	$4.0 \times 10^{26}$	$1.4 \times 10^{-7}$
	2000 atm.	927	1200	-119.9	21.8	$6.3 \times 10^{21}$	$5.4 \times 10^{-6}$
	5000 atm.	427	700	-133	41.5	$3.2 \times 10^{41}$	$2.7 \times 10^{-12}$
	5000 atm.	727	1000	-123	23.0	$1.0 \times 10^{23}$	$3.6 \times 10^{-8}$
	5000 atm.	927	1200	-124	22.6	$4.0 \times 10^{22}$	$5.4 \times 10^{-6}$

$$a \quad K_w = \frac{p(H_2O)^2}{p(H_2)^2 p(O_2)} ; \quad \ln K_w = - \frac{\Delta F}{RT}$$

b

Experimental data for all 1 atm. total gas pressures from Dwyer and Oldenberg, 1944.

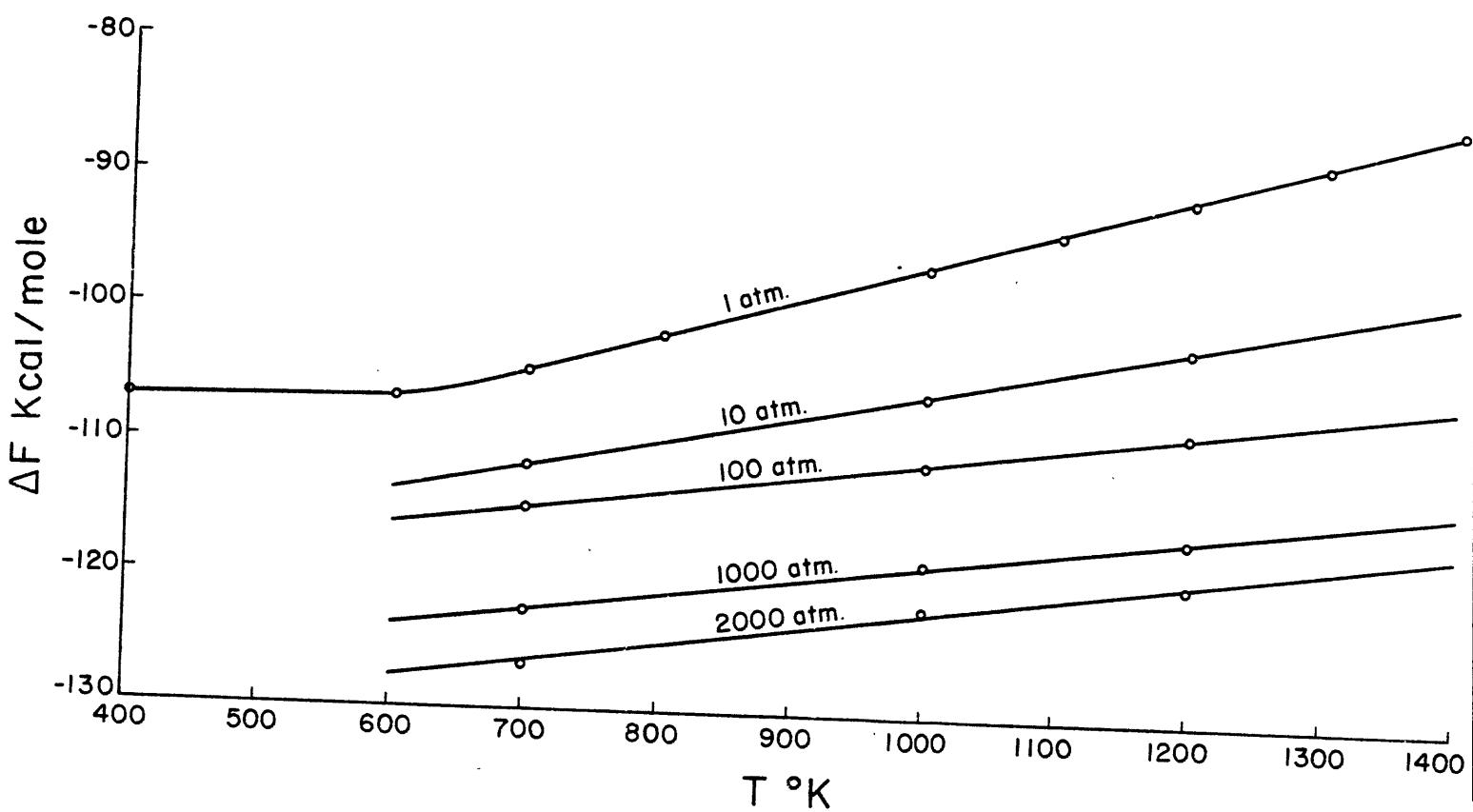


Fig. 17. Isobars showing variation of variation of free energy ( $\Delta F$ ) with temperature for the water reaction

ibrium constant for the water reaction at high pressures for the investigated series of temperatures.

#### Water reaction at high pressures and temperatures

As was the case for the magnetite-hematite reaction, in order to evaluate the free energy increase and equilibrium constant for the water reaction at high pressure it is necessary to evaluate the following thermodynamic equation:

$$\left[ \frac{d\Delta F}{dP} \right]_T = \Delta V_w$$

where  $\Delta F$  is the free energy increase and  $\Delta V_w$  the volume increase for the water reaction. In order to evaluate  $\Delta V_w$  for a series of temperatures and pressures it is necessary to know the molar volumes of  $N_2$ ,  $O_2$  and  $H_2O$  at these temperatures and pressures. Fortunately, the specific volume of  $H_2O$  has been experimentally determined by Kennedy (1950) for temperatures up to 1000°C and pressures up to 2500 bars. In addition by utilizing the equation of state as given by Taylor (1952),

$$\frac{PV}{nRT} = 1 + \frac{b}{V} + .625 \frac{b_0^2}{V^2} + .2869 \frac{b_0^3}{V^3} + .1920 \frac{b_0^4}{V^4}$$

it is a simple matter to graphically determine the molar volumes of  $N_2$  and  $O_2$  at high pressures and temperatures. The first and second virial coefficients,  $b$ ,  $b_0$  respectively, are given in Table 20. Thus it is possible to evaluate the volume increase  $\Delta V_w$  for the water reaction for any temperatures up to 1000°C and any pressures up to 2500 bars.

As for the magnetite-hematite reaction the equation

$$(\Delta F_p)_T = \left[ \Delta F_1 + \int_1^P \Delta V dP \right]_T$$

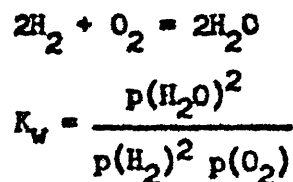
applies to the water reaction; where  $\Delta F_p$  is the free energy increase

at the pressure  $P$ ;  $\Delta F_1$  is the free energy increase at one atmosphere pressure and  $\int\limits_1^P \Delta V dP$  is the difference in the free energy increase for the two pressures, 1 and  $P$ , for the temperature  $T$ . Therefore, by plotting  $\Delta V$  versus  $P$  for a group of temperatures and measuring the area under those isotherms, the integral may be evaluated and by adding this value to the appropriate  $\Delta F_1$ , the free energy increase may be determined for any pressure,  $P$ , for the temperature of the specific isotherm. The  $\Delta V$  data have been calculated and plotted versus  $P$  for the 700°, 1000° and 1200°K isotherms. By a series of approximations the area beneath each of these isotherms has been determined for the pressures 10, 100, 1000, and 2000 atmospheres. Thus, the free energy increase for the water reaction was determined for these three temperatures at the four indicated pressures. These values of the free energy increase are listed in Table 23 and plotted versus  $P$  for the three isotherms in Figure 15. The graph, as in the magnetite-hematite reaction, shows that the change in the free energy increase is very marked in the pressure interval from 1-1000 atmospheres. Above this pressure the compressibilities of the gases becomes so large that the pressure effect is considerably less. The curves have been extrapolated to 5000 atmospheres in order to give an approximate value of  $\Delta F$  at that pressure.  $\Delta F$  versus  $T$ , for the isobars 10, 100, 1000, and 2000 atmospheres, are plotted in Figure 17. As in the case of experimental data (1 atmosphere isobar), there is a linear dependence of  $\Delta F$  on temperature, in addition the slopes of the isobars greater than one atmosphere are not much different from the slope of the experimentally determined curve of Dwyer and Oldenberg (1944).

Using the  $\Delta F$  data as calculated for high temperature and pressure is a simple matter to calculate the equilibrium constant for the water reaction by utilizing the following expression,  $\Delta F = -RT \ln K_w$ . This has been done and the values of  $K_w$  for the three temperatures 700°, 1000°, and 1200°K and for the pressures 10, 100, 1000, 2000, and 5000 atmospheres are listed in Table 23, along with the experimental values  $K_w$  for 1 atmosphere pressure. The values of  $\log K_w$  are plotted versus  $\frac{1}{T}$  for the same isobars in Figure 13. For all isobars there is the expected linear dependence of  $\log K_w$  on  $\frac{1}{T}$ . In general the slopes of the calculated isobars are not too different from the slopes of the experimentally determined 1 atmosphere isobar. Figure 13 may be used to give equilibrium constant for the water reaction for any significant thermologic temperature and pressure.

#### Calculation of $p(O_2)$ for the water reaction

With the equilibrium constant for the water reaction it is possible calculate the  $p(O_2)$  in equilibrium with pure  $H_2O$  for any significant temperature and pressure. A sample calculation is given below.



$$\text{Let } a = p(O_2)$$

$$2a = p(H_2)$$

P = total volatile pressure

$$P - 2a = p(H_2O)$$

$$\text{Therefore, } K_w = \frac{(P - 2a)^2}{(2a)^2} = \frac{(P - 2a)^2}{4a^3}$$

assume  $2a$  is much less than  $P$  (very little  $H_2O$  is actually dissociated),

then

$$a = \left[ \frac{P}{4K_w} \right]^{\frac{1}{3}}$$

$$p(O_2) = \frac{P^{\frac{2}{3}}}{(4K_w)^{\frac{1}{3}}}$$

Thus the equilibrium partial pressure of  $O_2$  for the water reaction is directly proportional to the two thirds power of the total water pressure and inversely proportional to the one third power of the equilibrium constant. Using the above method the equilibrium partial pressures of  $O_2$  for the water reaction have been calculated and are listed in Table 23; in addition the  $\log p(O_2)$  has been plotted versus  $\frac{1}{T_K}$  in Figure 16. The graph shows that regardless of the total water pressure in the system the equilibrium  $p(O_2)$  for the water reaction remains very nearly the same for any given temperature. The greatest range of  $\log p(O_2)$  is from -15.3 at 5000 atmospheres to -13.5 at 1 atmosphere for  $\frac{1}{T_K} = 1.75$ .

At higher temperatures the  $\log p(O_2)$  isobars actually cross in the region of  $\frac{1}{T_K} = 1.0$ , i. e.,  $1000^\circ K$ , so that above  $1000^\circ K$  the  $p(O_2)$  is greater for the higher total water pressures, but below this temperature the  $p(O_2)$  is actually less for the higher total water pressures. This relationship is explained by the fact that  $p(O_2)$  is a function of the equilibrium constant which, as was previously shown, is itself a function of temperature and pressure; so in effect the change in the value of  $K_w$  cancels out the effect that increased total water pressure has on the

value of  $p(O_2)$ . Thus, regardless of total pressure the  $p(O_2)$  is about the same for any given temperature. A plot of  $\log K_w$  versus  $\log P^2$  for any isotherm gives an almost straight line. This quantitatively substantiates the statement that the change in  $K_w$  with increased total water pressure essentially cancels out the effect of the increased pressure on the value of  $p(O_2)$ , according to the equation

$$p(O_2) = \left[ \frac{P^2}{4K_w} \right]^{\frac{1}{3}}$$

In evaluating the  $p(O_2)$  for the water reaction Kennedy (1948) ignored the fact that the equilibrium constant ( $K_w$ ) varied with the total water pressure, thus his values of  $p(O_2)$  for high pressures are consistently greater than for low pressures. Thus by calculating  $K_w$  for high pressures, it has been possible to arrive at a much more reliable figure for the  $p(O_2)$  in equilibrium with pure water for the high pressure range.

#### Influence of other volatiles on the water reaction

In order to apply the water reaction data in petrologic problems it is necessary to consider the influence that other substances, particularly volatiles, will have on the water equilibrium. To evaluate such effects requires not only a knowledge of all the thermodynamic and chemical equilibrium data for these other gases, but also it is necessary to know in what kinds of molecules and ions these gases exist. Obviously, these data are lacking for gases at such high temperatures and pressures; therefore no attempt is made to quantitatively evaluate the effects of other gases. However, these gases all of which would be involved in

oxidation-reduction reactions will cause the equilibrium  $p(O_2)$  in such a "real" system to be different from what it would be in a pure "ideal" water system as has been considered here.

COMPARISON OF THE WATER REACTION WITH THE MAGNETITE-HEMATITE  
REACTION

Now that the equilibrium constants for the water and the magnetite-hematite reactions have been evaluated for a group of petrologically significant temperatures and pressures, it is possible to discuss in a more quantitative fashion the various aspects of a system consisting of water, magnetite and hematite at these temperatures and pressures.

For purposes of discussion let us imagine as isolated a water system and a magnetite-hematite system both at the same pressure and temperature and both at chemical equilibrium. It is clear from Figure 16 that for any temperature below about 1300°K, regardless of the total pressure, the partial pressure of  $O_2$  in equilibrium with a pure water system is considerably greater than that in equilibrium with a pure magnetite-hematite system. Hence, below 1300°K there exists a disequilibrium between the water reaction and the magnetite-hematite reaction, so that if the two "isolated" systems are combined additional oxidation of magnetite will take place until the  $p(O_2)$  in equilibrium with  $H_2O$  drops to an identical value for that in equilibrium with magnetite and hematite. As water comes to chemical equilibrium with magnetite-hematite by this utilization of some of the excess  $O_2$  through the oxidation of magnetite, additional  $H_2$  is formed; so that at equilibrium at the lower  $p(O_2)$ , the

$p(H_2)$  is considerably greater than for a pure water system. Thus, if a rock contains magnetite and hematite and if it is assumed that equilibrium was established between these iron oxides and the water in the system at a given temperature and pressure [knowing from Figure 16 the equilibrium  $p(O_2)$  for the magnetite-hematite reaction], it is possible to calculate the requisite  $p(H_2)$  in order that  $H_2O$  could exist in chemical equilibrium with the two iron oxides. By using the appropriate values of  $p(O_2)$  for the magnetite-hematite equilibrium (Figure 16) and the appropriate values of the equilibrium constant for the water reaction, the requisite  $p(H_2)$  for chemical equilibrium in a water-magnetite-hematite system has been determined. These values are listed in Table 24, and  $\log p(H_2)$  is plotted versus  $\frac{1}{T}$  for the various isobars in Figure 18. In addition the equilibrium  $p(H_2)$  for the pure water system is listed in Table 24 and plotted in Figure 18. It is obvious that the  $p(H_2)$  is considerably greater for the water-magnetite-hematite equilibrium than it is for the pure water equilibrium. From Figure 18 it is possible to obtain an approximate value of the  $p(H_2)$  (for a particular temperature and pressure) which must have existed in a petrologic system in which water, magnetite and hematite were at chemical equilibrium. Thus, if it is possible to estimate the temperature and pressure under which a magnetite-hematite bearing metamorphic or metasomatic rock crystallized, it is possible to determine the equilibrium  $p(O_2)$  (Figure 16) and  $p(H_2)$  (Figure 18) for the crystallizing system.

At temperatures above about  $1300^{\circ}\text{K}$  it is clear from Figure 16 that the equilibrium  $p(O_2)$  for the magnetite-hematite reaction is greater than that for the water reaction. Under such conditions the  $p(H_2)$  in equilib-

Table 24. Equilibrium  $p(H_2)$  for a pure  $H_2O$  system and a  $H_2O$ -magnetite-hematite system for selected temperatures and pressures.

Total Gas Pressure	T°C	T°K	Pure $H_2O$ System		$H_2O$ -Magnetite-Hematite System	
			$p(H_2)$ atm.	$\log p(H_2)$	$p(H_2)$ atm.	$\log p(H_2)$
1 atm.	427	700	$4.03 \times 10^{-11}$	-10.40	$2.10 \times 10^{-5}$	-4.63
1 atm.	600	873	$1.40 \times 10^{-9}$	-7.85	$2.27 \times 10^{-5}$	-4.64
1 atm.	727	1000	$2.44 \times 10^{-7}$	-6.61	$3.14 \times 10^{-5}$	-4.50
1 atm.	927	1200	$6.72 \times 10^{-6}$	-5.17	$3.52 \times 10^{-5}$	-4.45
100 atm.	427	700	$3.2 \times 10^{-11}$	-10.49	$1.7 \times 10^{-4}$	-3.77
100 atm.	600	873	$1.1 \times 10^{-8}$	-7.96	$2.2 \times 10^{-4}$	-3.66
100 atm.	727	1000	$2.2 \times 10^{-7}$	-6.66	$3.4 \times 10^{-4}$	-3.47
100 atm.	927	1200	$6.4 \times 10^{-6}$	-5.18	$3.7 \times 10^{-4}$	-3.43
1000 atm.	427	700	$2.2 \times 10^{-11}$	-10.66	$1.5 \times 10^{-4}$	-3.35
1000 atm.	600	873	$1.0 \times 10^{-8}$	-8.00	$1.1 \times 10^{-3}$	-2.96
1000 atm.	727	1000	$3.0 \times 10^{-7}$	-6.52	$2.2 \times 10^{-3}$	-2.66
1000 atm.	927	1200	$1.1 \times 10^{-5}$	-4.96	$4.0 \times 10^{-3}$	-2.40
2000 atm.	427	700	$1.4 \times 10^{-11}$	-10.85	$1.0 \times 10^{-4}$	-3.40
2000 atm.	600	873	$9.0 \times 10^{-9}$	-8.05	$7.5 \times 10^{-3}$	-2.92
2000 atm.	727	1000	$2.8 \times 10^{-7}$	-6.55	$3.6 \times 10^{-3}$	-2.42
2000 atm.	927	1200	$1.1 \times 10^{-5}$	-4.96	$6.3 \times 10^{-3}$	-2.30

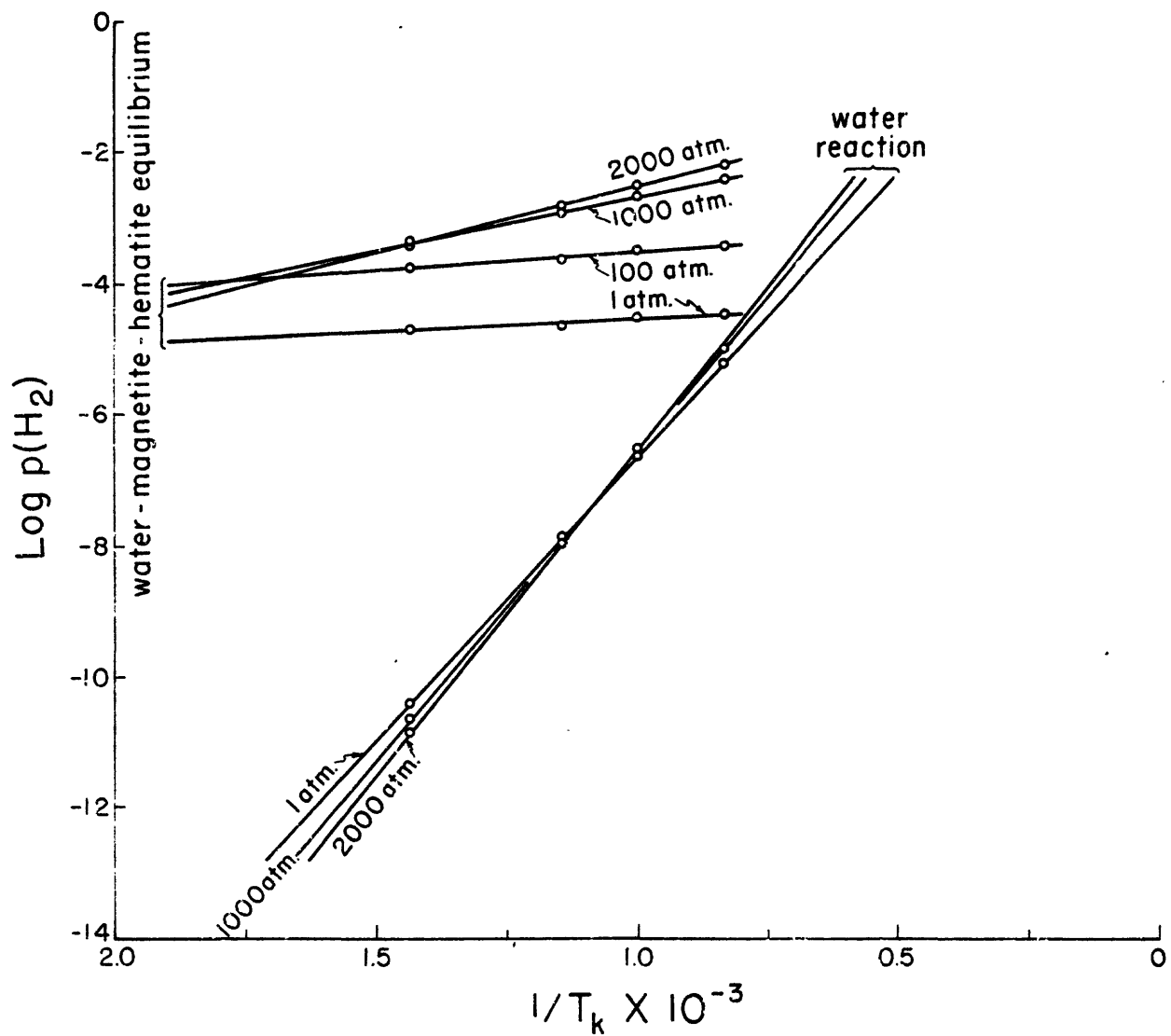


Fig. 18. Isobars showing variation of the equilibrium  $p(\text{H}_2)$  with temperature for the water reaction and for a water-magnetite-hematite system

xrium with a water-magnetite-hematite system will be considerably less than it would be for a pure water system at the same temperature and pressure. This is of course in consequence of the higher  $p(O_2)$  maintained by the dissociation of hematite.

Probably even more significant than the difference in  $p(O_2)$  values for the two reactions is the difference in slopes for the  $\log p(O_2)$  versus  $\frac{1}{T} \text{ K}^{-1}$  curves for the two reactions (Figure 16). Regardless of total pressure the slope of the  $\log p(O_2)$  curve for the water reaction is always less than the slope of the same curve for the magnetite-hematite reaction. Thus, it can be said that the equilibrium  $p(O_2)$  decreases more rapidly with decrease in temperature for the magnetite-hematite reaction than it does for the water reaction. Therefore, if water and magnetite exist at equilibrium at some definite pressure and temperature, as the system cools to lower temperatures, a disequilibrium is established, so that there is "leak" of  $O_2$  in the system, due to  $H_2O$  dissociation, and due to the arrest of  $O_2$  exchange for equilibrium between magnetite and hematite. If equilibrium is maintained during the cooling process, it is required that some of the magnetite be oxidized initially to its "normal"  $O_2$ , thus there is a continued formation of hematite. During such an equilibrium cooling process:

## CHAPTER 10

### SIGNIFICANCE OF THE IRON AND TITANIUM CAIDE PARAGENESIS IN THE EDISON UNIT

#### MAGNETITE-HEMATITE HEMIMITE

The thermodynamic treatment of the magnetite-hematite reaction (Chapter 9) has established the stability fields for magnetite and hematite for a series of temperatures and pressures. The univariant isobars for the magnetite-hematite reaction in Figure 16 separate the hematite field from the magnetite field; hematite alone is stable above the isobars and magnetite alone below the isobars. At points on the isobars magnetite and hematite exist at equilibrium at a  $p(O_2)$  as indicated on the ordinate. The thermodynamic treatment of the reaction has established data which would otherwise have to be established by experimental work. As the reaction is not very sensitive thermodynamically at the temperatures and pressures of the Edison Unit, the foregoing thermodynamic data may serve as a guide in designing applicable experiments.

If the mineral paragenesis of magnetite and primary hematite in the mixed gneiss subunit is considered to be an equilibrium assemblage, then the results of the thermodynamic calculations are applicable. In this case the paragenesis is represented by a point on one of the univariant isobars for the magnetite-hematite reaction in Figure 16. If it is assumed that the mixed gneiss subunit came to equilibrium at a temperature of 500°C and at a pressure between 1000 and 7000 atmospheres, then the equilibrium  $p(O_2)$  would be between  $10^{-24}$  and  $10^{-22}$  atmospheres.

(Figure 16). As water was undoubtedly present in the system the equilibrium  $p(H_2)$  would be high and have a value near  $10^{-3}$  atmospheres (Figure 18) for the temperature and pressures indicated above. Hence, in a petrologic system involving an equilibrium assemblage of magnetite and hematite it is possible to read from Figures 16 and 18 the equilibrium  $p(O_2)$  and  $p(H_2)$ , respectively, if the equilibrium temperature and total pressure may be estimated.

In rocks such as the quartz-feldspar gneiss and biotite-quartz-feldspar gneiss in which magnetite is present but primary hematite is absent, Figure 16, may be utilized to place maximum values on the  $p(O_2)$  for particular temperatures and pressures. If these rocks came to equilibrium at 500°C and at a pressure of 3000 atmospheres, then the maximum  $p(O_2)$  of the system would be about  $10^{-23}$  atm. In other words the iron oxide as willage in these rocks is represented by a point in the magnetite field of Figure 16 below the appropriate invariant isobar line. Similarly, the  $p(H_2)$  in equilibrium with  $H_2O$  and  $O_2$  in these rocks would be correspondingly greater the lower the  $p(O_2)$ .

It is possible that the  $p(O_2)$  in the quartz-feldspar gneiss and biotite-quartz-feldspar gneiss was just as high as that in the mixed gneiss subunit, but that hematite failed to crystallize because the equilibrium temperature was too high in the former rocks. In other words a high temperature would shift the iron oxide paragonesis to the right into the magnetite field away from the invariant isobar. Viewed in this way the magnetite paragonesis of these two rocks indicates a higher temperature of origin than for the mixed gneiss subunit. It is interesting that this idea is in agreement with the conclusions which are expressed

in Chapter 11 on the origin of the Edison unit and which were based on other observations.

#### MAGNETITE-MARTITE

The data presented in Figure 16 provide an excellent basis for explaining the origin of the ubiquitous martite in the mixed gneiss sub-unit. If, as before, it is assumed that the magnetite-peritoric hematite paragenesis is an equilibrium assemblage and that  $H_2O$ ,  $H_2$  and  $O_2$  were all in equilibrium with these oxides, the origin of martite can be explained as follows. As the system cooled from the equilibrium temperature, estimated to be  $500^{\circ}C$ , it is obvious from Figure 16 that a disequilibrium is established such that there is "excess"  $O_2$  in the system, due to  $H_2O$  dissociation, relative to the amount of  $O_2$  necessary for equilibrium between magnetite and hematite. This disequilibrium is caused by the fact that the slopes of the  $\log p(O_2)$  versus  $\frac{1}{T}$ , univariant isobars for the water reaction are considerably less than the slopes of the univariant isobars of the magnetite-hematite reaction (Figure 16). In other words the equilibrium  $p(O_2)$  decreases more rapidly with decrease in temperature for the magnetite-hematite reaction than for the water reaction. Hence, if equilibrium is maintained between the iron oxides and  $H_2O$ ,  $O_2$  and  $H_2$  during the cooling process, it is necessary that some of the magnetite be continually oxidized by this "excess"  $O_2$ , and there would be a continual formation of hematite at the expense of magnetite. In this interpretation secondary hematite or martite is regarded as a retrograde mineral, as it has originated during the cooling process of the rock in response to changing physical conditions.

The virtual absence of martite in either the quartz-K-feldspar gneiss or the biotite-quartz-feldspar gneiss is further evidence of their very low  $p(O_2)$ . It may be concluded that throughout the cooling process of these rocks the  $p(O_2)$  of the system was always low enough that the iron oxide paragenesis was represented by points within the magnetite field (Figure 16) i. e., below the univariant isobars. The very small proportion of martite in rare samples of the quartz-K-feldspar gneiss indicates that in some places the  $p(O_2)$  did reach a value which corresponded to a point on one of the univariant isobars. With regard to such samples it is concluded that because of the less rapid decrease of  $p(O_2)$  for the water reaction there was a point in the cooling history of those samples when the  $p(O_2)$  became equal to the equilibrium  $p(O_2)$  for the magnetite-hematite reaction, i. e., the  $p(O_2)$  isobars for the water reaction intersected those for the magnetite-hematite reaction, and with further cooling martite formed.

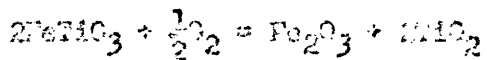
It is very significant that martite is present in the mixed gneiss subunit and absent in adjacent samples of the quartz-K-feldspar gneiss. According to the interpretation that martite is a retrograde mineral and recognizing the significance of the univariant isobars of Figure 16, this contact relationship indicates one or more of the following conclusions: (1) that the equilibrium temperature of the quartz-K-feldspar gneiss was considerably higher than that of the mixed gneiss subunit, (2) that the  $p(O_2)$  in the quartz-K-feldspar gneiss was much less than in the mixed gneiss subunit, (3) that the total gas pressure in the quartz-K-feldspar gneiss was somewhat lower than that in the mixed gneiss subunit, or that the gas composition differed radically in the two rocks, or (4) that the

quartz-K-feldspar gneiss formed at a somewhat different time than the mixed gneiss subunit and under quite different physical conditions, e.g., magmatic.

This discussion gives some indication of the additional understanding of the petrogenesis which detailed studies of the iron oxide paragenesis may offer. In particular such studies may reveal a great deal about the nature of the volatiles involved in petrogenesis. For example, it may be possible to estimate the actual volume or mole per cent of  $H_2O$  which existed in a petrologic system by determining the amount of martite which formed during the cooling history.

#### OXIDATION OF ILMENITE

The oxidation of ilmenite with the production of "mottled aggregates" composed of hematite and rutile is chemically expressed as follows:



As discussed in a previous section, the reaction appears to be thermodynamically equivalent to the magnetite-hematite reaction. This fact plus the very obvious secondary nature of the hematite-rutile aggregates in oxidized ilmenite indicate that the oxidation process is analogous to the oxidation of magnetite to form martite. Hence, it is believed that the oxidation of ilmenite is a retrograde process in response to the changing physical conditions during cooling. However, it remains to be explained why martite is present in some rocks, oxidized ilmenite in others, and in some rocks both are present. For example, in the biotite-quartz-feldspar gneiss the ilmenite tablets within magnetite are often

partially altered to hematite and rutile, but the host magnetite is not altered to martite. This relationship indicates that ilmenite is oxidized at a lower  $p(O_2)$  than magnetite. In other words a hypothetical univariant isobar for the oxidation of ilmenite would lie below that for the magnetite-hematite reaction in Figure 16 (for the temperature and pressure of formation of the biotite-quartz-feldspar gneiss). On the other hand in the mixed gneiss subunit magnetite is always partially altered to martite, but ilmenite may or may not be altered. This relationship indicates that a higher  $p(O_2)$  is needed to oxidize ilmenite than to oxidize magnetite. This is precisely opposite to the conclusions reached from the observations made on the biotite-quartz-feldspar gneiss. Inasmuch as the two oxidation reactions are thermodynamically so similar (Chapter 9), it is possible that very small changes in the actual solids, such as solid solution, structural changes, etc., or in the petrologic system might be sufficient to shift from one reaction to the other. In other words, because of the thermodynamic similarities the univariant isobar for the oxidation of ilmenite must lie very close to the univariant isobars for the magnetite-hematite reaction (Figure 16). Thus small changes from the ideal case which was assumed in the thermodynamic treatment could cause these curves to change relative position; so that in some cases magnetite would be more readily oxidized and in other cases ilmenite would be more readily oxidized.

#### SIGNIFICANCE OF INTERGROWTHS OF MAGNETITE WITH NON-MAGNETIC IRON AND TITANIUM OXIDES

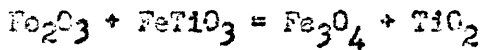
The simplest explanation for the intergrowths of non-magnetic iron

and titanium oxides with magnetite is that of the simultaneous crystallization of magnetite with the respective solid solution of the non-magnetic oxide. However, the morphologic regularity of these intergrowths and the absolute absence of any irregular intergrowths of non-magnetic oxides with magnetite suggest that a less random process than simultaneous crystallization may be responsible for the intergrowths.

Randohr (1939) postulated that intergrowths of magnetite with hematite-ilmenite were caused by the reduction of lenses of hematite to magnetite. In the light of the magnetite-hematite univariant isobars in Figure 16 and the interpretation of martite presented in a preceding section, Randohr's hypothesis appears inapplicable to the intergrowths of magnetite with non-magnetic oxides described here. Specifically, the application of his hypothesis requires that the petrologic system alternately changes from oxidation to reduction conditions. Applying Randohr's hypothesis and utilizing the textural relationships evident in the intergrowths of magnetite with non-magnetic oxides implies the following series of processes in order of occurrence: (1) initial equilibrium established between magnetite and primary hematite (solid solutions), (2) cooling from initial equilibrium temperature with production of martite, (3) exsolution of hematite-ilmenite solid solution with further production of martite during this cooling interval, (processes 2 and 3 probably take place throughout the same temperature interval), (4) reduction of hematite lenses in hematite-ilmenite intergrowths to form magnetite tablets (Randohr's hypothesis), no production of martite during this process, (5) return to the development of martite as indicated by the martized nature of the magnetite tablets intergrown with

the hematite-ilmenite. Hence, to apply Bamrohr's hypothesis requires a change from oxidation conditions (processes 1, 2, and 3) to reduction conditions (process 4) and back again to oxidation conditions (process 5). In terms of the magnetite-hematite univariant isobars in Figure 16 such a series of changes mean that the petrologic system alternately changed from positions above the univariant isobars (production of martite) to positions below the univariant isobars (production of magnetite). Very small changes in the  $p(O_2)$  could cause such shifts in equilibrium. However, as there is no independent evidence which indicates that the petrologic system deviated from the appropriate magnetite-hematite univariant isobar during the entire history of the rock, Bamrohr's hypothesis is discounted as requiring too many coincidental events. The fact that the morphology of the intergrown magnetite (flat tablets which extend across the entire grain, Plates 13, 15, 18, 19) differs from that of the hematite bodies (thick lenses, Plates 13, 14) is independent evidence that the former were not produced from the latter. Hence, Bamrohr's hypothesis is untenable from the textural as well as the physical-chemical standpoint.

Such considerations as above make the hypothesis of incongruent exsolution of an original solid solution of  $Fe_2O_3$ - $FeTiO_3$  to magnetite and rutile more tenable. It was noted (Table 22) that the thermodynamic constants for the chemical reactions involving the iron and titanium oxides are very similar; hence, the free energy increase in such a reaction as:



for any temperature and pressure would be very small. In other words under most physical conditions the relative stabilities of a hematite-

ilmenite assemblage is about equivalent to that of a magnetite-rutile assemblage. Thus, only small changes in the physical conditions would cause one assemblage to form at the expense of the other. From these considerations it is proposed that in the mixed gneiss subunit solid solutions of  $\text{Fe}_2\text{O}_3 \cdot \text{FeTiO}_3$  usually evolved as hematite and ilmenite, but that in some cases the physical aspects of the petrologic system were such that a magnetite-rutile assemblage was more stable than a hematite-ilmenite assemblage and hence the solid solution of  $\text{Fe}_2\text{O}_3 \cdot \text{FeTiO}_3$  evolved to magnetite and rutile.

## CHAPTER 11

### ORIGIN OF THE EDISON UNIT

#### INTRODUCTION

The origin of many of the pre-Cambrian rocks in the region is without question. However, the bulk of the gneisses have properties which are much more difficult to interpret and their origin is much more in question. For example, the Franklin Marble (Spencer, 1903) is clearly of metamorphic origin; however, associated amphibolites or hornblende gneisses are of doubtful origin. To interpret such rocks as the latter, requires not only a full understanding of their geologic occurrence and field relationships but also requires a great deal of detailed information pertaining to their mineralogy, the soil composition, etc., (Engel and Engel, 1952). Hence, the task of explaining the origin of the gneisses of the New Jersey Highlands is one of detailed field mapping plus detailed and laborious laboratory study. The second part of this report has been devoted to the presentation of descriptive data pertaining mainly to a single rock body (the Edison unit) in the Edison area. The subsequent sections are devoted to the interpretation of these data in an effort to explain the nature of the origin of the Edison unit and related magnetite deposits.

It is postulated that the Edison unit originated as the result of a series of complex events. It is believed that much of the material of which the unit is composed is of sedimentary origin. At the same time there is excellent evidence that much of the material has been introduced from other sources. It appears that the processes of metamorphism,

metasomatism and probably igneous injection have played the dominant roles in reconstituting an original sedimentary rock series into the form it has at present.

#### ORIGIN OF THE MIXED GNEISS SUBUNIT

It is postulated that the mixed gneiss subunit represents an original heterogeneous series of somewhat argillaceous and/or arenaceous sedimentary rocks which have been reconstituted to gneisses of the amphibolite grade by regional metamorphism and have been in part chemically reconstituted by metasomatic action.

**Sedimentary affinities.** Several factors testify to the original sedimentary affinities of the mixed gneiss subunit. The regional distribution of the Edison unit from one limb of the Beaver Lake anticline to the other is suggestive of "stratigraphic" continuity. The heterogeneous character of the mixed gneiss subunit as manifest by the marked chemical and mineralogic discontinuities (lithologic variegations) from layer to layer are certainly in part a reflection of a primary sedimentary heterogeneity. Specifically, such rock layers as the garnet-biotite-cillimanite-quartz gneiss have bulk compositions which must closely approach those of sedimentary rocks, e.g., argillaceous sandstones. In addition the local abundance of such minerals as garnet, biotite and sillimanite are evidence of sedimentary affinities. The presence of at least two kinds of rounded zircons in the mixed gneiss subunit is also good evidence of sedimentary affinity.

Perhaps the most conclusive quantitative evidence of the sedimentary affinity of the mixed gneiss subunit is the very high  $\text{SiO}_2$  content (Table 16)

and high quartz to feldspar ratios (Tables 4 and 5) in the magnetite-quartz-K-feldspar gneiss.

Sample 145, Table 16, has a mineral composition which corresponds very closely to that of the average magnetite-quartz-K-feldspar gneiss (compare the mode of 145, Table 4B to the means in Tables 4 and 5). Hence, the chemical composition of 145 (Table 16) must be very close to the average composition of the magnetite-quartz-K-feldspar gneiss and the mixed gneiss it must on the whole. The minimum  $\text{SiO}_2$  content of sample 1/5 is 76.4 per cent which is somewhat higher than most normal igneous rocks. Actually the  $\text{SiO}_2$  content may be as great as 80 per cent in which case the rock would correspond to no bonafide igneous rock. Certain alkaliites (Fuddington, 1929) and leucogranites (Larsen, 1943) contain 76 and 76.54 per cent  $\text{SiO}_2$  respectively. However, no granites are known to contain  $\text{SiO}_2$  in greater amounts, and as 76.4 per cent  $\text{SiO}_2$  is a minimum for the average magnetite-quartz-K-feldspar gneiss a normal igneous origin for this rock type is excluded. As is so conclusively pointed out by Chayes (1952), normal granites appear always to carry less than 40 per cent quartz and more than 50 per cent feldspar. Hence, a maximum quartz to feldspar ratio for normal igneous granites would be about 0.8. It seems fitting to note that this ratio for the samples of magnetite-quartz-K-feldspar gneiss (Tables 4 and 5) is generally greater than 0.9 and in many cases is greater than 1.0, and that the ratio for the mean of these samples is 1.08. In addition the quartz to feldspar plus ortho ratio is often greater than 0.8 and the mean of this ratio for the samples is 0.76 (Table 5) or nearly the maximum for the quartz-feldspar ratio for granites as determined by Chayes (1952). Again it appears evident that the magnetite-

quartz-K-feldspar gneiss and the mixed gneiss subunit have marked sedimentary affinities and not igneous affinities.

Metamorphism. That the mixed gneiss subunit has been subjected to regional metamorphism is beyond all doubt. The well developed metamorphic structures such as flow cleavage and lineation as well as the characteristic metamorphic fabric of the subunit prove that pre-existing rocks have been subjected to the agents of metamorphism. In addition much of the mineral assemblage is characteristic of metamorphic rocks, e.g., garnet, sillimanite. There is no evidence in the Wilson area to suggest that there has been more than one period of metamorphism (excepting minor retrograde metamorphic effects). As discussed previously the grade of metamorphism in the Wilson area as indicated by the pyroxene-syenite gneiss corresponds to the amphibolite facies of the Adirondacks (Buddington, 1952). The mineral assemblage in the mixed gneiss subunit is characterized by non-porphyritic K-feldspar, magnetite, quartz, biotite, manganese-almandite, sillimanite, etc. The non-porphyritic K-feldspar assemblage has its counterpart in similar rocks in the Adirondacks (Engel and Angel, 1953; and Buddington, 1953, p. 265) which have been interpreted as belonging to the amphibolite facies (Buddington, 1952, p. 74). Furthermore, the  $TiO_2$  content of magnetite from the magnetite-quartz-K-feldspar gneiss is low (Table 4A) and indicates a temperature of formation which corresponds to the lower range of the amphibolite facies of the Adirondacks (Buddington, 1953).

In addition the mineral assemblage of the mixed gneiss subunit corresponds to the sillimanite-almandine subfacies of the amphibolite facies (Turner, 1951, p. 456). This subfacies, "is distinguished above

all by the assemblage sillimanite-almandine-orthoclase (-plagioclase-biotite-quartz) in schists of pelitic composition," (Turner, p. 457). With the exception of the absence of plagioclase this assemblage corresponds to that in the mixed gneiss subunit. Thus, there is adequate evidence that the mineral assemblage of the mixed gneiss subunit belongs to the identical metamorphic assemblage as other rocks in the area, i. e., the amphibolite facies.

Metasomatism. There is a great deal of indirect evidence which suggests that the original sedimentary rocks of the mixed gneiss subunit have been chemically reconstituted during the regional metamorphism. This chemical reconstitution has been referred to as regional metasomatism. The term metasomatism as used in this paper does not necessarily imply that material has been introduced from extraneous and distant sources, although this may often be the case; the term also refers to the redistribution of material which has its origin in the immediate milieu. This definition is adopted because of the inherent difficulties in distinguishing between metasomatic material of distinct sources and that which stems from adjacent rocks (i. e., redistributed material).

The most obvious effect of metasomatism is the magnetite rich zones and general high magnetite content of the entire subunit. The origin and emplacement of this material will be discussed in a subsequent chapter.

It is believed that most of the potassium which is contained in K-feldspar in the mixed gneiss subunit is of metasomatic origin. That potash rich gneisses in the subunit could not be of normal igneous origin was clarified previously. Hence, the potassium which is so abundant in the mixed gneiss subunit must either have originated during the sedimentary

cycle or have to be introduced from an outside (distant) source.

Potassium enrichment during the sedimentary cycle might take place in either of two ways. First, it is possible that many of the original sediments of the mixed gneiss subunit were of arkosic composition and rich in alkali feldspar (Pettijohn, 1949, p. 258). Such arkoses could provide ample potassium for the formation of the mineral assemblage, but in addition would also supply a considerable amount of sodium (Pettijohn, 1949, p. 259). However, as described earlier the paucity of Na-feldspar or any sodium minerals in the mixed gneiss subunit is striking. If the arkose hypothesis is to be considered it must be postulated that either the arkose was very poor in Na-feldspar or that any Na-feldspar it may have contained has been completely removed from the mixed gneiss subunit. A second more likely mode of enrichment of potassium is through the presence of clay minerals such as montmorillonite and illite (Grim, 1953) in the original sedimentary rocks of the mixed gneiss subunit. The regional metamorphism of such clay minerals could lead to the development of much K-feldspar, and inasmuch as these clay minerals contain a greater proportion of Al than does K-feldspar the simultaneous development of sillimanite would be a natural consequence. However, many layers in the mixed gneiss subunit, rich in K-feldspar carry little or no sillimanite. Thus the question arises as to what happened to the excess Al which would have been associated with the potassium in the original clay minerals of such layers. It must be postulated that a considerable amount of redistribution of either potassium or aluminum or both took place during the regional metamorphism. Thus, certain layers were enriched in K (K-feldspar) while others in Al (sillimanite). Such a redistribution process

is deemed metasomatic according to the definition given above. Inasmuch as K is much enriched over Na in clay minerals (Grim, 1953) the above hypothesis would satisfactorily explain the paucity of Na-feldspar in the mixed gneiss subunit.

The ubiquitous K-feldspar pegmatite veins and lodes are additional evidence that K-metasomatism has been an important process in the mixed gneiss subunit. The pegmatites are believed to have been "fixed" relatively late and are excellent evidence that either K from the original sediments or from extraneous sources has permeated most of the mixed gneiss subunit. The pegmatites appear to carry more K-feldspar than the average kyanite-quartz-K-feldspar gneiss and have a composition similar to that of a potash granite. It is proposed that the pegmatites represent an unconsolidated crystallized product of some metasomatic "fluids" which permeated the mixed gneiss subunit.

Of course it is quite possible that the K in the mixed gneiss subunit came from an extrusive source. Such potash metasomatism has been noted in the Adirondacks (Engel and Engel, 1953) where it is apparently related to large masses of hornblende granites. Similar granites are present in this region and could have supplied the K to the mixed gneiss subunit. However, other than the correlation in time and space between the hornblende granite and mixed gneiss there is no specific evidence available to identify the former rock as the primary source of K.

According to the idea originally proposed by Goldschmidt (1921) alkali metasomatism may take place by the diffusion of K and Na by excess  $\text{Al}_2\text{O}_3$  in the precipitating rock. In the mixed gneiss subunit the presence of sillimanite indicates that this process may have taken place. Specific-

cally, if the original sediment was rich in aluminous constituents (clay minerals), K from an extraneous source might be readily fixed by the chemical combination with Al and Si to form K-feldspar. As indicated previously, the variable proportions of sillimanite and K-feldspar in the mixed gneiss subunit probably depended upon the bulk chemical composition of the immediate milieu. Thus, layers rich in sillimanite are poor in K-feldspar (Figure 4). This probably indicates that no K-fluids penetrated these layers. On the other hand K-feldspar rich layers are generally poor in sillimanite. This indicates that the original sedimentary layer was permeated by K-fluid and all the excess Al was used up in the formation of K-feldspar. Goldschmidt's concept is applicable to the mixed gneiss subunit regardless of whether the K came from the original sediments or from an extraneous source. In either case the absolute fixation of K in the subunit would depend upon the presence of excess Al for the formation of K-feldspar.

In summary it is concluded that the best single explanation of the K metasomatism so characteristic of the mixed gneiss subunit is that the K from the original clay mineral rich sediments was mobilized during the regional metamorphism and fixed by the combination with Al and Si to precipitate K-feldspar.

#### ROCKS IN THE LIME RICH SUBUNIT

It is postulated that the lime rich subunit originated by the regional metamorphism and metasomatism of an original series of carbonaceous sedimentary rocks. Thus the genesis of the lime rich subunit is

considered to be essentially identical to that of the mixed gneiss sub-unit. The principal differences between the two are considered to be a reflection of the chemical differences between the original sediments.

Sedimentary affinity. The "stratigraphic" like distribution, the heterogeneous nature with alternating layers of distinct chemical and mineralogic compositions and the presence of metagrayzites and calcite rich layers all testify to the marked sedimentary affinities of the lime rich subunit. As is indicated on Plate 1 the lime rich subunit lenses cut abruptly into the mixed gneiss subunit. One small body of gneiss of lime rich type has been mapped well to the southwest within the mixed gneiss subunit. It is postulated that the structural relationships between these two subunits is simply a reflection of an original sedimentary relationship in that a series of calcareous sediments (lime rich subunit) rather abruptly lensed out in favor of argillaceous sediments (mixed gneiss subunit).

Mineralogic. The somewhat different mineral assemblage in the lime rich subunit from that in the mixed gneiss subunit might suggest that they belong to different metamorphic facies. However, such differences as exist can be explained on the basis of chemical differences in each milieu. The absence of pyrope & and hornblende in the mixed gneiss subunit can be related to the paucity of Ca. On the other hand the absence of sillimanite in the lime rich subunit can be related to the rather high content of Ca which utilized all the Al to form such aluminous minerals as kyanite and epidote instead of sillimanite. The composition of the plagioclase ( $An_{20-30}$ ) in the lime rich subunit is characteristic of metamorphic rocks of a higher grade than the albite-epidote amphibolite

facies (Turner 1951, p. 446). The microcline in the mixed gneiss subunit and lime rich subunit are essentially identical. In both cases the microcline is non-perthitic which indicates both crystallized at about the same temperature (Bowen and Tuttle, 1950). It is clear that the lime rich subunit belongs to the same metamorphic facies as the mixed gneiss subunit, i. e., amphibolite facies.

In addition the mineral assemblage of the lime rich subunit corresponds to the assemblage in rocks of the staurolite-hkyrnite subfacies (amphibolite facies) which have excess potash (Turner, 1951, p. 455). This subfacies is characterized by an assemblage of such minerals as microcline, plagioclase, biotite, hornblende, diopside, epidote, grossularite and quartz (Turner, p. 456). The high potash content prevents the formation of either staurolite or kyanite (sillimanite). According to the facies classification of Turner the mixed gneiss (sillimanite-aluminite subfacies) and lime rich (staurolite-aluminite) subunits belong to different subfacies of the amphibolite facies. In other words the difference in bulk composition between the two aluminite subunits for the different mineral assemblages which were apparently developed under similar conditions of pressure and temperature.

**Metasomatism.** Although quantitative chemical and mineralogic data are lacking for the lime rich subunit, it is postulated that K-metasomatism has been an important process in the genesis of this subunit. It is possible that the source of the K was from the mixed gneiss subunit although it is equally possible that the K could have come directly from clay minerals in the original sediments of the lime rich subunit. As before it is quite possible that the major source of the K and perhaps

other elements could be from extraneous distant sources. If this is the case there is no clear evidence to substantiate it.

The presence of Na-feldspar (oligoclase) and scapolite pose a problem as to the source of the Na. This is somewhat of an enigma; however, it could be argued on theoretical grounds (Ranborg, 1952) thatasmuch as Ca forms a major constituent in the lime rich subunit, Na-feldspar and Na-scapolite are stable phases in that milieu and consequently there exists a chemical potential or gradient in favor of the "migration" of Na from adjacent rocks to the lime rich subunit. According to such a theory any Na contained in the mixed species clinopyroxene may have been "extracted" and redeposited in the lime rich subunit.

#### ORIGIN OF THE BIOTITE-QUARTZ-FELDSPAR GNEISS

The origin of the biotite-quartz-feldspar gneiss is very difficult to ascertain. However, because of its close similarities to certain gneisses in the Alluvial Valley which were studied with a high level of detail (Engel and Engel, 1953), it is postulated that the biotite-quartz-feldspar gneiss may have an origin similar to them.

In Table 1 a chemical analysis of a biotite-quartz-oligoclase gneiss (16-1163) from the New Jersey Highlands (5 miles northeast of the Alluvial area) is presented along with the analysis of a similar gneiss from the Alluvial Valley (Engel and Engel, 1953). For comparison the average composition of a Franciscan gneissic gabbro (Paliotto, 1943) and the average composition of eleven pyroxenite gneisses from widely separate localities (Pettijohn, 1949, p. 250) are included in the table. The chemical

compositions of the biotite-quartz-oligoclase gneiss from the Adirondacks is so similar to that of the graywacke sandstones that Engel and Engel have concluded that it is most likely the metamorphosed equivalent of a graywacke sediment. The same conclusion seems justified for the biotite-quartz-oligoclase gneiss of the New Jersey Highlands, inasmuch as its composition is so similar to that of the Adirondack gneiss and the two graywacke sandstones. Although no chemical analyses of the biotite-quartz-feldspar gneiss of the Elgin area is available, some of the samples are mineralogically very similar to biotite-quartz-oligoclase gneiss of the Adirondacks and New Jersey Highlands (Table 9) and would very likely have a chemical composition similar to those of the rocks listed in Table 1. Analogous to the biotite-quartz-oligoclase gneiss of the Adirondacks, the biotite-quartz-feldspar gneiss of the Elgin area is believed to have been originally a sedimentary rock of graywacke composition.

It is obvious from Table 9 that most of the samples of biotite-quartz-feldspar gneiss in the Elgin area carry a large proportion of K-feldspar. This is not the case with either of the two samples of gneiss listed in Table 1. Engel and Engel (1953) have found that in the Adirondacks the biotite-quartz-oligoclase gneiss has been modified by K-metasomatism so that K-feldspar is often a major mineral in such gneisses. The Adirondack gneiss listed in Table 1 is their example of unmodified gneiss. They have been able to relate the degree of K-metasomatism to the purity of major granite minerals and have postulated that the K-enrichment comes from such minerals. Accompanying the K-metasomatism the original biotite-quartz-oligoclase gneiss of the Adirondacks shows both textural and

mineralogic modifications. With an increase in the proportion of K-feldspar the original gneisses, "blend by subtle transitions into granite augen gneiss and gneissic granite," (op. cit., 1953, p. 1059). The K-feldspar content of the biotite-quartz-feldspar gneiss of the Edson area corresponds most closely to facies of the Hermon type granite gneiss (op. cit., 1953, p. 1066, Figure 7), which is believed to be a highly modified facies of the biotite-quartz-oligoclase gneiss of the Adirondacks. On the other hand the fabric of the biotite-quartz-feldspar gneiss of the Edson area corresponds to that of less modified facies of the biotite-quartz-oligoclase gneiss of the Adirondacks (loc. cit., Figure 7). Specifically, the fabric corresponds to the migmatitic and well foliated (with minor porphyroblastic development) stage of the Adirondack gneiss. Foliation and migmatitic layering by biotite alkali-feldspar-quartz-K-feldspar gneiss are both well developed in the biotite-quartz-feldspar gneiss of the Edson area, and K-feldspar porphyroblastic development is of subordinate importance. Thus the overall fabric of the gneiss in the Edson area is in contrast to the typical facies of the Hermon granite gneiss in which porphyroblastic K-feldspar is at the early stages of foliation and foliation and migmatitic develop, but are of subordinate importance (loc. cit., Figure 7). Thus it is concluded that although there apparently the biotite-quartz-feldspar gneiss of the Edson area may be a well developed stage of metasomatism of a biotite-quartz-oligoclase gneiss, the fabric of the gneiss does not indicate a similar stage of metasomatism but instead indicates an early stage of crystallization. On a much smaller scale the increase in K-feldspar in the biotite-quartz-feldspar gneiss toward the contact of the quartz-K-feldspar gneiss (Table 2,

Figure 6) in the Edison area is analogous to the similar changes in the biotite-quartz-oligoclase gneiss toward the contacts of large granite masses in the Adirondacks. The biotite-quartz-feldspar gneiss of the Edison area is considered to be a small scale facsimile of similar gneisses in the Adirondacks which are interpreted as regional metamorphosed and K-metasomatized graywacke subunits.

Analogous to the similar gneisses in the Adirondacks the biotite-quartz-feldspar gneiss probably belongs to the amphibolite facies. The slightly porphyritic character of the K-feldspar indicates that the gneiss may represent a mineral facies of slightly higher temperature than either the mixed gneiss or the lime rich subunit. This could be explained by the proximity of the biotite-quartz-feldspar gneiss to the quartz-K-feldspar gneiss and the igneous granites to the southeast. More difficult to explain is the presence of monoclinic K-feldspar porphyroblasts in the biotite-quartz-feldspar gneiss while the matrix K-feldspar is well twinned orthoclase. There is no evidence to suggest that the porphyroblasts belong to a different period of crystallization from that of the matrix feldspar. Therefore, it is postulated that all the K-feldspar in the biotite-quartz-feldspar gneiss crystallized at the same time and as monoclinic K-feldspar, but upon cooling only the small grains inverted to the triclinic polymorph (Jones, 1959). It is postulated that the inversion process of the large porphyroblasts was inhibited due to their rather large size. It seems possible that the ease of inversion may depend upon surface effects which would be magnified in small grains, but minimized in large grains. Similar mixtures of triclinic and monoclinic K-feldspar have been noted before (Warren, 1954; Mackenzie, 1954) and have been interpreted in a similar manner.

### ORIGIN OF THE QUARTZ-K-FELDSPAR GNEISS

It is postulated that the quartz-K-feldspar gneiss originated by the crystallization of a relatively mobile fluid (magma?) which originated within the mixed gneiss subunit. Thus, it is believed that the origins of all the rocks of the Edison unit are closely related.

The uniform nature of the quartz-K-feldspar gneiss as observed in the field, the very uniform mineral composition as found by modal analyses of random samples (Table 3 and Figure 5) and the relatively undeformed nature of the fabric of the quartz-K-feldspar gneiss are evidence that the gneiss originated by the replacement and crystallization of a fluid of uniform composition during a late stage of the regional metamorphism. The uniform nature of the rock also indicates that the parent fluid was uncontaminated by adjacent rocks. In addition the presence of a single type of euhedral sillon in the quartz-K-feldspar gneiss in contrast to the two varieties of rounded sillon in the mixed gneiss subunit is good evidence that the former rock crystallized directly from a fluid and was not contaminated by adjacent rocks. The porphyritic nature of the K-feldspar and the rather high  $TiO_2$  content of the magnetite (Table 15) both indicate that the quartz-K-feldspar gneiss crystallized at a somewhat higher temperature than the mixed gneiss and Ti-rich schistite. Specifically, the  $TiO_2$  content of the magnetite corresponds to that in "hornblende rich granitized rocks, formed at temperatures lower than magmatic," (Brillington, 1953).

Although it is certain that the biotite-quartz-feldspar gneiss in the Edison area has been affected by K-metamorphism, it is evident that

there is not a continuous textural or mineralogic variation between that gneiss and the quartz-K-feldspar gneiss (Tables 8 and 9). There is a distinct textural and mineralogic (chemical) discontinuity between the two. Rather than postulate that the quartz-K-feldspar gneiss is the ultimate product of K-metasomatism of the biotite-quartz-feldspar gneiss, it seems more logical to postulate that the quartz-K-feldspar gneiss formed by the direct crystallization of K-rich-fluids (magm?) and that the fluids penetrated and partly modified the adjacent biotite-quartz-feldspar gneiss. In other words the quartz-K-feldspar gneiss is a primary rock and not the product of a modified pre-existing rock.

Mineralogically the quartz-K-feldspar gneiss is most similar to garnet alaskite of the Mironlachs (Buddington, 1951). In Table 25 the average modal composition of these two rocks is compared. The two rocks have very similar mineralogy but differ somewhat in their bulk composition. The quartz-K-feldspar gneiss has much more quartz and much less plagioclase than the garnet alaskite. Although the absolute content of K-feldspar in the two rocks is similar, the ratio of K-feldspar to Na-feldspar is considerably greater in the gneiss of the Indiana area. This is the most important mineralogic difference between the two rocks. Although sillimanite and horblende are absent from the quartz-K-feldspar gneiss and present in the garnet alaskite, the other accessory minerals are common to both the rocks. Buddington (1951) has noted that along the margins of igneous rocks in the Mironlachs adjacent biotitic gneisses have been intruded and replaced by alaskite and a slightly biotitic, sillimanitic and garniferous felsic has developed. Therefore, he interprets the garnet alaskite as the product of contamination between alaskite

Table 25. Average mineral composition of the quartz-K-feldspar gneiss of the Edison Area and garnet alaskite of the Adirondacks.

	A	R12-B
Quartz	40.2	24.0
K-feldspar	50.8	56.6
Plagioclase	0.6	10.1
Micaite	0.8	-
Accessory	7.6 <sup>a</sup>	7.6 <sup>b</sup>

A = Average mineral composition of sixteen samples of quartz-K-feldspar gneiss, Edison Area, New Jersey.

R12-B = Garnet alaskite intercalated with gneiss, Newvine Mine, Tupper Lake Quadrangle, N.Y., 1000 feet. (Cited from A. P. Knobell, 1951).

<sup>a</sup> Includes magnetite, chlorite, pyroxene, sulfide and zircon

<sup>b</sup> Includes magnetite, ilmenite, sphene, garnet, zircon, sulfide and hornblende

fluid (magma) and biotitic gneisses. He postulates that the alaskitic fluid originated as a volatile-rich differentiate of certain granite magmas in the Adirondacks.

It is possible that the quartz-K-feldspar gneiss originated in a way similar to that of the garnet alaskite of the Adirondacks. The presence of garnet in the former rock suggests that it may have been contaminated by the adjacent biotite-quartz-feldspar gneiss, although there is no positive correlation between the presence of the latter rock and the abundance of garnet. Furthermore, sillimanite is absent from the quartz-K-feldspar gneiss even in zones which are intimately mixed with the biotite-quartz-feldspar gneiss. The very low K-feldspar content (high K-feldspar to Na-feldspar ratio) and very high quartz content of the quartz-K-feldspar gneiss in comparison with the garnet alaskite is very difficult to reconcile if both rocks had the same origin. To explain these differences it would be necessary to postulate that it is possible to obtain quite different kinds of differentiates from the fractionation of granite magma. It is concluded that the quartz-K-feldspar gneiss could not have precisely the same origin as the garnet alaskite of the Adirondacks.

It seems likely that the K-enrichment of the mixed gneiss and limestone subunit is related to the quartz-K-feldspar gneiss. It is possible that the latter gneiss crystallized directly from the fluids which modified and eventually reconstituted the former gneisses. If such fluids originated within the mixed gneiss subunit, as was previously proposed, through a process of metamorphic differentiation during regional metamorphism, then the quartz-K-feldspar gneiss would represent the "lowest

"melting" residue of the mixed gneiss subunit. Very likely the pegmatites within the mixed gneiss subunit are the counterpart to the quartz-K-feldspar gneiss in having crystallized from these same K-rich-fluids. In a sense the quartz-K-feldspar gneiss might be considered as a very large "pegmatite" lode of the identical origin as the small pegmatites.

Therefore, the principal difference between the origin of the quartz-K-feldspar gneiss of the Ellison area and the garnet alaskite of the Adirondacks is related to the mode of origin of the alaskite fluids from which they crystallized. In the former case this fluid is believed to have originated through a process of metamorphic differentiation of original Grenville type sediments, whereas in the latter case the fluid is believed to have originated as a late product of the differentiation of a granite magma.

## CHAPTER 12

### ORIGIN OF THE MAGNETITE DEPOSITS IN THE EDISON AREA

#### INTRODUCTION

In order to explain the genesis of the magnetite deposits in the New Jersey Highlands two fundamental questions must be answered: (1) What process or processes caused the initial enrichment of iron?, and (2) What was the nature of the process or processes whereby the iron was displaced? Obviously, these two questions are closely related and the explanation of either one will probably indicate or restrict the answer of the other.

Most previous geologists have related the actual enrichment of iron to a phase of magmatic activity, and generally propose that the iron was carried and displaced by some sort of an "igneous magma." An early idea of Rogers (1898, 1899) was that the magnetite particles were brought along from the "magmatic injection of fluid base" into igneous rocks. Rogers apparently believed that the magnetite particles were magmatic in the strictest sense, i. e., a magnetite magma (Rogers 1907). Spence (1904) and Bayley (1910) both expressed the opinion that the magnetite deposits were products of igneous activity. Bayley (1910, p. 149) clarified this opinion by stating the following:

In all cases the ores are regarded as being of magnetite origin—that is, the source of their material is thought to have been the deep-seated rocks, portions of which, upon being intruded into the overlying rocks, solidified as the various gneisses now constituting the principal rocks of the Highlands ridge.

Bayley (1910, p. 151) clarified his views as to the nature of the emplacement process:

Very probably the vehicle of transportation was a hot aqueous solution or possibly a vapor which emanated from the same magmatic source . . .

and further,

The channels through which the solutions circulated presumably afforded the most favorable opportunities for deposition of mineral matter, and such portions of the rock naturally became richer in magnetite . . . In some places there may have been replacement of the silicates by magnetite . . .

Modern opinion regarding the genesis of the magnetite deposits does not differ much from that expressed by Bayley and is summed up by Sims (1952) in several statements:

The source of ore-forming fluids was a cooling igneous mass. The process whereby the residual liquor of a magma undergoing progressive crystallization is continually enriched in volatile components has been described by Bowen (1928, p. 273). During crystallization the residual liquor is progressively enriched in  $H_2O$  and other mineralizers, but there is no general agreement whether the mineralizers given off by the cooling igneous mass escape as a liquid or a vapor phase.

Both field and laboratory evidence suggest that all the magnetite deposits originated by magmatic replacement of favorable host rocks.

The ore-forming fluids did not, therefore, have large openings through which to migrate, but instead had to migrate along intergrain boundaries, discontinuous small fractures, and granulated zones that were rendered more permeable than the surrounding rock by micro-crystallization. To penetrate for long distances in these zones the fluids must have had a high degree of fluidity, and were either pneumatolytic or hydrothermal, or were probably both. Evidence is strong against the tenet that the magnetite was introduced as a liquid melt, as suggested by Glazi (1947).

Sims (1953, p. 233) is very specific about the origin of the magnetite deposits which he has studied and states:

The magnetite deposits in the Dover district were derived from the granite magma that consolidated to form hornblende

granite and alaskite. During the progressive crystallization of this magma a more mobile and highly volatile portion of the magma was concentrated adjacent to inclusions and in the crests of certain large anticlines. This magma which consolidated to form alaskite, was split off prior to the crystallization of the pegmatites. Further differentiation of the alaskitic magma by progressive crystallization concentrated the volatiles still more and these ferriferous fluids escaped from the crystal system, migrated along the microbrecciated zones, and replaced the rocks within these zones to form magnetite bodies.

In contrast to a magnetic origin of the iron others have postulated that the initial iron enrichment took place during a sedimentary cycle and that the magnetite deposits are metamorphosed sedimentary iron beds, (Kittoe, 1857). Landergren (1948) is strongly in favor of initial iron enrichment during a sedimentary (exogene) cycle but suggests that this iron has in many cases been moved around or redeposited during subsequent orogeny. Using his terminology Landergren postulates that the initial iron enrichment took place during the exogene (sedimentary) cycle but that this sedimentary material,

... entered into an endogenic phase of development in an orogenic cycle.

In this way Landergren points out that the magnetite deposits can tell on the character of deposits formed entirely through endogenic processes, i. e., products of igneous activity. Landergren (1948, p. 174) sums up his point of view as follows:

All the geological features indicate that the enrichment of iron took place before those endogenic phenomena which have obscured these trends and which have given the iron ores the indisputable geological character of what we call a magnetic ore.

Landergren prefers not to commit himself on the possible ways in which iron may be transported, e.g. solution transfer, gaseous transfer or solid

diffusion. Instead he sums up his position by the following general statement (*op. cit.*, p. 158):

A remobilization of iron in the endogene phase of development may take place under certain conditions depending on the composition of the material entering in the endogene phase, on the content of volatiles present, and on the temperature.

An extreme view which has some aspects in common with Landergren's opinions is that the iron enrichment took place by a process related to metamorphic differentiation, and that during regional metamorphism and metasomatism iron was "driven out" of some rocks, and concentrated and fixed in other sites (Ranberg 1952, pp. 265-266; Devore, 1953). Proponents of this hypothesis generally propose solid state diffusion or grain boundary migration as the mechanism of transport of the iron.

It is proposed that the magnetite deposits in the Milion area are of complex origin. Although it is postulated that the initial concentration of the bulk of the iron in these deposits is directly related to igneous activity as Dins (1953) has explained, it is believed that none of the area was initially concentrated during a sedimentary (endogene) cycle. Furthermore, it is postulated that the magnetite deposits are of metasomatic origin in the sense that the original rocks of the mixed gneiss subunit have been chemically reconstituted with reference to the distribution of iron. It is concluded that the magnetite deposits were formed contemporaneously with the regional metamorphism and metasomatism of the mixed gneiss subunit, and are therefore para-tectonic and represent an almagat style type developed during these processes. In other words, it is believed that the magnetite was introduced via iron rich fluids into the host rocks during their formation, i. e., during regional meta-

morphism and metasomatism, and not after their formation. The mechanism of iron transport significant to the genesis of these magnetite deposits is not certain, but several aspects of this problem are discussed.

#### SOURCE OF IRON FOR MAGNETITE DEPOSITS

Several lines of evidence indicate that the initial source of the iron was from residual solutions formed from the progressive crystallization of granitic magma. First, there are experimental data (Bowen and Schairer, 1935) and petrologic data (Wager and Deer, 1939, p. 153; Renner, 1929, p. 272) which indicate that the absolute content of iron increases in the residual liquids of synthetic melts and basaltic magma, respectively. However, the application of these data to granitic magma may not be entirely justified. Sims (1953) believes that the presence of magnetite in a variety of host rocks such as gneiss, schist, and granite is good evidence that the initial iron enrichment did not take place during a sedimentary cycle. Apparently Sims would expect less variation in the host rock in the case of sedimentary iron deposits. Within the Franklin Furnace area magnetite deposits occur in many kinds of rocks, hence Sims' reasoning is somewhat applicable but does not rule out the possibility that the iron could be of extrusive origin and incorporated in other host rocks during an endogenic cycle (a la Buddington, 1948).

The regional association of magnetite deposits with granitic igneous rocks is evidence that the initial iron enrichment took place during a magmatic cycle. Buddington (1939, p. 178) has pointed out that Allisondale magnetite deposits are always in a host rock of Greenville type and are

always located in the highland portion of the northwest Adirondacks where about 85 per cent of the rocks are of igneous origin. In the Grenville lowlands in the extreme northwest Adirondacks magnetite deposits are absent and only about 15 per cent of the rocks are of igneous origin. Actually the magnetite deposits in the Adirondacks are lodged in bodies of Grenville type gneisses which are completely surrounded by granitic rocks. This consistent association adds strength to the hypothesis of a magnetic origin of the iron. It is clear that the cores of the mixed gneiss subunit are associated with rocks of igneous origin, e.g., hornblende granites and alkaliite, pyroxene granites and alkaliites. The similarity of this association to those in the Adirondacks is some evidence that granites were the source of the iron.

There is additional evidence that the granitic rocks could be the source of the iron. For example enclosed in the pyroxene granite just southeast of the Ellicott area is a small magnetite-rich pegmatite. The Gables Mine (Barley, 1910) is such a small magnetite-rich pegmatite completely enclosed by pyroxene granite. It is located several miles to the southwest of the Ellicott area. These and other small magnetite deposits are apparently unrelated to any Grenville type gneiss, and always appear enclosed by large masses of granite. In most cases these bodies are mineralogically like a magnetite-rich pegmatite; however, there are no other magnetite bodies which are also closely associated with granite which contain little or no feldspar and which may be classed as non-pegmatitic. If as is ordinarily believed, pegmatites represent a relatively late stage of crystallization, then the magnetite pegmatites are evidence

that considerable iron enrichment took place during the fractional crystallization of the granite magma. The non-pegmatitic magnetite bodies are also indicative of late stage enrichment of iron, but perhaps they owe their distinctive composition to a process of enrichment different from fractional crystallization, e. g., gaseous transfer, liquid immiscibility. In any case it is proposed that such residual fluid from which these small magnetite bodies crystallized, may have been the immediate source of the major part of the iron deposited in the mixed granites subunit.

There is evidence that some of the iron in the mixed granites subunit is of sedimentary origin. This evidence is related to the quantitative distribution of magnetite and primary hematite. The apparently high ratio of hematite to magnetite in rocks of decided retro-sedimentary character, such as sillimanite granites in the mixed granite subunit and in rocks in the lime rich subunit, may be explained if all the ferric iron in primary hematite is of sedimentary origin. In this case the high oxidation state of the iron is inherited from the sedimentary cycle, and therefore, retro-sedimentary rocks which have not been chemically reconstituted (as by magnetite-rich fluids) would be expected to have a high proportion of hematite. In addition the linear increase of the magnetite-hematite ratio with increase in total iron content (Figures 10 and 11) may be explained if the iron in hematite is of a sedimentary origin and is equally distributed in the original sediments. In this case the curve is an expression of the gradual dilution of this sedimentary ferric iron as magnetite was added by a metasomatic process to the original rock. The sporadic distribution of points around the linear trend (Figure 10)

is easily explained as due to the irregular proportion of ferric iron in the original sediment.

It might be argued that during progressive crystallization of a parent granite magma the residual solutions were enriched in ferric iron above that necessary to form magnetite. Hence, hematite could crystallize directly from such fluids and be of true endogenic origin. However, the magnetite bodies previously discussed which are associated with granites and believed to represent the crystallized product of residual fluids from those granites do not contain primary hematite. In addition many of the magnetite deposits in the Granville rocks of the Adirondacks (Howard, 1951) and New Jersey (Sims, 1953) carry little or no primary hematite, whereas those which do carry primary hematite contain considerably less than the rocks of the mixed gneiss subunit. Thus, there appears to be good evidence that the magnetite ore fluids carried little or no ferric iron in excess of that necessary to form magnetite. It might be proposed that such iron bearing fluids could be oxidized when brought into contact with the mixed gneiss subunit. For example a relatively high  $H_2O$  content of these granites might cause considerable oxidation of a magnetite ore fluid. Utilizing the equilibrium data presented in Chapter 3, it is possible to estimate the amount of  $H_2O$  necessary to oxidize a given quantity of magnetite (as the solid phase). Simple calculations show that it would require approximately 100 moles of  $H_2O$  to oxidize a mole of magnetite to hematite if the temperature and pressure were 900°C and 2000 atm., respectively. Thus if this process took place it would require preposterously large volumes of  $H_2O$  to form the amount of primary hematite in the mixed gneiss subunit. This mode of origin of

the primary hematite appears unlikely unless non-equilibrium conditions prevailed in which case unlimited oxidation could take place. In summary it appears as if at least some of the ferric iron in the mixed gneiss subunit originated during the exogene cycle when the original sediments of the mixed gneiss subunit formed.

There are difficulties in regarding the residual fluids of a granite magma as the immediate source and carrier of the iron. In the first place very little is known about the nature of the differentiation process which leads to this iron enrichment. While it is clear that iron is enriched in the residual solution of a bimictic magma there are few data available pertaining to granitic magmas. Of course the associated magnetite bodies discussed above are indirect positive evidence that the residual fluids are enriched in iron; however, such bodies are always very small so that some doubt is created as to whether sufficiently large quantities of iron to form such magnetite deposits as in the Wilson area could be concentrated by the progressive crystallization of varying ratios of granite. Furthermore, despite the regional proximity of "source" granites, there is no evidence which establishes a direct tie between the magnetite deposits of the Wilson area and any particular granite mass. All the granites and alkali-silicates contain magnetite as an accessory mineral. In the case of some of the peraluminous granites in the Franklin Falls area secondary magnetite may total 3-7 volume per cent. It is difficult to imagine that the residual fluids of a granite or alkali-silicate magma could become greatly enriched in a constituent (magnetite) which was actually crystallizing from the magma. Enrichment through crystallization differentiation implies that the

crystalline product contains less of the particular constituent than the residual product. As these "parent" granites and alkali-silicates contain several per cent magnetite, it is implied that their magmas must have been very rich in  $\text{FeO}$  and  $\text{Fe}_2\text{O}_3$ . Therefore, as there is evidence that at least some of the iron in the mixed gneiss subunit is of sedimentary (exogenic) origin, perhaps Landergren's (1948) hypothesis should receive more consideration. Perhaps all the iron in the mixed gneiss subunit is of sedimentary origin and has been completely redistributed during the regional metamorphism and metasomatism (endogenic cycle), so that the magnetite deposits have taken on the geological character of "magmatic" deposits for which the source of the iron was from the differentiation of granitic magma.

#### MODE OF TRANSPORTATION OF THE IRON

An additional problem arises when the nature of the residual fluid is considered. The concept of a magnetite magma has been considered by previous geologists (Rogers, 1940; Chord, 1947) and recently discounted by Sims (1953). In the case of the magnetite deposits in the mixed gneiss subunit there is absolutely no evidence to suggest that such an ore magma was injected into the gneiss. Most investigators postulate that the residual iron-rich fluids were either hydrothermal or peridotolytic or both.

It is well known that ferric and ferrous iron form very volatile halogen complexes; hence, it has frequently been proposed that iron has "boiled off" of the residual granite regions as such gaseous complexes.

This mechanism of gaseous transfer offers both an explanation of how the iron was initially concentrated from the parent magma and how the iron was transported. Aside from its simplicity, there is no geologic evidence to indicate that such a process was important in the formation of the magnetite deposits in the mixed gneiss subunit. The absence or paucity of halogen compounds in the magnetite deposits or the associated rocks makes this process even less tenable.

Very little is known about the solubility of magnetite in aqueous solutions at high temperatures and pressures. Holser (1952, 1953) has carried out some experimental work which indicates that the solubility of magnetite in pure H<sub>2</sub>O is very slight but that in mildly acid water it increases greatly. However, much more information is needed before it can be positively concluded that large amounts of iron can be carried in an aqueous solution.

Nevertheless, it is believed that large quantities of iron were transported to and within the mixed gneiss subunit by some sort of iron ore fluid. Such a fluid regardless of its exact physical nature (gas, liquid, e'c.) would be expected to have a characteristic chemical composition. Evidence for this was cited in the section on the geochemistry of phosphorus, where it was shown that phosphorus and iron "join together" as though they were both present in an ore fluid in a constant ratio. In addition the relative concentration of manganese (in gneiss) and barium (in K-feldspar) in magnetite rich layers is evidence that an iron ore fluid with a distinct chemical composition entered into the formation of the magnetite deposits. Furthermore, the inverse relationship between the

content of magnetite and primary hematite, (Figures 10 and 11) indicates that an iron ore fluid with a ferrous/ferric iron ratio distinct from that in the original sediments of the mixed gneiss subunit entered into the formation of the magnetite deposits. Therefore, there appears to be ample geochemical evidence that some sort of an iron ore fluid with a characteristic chemical composition did play an important part in the genesis of the mixed gneiss subunit and the related magnetite deposits.

#### MODE AND TIME OF REPLACEMENT OF THE MAGNETITE

Whatever the precise nature of the process whereby iron was transported and emplaced in the mixed gneiss subunit; gaseous phase, hydrothermal phase, etc., it is clear that it was a pervasive or percolative process. Although there are zones and layers in the mixed gneiss subunit which are very rich in magnetite, it should be emphasized that the magnetite occurs throughout the subunit and ranges in size of distribution from disseminated grains to lamellar aggregates of several grains and progressively to layers of over 50 per cent magnetite. There is no evidence that an ore magma has forcibly intruded the mixed gneiss subunit. Chemical processes appear to have been far more important than mechanical processes. There is no evidence that any openings (cracks, fissures, microlaccolith, etc.) were available for the ore fluids. Instead, the magnetite must have either selectively replaced pre-existing mineral materials in order to make room for itself.

The magnetite-quartz gneiss layers in the mixed gneiss subunit might indicate that magnetite has preferentially replaced K-feldspar during the

genesis of the magnetite rich layers. However, it is apparent from Figure 3 that in the magnetite-quartz-K-feldspar gneiss there is no preferential enrichment of magnetite at the expense of K-feldspar. If this were the case, the ratio of quartz to K-feldspar should show a continual increase with increase in magnetite. The figure shows that there is no such relationship. Furthermore, there is a sharp mineralogic discontinuity between the samples of magnetite-quartz-K-feldspar gneiss and the magnetite-quartz gneiss (Figure 3). If the latter rock originated by the preferential replacement of K-feldspar of the former rock by magnetite, then a continual mineralogic variation would be expected.<sup>1</sup>

- 
1. There are several possible explanations of the origin of the magnetite-quartz gneiss layers. First, such layers may represent original pure sandstone layers which have been partially replaced by magnetite during the regional metamorphism and metasomatism. The absence of aluminum in such sandstone layers would prevent the fixation of any potassium (K-feldspar). Second, such layers might represent the actual crystallization product of the iron ore fluid. In that case the fluid would be composed mostly of iron and silicon so that the ultimate product of replacement would have a similar composition. Last, it seems possible that magnetite-quartz gneiss layers could actually be actinolite-rich hornfelsation (taconite). Their bulk composition is similar enough to taconite to make such a hypothesis tenable (J. Ge., 1954). If this latter case is actually true, then several problems related to the origin of the iron deposits may be explained. First, such layers could provide the source of all the iron. Second, the concentration of the magnetite crystals into certain zones and layers would be a consequence of the original sedimentary stratification. Furthermore, the contact relations between the magnetite-quartz gneiss and magnetite-quartz-K-feldspar gneiss (Plate 20) which indicate that the latter rock may have been younger than the former, could be explained as due to Metasomatism of the older iron rich (taconite) layer. The heavy magnetite rich layer in the magnetite-quartz-K-feldspar gneiss at the contact with the magnetite-quartz gneiss (Plate 20) could be regenerated iron stemming from the latter rock as a result of the Metasomatism.

There is no evidence which indicates that the metasomatic emplacement of the iron postdated the regional metamorphism and metasomatism of the mixed gneiss subunit. The magnetite deposits are structurally equivalent to other masses of rock within the subunit, i. e., foliated, linedated, folded. The fabrics of the magnetite-rich layers and the magnetite-quartz-K-feldspar gneiss appear equivalent. The fabric of magnetite grains appears similar to the fabric of associated silicate grains. If the silicate grains are markedly deformed so are the magnetite grains (Plate 4). In undeformed samples of magnetite-quartz-K-feldspar gneiss the magnetite grains are again texturally equivalent to the silicate grains; i. e., undeformed (Plates 3 and 5). There are no reaction rims between magnetite and adjacent silicates. The data all indicate that the entire mineral assemblage in the mixed gneiss subunit crystallized and grew to equilibrium at the same time, and that as indicated by the nature of the fabric and structure of the rocks in the subunit this entire assemblage developed during the period of regional metamorphism and metasomatism.

According to this view the metasomatic emplacement of the magnetite is but another phase of the metamorphic and metasomatic processes which took place in the mixed gneiss subunit. The replacement of minerals by magnetite is similar to the process that was going on in the case of K-feldspar, i. e., it was enriched in certain layers at the expense of other minerals and depleted in other layers. In layers where magnetite was added other constituents were "flushed out" into adjacent layers. In some places magnetite grew at the expense of silicates and in other places silicates grew at the expense of magnetite. In essence the entire process is deemed as metamorphic in nature in that mineral grains grow

outward from centers (nuclei) continually replacing surrounding mineral grains, continually increasing in size and continually changing the nature of the grain boundary interface with adjacent grains. The relationships seen today either represent final equilibrium arrangement (with regard to mineral phases, their grain sizes and shapes, etc.) or a stage of crystallization leading to such a final equilibrium.

#### SUMMARY

In final summary it is believed that the magnetite deposits in the mixed granite gneiss are a, sial rock types developed along with other rocks during the upper-level metamorphism and metasomatism. It is believed that the initial source of most of the magnetite was from residual fluids which developed by the successive crystallization of granitic pegmatites. It is proposed that the magnetite pegmatites which are associated with granites in the region may represent the crystallized product of such residual fluids. Much, however, is far yet believed true at least some of the ferrous iron in the mixed granite gneiss is of sedimentary (igneous) origin. The actual nature of the iron rich residual fluids is problematical. However, it is certain that the fluids were of a nature as to penetrate and redistribute highly soluble other constituents. There is no doubt as that the fluids were largely for the purpose by mechanical processes (fracturing, etc.). Hence, the mixed granite deposits are of very complex origin and represent the culmination of a whole series of complex geological processes.

Plate 1. Geologic Map of the Area of the Edison  
Magnetite Deposits, Sussex County, New  
Jersey.

PRE-CAMBRIAN

IGNEOUS ROCKS

Hypersthene granite (ghy)

Greenish buff, fine to medium grained, gneissoid granite. Composed of quartz, microperthite and microantiperthite with accessory hypersthene, biotite and magnetite. Biotite-quartz-feldspar gneiss and pegmatite layers are common.

Pyroxene granite (gp)

Green, medium grained, gneissoid granite and alaskite. Composed of quartz, microperthite and microantiperthite with accessory ferro-hedenbergite, ilmenomagnetite, ilosite and hornblende; rather uniform.

Biotite alaskite (ga)

Pink, medium to coarse grained, gneissoid to massive granite of uniform composition. Composed of perthitic microcline and quartz with accessory oligoclase, biotite, apatite and hornblende. Amphibolite layers are common.

Hornblende granite (gh)

Pink to buff, medium to coarse grained gneissoid granite. Composed of quartz and microperthite with accessory olivoclase, hornblende, biotite and magnetite. Amphibolite and pegmatite layers are abundant.

Contaminated hornblende granite (ghc)

Medium grained, gneissoid granite. Composed of quartz and microperthite with accessory hornblende and magnetite. Contaminated with hornblende-pyroxene gneisses, amphibolites and local lenses of pyroxene skarn.

### Pyroxene syenite gneiss (gns)

Medium grained, uniform syenite gneiss. Composed of oligoclase, perthitic microcline and ferroaugite with accessory ilmenomagnetite, ilmenite, hornblende, quartz and relic microperthite.

### METASEDIMENTARY, METASOMATIC AND MIXED GNEISSES

#### Epidote-scapolite-quartz gneiss and related facies (lime rich subunit) (gne)

Medium grained, well-layered gneiss. The gneiss is composed of variable proportions of the following minerals: quartz, microcline, plagioclase, epidote, scapolite, pyroxene, hornblende, biotite, garnet, calcite, zoisite, sphene and ores. Typical facies include epidote-scapolite-quartz gneiss, hornblende and pyroxene-quartz-feldspar gneiss, and biotite-hornblende-quartz-feldspar gneiss, etc.

#### Mixed gneisses with magnetite concentrations (mixed gneiss subunit) (gm)

A complex group of gneisses composed mostly of quartz, K-feldspar and magnetite with hematite, ilmenite, rutile, biotite, garnet, sillimanite, plagioclase, apatite, spinel, normazite and corundum. Generally medium grained, gneissic, and extremely heterogeneous. Magnetite-quartz-feldspar gneiss is the predominant facies, whereas magnetite-quartz-gneiss, garnet-biotite-sillimanite-quartz gneiss, biotite-quartz-feldspar gneiss, magnetite rich layers and rich pyrrhotite are present.

#### Quartz-K-feldspar gneiss (qnf)

Pink to buff, fine grained, even grained and ovoidal; granofels due to streaks and porphyroblastic segregates of garnet; otherwise massive. Composed of K-feldspar and quartz with garnet, ilmenite-pyrite and biotite. Locally interlayered with ilmenite-quartz-feldspar gneiss, clackite and pyrrhotite.

#### Garnetiferous-biotite-quartz-feldspar gneiss (gbq)

Grayish, medium grained gneiss with local K-feldspar porphyroblasts. Consists of oligoclase, perthitic microcline and quartz with biotite, garnet and magnetite. Granofels, pyrrhotite and quartz-K-feldspar gneiss are intimately interlayered.

Garnet-biotite-quartz-feldspar gneiss and related facies (gng)

Medium to coarse grained gneiss. Composed of quartz, oligoclase and perthitic microcline with garnet, biotite, hypersthene, hornblende and magnetite. Somewhat heterogeneous with layers of amphibolite, granite, pegmatite and rare scapolite-pyroxene gneiss.

gneiss of uncertain origin

Quartz-oligoclase gneiss (gno)

White, medium to coarse grained and very gneisic. Composed of quartz and oligoclase with biotite, chlorite, microcline, epidote, garnet and ores. Amphibolite and pegmatite layers are common.

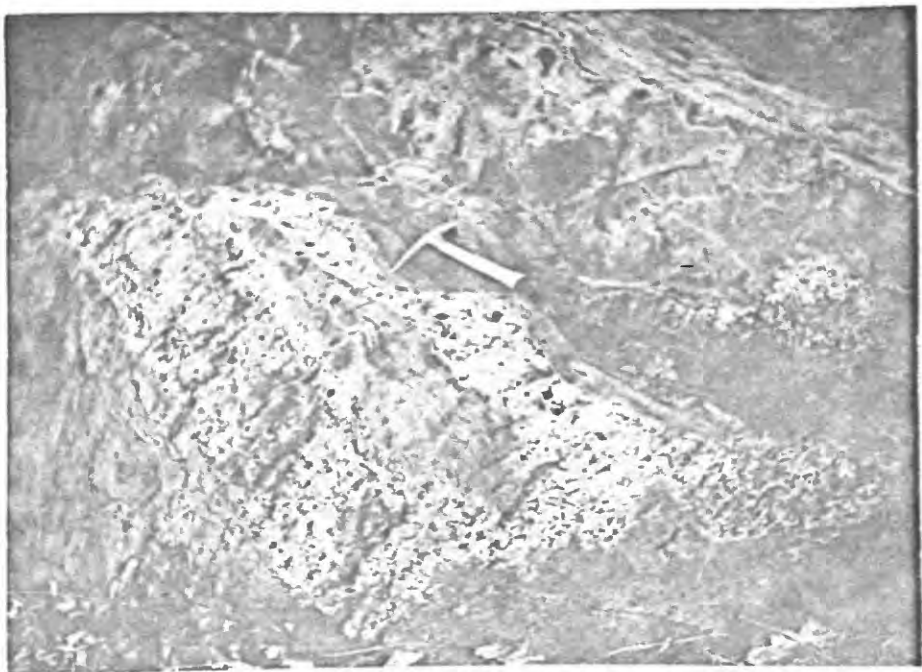


Plate 2. Amphibolite layer intruded by pegmatite.

The pegmatite (white) is a large lenticular mass which surrounds the amphibolite (gray). It is true that the internal boundaries of the pegmatite are conformable to the foliation, but the ends of the pegmatite cross-cut the foliation. There are also thin "injection" layers of pegmatite within the amphibolite. The plate illustrates the typical relations between the older "traville type" gneisses and the younger igneous rocks.

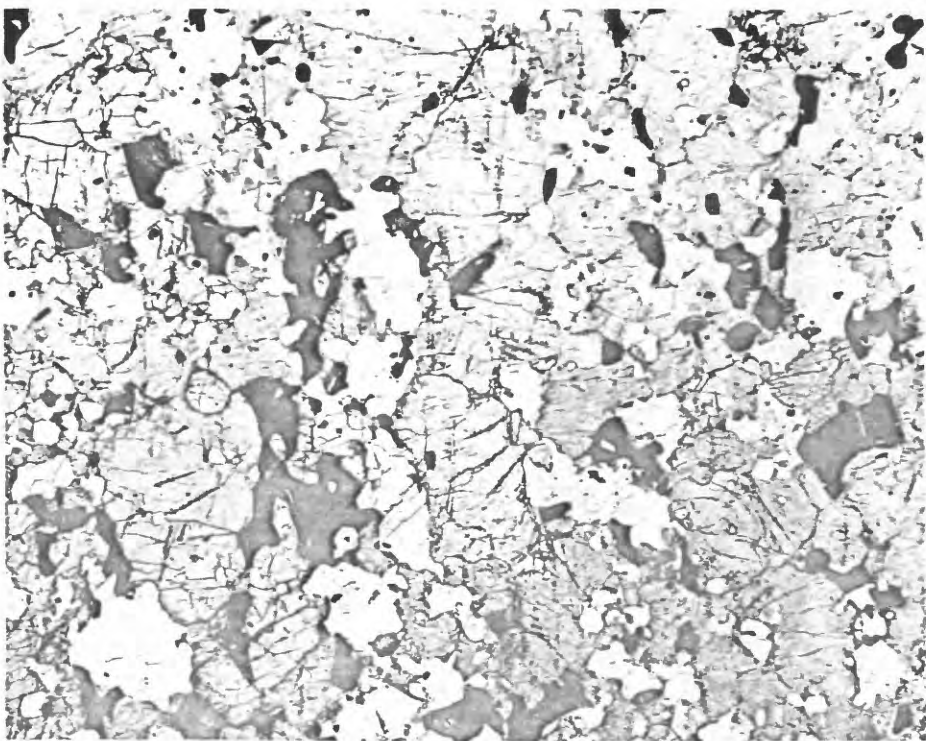


Plate 5. Photomicrograph sample 149, magnetite-quartz-K-feldspar gneiss from the Edison Area. (white = quartz; gray = stained K-feldspar; black = ores; ordinary light, x 9)

The principal minerals are xenoblastic and have highly cutured grain boundaries. Texturally all the minerals are equivalent.



Plate 4. Photomicrograph sample 143, magnetite-K-feldspar-quartz gneiss from the Edison Area. (white = quartz; gray = stained K-feldspar; black = ores; ordinary light, x 11)

The principal minerals are xenoblastic and have sutured grain boundaries. Note the lenticular shape of the magnetite and the equidimensional shape of the K-feldspar.

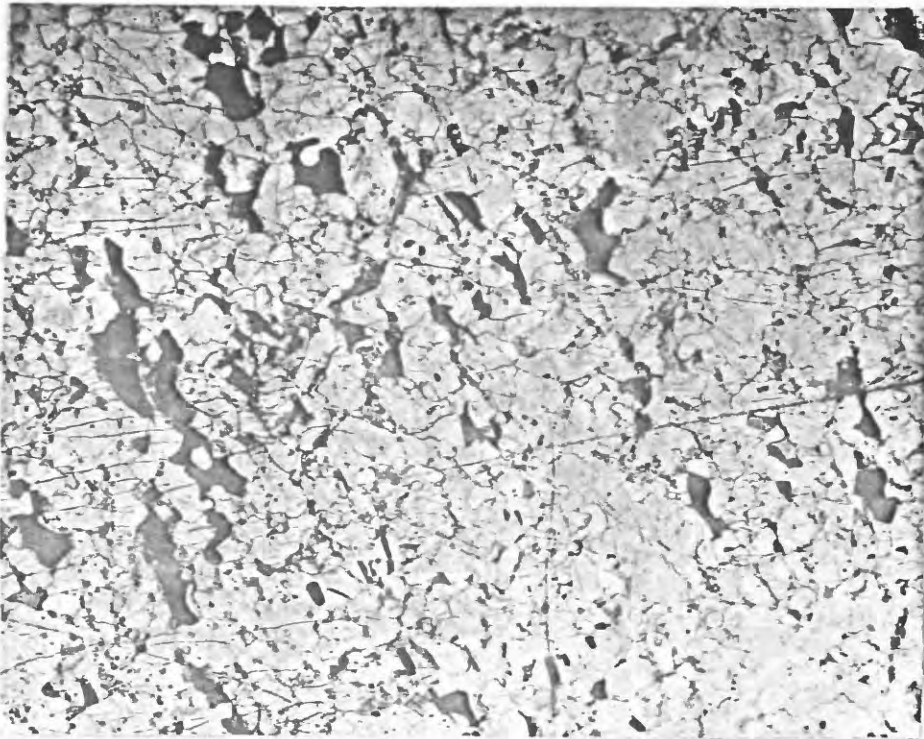


Plate 5a. Photomicrograph sample 145, magnetite-quartz-K-feldspar gneiss from the Elton Area. (light gray = quartz; gray = stained K-feldspar; dark gray and high relief = sillimanite; black = ores; ordinary light, x 11)

Magnetite, quartz and K-feldspar are xenoblastic and have sutured grain boundaries and appear to be texturally equivalent. Sillimanite is subhedral and is often elongated parallel to the side pinacoid.

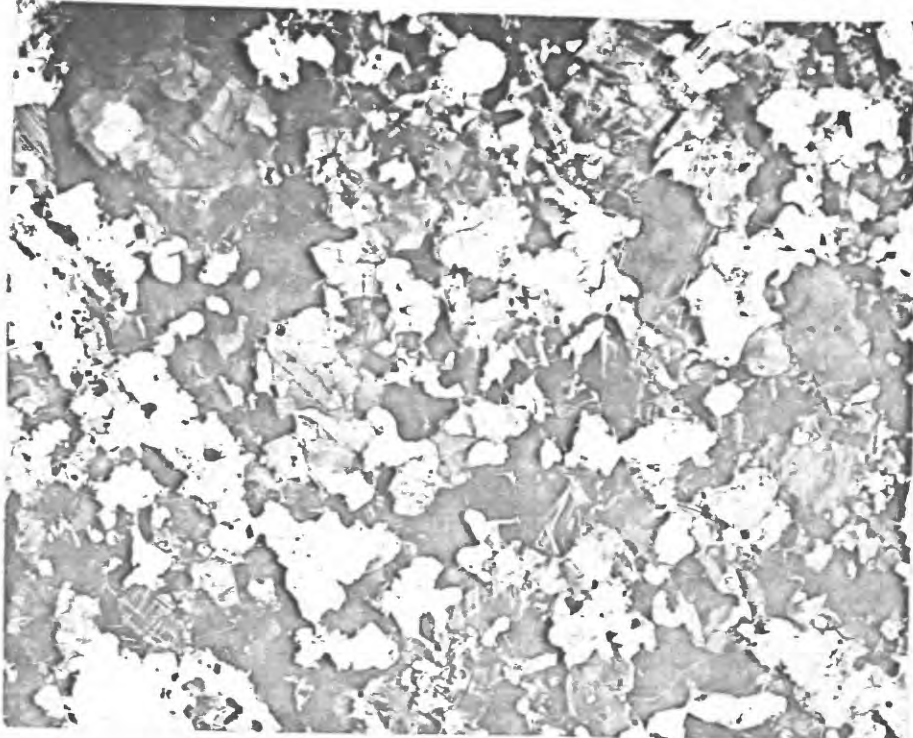


Plate 5b. Photomicrograph sample 145, (crossed nicols, x 11).

Zenoblastic shapes and sutured grain boundaries are apparent. Microcline grid twinning and strain shadows in quartz are illustrated.

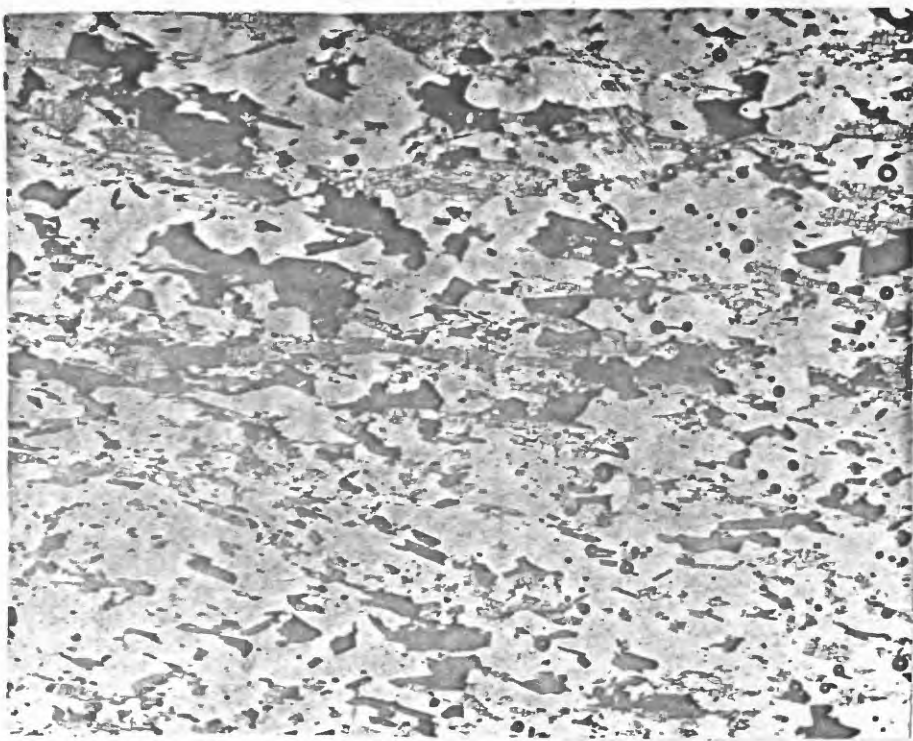


Plate 6a. Photomicrograph sample B-151f, magnetite-biotite-sillimanite-quartz gneiss (meta-quartzite?) from the Edison Area. (white = quartz; gray and high relief = sillimanite; dark gray = biotite; black = ores; ordinary light, x 9)

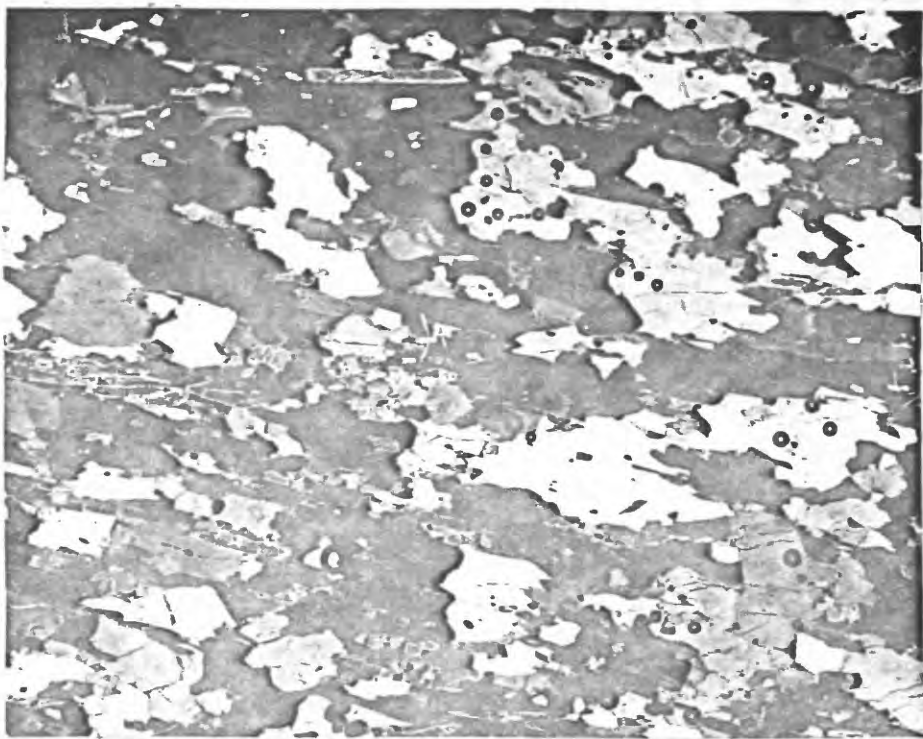


Plate 6b. Photomicrograph sample B-151f, (crossed nicols,  
 $\times 14$ )

Magnetite and quartz are xenoblastic with irregular grain boundaries. Some subhedral hematite plates are visible. Sillimanite is subhedral and elongated parallel to the side pinacoid. Note the strong preferred orientation of all the minerals. The fabric of all the minerals appears equivalent.

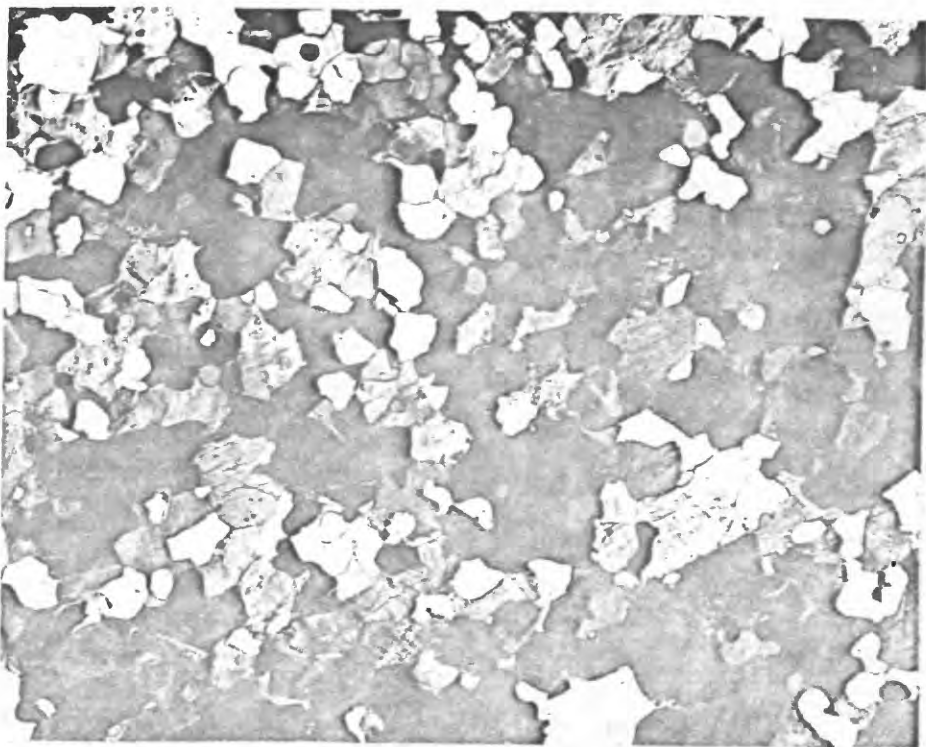


Plate 7. Photomicrograph sample Ed-177, quartz-K-feldspar gneiss from the Edison Area. (crossed nicols, x 14)

Quartz and K-feldspar are xenoblastic, equidimensional and have smooth (not sutured) grain boundaries. Microcline grid twinning is visible in portions of some grains.

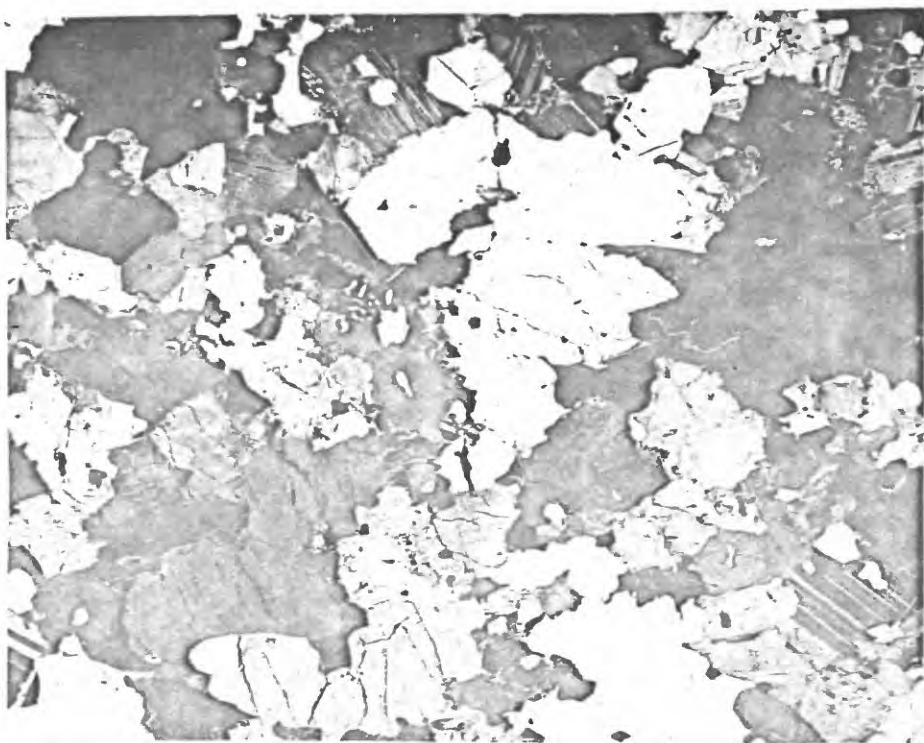


Plate 3. Photomicrograph sample Ed-24la, biotite-quartz feldspar gneiss from the Edison Area. (crossed nicols, x 9)

Minerals are mostly xenoblastic with sutured grain boundaries. Note twinned plagioclase, faintly twinned microcline, large anhedral quartz grains, symplectites and biotite plates.

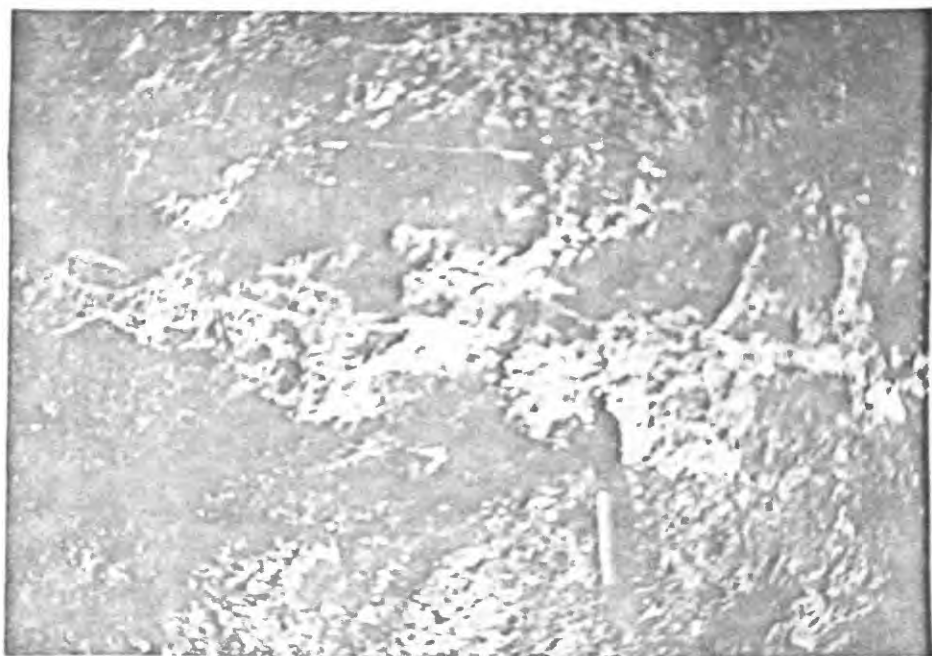


Plate 9. Pegmatite lode in the mixed gneiss subunit.

Pegmatite (white) cross-cuts the foliation of magnetite-quartz-K-feldspar gneiss, sillimanite gneiss and magnetite rich layers. The foliation is parallel to the pen and the trend of the pegmatite lode is parallel to the pencil. Note the thin "injection" layers which extend out from the body of the pegmatite into the surrounding gneiss.



Plate 10. Interlayers of biotite alaskite, biotite-quartz-feldspar gneiss and quartz-K-feldspar gneiss in the Edison Area.

The pen is parallel to the foliation and rests on a layer of biotite-quartz-feldspar gneiss. To the right of the pen a layer of biotite alaskite which cross-cuts the foliation and weathers out in greater relief is visible. To the left of the pen a layer of quartz-K-feldspar gneiss which weathers out with very little relief is visible. All the layers lense out very abruptly into one another.

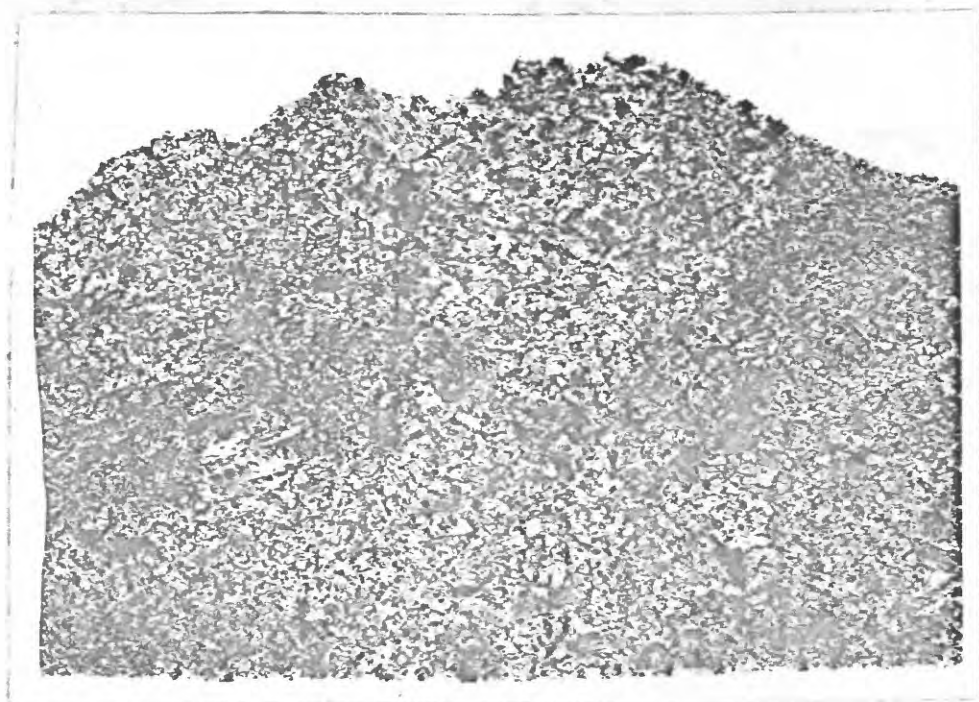


Plate 11. Handspecimen (3d-2544) which illustrates interlayering of biotite alaskite, biotite-quartz-feldspar gneiss and quartz-K-feldspar gneiss. (Specimen about 6 inches long).

The contacts between the layers are abrupt but are the natural grain boundaries between minerals. The contacts are inked. The layer on the left is medium grained biotite-quartz-feldspar gneiss with a monoclinic K-feldspar porphyroblast (2544-c). The middle layer is coarse grained biotite alaskite. The layer on the right is fine grained quartz-K-feldspar gneiss.

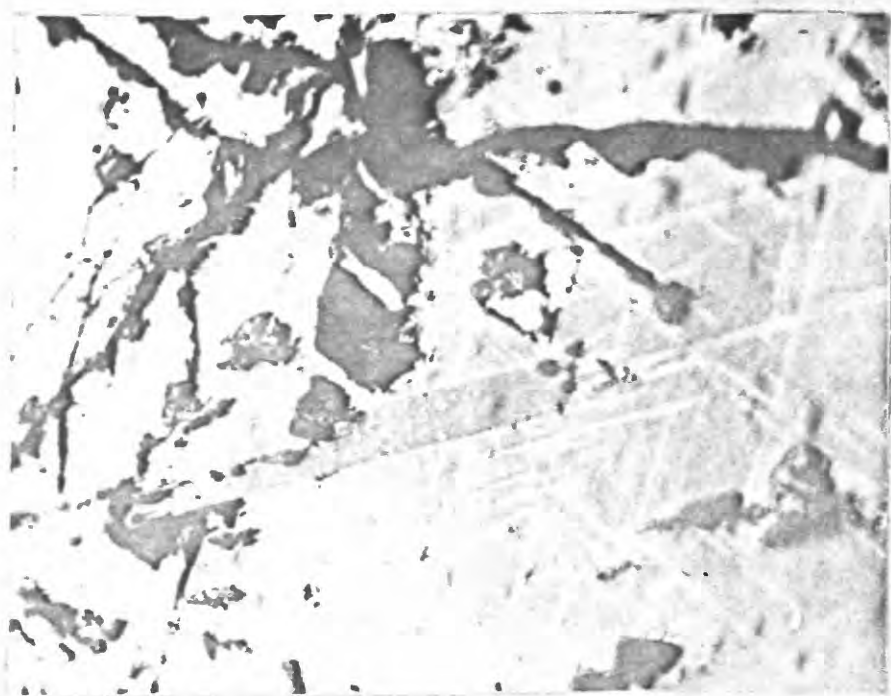


Plate 12. Photomicrograph sample 144, ilmenomagnetite with martite. (white = hematite or martite; light gray = magnetite; dark gray = ilmenite; reflected light,  $\times 570$ )

The martite forms an octahedral network of films and spikes. The ilmenite tablet is also parallel to the octahedral plane and appears to form a barrier to the growth of the martite.

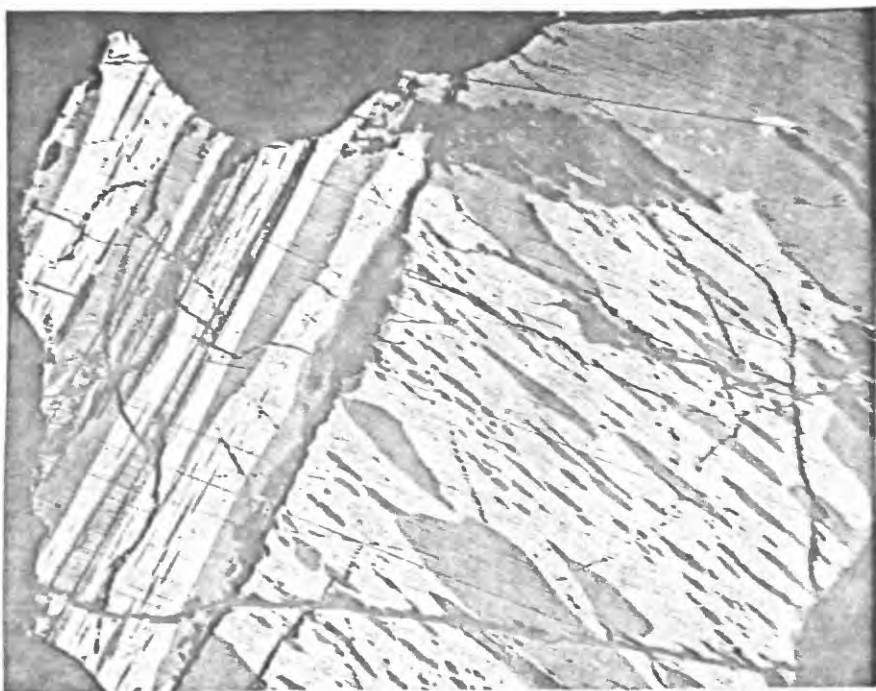


Plate 13. Photomicrograph sample 149, ilmenohematite and magneto-ilmenohematite; (white = hematite; medium gray = magnetite; dark gray = ilmenite; reflected light,  $\times 250$ )

The grain on the right is ilmenohematite. Large lenses of ilmenite are apparent and very fine films of ilmenite are faintly visible in the host hematite.

The grain on the left is magneto-ilmenohematite. Note the ilmenite salvage which completely surrounds each magnetite tablet.

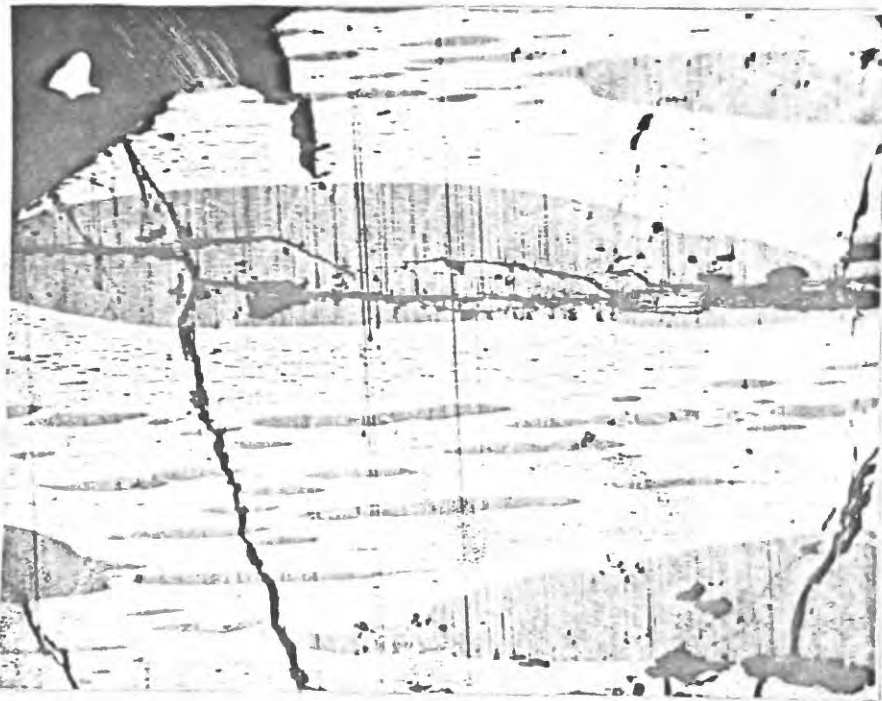


Plate 14. Photomicrograph sample 149, ilmenohematite.  
(white = hematite; gray = ilmenite; reflected  
light,  $\times 570$ )

The host hematite contains large and medium sized lenses of ilmenite and extremely fine films of ilmenite. There is a size discontinuity between the lenses and the films. The large lenses of ilmenite contain similar fine films of hematite. The large lenses of ilmenite formed during the early stage of the exsolution history; whereas the films of ilmenite and hematite formed during the last stage of the exsolution history. Note the rhombchedral twin lamallae.



Plate 15. Photomicrograph sample 149, magneto-ilmenite;  
(white = hematite; medium gray = magnetite;  
dark gray = ilmenite; reflected light,  $\times 250$ )

The host ilmenite contains large lenses and very fine films of hematite. There is a size discontinuity between the large lenses and fine films. The large lenses of hematite contain similar fine films of ilmenite. The large lenses of hematite formed during the early stage of the exsolution history and the fine films of hematite and ilmenite formed during the last stage of exsolution. The magnetite tablets are always surrounded by an ilmenite salvage and often lens out abruptly into the host ilmenite. Note the two patches of altered ilmenite (mottled aggregate) on the far right of the grain.

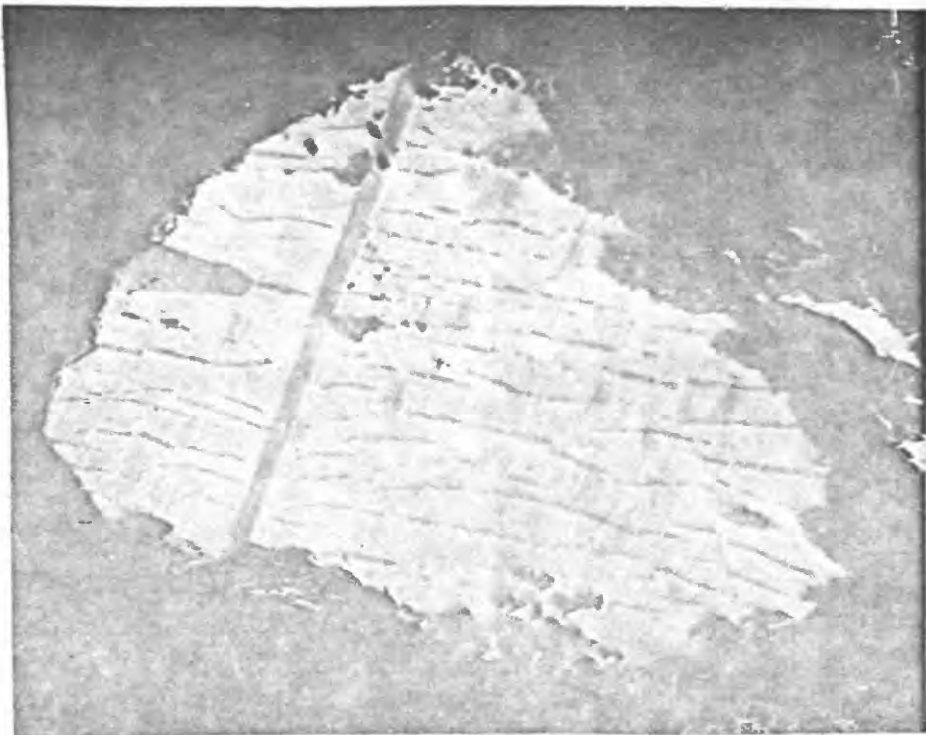


Plate 16. Photomicrograph sample 145, ilmeno-rutilehematite.  
(light gray host = hematite; gray lenses = ilmenite  
and rutile; gray flat disks = rutile; reflected  
light, x 920)

The rutile bodies are oriented parallel to the basal and rhombohedral planes. Ilmenite is subordinate to rutile.

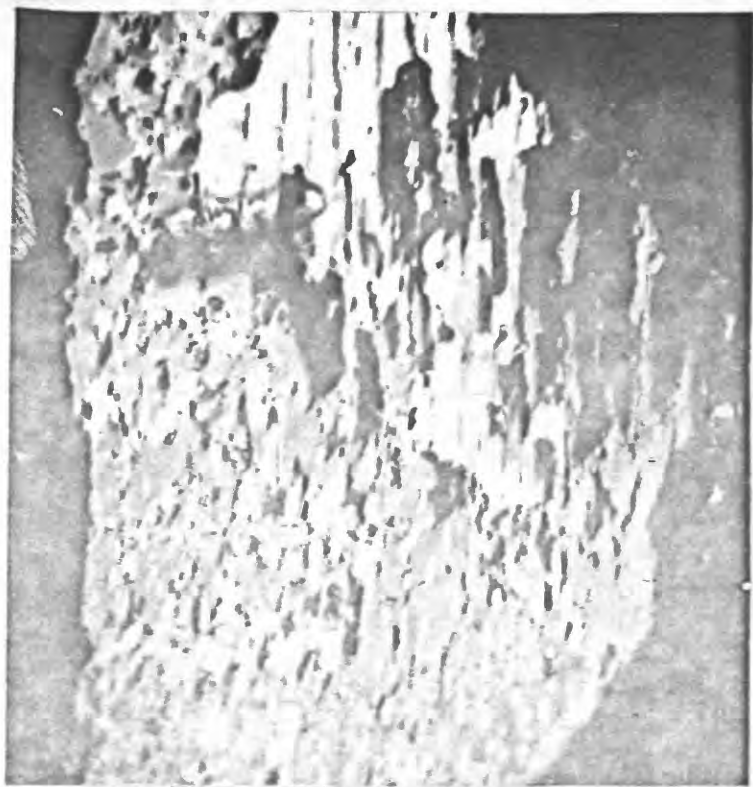


Plate 17. Photomicrograph sample 153, honorutile.  
(medium gray = rutile; white = hematite;  
reflected light,  $\times 570$ )

Rutile is host to large and small lenses of  
hematite.

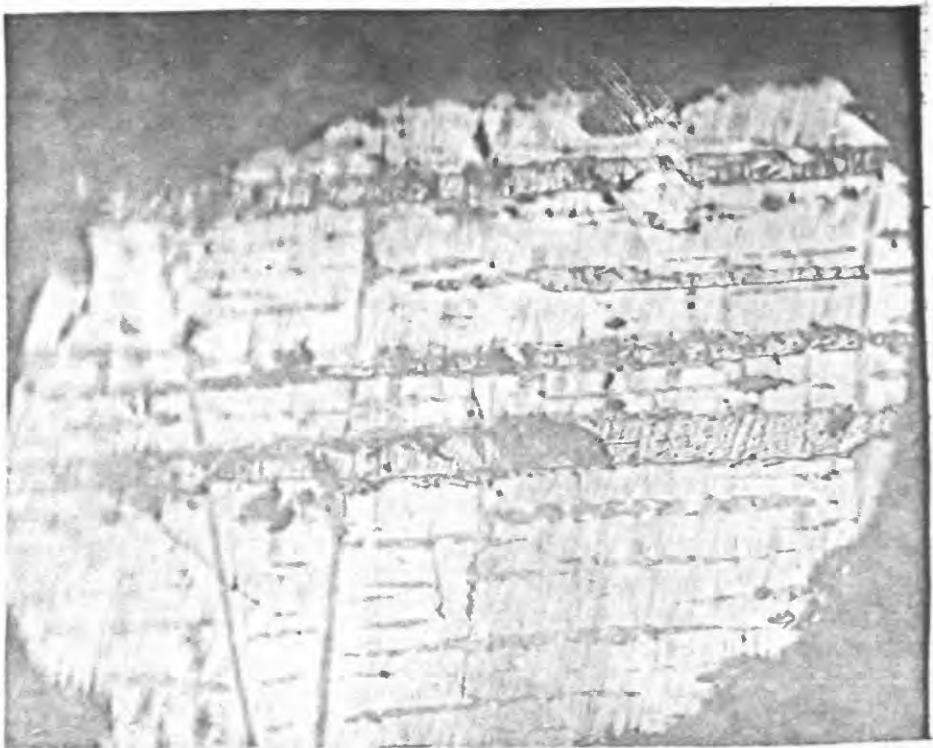


Plate 18. Photomicrograph sample 153, magneto-rutilehematite.  
(light gray = hematite; medium gray = magnetite;  
dark gray = rutile; reflected light,  $\times 750$ )

Hematite is host to basal lenses and rhombohedral disks of rutile and basal tablets of magnetite. The magnetite has been etched with HCl.

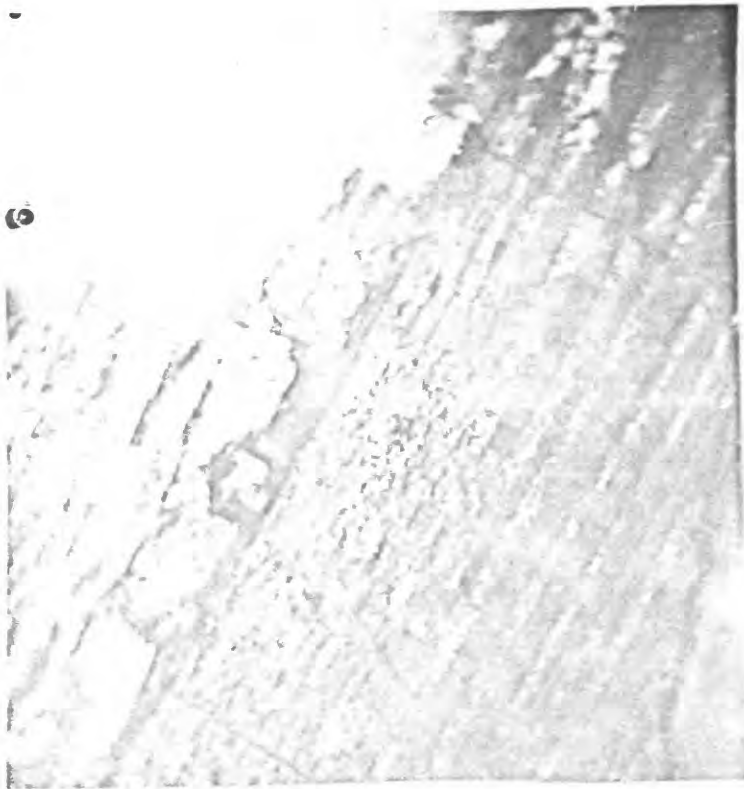


Plate 19. Photomicrograph sample 154, magneto-rutile.  
(medium gray and white = rutile; very dark  
gray = magnetite, reflected light, crossed  
nicols, x 130)

Rutile appears in two colors due to strong internal reflections. Magnetite tablets are etched with HCl and generally extend across the entire host grain of rutile.

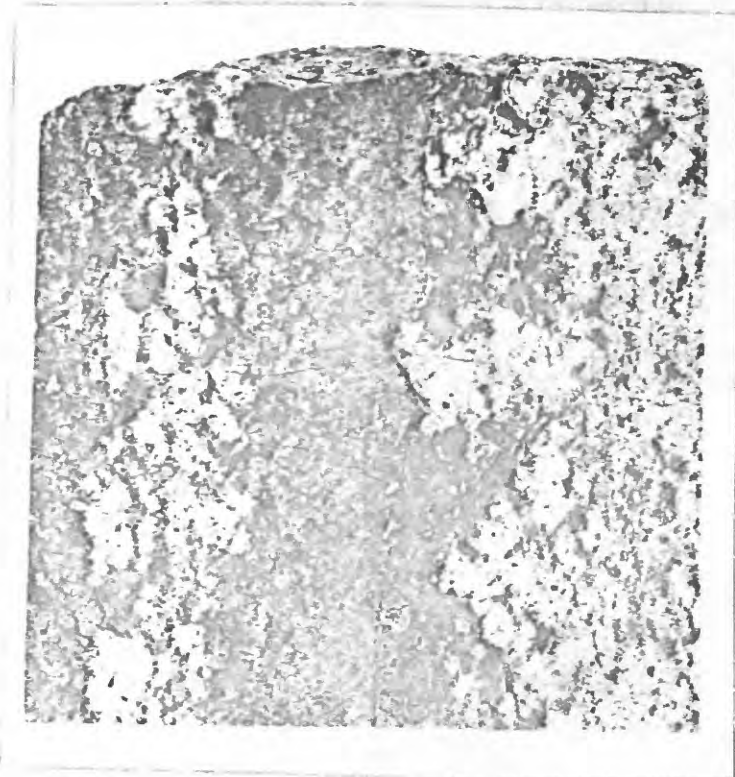


Plate 20. Handspecimen showing contact relations between magnetite-quartz-K-feldspar gneiss and magnetite-quartz gneiss (x 1)

The contact between the two rock types is inked. Magnetite-quartz-K-feldspar gneiss is on the right and magnetite-quartz gneiss is on the left. The contact is the natural grain boundary between the minerals. Note the marked enrichment of magnetite in the magnetite-quartz-K-feldspar gneiss at the contact. Note the isolated lense of magnetite-quartz-K-feldspar gneiss with K-feldspar porphyroblasts within the magnetite-quartz gneiss.

REFERENCES CITED

- Barth, T. F. W. (1952) *Theoretical Petrology*. New York: John Wiley and Sons, Inc.
- Bascom, P. and Stose, G. W. (1938) Geology and mineral resources of the Honeybrook and Phoenixville quadrangles, Pennsylvania. U. S. Geol. Survey Bull. 891, p. 1-145.
- Bayley, W. S. (1910) Iron mines and mining in New Jersey. New Jersey Geol. Survey, Final Report Ser., vol. 7.
- Bayley, W. S. and others (1903) U. S. Geol. Survey, Bull. 311, Part 4, Folio (no. 157).
- \_\_\_\_\_, (1914) U. S. Geol. Survey, Bull. 414, Part 4, Folio (no. 391).
- Birch, F., Price, Schaffer, J. F., and Spurr, H. D. (1942) A method of physical analysis. Geol. Soc. Amer., Spec. Paper 26.
- Berlet, P. and Coffroy, J. (1952) Nécessité d'ilménite dans les lamelles du Tahalra. Bull. de la Soc. Frans. Min. et de Cristallog. LXXV, p. 580-584.
- Bowen, N. L. (1923) *The Evolution of the Igneous Rocks*. Princeton University Press.
- Bowen, N. L. and Schairer, J. F. (1935) The system  $MgO-CaO-Al_2O_3$ . Am. Jour. Sci. 22, p. 161-163.
- Bowen, N. L. and Tuttle, O. F. (1950) The system  $MgO-Al_2O_3-KAlSi_3O_8-Al_2O_3$ . Jour. Geol., 58, p. 474-511.
- Brown, A. S. (1937) *A Field Guide to the Igneous Intrusions of New England*. Geol. Soc. Amer. Mem. 7, 354 pages.
- \_\_\_\_\_, (1943) Origin of granitic rocks of the Northeast Adirondacks, in Gilluly, James (Editor), *Origin of Granites*. Geol. Soc. Amer. Mon. 28, p. 21-43.
- \_\_\_\_\_, (1951) Geology of the Northwestern Adirondack magnetite district, New York. U. S. Geol. Survey, Prof. Paper (in preparation).

- (1952) Chemical petrology of some metamorphosed Adirondack gabbroic, syenitic and quartz syenitic rocks. *Am. Jour. Sci.*, Bowen volume.
- Barington, A. F., Fahey, J., and Vlasisidis, A. (1953) Iron and titanium oxide minerals of Adirondac rocks and their magnetic properties. Abstract, Amer. Min.
- Bell, J. (1952) The fiber-reinforced local fine-granites of New Jersey. *Jour. Geol.*, 60, p. 257-258.
- Bell, J. (1952) The granofels facies of pitch-fiber-quartzite. An intermediate facies in the evolution. *Amer. Min.*, 37, p. 337-352.
- Bell, J., Jr. and Edward, J. (1950) Synthetic fiber-quartzite. *Jour. Geol. Soc. Am.*, 61, p. 575-577.
- Bell, J. Jr. (1952) Geology of New Jersey, I. Rock.
- Bell, J. Jr., Bell, C. R., and Edwards, K. L. (1951) High-pressure granofels facies of pitch-fiber-quartzite, quartzite and quartzite-schist. *Amer. Jour. Min.*, 36, p. 31-43.
- Bell, J. Jr. and McNeely (1953) The granofels facies of pitch-fiber-quartzite. *Jour. Geol.*, 61, p. 1-12.
- Bell, J. Jr. and Berry, R. W. (1945) The system feldspar + K<sub>2</sub>TiO<sub>3</sub> - quartz - feldspar and related equilibria. *Jour. Amer. Chem. Soc.*, 67, p. 1393-1412.
- Bell, J. Jr. (1946) The system K<sub>2</sub>TiO<sub>3</sub>-K<sub>2</sub>O: II. Equilibrium and thermodynamics of liquid acids and other phases. *Jour. Amer. Chem. Soc.*, 68, p. 721-736.
- Bell, J. Jr. (1950) The solid solution of K<sub>2</sub>TiO<sub>3</sub>. *Jour. Amer. Chem. Soc.*, 72, p. 1777-1780.
- Bell, J. Jr. (1953) The solid solution of K<sub>2</sub>TiO<sub>3</sub>. *Jour. Amer. Chem. Soc.*, 75, p. 1702.
- Bell, J. Jr., Edwards, J. (1952) The solid solution of K<sub>2</sub>TiO<sub>3</sub>. *Jour. Amer. Chem. Soc.*, 74, p. 317-318.
- Bell, J. Jr. (1953) Olivine-schists - microstructures and crystallography. *Proceedings, Australian Institute of Mining and Metallurgy*, p. 31-52.
- Bell, J. Jr. (1952) The ore minerals and their textures. *Jour. Roy. Proc. of the Royal Society of New South Wales*, 1952, p. 25-46.

- Engel, A. E. J. and Engel, Celeste G. (1952) Origin and evolution of hornblende-andesine amphibolites and kindred facies. *Geol. Soc. Amer. Bull.*, 63, p. 1435-1436.
- \_\_\_\_\_(1953) Grenville series in the northwest Adirondack Mountains, New York. *Geol. Soc. Amer. Bull.*, 64, p. 1013-1093.
- Foster, G. R. (1914) The role of garnet in certain gneisses in the Highlands of New England. *Trans. Geol. Soc., 22*, p. 594-612; 654-702.
- \_\_\_\_\_(1922) The origin of the gneisses. *Trans. Geol. Soc., 27*, p. 171-213.
- Goldschmidt, V. M. (1930) Chemical evolution of the earth. In: *The Elements*, N. L. Bowen (Ed.), McGraw-Hill, New York, p. 261-364.
- Hall, C. T. (1932) Garnet in the Mississippian, Cambrian, Ordovician, Silurian, and Devonian rocks of New England. *Geol. Soc. Amer. Bull.*, 43, p. 141-151.
- Hall, C. T. (1946) Garnet in metamorphic rocks. *Geol. Soc. Amer. Bull.*, 57, p. 101-112.
- Hall, C. T. (1951) The garnet facies. *Geol. Soc. Amer. Bull.*, 62, p. 101-112.
- Ondrejetic, V. M. (1941) The Fujikobashi garnet facies in Japan. *Geol. Society of America Bull.*, 52, p. 11-20.
- Smithson, J. R. and Hall, C. T. (1954) The garnet facies. III: Stability relations. *Geochimica et Cosmochimica Acta*, 18, p. 1-10.
- Sommer, Z. and Rubin, H. J. (1954) The identification and determination of plagioclase feldspars by the X-ray powder method. *Min. Mag.*, 74, No. 904, p. 326-335.
- Spurr, J. W., Jr., Hall, C. T., Smithson, J. R., and Hall, C. A. (1955) The garnet facies. IV: The stability relations of the garnet-clinopyroxene-plagioclase system. *J. Geol.*, 63, p. 117-131.
- Taylor, R. F. (1953) The garnet facies in the Adirondack rocks, Part I. *Geol. Soc. Amer. Bull.*, 64, p. 1013-1093.
- Weller, R. L. (1954) Petrography of orthoclase and plagioclase in the garnet facies of the Adirondack metasediments. *J. Geol.*, 62, p. 121-136.
- Wess, H. K. (1949) Chemical composition and optical properties of common clinopyroxenes, Part I. *Amer. Min.*, 34, p. 621-665.

- Holser, W. T. (1952) Hydrothermal geochemistry of magnetite—progress report. *Geol. Soc. Amer. Bull.*, 63, Abstract 1264.
- Holser, W. T. and Schneer, C. J. (1953) Deposition of high temperature, nonmagmatic magnetite. *Geol. Soc. Amer. Bull.*, 64, Abstract 1435.
- Hotz, P. F. (1953) Geology and magnetite deposits of the Hudson Valley and Catskill districts, New York and New Jersey. U. S. Geol. Survey Bull. 920-P.
- Jones, Harold (1951) The hydrology of iron formations. *Am. Geol.*, 48, no. 1, p. 1-43.
- Klemm, Elmer (1952) A Paleozoic stratigraphy of the Hudson River Valley, Vol. II. University of State of New York.
- Klemm, E. (1953) Paleozoic stratigraphy of the Hudson River Valley, Vol. III. Paleozoic, Part 2. U. S. Geol. Survey Bull. 920.
- Klemm, E. (1954) Paleozoic stratigraphy of the Hudson River Valley, Vol. IV. Paleozoic, Part 3. U. S. Geol. Survey Bull. 920.
- Landes, G. (1910) Iron-ore veins of the Hudson River Valley. *Geol. Soc. Amer. Bull.*, 21, p. 562-584.
- McNeill, L. (1956) New Jersey Coal, Valley Creek, N. J., Oct. 1955, p. 111-248, Bureau.
- \_\_\_\_\_, (1957) New Jersey Coal. Survey Bull. Part of Geologic Report and State Coal Law 1956, p. 5-61.
- Morley, R. (1953) On the paleogeology and tectonics of the eastern United States. *Bull. Amer. Geol. Soc.*, 62, p. 1-12.
- Morgan, F. C. (1953) The Paleozoic history of the Hudson River Valley, N. Y. *Geol. Soc. Amer. Bull.*, 64, p. 113-128.
- \_\_\_\_\_, (1954) Paleogeography of the Hudson River Valley, N. Y. *Geol. Soc. Amer. Bull.*, 65, p. 272-277.
- \_\_\_\_\_, (1952) Mineralization of the Hudson Valley, N. Y. *Am. J. Geol.*, 60, p. 456-450; 549-574.
- Leonard, E. F. (1951) Magnetite deposits of St. Lawrence County, New York. Princeton University, Unpublished Ph.D. thesis.

- Mackenzie, W. S. (1954) The orthoclase-microcline inversion. Min. Mag., XXX, p. 354-366.
- McKinstry, H. E. (1948) Mining Geology. New York: Prentice-Hall.
- Miyashiro, Akiko (1953) Calcium-poor garnet in relation to metamorphism. Geochimica et Cosmochimica Acta, 4, p. 179-203.
- Mjøsnesen, F. (1946) A ferro-orthosilicate ore from Skjera Ulvsk. G.P.P. 68, p. 572-573.
- Munn, F. L. (1889) Geological studies of the Archaean rocks in the Jersey Coal Survey, Ann. Dept. State Geologist for 1889, p. 12-72.
- MacDonald, R. R. (1954) Chemical composition of igneous rocks. G. & G. Soc. Amer. Bull., 65, p. 1027-1032.
- McLaughlin, F. J. (1949) Geology of New York. New York: Harper and Brothers.
- Michel, A. and Vans, P. R. (1951) Fluorine in the pegmatitic rocks of the Maltese range. Geol. M. G., 59, p. 402-410.
- Montbard, Ile (1953) Sur le comportement de l'oxyde de titane dans les pegmatites variées des environs de Sen. Ann. G. G. C., 5, p. 164-214.
- Perdillier, E. and Michel, A. (1959) Etudes des composants définis et des silicates solides qui peuvent former l'oxyde de titane  $TiO_2$  et les oxydes de fer. C. R. Acad. Sci. Paris, 239, p. 1233-33.
- Potter, R. T. (1876) Notes on the samples of iron collected in New Jersey, in Murphy, Raphael, Report on the Mining Territories of the United States (exclusive of the precious metals). U. S. 10th Census, 15, p. 175-177.
- Ridley, H. (1952) The origin of ultramafic and mafic rocks. In: H. Ridley, Vol. 1, Chap. 1.
- Röderer, G. (1955) Beobachtungen über Olivinit, Pyroxinit, Enstatit und Chromit, an der Lagerstätte des  $Fe_2O_3$ , Fe<sub>2</sub>O<sub>3</sub>, NiO. N. J. Geol. f. Min., 24.
- (1959) Wichtige neue Beobachtungen an Magnesit, Olivinit, Ilmenit und Putil. Abhandlungen der Preussischen Akademie der Wissenschaften. Math.-Naturw. Klasse, Nr. 14.

- (1950) Die Erzminerale und Ihre Verwachsungen. Akademie-Verlag, Berlin.
- (1953) Ultraspinel and its significance in titaniferous iron ores. Economic Geol., 48, p. 677-683.
- McIntosh, J. R. and Jeffreys, J. W. E. (1948) The thermodynamics of silicate minerals of iron in iron and steelmaking from 9° to 2400°C. I. Silicates. Journ. Iron Steel Inst. (London), 166, p. 261-270.
- Poggen, H. T. (1936) A. 1st on the Geological Survey of the State of New Jersey, p. 137-144, Philadelphia.
- (1940) Final Report on the Geology of the State of New Jersey, p. 10-12, 26, Philadelphia.
- Porter, W. D. and others (1952) Selected values of chemical elements in common minerals. Circular of the National Bureau of Standards, 50, U. S. Government Printing Office.
- Reed, F. A. (1941) Die Ultraspinel und Titanit im Magnetit, Titanit und Magnetit-Gabbro; in System Fe<sub>2</sub>O<sub>3</sub>-MgO. Z. Mineral. Petrol. Phys., 41, p. 1-25.
- Reed, F. A. (1947) The genesis of intrusive magnetite and titaniferous gabbro. Econ. Geol., 42, p. 634-656.
- Sims, P. K. (1952) Petrology and ores of the Cedar Region, New Jersey. Ph.D. Dissertation, Princeton University.
- (1953) Geology of the Beaver magnetite district, Morris County, New Jersey. U. S. Geol. Survey Bull. 932-E, p. 245-305.
- Sims, P. K. and Leonard, A. F. (1952) Geology of the Cedar Valley district, Morris County, New Jersey. New Jersey, Div. Min. Resources and Geol., Geol. Surv., B. 62, 46 pp.
- Smith, L. C. & S. (1951) Geology of the Franklin Province of New Jersey. Geol. Survey Bull. 921-B, U. S. Geol. Survey.
- Spence, A. G. (1952) Geology of Franklin, New Jersey. Economic Geol., 47, p. 1-1577.
- Spencer, A. G. (1954) Genesis of the magnetite deposits in Sussex County, New Jersey. Mining Mag., 10, p. 377-381.
- Spencer, A. G., McMillan, W. P., and others (1958) U. S. Geol. Survey, Geol. Atlas, Franklin Furnace folio (no. 161).

- Sundius, N. (1946) The classification of hornblendes and the solid solution relations in the amphibole group. *Sveriges Geol. Unders. Ser. C.* #430 Arsbok 40.
- Taliaferro, W. L. (1943) Franciscan-Knoxville problem. *Amer. Assoc. Petr. Geol. Bull.* 27, p. 109-219.
- Taylor, James (1952) Detonation in confined explosives. Oxford: Clarendon Press.
- Taylor, F. J. and Verhoogen, J. (1951) *Igneous and Metamorphic Petrology*. New York: McGraw-Hill Book Company.
- Tennell, G. V. (1946) *The British Isles of the Atlantic. London*, Methuen and Co., 9th edition.
- Vance, H. S. and Price, W. A. (1950) Geological investigation of the West Point area; Part III. The geology of the eastern part of the area, including the Tuckahoe River, the Little River, and the northern part of the New River, p. 124-15.
- Vance, H. S. (1951) The geology of the eastern part of the New River, the Little River, and the northern part of the New River. *Geological Survey of Canada, Memoir 183*, 1951, 100 pp.
- Vance, H. S. (1951) Geological investigation of the West Point area, Part IV, and its relation to the adjacent areas. *Geological Survey of Canada, Memoir 183*, 1951, 100 pp.
- Vance, H. S. (1952) The West Point area, West Virginia, and its relation to the adjacent areas. *Geological Survey of Canada, Memoir 184*, 1952, 100 pp.